UNIVERSIDADE FEDERAL DE PERNAMBUCO

CENTRO DE BIOCIÊNCIAS

PROGRAMA DE PÓS-GRADUAÇÃO EM INOVAÇÃO TERAPÊUTICA

RAFAEL RAMOS DA SILVA

AVALIAÇÃO DAS ATIVIDADES BIOLÓGICAS DE DERIVADO OXAZOLIDÍNICO E INCREMENTO DE SOLUBILIDADE BASEADO EM CICLODEXTRINA

Recife

2017

RAFAEL RAMOS DA SILVA

AVALIAÇÃO DAS ATIVIDADES BIOLÓGICAS DE DERIVADO OXAZOLIDÍNICO E INCREMENTO DE SOLUBILIDADE BASEADO EM CICLODEXTRINA

Tese apresentada ao Programa de Pós-Graduação em Inovação Terapêutica da Universidade Federal de Pernambuco, para a obtenção do Título de Doutor em Inovação Terapêutica

Área de concentração: Farmácia

Orientador: Profº. Dr. César Augusto Souza de Andrade
Coorientador: Profª. Drª. Maria Danielly Lima de Oliveira
Profª. Drª. Maira Galdino da Rocha Pitta

Recife

2017

Dados Internacionais de Catalogação na Publicação (CIP) de acordo com ISBD

Silva, Rafael Ramos da

Avaliação das atividades biológicas de derivado oxazolidínico e incremento de solubilidade baseado em ciclodextrina / Rafael Ramos da Silva - 2017.

162 folhas: il., fig., tab.
Orientador: César Augusto Souza de Andrade
Coorientadoras: Maria Danielly Lima de Oliveira
Maíra Galdino da Rocha Pitta
Tese (doutorado) – Universidade Federal de Pernambuco. Centro de Biociências. Programa de Pós Graduação em Inovação Terapêutica. Recife, 2017.
Inclui referências, apêndices e anexo

1. Oxazolidina 2. Ciclodextrina 3. Atividades antitumoral I. Andrade, César Augusto Souza de (orient.) II. Oliveira, Maria Danielly Lima de (coorient.) III. Pitta, Maíra Galdino da Rocha (coorient.) IV. Título

620.5 CDD (22.ed.) UFPE/CB-2018-345

Elaborado por Claudina Karla Queiroz Ribeiro CRB4/1752

RAFAEL RAMOS DA SILVA

AVALIAÇÃO DAS ATIVIDADES BIOLÓGICAS DE DERIVADO OXAZOLIDÍNICO E INCREMENTO DE SOLUBILIDADE BASEADO EM CICLODEXTRINA

Tese apresentada ao Programa de Pós-Graduação em Inovação Terapêutica da Universidade Federal de Pernambuco, para a obtenção do Título de Doutor em Inovação Terapêutica

Aprovada em: 31/07/2017.

BANCA EXAMINADORA

_____

Profº. Dr. César Augusto Souza de Andrade (Orientador)
Universidade Federal de Pernambuco

_____

Profª. Drª. Maria Danielly Lima de Oliveira (Examinador Interno)
Universidade Federal de Pernambuco

_____

Profº. Dr. Moacyr Jesus Barreto de Melo Rêgo (Examinador Interno)
Universidade Federal de Pernambuco

_____

Prof. Dr. Isaac Aarón Morales Frías (Examinador Externo)
Universidade Federal de Pernambuco

_____

Prof. Dr. Thiago Ubiratan Lins e Lins (Examinador Externo)
Universidade Federal de Pernambuco

A minha esposa **Marcella Ramos**, por vivenciar cada batalha do cotidiano e compartilhar comigo cada vitória enfrentada até aqui. Seu amor e amizade garantiram o apoio necessário para encarar estes desafios sempre com força de vontade e bom humor.

AGRADECIMENTOS

A Deus, pois sem sua permissão nada disso teria sido possível.

Ao Prof. Dr. César Augusto Souza de Andrade, meu orientador, pelo incentivo, amizade, compreensão, confiança e apoio para progredir na carreira acadêmica demonstrados nestes anos de convivência.

A Profa. Dr. Maria Danielly Lima de Oliveira, pela amizade, ajuda, incentivo e confiança durante a realização deste e de outros trabalhos realizados.

A Profa. Dr. Maira Galdino da Rocha Pitta, pela compreensão, profissionalismo e apoio transmitidos durante os anos de convivência em seu laboratório.

A Profa. Maria do Carmo de Alves de Lima (Nena) pela amizade e por me receber de braços abertos e disposta a ajudar no necessário durante a execução deste trabalho.

Ao Prof. Reginaldo Gonçalves de Lima Neto pela generosidade e colaboração envolvidas durante alguns experimentos realizados deste trabalho.

Ao Prof. Dr. Celso Pinto de Melo, pela confiança e ajuda durante a realização de experimentos em seu laboratório de Polímero Não Convencionais (PNC).

Aos colegas do PNC (Sandro Vagner, Juan Medina, Alícia Guajardo, Jarib Alcarraz), do LINAT (Marina Ferraz e Fernanda Gomes) e Bionano (Karen Yasmin, Kalline Lourenço, Felipe Rocha e Isaac Moráles) pela ajuda prestada na utilização de alguns equipamentos neste trabalho e colaboração em outros trabalhos.

Ao Prof. Marcelo Zaldini Hernandes e ao Marcelo Montenegro Rabello do laboratório pela contribuição nos estudos teóricos do laboratório LQTM.

A Paulo Germano, secretário do PPGIT, pelos serviços prestados a mim durante este período sempre com dedicação e eficiência.

A FACEPE, pelo suporte financeiro.

Ao CETENE, pelo apoio na utilização de equipamentos necessários neste estudo.

A minha esposa, Marcella Ramos, pelo amor, compreensão e apoio em todos os meus planos desde sempre.

Aos meus pais Severino e Rosilda pelo amor e dedicação incondicionais e aos meus irmãos Rosy, Chris e Robson, por fazer parte dessa família e por respeitaram minhas escolhas.

RESUMO

Os derivados oxazolidinicos (DOx) foram descritos como compostos com atividade antimicrobiana e antitumoral. No entanto, um dos entraves desta molécula está em sua baixa solubilidade em água e consequentemente reduzida biodisponibilidade. Portanto, a utilização de complexos de inclusão baseados em ciclodextrina (CD) pode contribuir para uma melhoria desta limitação. Neste contexto, realizamos um estudo *in silico* para avaliar a capacidade de interação entre um novo DOx (LPSF/NB-14) e 2-hidroxi-beta-ciclodextrina (2-HPβCD) para formação de um complexo de inclusão. Posteriormente, desenvolvemos complexos de inclusão baseados em 2-HPβCD baseados na técnica de co-evaporação. Em seguida, técnicas de caracterização analítica foram realizadas através de microscopia eletrônica de varredura (MEV), infravermelho transformado de Fourier (IVTF), espectroscopia de ressonância magnética nuclear (RMN-^{1}H), difração de raios X e análises térmicas. Posteriormente, um estudo de perfil cinético da liberação de DOx, teste de citotoxicidade usando células mononucleares de sangue periférico (PBMCs) e testes de atividade biológica em linhagens bacterianas e fúngicas foram realizados. Os estudos *in silico* apresentaram as possíveis orientações com valores entre -5,9 kcal/mol e -5,6 kcal/mol, demonstrando a viabilidade da incorporação do DOx na 2-HPβCD. O aumento máximo de solubilidade foi obtido a 70mM de DOx usando 400 mM de 2-HPβCD, resultando em um incremento vinte vezes maior da solubilidade em água em relação ao DOX puro. As análises de MEV revelaram uma mudança significativa na morfologia das moléculas após o processo de inclusão. Os espectros de FTIR indicaram a formação de complexos de inclusão, considerando a diminuição da intensidade das bandas de absorção dos grupos funcionais do DOx. RMN-^{1}H apresentou mudanças químicas que indicaram estequiometria 1:1 de DOx:2-HPβCD. O complexo de inclusão também indicou diferentes comportamentos térmicos em comparação com o DOx puro. O perfil cinético da libertação de DOx em 2-HPBCD demonstrou uma maior liberação do composto em relação à sua mistura física em meio aquoso. O composto não exibiu citotoxicidade na forma pura ou após a síntese do complexo de inclusão. Em conclusão, estudos *in silico* forneceram uma visão mais importante sobre as interações entre DOx e 2-HPβCD. O perfil farmacocinético apresentou um curto tempo de liberação e alta quantidade de massa em meio sem citotoxicidade em PBMCs. O DOx não apresentou atividade bactericida no entanto, apresentou atividade fungicida em duas espécies de dermatófitos (*T. rubrum e T.* mentagrophytes) em concentrações de 16 µg/mL. Os ensaios de MTT em células tumorais demonstraram que os complexos de inclusão contendo DOx apresentaram diferenças na viabilidade celular com uma atividade

melhor para a linhagem MCF-7. Desta forma foi possível demonstrar que o complexo de inclusão contribuiu para a melhoria da solubilidade e da atividade biológica deste novo derivado.

Palavras-chave: Oxazolidinas. Fungicida. Antitumoral. Ciclodextrinas. Complexo de inclusão.

ABSTRACT

Oxazolidinic derivatives (OxD) have been described as compounds with antimicrobial and antitumor activities. However, OxD have low solubility in water and consequently reduced bioavailability. Also, the use of host-guest inclusion complex of OxD in 2-hydroxy-beta-cyclodextrin (2-HPβCD) contributes to the improvement of the solubility and bioavailability. In this context, we initially carried out an in silico study to evaluate the interaction capability between OxD (LPSF/NB-14) and 2-HPβCD for the formation of an inclusion complex. Subsequently, we developed inclusion complexes based on co-evaporation technique. The analytical characterization was performed by scanning electron microscopy (SEM), Fourier transform infrared (FTIR), nuclear magnetic resonance (1H-NMR) spectroscopy, X-ray diffraction, and thermal analysis. The kinetic profile study of OxD release, cytotoxicity test using peripheral blood mononuclear cells (PBMCs), and antimicrobial activities were evaluated. The *in silico* studies showed the molecule orientations with values ranging from -5.9 to -5.6 kcal/mol, demonstrating the viability of the inclusion complex. The maximum solubility was obtained at 70 mM OxD using 400 mM 2-HPβCD, resulting in a twenty-fold increase in water solubility. SEM analysis revealed a significant change in the morphology of the molecules after the inclusion process. FTIR spectra indicated the formation of the inclusion complexes, considering the decrease in the intensity of the absorption bands of the OxD functional groups. ^{1}H-NMR showed chemical changes indicating 1:1 stoichiometry of OxD:2-HPβCD. The inclusion complex also indicated different thermal behaviors compared to pure OxD. The OxD release profile demonstrated a greater release of the compound relative to its physical mixing in an aqueous medium. The compound did not exhibit any significant cytotoxicity either in its pure form or after 2-HPβCD association. In conclusion, in silico studies provided an important insight into the interactions between OxD and 2-HPβCD. The pharmacokinetic profile showed a short release time and high amount of mass without cytotoxicity in PBMCs. The OxD did not present bactericidal activity. However, OxD (16 μg/mL) is effective against two species of dermatophytes (*T. rubrum* and *T. mentagrophytes*). MTT assays in tumor cells demonstrated differences in cell viability with improved activity for MCF-7 lineage. In this way, it was possible to demonstrate that the inclusion complex contributed to the improvement of the solubility and the biological activity of this new derivative.

Keywords: Oxazolidines. Fungicidal. Antitumor. Cyclodextrin. Inclusion complex.

LISTA DE FIGURAS

LISTA DE TABELAS

LISTA DE ABREVIATURAS E SIGLAS

AIDS	Síndrome da imunodeficiência adquirida. Do inglês, *Acquired Immune Deficiency Syndrome*
ATCC	Coleção de tipos de cultura americana. Do inglês, *American Type Culture Collection*
CD	Ciclodextrina
CE	Coeficiente de Encapsulamento
CIM	Concentração Inibitória Mínima
CNPq	Conselho Nacional de Desenvolvimento Científico e Tecnológico
DE	Alemanha. Do alemão, Deutsch
DMSO	Dimetilsulfóxido
DNA	Ácido Desoxirribonucléico, Do inglês, deoxyribonucleic acid.
DO	Densidade Ótica
DOX	Derivado Oxazolidínico
DRX	Difração de Raio X
DSC	Calorimetria diferencial de varredura. Do inglês, *differential scanning calorimetry*
EIV	Espectroscopia de Infravermelho
ELISA	Ensaio de imunoabsorção enzimática. Do inglês *Enzyme-Linked Immunosorbent Assay)*
et al.	e outro
HIV	Vírus da Imunodeficiência adquirida. Do inglês, *Human Immunodeficiency Virus*
HP-β-CD	Hidroxipropil-beta-ciclodextrina

INCA	Instituto do Câncer
IV	Infravermelho
K	Constante
LPSF	Laboratório de Planejamento e Síntese de Fármacos
LZ	Linezolida
MALDI-TOF	ionização por dessorção a laser assistida por matriz – tempo de vôo, Do inglês, *Matrix Associated Laser Desorption-Ionization - Time of Flight*
MH	Miller-Hinton
MIC	Concentração Mínima Inibitória. Do inglês, *Minimal Concentration Inhibitory*
MRSA	*Staphylococcus aureus* resistente à meticilina. Do inglês, *Methicillin-resistant Staphylococcus aureus*.
MTT	ácido 3,4,5-trimetoxi-cinâmico
NIAID	Instituto Nacional de Alergia e Doenças Infeciosas. Do inglês, *National Institute of Allergy and Infectious Diseases*
PAM	Peptídeo Antimicrobiano
PBMC	Células mononucleares de sangue periférico, Do inglês *Peripheral Blood Mononuclear Cells*
PBS	Tampão Fosfato. Do inglês, *Phosphate Buffered Saline*
PPAR	receptores ativados por proliferador de peroxissoma. Do inglês, *Peroxisome proliferator-activated receptor*
PPGIT	Programa de Pós-Graduação em Inovação Terapêutica
PVDF	Fluoreto de polividileno
RF	Radiofrequência
RMN	Ressonância Magnética Nuclear
RNAt	Ácido ribonucleico transportador

SDA	Ágar Sabouraud Dextrose. Do inglês, *Sabouraud Dextrose Ágar*
TG	Termogravimetria
TR	Termo de Referência
UK	Reino Unido. Do inglês, *United Kingdom*
UV	Ultravioleta

LISTA DE SÍMBOLOS

α	Alfa
β	Beta
γ	Gama
θ	Teta
λ	Lambda
μ	Micro
^{o}C	Grau Celsius

SUMÁRIO

1 INTRODUÇÃO

As doenças bacterianas ou fúngicas ainda representam um fator de ameaça à saúde pública devido a fatores de virulência e linhagens resistentes a antibióticos convencionais (PENCHOVSKY e TRAYKOVSKA, 2015). Por outro lado, as complicações associadas ao desenvolvimento do câncer também exercem um fator impactante nas sociedades modernas com uma maior incidência anualmente (PENCHOVSKY e TRAYKOVSKA, 2015). No entanto, para ambos os casos, há uma constante busca por novos medicamentos contribuam para um melhor efeito terapêutico e, ao mesmo tempo, apresentem mínimos efeitos adversos.

Diante desta problemática, novas pesquisas vêm obtendo novos compostos, como os derivados da oxazolidina (DOx) que apresentam atividade comprovada contra determinados tipos de bactérias e fungos e, numa proporção menor, atividade antitumoral (SORABJEE e GARJE, 2004). Contudo, estes compostos apresentam pouca solubilidade em água, o que dificulta sua administração. Para enfrentar esta barreira, estratégias para o incremento da solubilidade pode ser aplicado através da substituição grupos funcionais à oxazolidina ou a incorporação destas drogas em complexos de inclusão, sendo a ciclodextrina (CD) mais comumente utilizada. A versatilidade destas moléculas, permite que drogas pouco solúveis em água, possam garantir um aumento na biodisponibilidade e diminuição de potencial tóxico (ALVES, FERNANDES, DE SOUZA*, et al.*, 2014; CAMPOS, JÚLIA FURTADO *et al.*, 2017).

Sendo assim, o presente estudo objetivou desenvolver uma alternativa terapêutica, avaliando a atividade biológica de DOx em forma livre e presentes em complexos de inclusão baseado em ciclodextrina. Inicialmente este estudo visou avaliar a atividade biológica em bactérias, fungos e células tumorais e células do sangue periférico. Após esta etapa, o estudo focou nos testes de preparação e caracterização físico-química e morfológica dos complexos de inclusão. A etapa seguinte deste estudo procurou avaliar comparativamente a atividade biológica nos alvos biológicos entre os DOx em sua forma livre em relação aos complexos de inclusão. Adicionalmente, testes de citotoxicidade em células mononucleares de sangue periféricos de pacientes sadios foram utilizados para avaliar toxicidade. Por último, os complexos de inclusão foram testados nas mesmas condições em relação a droga livre para avaliarmos se a atividade antimicrobiana/antitumoral foi incrementada em função da melhoria na solubilidade dos DOx.

2 OBJETIVOS

2.1 OBJETIVO GERAL

Avaliar a atividade biológica do novo derivado oxazolidínico LPSF/NB-14 e desenvolver uma estratégia para o incremento de solubilidade deste composto.

2.2 OBJETIVOS ESPECÍFICOS

I. Avaliação da atividade antimicrobiana através de testes de susceptibilidade em bactérias e fungos
II. Desenvolvimento de um incremento de solubilidade para o derivado oxazolidínico LPSF/NB-14 baseado em ciclodextrina;
III. Caracterização analítica através de microscopia eletrônica de varredura (MEV), infravermelho transformado de Fourier (IVTF), espectroscopia de ressonância magnética nuclear (RMN-^{1}H), difração de raios X e análises térmicas dos complexos de inclusão baseado em ciclodextrina contendo o derivado oxazolidínico LPSF/NB-14;
IV. Avaliação comparativa da atividade biológica de LPSF/NB-14 e de seus complexos de inclusão em tumorais de câncer de mama (MCF-7 e T-47D) e em células mononucleares do sangue periférico.

3 REVISÃO DE LITERATURA

3.1 INFECÇÕES BACTERIANAS

As infecções bacterianas são doenças que ocorrem a partir da proliferação de bactérias que podem causar danos prejudiciais ao nosso organismo. Estas infecções são adquiridas por transmissão interpessoal (ex: tuberculose) (RITZ e CURTIS, 2014), contato sexual (ex: sífilis, gonorréia) (LEE e CLARKE, 2004), ingestão de alimentos (ex: salmonelose) (SADKOWSKA-TODYS e CZARKOWSKI, 2014) ou água contaminada (ex: cólera, febre tifoide) ou adquiridas em processos cirúrgicos (ex: infecções estafilocócicas) (ANDERSON e KAYE, 2009).

Em certos casos, essas bactérias podem envolver órgãos internos, como na pneumonia bacteriana ou na meningite bacteriana. As bactérias *Streptococcus pneumoniae*, sempre causam doenças dentro do corpo, sejam invasivas (pneumonia) ou não invasivas (sinusite, otite média aguda) (LESNAKOVA *et al.*, 2007).

Outras bactérias como a *Escherichia coli* geralmente estão presentes no organismo sem causar prejuízo, porém são classificadas como oportunistas. Isso resulta de uma proliferação descontrolada quando o sistema imune está deprimindo, fazendo com que a *E. coli*. produza danos. Estes tipos de infecções (oportunistas) se tornaram mais comuns decorrente da AIDS, aumento do número de transplante de órgãos, utilização de imunossupressores e uso indiscriminado de antibióticos principalmente em países emergentes (JAFARI *et al.*, 2013).

Estas doenças podem afetar diretamente os tecidos e consequentemente, prejudicar o funcionamento normal dos organismos. Outro fator é a presença das endotoxinas presentes em bactérias patogênicas que afetam as células do hospedeiro. Essas toxinas, em geral, são liberadas quando uma bactéria morre e pode ser responsável pela sepse ou choque séptico (RONCO, 2014). A depender da doença, o diagnóstico laboratorial pode ser realizado através de teste sanguíneo (ex: hemograma), escarro ou cultura microbiológica através de coleta *in situ*. Outros exames como radiografia de tórax ou análise de biópsias auxiliam no diagnóstico de doenças respiratórias causadas por bactérias. Nos casos de meningite, uma punção medular para análise de líquido cefalorraquidiano (LCR) pode evidenciar o diagnóstico de meningite (WASHINGTON, 1996). Estima-se que em 2010, 16 milhões de pessoas morreram por causas infeciosas.

Contudo, este número pode reduzir para 13 milhões devido aos avanços de novos antibióticos para espécies mais comuns e algumas resistentes (DYE, 2014).

A enterobactérias fazem parte de uma família (Enterobacteriaceae) que possui mais de 25 gêneros diferentes, centenas de espécies e subespécies e milhares de sorotipos. Em geral, esta família é diferenciada por propriedades bioquímicas, estruturas antigênicas e hibridização e sequenciamento de ácidos nucléicos. Os gêneros dessa família podem ser classificados como patógenos primários (sempre causam doença) como Shigella e Salmonella e patógenos oportunistas (dependem da condição do hospedeiro). As do gênero Shigella e Salmonella (gram-negativos) atuam no trato gastrointestinal enquanto a Enterobacter (gram-positivas) podem se disseminar pela através da corrente sanguínea e afetar vários órgãos (GROSE e CASJENS, 2014) .

As que pertencem ao gênero Salmonella podem provocar gastroenterite aguda ou intoxicação alimentar onde podem ser infectantes em algumas fontes: animais de estimação, ovos e carne de frango mal cozidos, utensílios de cozinha contaminados porém requer uma elevada carga microbiana para a infecção. Em alguns casos ela pode ser autolimitada em indivíduos saudáveis (antibióticos e agentes antidiarreicos podem prolongar os sintomas). Outra espécie, a Salmonella Typhi é responsável pela febre tifoide e outras febres entéricas com envolvimento particularmente do fígado, baço, intestino, mesentério e capacidade de disseminação para outros órgãos (ENG *et al.*, 2015).

As bactérias do gênero *Shigella* podem causar disenteria pois em humanos, o intestino grosso é o principal reservatório onde são transmitidos por via fecal-oral. No entanto outras espécies podem desenvolver sintomas diferentes: *S. dysenteriae* (toxina Shiga e pode causar síndrome hemolítico urêmica) , *S. flexneri* (doença periodontal), *S. boydii, S. sonnei* (mais comum). Além disso, menos de 200 bacilos são necessários para a infecção em indivíduos saudáveis (elevada virulência) (SCHROEDER e HILBI, 2008).

Enterococcus faecalis é uma bactéria Gram-positiva comensal (flora normal) do sistema digestivo humano e de outros mamíferos. Amplamente encontrada no ambiente, pode causar infecção urinária, meningite e bacteremia, especialmente em ambientes hospitalares. *E. faecalis* constituem 85 a 90% das espécies de *Enterococcus* identificados nos humanos, sendo essa espécie a menos propensa ao desenvolvimento de resistência a antibióticos (BEGANOVIC *et al.*, 2018).

O tratamento para a maioria das infecções bacterianas é realizado através da administração de antibióticos de amplo espectro que além de debelar, impedem a reprodução de mais de uma espécie bacteriana. A penicilina, o primeiro antibiótico descoberto, ainda é utilizado para algumas infecções. No entanto, outros antibióticos de amplo espectro são amplamente utilizados: a amoxicilina, bacitractina, eritromicina, cefalosporina, fluroquinilonas e tetraciclina. Algumas antitoxinas são também administradas para combater os efeitos de toxinas bacterianas, como nos casos de tétano ou botulismo (MCGUIRE *et al.*, 2015).

3.1.1 RESISTÊNCIA BACTERIANA

Os antibióticos, também denominados de agentes antimicrobianos têm sido utilizados nos últimos 70 anos para tratar pessoas com doenças infecciosas. Desde de 1940, essas drogas auxiliaram no tratamento e cura das infecções e consequentemente, reduziram o número de óbitos causados por microrganismos. No entanto, devido a uma a falta de controle na venda destes medicamentos e/ou ampla utilização de forma indiscriminada, alguns microrganismos adaptaram-se a essas drogas, tornando-as menos efetivas (PENCHOVSKY e TRAYKOVSKA, 2015).

As bactérias resistentes têm sido motivo de preocupação no controle as doenças infecciosas. Isso é decorrente do fato que o desenvolvimento de novos antibióticos não tem acompanhado a evolução destas bactérias. Em países desenvolvidos como os EUA e a países da Europa têm tratado essa problemática, buscando mapear novos casos que envolvam estes tipos de bactérias através de estudos realizados por centros de prevenção e controle de doenças (HAWKEY e JONES, 2009; DE KRAKER *et al.*, 2013).

O mecanismo de resistência resulta de mutações genéticas que reduzir ou neutralizar o efeito dos antibióticos. Uma destas mutações pode tornar uma determinada bactéria menos vulnerável a droga. Uma vez que as bactérias resistentes sobrevivem a determinadas doses em relação àquelas mais vulneráveis, elas se replicam e podem ser transmitidas para outras linhagens, resultando em cepas mais evoluídas. Na maioria dos casos, a resistência bacteriana é induzida através da automedicação ou administração inadequada de antibióticos por tempo incorreto (GOULD, 2008). A cada ano nos EUA, pelo menos 2 milhões de pessoas são infectadas com bactérias que são resistentes a antibióticos e aproximadamente 23.000 pessoas morrem ao ano por essas infecções. Desde 2012, novos casos de resistência bacteriana ao tratamento de drogas foram

relatados, o que demanda o uso de medicamentos mais caros e desenvolvimento de novos fármacos (GOULD, 2008).

Em 2013, havia cerca de 480.000 novos casos de tuberculose multirresistente (TB-MR) enquanto que a extensivamente resistente tuberculose (TB-ER) foi encontrada em 100 países. A TB-MR requer medidas de tratamento que duram mais tempo e são menos eficazes se comparada aos casos de tuberculose não-resistente (WHO, 2015).

Existem proporções elevadas de resistência aos antibióticos em bactérias que causam infecções comuns como infecções do trato urinário, pneumonia, infecções da corrente sanguínea que estão presentes em todas as regiões do mundo. Um percentual elevado de infecções hospitalares tem sido causado por bactérias altamente resistentes, como a *Staphylococcus aureus* resistente à meticilina (MRSA) e bactérias gram-negativas multirresistentes (enterococos vancomicina-resistentes) (WHO, 2015).

A resistência bacteriana é um problema complexo e multifatorial. Como tal, as intervenções individuais, isoladas têm pouco impacto. A necessidade de combater este problema exige uma ação coordenada entre a população, políticos e profissionais de saúde para minimizar o surgimento e propagação da resistência antimicrobiana.

3.2 INFECÇÕES FÚNGICAS

Em geral, se o sistema imune da pessoa infectada for competente, estes tipos de infecções não se espalham por órgãos do corpo. Por outro lado, há situações em que a queda nas defesas do organismo favorecem estas infecções. Adicionalmente, o uso prolongado de antibióticos pode interferir no balanço normal entre bactérias e fungos presentes num mesmo microambiente (ex: trato digestivo, vagina) humano. Desta forma, com a diminuição do número normal de bactérias nessas regiões, os fungos crescem de forma excessiva. Nestas situações, a restauração da microbiota, em geral, soluciona o problema. No entanto, algumas podem ser prejudiciais à saúde. Esses acometimentos envolvem, por exemplo, infecções na corrente sanguínea e meningite por fungos. Embora estas sejam menos frequentes que as infecções de pele e pulmonares, podem ser mortais se não tratadas a tempo (MAERTENS *et al.*, 2001; MUSKETT *et al.*, 2011; LANTERNIER *et al.*, 2013) .

A maioria das infecções fúngicas se desenvolve lentamente (meses ou anos) e podem passar despercebido da atenção médica. No entanto, pessoas com acometimento

imune, estas manifestações clínicas podem ser agressivas. Além da rápida propagação, geralmente acarretam óbito. O sistema imune pode ser enfraquecido por drogas imunossupressoras destinados para evitar rejeição em transplante de órgão ou como quimioterápicos para tratamento doenças como a AIDS e neoplasias (ARMSTRONG-JAMES *et al.*, 2014; GAVALDA *et al.*, 2014). Os fatores de risco e outros acometimentos estão presentes na Tabela 1.

Tabela 1 - Drogas imunossupressoras e doenças que favorecem o desenvolvimento de infecções fúngicas.

Drogas Imunossupressoras	Doenças
Quimioterápicos	AIDS, queimaduras graves
Corticosteroides	Diabetes, linfomas (Hodgkin e não Hodgkin)
Drogas imunossupressoras para pós-transplante (ex: azatioprina, metotrexato, ciclosporina)	Leucemia, distúrbios pulmonares (ex: enfisema)

Os agentes etiológicos responsáveis pelas infecções fúngicas variam em características, formas e locais de acometimento. Pode-se destacar algumas das mais comuns: a candidíase, a criptococose e as dermatofitoses (CARILLO-MUNOZ e TUR-TUR, 1997; LANTERNIER *et al.*, 2013)

3.2.1 Candidíase

A *Candida* é normalmente encontrada na pele, no trato gastrointestinal, e em mulheres, na região genital. Em geral, a *Candida* não ocasiona problemas no entanto, indivíduos com imunidade deficiente podem ser afetados (ex: diabetes, câncer, gestantes). A candidíase também ocorre comumente em pessoas que estão sob uso de antibióticos (CHOI *et al.*, 2013; YAPAR, 2014).

A candidíase é uma infecção causada por várias espécies de *Candida,* especialmente pela *Candida albicans*. Os tipos mais comuns de candidíase são infecções superficiais que acometem a boca, vagina ou pele e causam manchas vermelhas, prurido, irritação ou ambos (RIBEIRO *et al.*, 2004). O agravamento maior pode ocorrer pela entrada do fungo na corrente sanguínea (chamada candidemia). Nestes casos os fungos podem proliferar-se em outras partes do corpo, como válvulas cardíacas, esôfago, fígado,

rins, olhos e até causar óbitos (DARWAZAH *et al.*, 1999; SHI *et al.*, 2008; PAPPAS *et al.*, 2016) **(Fig.1)**.

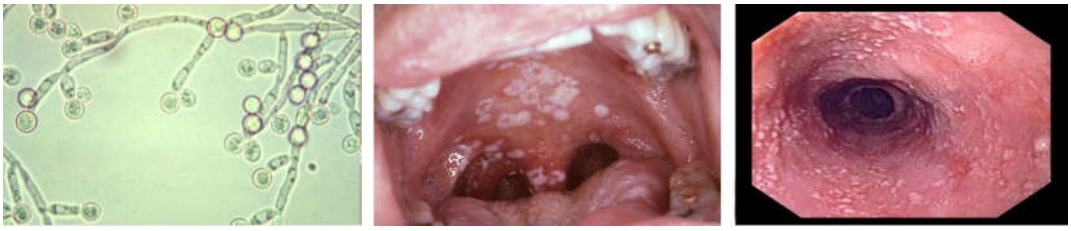

Figura 1 - Fungos do gênero *Candida sp.* e manifestações clínicas da candidemia na mucosa bucal e invasiva no esôfago (esquerda para direita).

A maioria das infecções por *Candida* são aparentes. A forma de detecção é examinada por microscopia e enviada para cultura microbiológica que posteriormente pode ser diferenciada meios de cultura especiais (ex: CHROMAgar) (SIVAKUMAR *et al.*, 2009). Adicionalmente, existem outras metodologias como a utilização de métodos imunológicos (ex: ELISA) ou através de biologia molecular (ex: SDS Page) (RODRIGUES *et al.*, 2004; AVNI *et al.*, 2011).

O tratamento é tópico com antifúngicos clotrimazol e nistatina. Em outras situações, de uso oral, pode-se administrado fluconazol. Porém nos casos de candidemia, utiliza-se a anfotericina B intravenosa e outras alternativas terapêuticas como o uso de posaconazol, voriconazol, casporfungina, micafungica e anidulafungina (GARCIA-CUESTA *et al.*, 2014; DOVNIK *et al.*, 2015).

3.2.2 Criptococose

A criptococose é uma doença causada por fungos do gênero Criptococcus. O *Criptococcus* é encontrado principalmente no solo contaminado com fezes de aves (ex: pombo). Apesar de haver aproximadamente 100 espécies diferentes, apenas duas espécies mais comumente causam doenças: *C. neoformans* e *C. gatti* (BOVERS *et al.*, 2008). Estas duas espécies representam cerca de 80% das infecções associadas a este gênero. Algumas manifestações clínicas podem ser assintomáticas ou apresentar dores de cabeça e confusão, tosse, peito dolorido ou erupção cutânea dependente do local acometido (ESPINEL-INGROFF E KIDD, 2015).

A infecções causadas por este tipo de fungo atuam sobre pacientes imunodeficientes e são mais prevalentes em países subdesenvolvidos (ILLNAIT-ZARAGOZI *ET AL.*, 2014). Este tipo de infecção recebeu destaque devido a epidemia causada pelo HIV e que ainda está presente no mundo todo. Mesmo pessoas HIV negativas possuem um risco de 6% de desenvolver sintomas clínicos associados ao *Criptococcus* (LA HOZ E PAPPAS, 2013). Há casos de infecções de pessoas com linfoma de Hodgkin e em pessoas com uso prolongado de corticosteroides. Entretanto, a criptococose também pode se desenvolver em pessoas com um sistema imune normal (ROMANO *ET AL.*, 2001; GONG *ET AL.*, 2013).

Os locais mais acometidos ocorrem nos tecidos que cobrem o cérebro e as meninges, pulmão ou pele. Sem um tratamento adequado outros órgãos podem ser afetados. Os sintomas da meningite criptocócica envolvem dor de cabeça e confusão. Nos pulmões pode ser assintomático ou marcado por tosse, dor no peito e em casos graves, dificuldade de respirar. Na pele há a presença de erupções cutâneas com a presença de exsudato inflamatório (GONG *et al*., 2013) **(Fig.2)**.

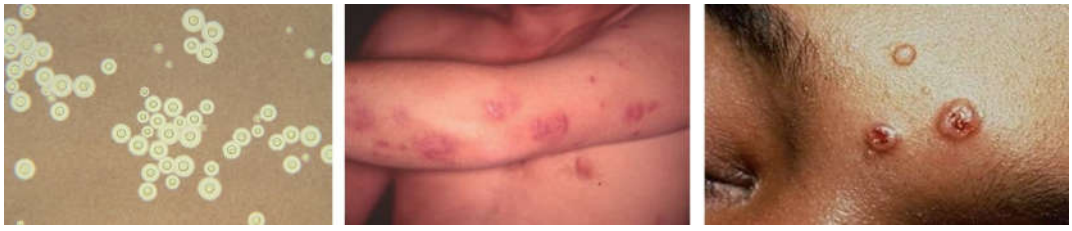

Figura 2 - Fungos do gênero *Cryptococcus sp.* e manifestações clínicas da criptococose cutânea (esquerda para direita).

O diagnóstico baseia-se em exame direto por microscopia e a cultura isolada da levedura. No entanto, estes métodos apresentam desvantagens quanto ao tempo de identificação genotípica. A automação diminui o tempo de análise, demonstrando resultados em até 72 horas (API 20C AUX e Vitek) (MAHABEER *ET AL.*, 2014). A identificação final depende de testes complementares e análise clínica. Outras metodologias têm sido implementadas e apresentaram bons resultados como MALDI-TOF-MS (FIRACATIVE *et al*., 2012).

Os antifúngicos são administrados oralmente em acometimentos de pele e respiratórios (fluconazol) e em casos mais graves (meningite), intravenosamente (ex: anfotericina B e flucitosina). Em pacientes com HIV o tratamento é permanente, porém

pode ser interrompido a depender da normalidade dos níveis linfocitários por pelo menos 6 meses (TORRES-RODRIGUEZ *et al.*, 2008; MAZU *et al.*, 2016).

3.2.3 Dermatofitoses

São doenças que acometem humanos e animais no mundo por fungos denominados, dermatófitos. Algumas dessas espécies representadas pelo *Microsporum gypseum, Trichopyton rubrum e Trichopyton mentagrophytes*. Estes fungos invadem tecido queratinizados como cabelos, pele e unha para produzir uma manifestação clínica conhecida como tínea. A tínea é classificada de acordo com o local acometido: corporis (corpo), pedis (pé), capitis (capilar), barbar (barba), manum (mão) e onicomicoses (unha) **(fig. 3)**.

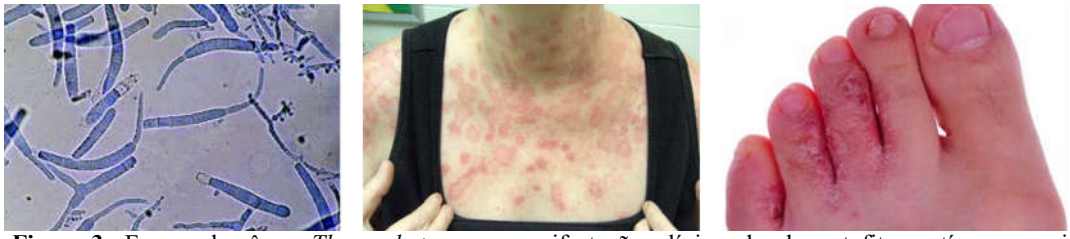

Figura 3 - Fungos do gênero *Thrycophyton sp.* e manifestações clínicas das dermatofitoses: tínea corporis e tínea pedis (esquerda para direita).

É importante ressaltar que estes restringem-se apenas as camadas mais externas e dificilmente penetração em tecidos mais profundos da pele. No entanto, pacientes com neoplasias, geralmente imunocomprometidos, são mais favoráveis a estes tipos de infecção e ao desenvolvimento de complicações (IRIMIE *et al.*, 2015).

Os tratamentos atuais limitam-se ao uso tópico e que também podem apresentar limitações quanto a toxicidade, indução de resistência e tempo de tratamento (WEITZMAN e SUMMERBELL, 1995). Estes fatores influenciam na continua necessidade de desenvolver novas alternativas terapêuticas. Há pesquisas atuais objetivando a utilização de plantas medicinais e de novas formas farmacêuticas sintéticas (AYATOLLAHI e KAZEMI, 2015).

3.3 O CÂNCER

O câncer representa um conjunto de mais de 100 doenças que apresentam um característica em comum: o crescimento desordenado (origem maligna) de células que

invadem tecidos e órgãos e apresentam risco de se espalhar (metástase) para outras regiões do corpo (DUNN e KRAMER, 2016).

As células envolvidas nesta doença podem apresentar agressividade e crescimento incontrolável, levando a formação de tumores (acúmulo de células do câncer) ou neoplasias malignas. No entanto, algumas células podem apresentar crescimento vagaroso, localizado, bem definido e semelhante ao tecido local, característica de tumores benignos. Este tipo apresenta baixo risco de vida (MALEY *et al.*, 2017).

.Os tipos de câncer variam de acordo com a célula afetada. A depender do tipo de célula, pode haver diferentes tipos de câncer como por exemplo, na pele. Os cânceres de origem epitelial é denominado de carcinoma. Se este for iniciado em tecidos conjuntivos (ex: cartilagem, músculos ou ossos) é denominado de sarcoma. Outro aspecto do câncer que diferenciam os tipos entre si estão associados a velocidade de multiplicação, capacidade de invasão em tecidos e órgãos próximos ou distantes (metástases) (MALEY *et al.*, 2017).

3.3.1 As causas do câncer

As causas do câncer são variáveis, podendo ser influenciadas por fatores externos (ambientais) ou internos. Os fatores externos estão associados ou meio ambiente e aos hábitos ou costumes de um indivíduo dentro de um ambiente sociocultural. Os fatores internos são associados a genética e a imunidade a agressões externas. Estes fatores apresentam um potencial de interagir de diferentes formas, o que resulta no aumento da probabilidade de transformações malignas em células normais (WHO, 2015).

O percentual de cânceres associados aos fatores externos varia de 80 a 90% devido ao uso de cigarro (câncer de pulmão), exposição solar excessiva (câncer de pele) e alguns vírus associados a casos de leucemia além de componentes alimentares em produtos industrializados, embora, o tema ainda é seja amplamente discutido. A manifestação do câncer também é maior em idosos, devido a exposição prolongada a diferentes fatores de risco durante a vida podendo ser cancerígenos e alterando o DNA destas células (MALEY *et al.*, 2017).

Os fatores internos associados a hereditariedade são mais raros, no entanto, o fator genético apresente um papel na oncogênese. Alguns tipos de câncer podem ter uma forte relação familiar ou exposição a uma causa comum. Grupos étnicos também podem

apresentar predominantemente um tipo de câncer do que em outros grupos (ex: leucemia linfocítica rara em orientais) (MALEY *et al.*, 2017)..

Dados do Instituto Nacional de Câncer (INCA), o câncer de pele, próstata e mama foram os mais incidentes. De acordo com a estimativa do INCA em 2016, o câncer mais incidente em homens foi o de próstata com 61.200 novos casos, enquanto o câncer de mama com 57.960 novos casos foi mais incidente em mulheres (Fig. 4).

Localização primária	casos novos	%			Localização primária	casos novos	%
Próstata	61.200	28,6%	Homens	Mulheres	Mama Feminina	57.960	28,1%
Traqueia, Brônquio e Pulmão	17.330	8,1%			Cólon e Reto	17.620	8,6%
Cólon e Reto	16.660	7,8%			Colo do Útero	16.340	7,9%
Estômago	12.920	6,0%			Traqueia, Brônquio e Pulmão	10.890	5,3%
Cavidade Oral	11.140	5,2%			Estômago	7.600	3,7%
Esôfago	7.950	3,7%			Corpo do Útero	6.950	3,4%
Bexiga	7.200	3,4%			Ovário	6.150	3,0%
Laringe	6.360	3,0%			Glândula Tireoide	5.870	2,9%
Leucemias	5.540	2,6%			Linfoma não Hodgkin	5.030	2,4%
Sistema Nervoso Central	5.440	2,5%			Sistema Nervoso Central	4.830	2,3%

Figura 4 - Distribuição proporcional dos dez tipos de câncer mais incidentes estimados para 2016 por sexo, exceto pele não melanoma (número de casos a cada 100 mil habitantes).

O câncer de mama ainda é o mais comum entra as mulheres no Brasil e no mundo, depois do de pele não melanoma. Ele representa cerca de 28,1% de novos casos ao ano, segundo estimativa de 2016. Embora, esta doença acometa homens, sua incidência é de apenas 1% do total de casos (INCA, 2016).

O surgimento destes doenças está associada aos fatores de risco, qualidade assistência prestada, na qualidade da informação e no envelhecimento da população. Em geral, como acontece nos países da Europa, Estados Unidos e Canadá, quanto maior a proporção de pessoas idosas, maior as taxas de incidência, principalmente ao envelhecimento relacionado ao de mama e próstata. É importante ressaltar o desafio de campanhas de prevenção e acompanhamento em indivíduos que se enquadrem nos grupos de risco, seja pela idade ou por fatores hereditários (INCA, 2016).

A idade de risco surge após os 35 anos e cresce progressivamente após os 50 anos. Este dado é apresentado tanto em países em desenvolvimento quanto desenvolvidos. Dentre os tipos de câncer de mama, podem variar conforme evolução (rápida ou lenta). No entanto, a detecção precoce favorece um bom prognóstico e boa resposta aos tratamentos (INCA, 2016).

3.3.2 Tratamentos para o Câncer

Existem muitos tipos de tratamento contra o câncer, os quais dependem do tipo de câncer e do seu avanço. O número de tratamentos é variável entre pessoas. Algumas podem depender de apenas um tratamento enquanto outras poderão ter uma combinação de tratamentos, como cirurgia com quimioterapia e /ou radioterapia (NIH, 2018).

A cirurgia é um procedimento invasivo em que um cirurgião remove o câncer sólida de alguma parte acessível do corpo. Quando este procedimento não é possível de realizar, outra opção mais próxima é a radioterapia. A radioterapia é um tipo de tratamento para o câncer que usa altas doses de radiação para matar células cancerosas e reduzir tumores de forma controlada e localizada. Por outro lado, a quimioterapia é um tipo de tratamento do câncer que usa drogas para matar as células cancerígenas de forma sistêmica que pode resultar em efeitos colaterais. Em alguns casos utiliza-se a imunoterapia como tratamento auxiliando o sistema imunológico a combater o câncer. Em outros casos, a terapia hormonal pode ser usada como tratamento que age retardando ou impedindo o crescimento de cânceres (por exemplo, câncer de mama e próstata) (WHO, 2015).

Outra alternativa está nos transplantes de células-tronco em casos de neoplasias na medula óssea e/ou que ajudam na restauração das células-tronco formadoras de sangue em pacientes com câncer que tiveram suas células destruídas por doses muito altas de quimioterapia ou radioterapia. A última alternativa para o tratamento do câncer é a chamada medicina de precisão. Nesta modalidade os médicos selecionam os tratamentos com maior probabilidade de ajudar os pacientes com base na compreensão genética de sua doença.

3.4 DERIVADOS DE OXAZOLIDINAS (DOX) E SUAS APLICAÇÕES

As oxazolinas são compostos heterocíclicos que consistem em um anel heterocíclico formado por de cinco membros contendo, no mínimo, um átomo de oxigênio e um de nitrogênio (**Fig. 5a**). Além delas possuir estrutura única e diversas aplicações, também serve como elemento estrutural para produtos naturais e farmacêuticos (SHAGHAFI *et al.*, 2011).

As aplicações terapêuticas destes compostos têm sido utilizadas como anticonvulsivantes, inibidor de polimerização de tubulina, agente anticâncer que compreende elementos oxazolidínicos 3,5-disubstituídos e até atividade antimicrobiana de alcaloide contendo oxazol. As oxazolidinas, também chamadas de 1,3-oxazolidinas, são a forma reduzida das oxazolinas **(Fig. 5b)**. As isoxazolidinas são os isômeros da oxazolidinas onde o nitrogênio e o oxigênio são átomos adjacentes **(Fig. 5c)**.

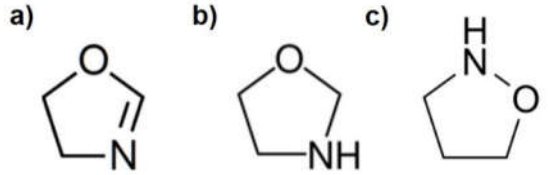

Figura 5 – A oxazolina (a) e seus derivados: oxazolidinas (b) e isoxazolidinas (c).

As oxazolidinonas são uma classe de compostos que contém 2-oxazolidona em sua estrutura e são utilizados como antimicrobianos. O efeito antibacteriano das oxazolidinonas ocorre através da inibição da síntese proteica, atingindo uma etapa inicial que envolve a ligação da N-formilmetionil-RNAt para o ribossomo (SHINABARGER, 1999). Algumas das mais importantes oxazolidinonas (ex: linezolida, posizolida, cicloserina) são a última geração de antibióticos utilizados contra bactérias gram-positivas, incluindo o *Staphylococcus aureus* resistentes à meticilina (MRSA). Estes antibióticos são considerados como último recurso quando outras terapias antibióticas falham.

A linezolida (LZ), também conhecida como Zyvox (Pfizer, USA), é um agente antibacteriano sintético com atividade *in vitro* comprovada contra bactérias gram-positivas, gram-negativas e algumas espécies anaeróbicas. A LZ atua ligando aos sítios no ribossomo bacteriano que impede a formação de um complexo de 70S ribossomal. Este componente é essencial para o processo de transdução e síntese proteica. A LZ está disponível através de administração intravenosa e também apresenta vantagens quanto a sua biodisponibilidade oral (SORABJEE e GARJE, 2004).

A posizolida, (AZD5847), uma nova oxazolidinona desenvolvida pela Astrazeneca (Londres, UK) foi comparada a LZ. Este novo composto obteve atividade comprovada contra bactérias gram-positivas, gram-negativas e algumas espécies anaeróbicas em 98% das linhagens testadas. No entanto, a atividade em bactérias do gênero *Staphylococci* e *Enterococci* foi bacteriostática (VILLEMAGNE *et al.*, 2012). Em

contrapartida, a posizolida apresentou uma concentração mínima inibitória (CMI) satisfatória (≤ 2 μg/mL) para *Mycobacterium tuberculosis*, no qual direcionou a sua utilização para o combate à tuberculose devido a resultados do estudo de fase clínica 2 realizado em 2013 na África do Sul (NIAID, 2013).

A cicloserina também conhecida como seromicina é um composto isaxolidínico também indicado para o tratamento da tuberculose sendo classificado como droga de segunda linha. A utilização deste medicamento é restrita apenas para linhagens de *M. tuberculosis* resistente a múltiplas drogas em 64 μg/mL. Adicionalmente, esta droga pode causar efeitos neurológicos adversos devido a sua capacidade de penetrar no sistema nervoso central (PROSSER e DE CARVALHO, 2013).

Ainda há outras drogas comerciais que ainda estão em estudos de fases clínica como a Tedizolida (Sivextro), o qual foi aprovada para infecções de pele. Há também a Radezolida (RX-1741) que ainda está em estudos de fase clínica 2 (LEMAIRE *et al.*, 2010). A necessidade de avaliar o potencial antifúngico está na limitação de agentes antifúngicos convencionais que estão sendo administrados para o combate destas doenças. Existem relatos sobre testes antifúngicos de DOx em fungos que ainda são inconclusivos (DEVI *et al.*, 2013).

Outra atividade apresentada por estes derivados foi a utilização de uma oxazolidinona (guanidínio-4-oxazolidinona dibrominada), denominada de Synozolidinona C. Este composto apresentou atividade antitumorais em linhagens celulares de melanoma, carcinoma de mama e cólon entre outras (TADESSE *et al.*, 2011). Outro estudo utilizando derivados da linezolida sugeriu que os compostos com substituintes etil e acril apresentaram uma atividade mais promissora e induzindo a apoptose de células tumorais de adenocarcinoma de próstata através da caspase-3 e caspase-9 (NARESH *et al.*, 2014).

Adicionalmente, Agrawal *et al.*, sugeriu que a ação de alguns derivados também atue sobre os receptores gama ativados por proliferador de peroxissoma (do inglês, pero*xisome proliferator-activated receptor gamma*). O presente composto utilizado no experimento (5-{4-[3-(4-ciclohexil-2-propilfenoxi)propoxi]fenil}-1,3-oxazolidina-2,4-diona demonstrou em ensaios metabólicos que o derivado atuou como enzima do citocromo P450 (AGRAWAL *et al.*, 2005). Outros experimentos demonstraram a atuação dos derivados (oxazol-5-onas) como agonistas parciais do *PPAR gamma*, onde

apresentaram citotoxicidade contra células de câncer de mama (PAL *et al.*, 2014). Este receptor apresenta suma importância, pois ligantes podem acarretar tanto a inibição da proliferação ou a indução de apoptose (GROMMES *et al.*, 2004; THEOCHARIS *et al.*, 2004). Além disso, alguns estudos têm apresentado que ligantes do *PPAR gamm*a parecem exercer propriedade antitumorais *in vitro* e induzir a parada ou encolhimento celular em murinos (ELSTNER *et al.*, 1998; MUELLER *et al.*, 1998; SUH *et al.*, 1999; PIGHETTI *et al.*, 2001).

3.5 O DERIVADO OXAZOLIDÍNICO (DOX) LPSF/NB-14

O DOx LPSF/NB-14 é um composto é formado por um anel de oxazolidina e um grupo tiol (-SH) na posição do carbono 2. Sabe-se que a presença do enxofre na estrutura química de compostos químicos confere um potencial antimicrobiano (BARTHOLOMEW *ET AL.*, 1954) além de possuir um grupo etil (CH_2-CH_3) ligados ao nitrogênio na posição 3. Este composto LPSF/NB-14 **(Fig. 6)** também apresenta um grupamento benzilideno ligado ao carbono 5 de sua estrutura.

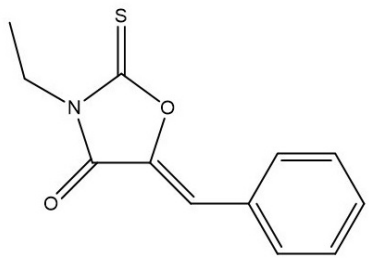

Figura 6 - Estrutura química do LPSF/NB-14 (PM: 222.20 mol/g).

Com relação a atividade biológica, algumas oxazolidinadionas 3,4-dissubistituídas semelhantes apresentaram atividade citotóxica em linhagem leucêmicas. Estudos prévios sugerem um mecanismo de ação através da indução por apoptose (ALVES, FERNANDES, DE SOUZA*, et al.*, 2014; CAMPOS, JÚLIA FURTADO *et al.*, 2017). No entanto, alguns destes compostos ainda não possuem atividade biológica comprovada como o LPSF/NB-14 (Patente BR1020150160607).

3.6 AS CICLODEXTRINAS

As ciclodextrinas são oligossacarídeos cíclicos que são formados por diferentes quantidades de glicopiranose unidas por ligações glicosídicas α-(1,4) **(Fig. 7)**. A descoberta destas moléculas surgiu em 1891 por Villiers que obteve uma pequena quantidade de dextrinas a partir da digestão do amido por ação de um microrganismo (*Bacillus amylobacter*). O achado foi descrito como cristais radiais obtidos por armazenamento em álcool com a composição de múltipla da fórmula ($C_6H_{10}O_3$). $3H_2O$ (DEL VALLE, 2004).

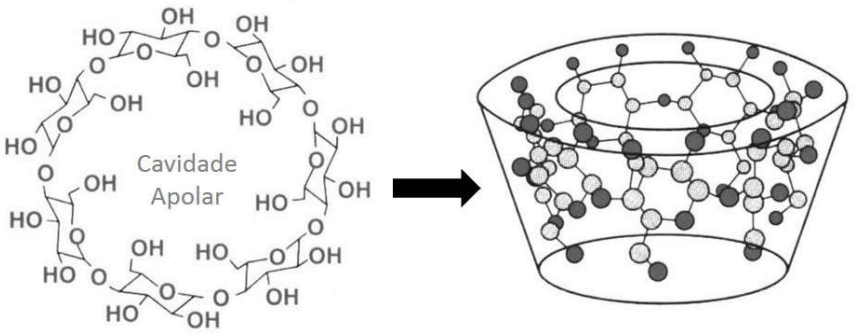

Figura 7 – Estrutura molecular e visão tridimensional da β-ciclodextrina. (Adaptado de www.u.arizona.edu).

Em 1911, Schardinger aprimorou a técnica de Villiers com outro microrganismo (*Bacillus macerans*), onde obteve maior rendimento na obtenção destas dextrinas cristalinas onde as denominou como α e β. Em 1942, as estruturas das dextrinas α e β foram determinadas através da cristalografia de raios-X e posteriormente descobriu-se a dextrina do tipo γ (1948) e outra com maiores resíduos: δ, ξ, ζ, ν, com 9 a 12 unidades (EASTBURN E TAO, 1994).

O interesse nestas moléculas foi enfatizado devido a capacidade de formar complexos de inclusão. A forma tridimensional desta molécula apresenta um formato semicircular tipo cone truncado. A cristalografia destas moléculas identificou a presença de grupos hidroxilas (-OH) presentes nas ciclodextrinas nas regiões externas e na cavidade interna da molécula. Esta caracterização permitiu definir que a área exterior da molécula é hidrofílica enquanto a cavidade é apolar (SZEJTLI, 1989). Devido a estas propriedades, as ciclodextrinas demonstraram ser úteis para formar complexos de inclusão com compostos hidrofóbicos e consequentemente, para aumento de solubilidade

(JOUDIEH *et al.*, 2009). Para obter estes complexos de inclusão é necessário que a ciclodextrina tenha tamanho suficiente para comportar a molécula alvo. A utilização das CD pode ser feita em diferentes proporções molares em função da molécula alvo (ciclodextrina/droga), sendo as frações molares mais comuns 1:1 e 1:2. Pode-se exemplificar a Linezolida que foi com a β-CD e associada a sua ligação ao BSA porém, sua atividade após a formação do complexo de inclusão não foi avaliada (JOUDIEH *et al.*, 2009).

3.6.1 Caracterização do complexo de inclusão de CD

Um conjunto de técnicas são necessárias para avaliar a formação de complexos de inclusão com as CDs tanto no estado sólido quanto em meio líquido. As metodologias aplicadas mais comuns são o diagrama de solubilidade de fases, análise térmica, espectroscopia de infravermelho, difração de raios-X, microscopia eletrônica de varredura e ressonância magnética nuclear. Adicionalmente, a simulação computacional pode ser aplicada de forma a complementar os resultados obtidos pelas técnicas anteriores.

3.6.1.1 Diagrama de solubilidade de fases de CD

Este tipo de metodologia foi estabelecido por Higuchi e Connors (1965) e é comumente utilizado para estabelecer uma relação ótima dos complexos de inclusão. Esta técnica envolve o monitoramento da solubilidade de um composto pela adição a quantidades crescentes de CDs enquanto o substrato é mantido nas mesmas concentrações (HIGUCHI & CONNORS, 1965).

A interação entre a droga e a CD é mantida devido a constante de equilíbrio (Kc). A natureza do complexo e seus valores numéricos de Kc são derivados das propriedades do complexo e concentrações de CD em função da droga. O aumento da solubilidade de drogas hidrofóbicas neste caso é alcançado em função do aumento das concentrações de CDs. O perfil de solubilidade pode ser variável demonstrando um tipo de complexo formado bem como a estequiometria fármaco:CD (DAVIS E BREWSTER, 2004).

Os perfis das bandas de absorção irão demonstrar o tipo de perfil observado e qual são os processos que envolvem a participação da droga e do complexo de inclusão com

CD (**Fig. 9**). Higuchi e Connors estabeleceram que há dois perfis distintos: A e B. O perfil Al demonstra um aumento linear da solubilidade da droga em função da concentração de CD (Kc=1:1). O perfil Ap demonstra um desvio positivo de linearidade onde a solubilização é mais efetiva proporcionalmente em altas concentrações (Kc=1:>1). O último perfil, o An há um desvio negativo de linearidade onde demonstra que a CD é pouco eficiente em altas concentrações (Kc = 1:<1).

A apresentação do perfil B (Bs e Bi) demonstram que a formação dos complexos de inclusão demonstram uma solubilidade aquosa limitada. Este tipo de perfil é mais observado nas ciclodextrina natural (α, β e γ). Há casos em que a o fármaco pode interagir no complexo de inclusão e torná-lo insolúvel fazendo com que parte fique prescipitada e seja observada graficamente como um decréscimo do perfil de absorção (HIGUCHI & CONNORS, 1965).

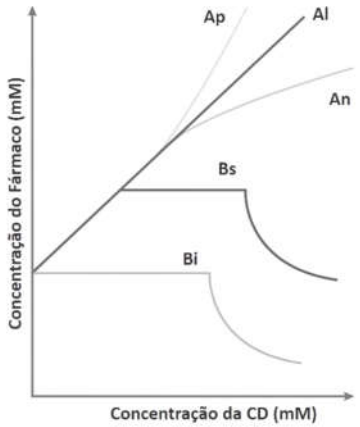

Figura 8. Tipos de diagramas de solubilidade de fases obtidos a partir da complexação de fármacos com ciclodextrinas. Al: linearidade, Ap: desvio positivo, An: desvio negativo, Bs e Bi: complexos com solubilidade aquosa limitada.

3.6.1.2 Espectroscopia de Infravermelho de CD

A espectroscopia de infravermelho (EIV) trata-se de uma técnica que estuda a interação da radiação eletromagnética com a matéria. A EIV tem sido amplamente utilizada para análise de vários compostos orgânicos ou inorgânicos, onde pode fornecer informações sobre os grupos funcionais da amostra, de acordo com sua natureza física. A identificação de uma molécula ocorre por movimentos rotacionais e vibracionais dos grupos moleculares e ligações químicas da estrutura química no comprimento de onda do

infravermelho. Essa absorção de radiação infravermelha provoca, portanto, aumento da amplitude das vibrações moleculares. A interpretação destes fenômenos é a EIV por Transformada de Fourier (Em inglês, *FTIR*) (SILVERSTEIN *et al.*, 2000; LOPES e FASCIO, 2004).

FTIR consiste, basicamente, na geração de um gráfico, utilizando-se de um interferômetro tipo Michelson constituído por um espelho fixo, um espelho móvel e um divisor de feixe. Ademais, a radiação incidente é separada através do divisor. Parte dessa radiação é direcionada ao espelho fixo e outra parte ao espelho móvel, onde é refletida e passa novamente pelo divisor de feixe e é recombinada, no qual um filme semirefletivo divide o plano de dois espelhos (*beam splitter*) em partes iguais. Os sinais obtidos são processados pelo cálculo da transformada de Fourier onde serão convertidos de forma gráfica considerando as coordenadas de tempo x intensidade do sinal. A esse tipo de gráfico denomina-se interferograma (LOPES e FASCIO, 2004) **(Fig. 9).**

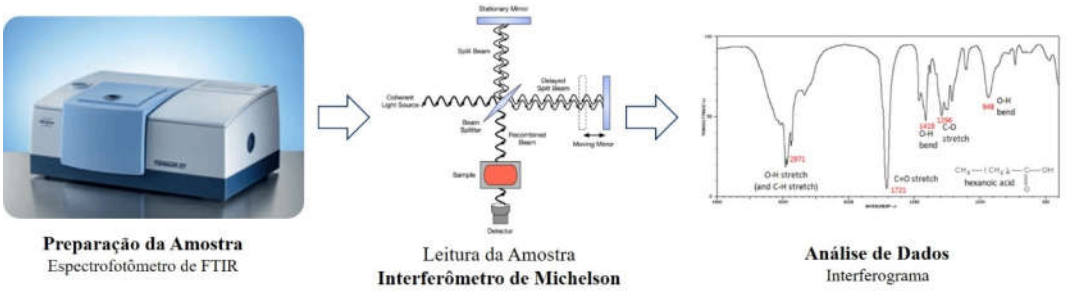

Figura 9 - Esquema de leitura e análise de dados através da espectroscopia de infravermelho por transformada de Fourier.

Essas bandas contem evidências de grupos funcionais na estrutura de uma molécula analisada. Isso ocorre porque os átomos interagem com a radiação eletromagnética em um processo de vibração molecular ao redor das ligações covalentes que os ligam (SILVERSTEIN *et al.*, 2000). Basicamente, há duas vibrações: a vibração de estiramento e a vibração angular. No primeiro caso, a vibração de estiramento, também denominada de *stretching*, os átomos aumentam ou diminuem sua distância mantendo-se no mesmo eixo. No segundo caso, a vibração angular (*bending*), as posições dos átomos mudam em relação ao seu eixo de ligação original (SILVERSTEIN *et al.*, 2000).

As posições das bandas no espectro podem ser apresentadas em número de ondas em centímetros invertidos (cm^{-1}) ou em micrômetros (μm). Cada grupo funcional costuma apresentar-se em determinadas regiões, o que ajuda a evidenciar ou confirmar a molécula em análise. As regiões que correspondem as faixas mais comuns são entre 4000-400 cm^{-1} (Tabela 2). Na região de alta energia são observadas hidroxila de álcool, ácido

carboxílico, fenol, enol, vibrações de NH de aminas primárias e secundárias, grupo carbonila e outros (SILVERSTEIN, 2000). Em casos em que há a ausência de bandas na região de 900 - 690 cm^{-1} é um indicativo de ausência de anéis aromáticos na molécula (SILVERSTEIN *et al.*, 2000; LOPES e FASCIO, 2004).

Tabela 2 – Bandas de absorção no infravermelho. Adaptado de SILVERSTEIN, 2000.

Ligação	Tipo de composto	Intervalo de frequência	Intensidade
C-H	Alcano	2850 a 2970	Forte
C-H	Alceno	1340 a 1470 3010 a 3095 675 a 995	Forte Média Forte
C-H	alcinos	3300	Forte
C-H	Anéis aromáticos	3010 a 3100 690 a 900	Média Forte
O-H	Alcoois e fenóis (mon) Alcoois e fenois/ponte de H	3590 a 3650 2500 a 2700	Variável Alargada
N-H	Aminas e Amidas	3300 a 3500	Média
C=O	Aldeidos, cetonas, ac. Carboxilicos, esteres	1690 -1760	Forte

Este método é indispensável para caracterização de compostos orgânicos em geral, pois permite a detecção de grupos funcionais. Moléculas hospedeiras não complexadas apresentam padrões de banda de absorção característico como do grupo carbonila (1600 cm^{-1}). No entanto, quando estas moléculas estão contidas nos complexos baseados em CD, pode haver um deslocamento destas bandas, encobrimento ou diminuição das bandas de absorção dos grupos funcionais (HEISE *et al.*, 2010; MANGOLIM *et al.*, 2014).

3.6.1.3 Ressonância Magnética Nuclear (RMN)

A ressonância magnética é um fenômeno que se relaciona com campos magnéticos e ondas eletromagnéticas de radiofrequência (RF). Foi descoberto em 1946, de forma independente por Bloch e Purcell, que lhes rendeu o prêmio Nobel de Física em 1952. Inicialmente, esta técnica foi utilizada primeiramente em química analítica e bioquímica e partir dos anos 80 seu uso foi destinado na medicina para diagnóstico por imagem em humanos (MAZOLLA, 2009).

As informações obtidas pela RMN provem das propriedades magnéticas naturais dos átomos. A base física deste fenômeno é dada pela existência dos tipos de movimentos dos núcleos atômicos: o movimento giratório em torno de si mesmo (“spin”) e o movimento em torno do eixo gravitacional (movimento de precessão). Os movimentos geram um campo magnético ao redor de cada núcleo, especialmente os átomos que possuem um número ímpar de próton e nêutrons onde adquirem maior atividade magnética. Devido a abundância tanto no meio quanto em tecidos orgânicos, deutério é bastante utilizado, seja em química analítica quanto na medicina (BEHROOZMAND *et al.*, 2015) **(Fig. 10).**

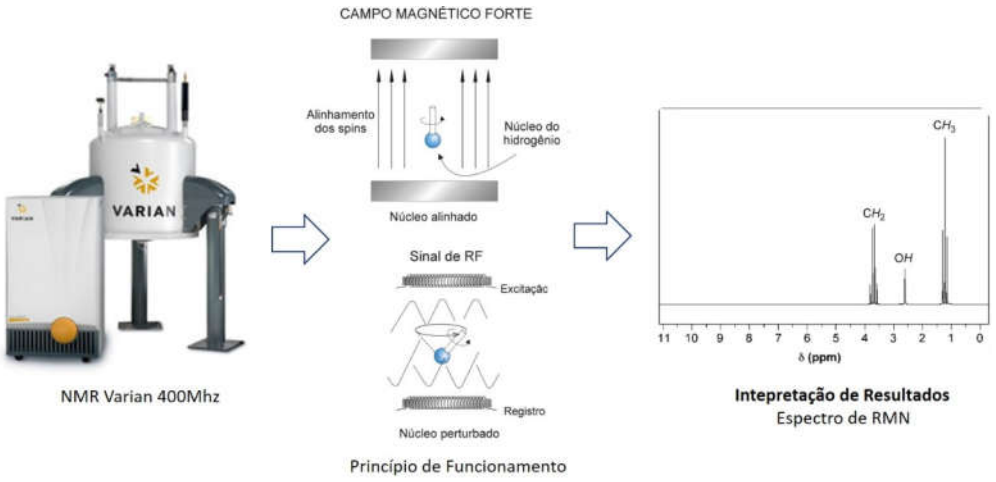

Figura 10 - Esquema de preparação, leitura e análise de dados através da ressonância magnética de ^{13}C e/ou ^{1}H.

Ao introduzir um campo magnético, estes átomos (H) se magnetizam temporariamente fazendo com que seus núcleos de alinhem criando um vetor de magnetização (longitudinal). Um fator de relevância neste processo, é que as partículas carregadas apresentavam órbitas circulares que se sobrepõe a frequência precessional em torno do campo externo conhecida, como frequência de Larmor. Quando se aplica um pulso de radiofrequência, o objetivo é mudar o plano de magnetização (longitudinal para o transversal), ou seja, o pulso de radiofrequência deve ser perpendicular ao campo magnético externo. Desta forma a variação da magnetização transversal é o que o equipamento pode detectar. A precessão da magnetização transversa induz sinais elétrico no cabo da bobina (MAZOLLA, 2009).

A RMN é utilizada para determinação de um dado composto nos complexos de inclusão. Essa técnica permite elucidar a estrutura do complexo e identificar as frações

da molécula que podem estar interagindo com a estruturas da CD (cavidade). A interação entre a molécula hospedeira e os complexos de inclusão apresentam alterações nos sinais espectrais de ambas as moléculas. A comprovação destes resultados são observados diante de análises comparativas entre as moléculas isoladas e os complexos de inclusão (TOMA e TOMA, 2007).

3.6.1.4 Difração de Raios X (DRX)

Esta técnica mede a intensidade de raios-X difratados por uma amostra sólida em diferentes ângulos. Essa metodologia baseia-se na lei de Bragg que está relacionada ao espalhamento de ondas incidentes provocados por estruturas cristalinas. Essa detecção pode ser observada através de um filme fotográfico ou um detector **(Fig. 13)**.

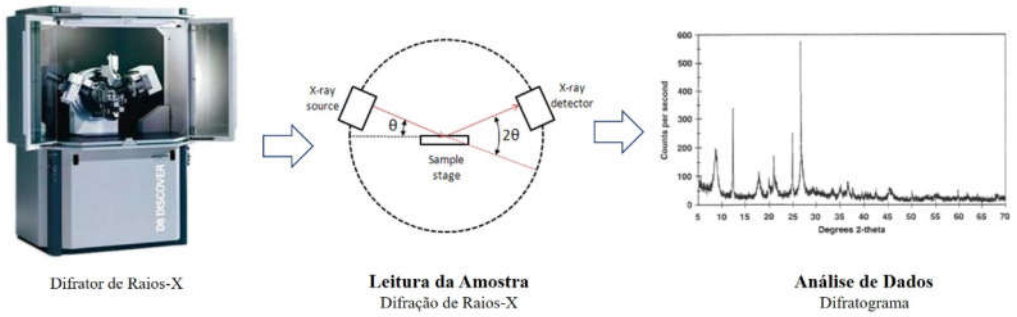

Figura 11 - Esquema de preparação, leitura e análise de dados através da difração de raios-x.

As moléculas hospedeira, geralmente apresentam picos de intensidade em vários ângulos diferentes, o que caracteriza estes compostos pela sua cristalinidade. No entanto, as CD apresentam ligações de hidrogênio tanto intra quanto intermoleculares, o que torna este material mais amorfo. Ou seja, diferentemente de compostos cristalinos, não há a presença de picos característicos. A determinação dos complexos de inclusão baseia-se na comparação dos perfis nos difratogramas entre as moléculas hospedeiras e os complexos de inclusão contendo estas moléculas. Em geral, quando há a formação de complexos contendo CD, ocorre a diminuição ou a total redução da intensidade dos picos da molécula hospedeira (MENDONÇA *et al.*, 2012).

3.6.1.5 Análises Térmicas de CD

A análise térmica destina-se a estudar o comportamento dos materiais à medida que mudam com a temperatura. Há uma variedade de métodos, no entanto, os mais comuns destinados a avaliar o comportamento térmico das ciclodextrinas em relação a um composto são pela calorimetria diferencial de varredura (DSC, do inglês *Differential Scanning Calorimetry*) e pela termogravimetria (TG). Na DSC o fluxo de calor é avaliado em função da temperatura ou tempo. Na TG, observa-se a mudança de massa em função da temperatura ou tempo (GIORDANO, *et al*., 2001). Existem equipamentos que podem fazer a análise térmica simultânea (STA) onde geralmente se aplica simultaneamente a TG e a DSC numa mesma amostra e em um único instrumento **(Fig. 12).**

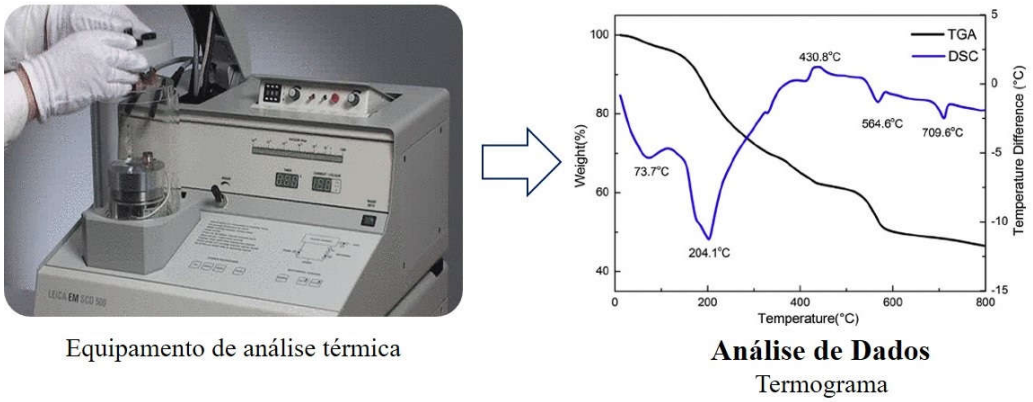

Figura 12 - Esquema de preparação, leitura e análise de dados através da análise térmica (calorimetria diferencial de varredura e termogravimetria).

As condições de ensaio são perfeitamente idênticas para os sinais TGA e DSC (mesma atmosfera, pressão de vapor da amostra, taxa de aquecimento, contato térmico com o cadinho e sensor da amostra, efeito de radiação, etc.). As medições podem ser realizadas no ar ou sob um gás inerte (por exemplo, azoto ou hélio) (GIORDANO *et al*., 2001).

4 METODOLOGIA

4.1 REAGENTES E MATERIAIS

O DOx LPSF/NB-14 (5-benzil-3-etil-2-tiooxazolidin 4-ona) foi gentilmente cedido pelo Laboratório de Planejamento e Síntese de Fármacos da UFPE. A 2-hidroxipropil-beta-ciclodextrina (HP-β-CD), acetona, acetonitrila, metano, MTT Formazan, DMSO, clorafenicol e fluconazol foram obtidos da Sigma-Aldrich (St. Louis, MO, USA). O Ficoll-Paque PLUS foi obtido da GE Healthcare (Little Chalfont, UK). O Ágar Mueller-Hinton (MH), Ágar SABOURAUD e meio RPMI 1640 foram obtidos da Life Technologies (Carlsbad, CA, USA). O Água Nutriente Difco™ foi obtido da BD (Franklin Lakes, NJ, USA). A placas de microtitulação planas de 96 poços foram adquiridas da TPP (Trasadingen, Suíça). filtros de seringa PVDF de 0,45 μm (Dueren, DE. Os solventes utilizados foram o tampão fosfato (PBS 0,9%, (pH 7.4) e água deionizada obtida de sistema Millipore (Billerica, MA, USA).

4.2 LINHAGENS BACTERIANAS

A cepa de bactéria gram-positiva foi de *Stahylococcus aureus* MRSA (ATCC® 29213) enquanto as cepas gram-negativas foram *Salmonella typhimurium* (ATCC® 14028), *Shigella flexneri* (ATCC® 12022) e *Enterobacter cloace* (ATCC® 13047). Todas as bactérias foram mantidas em Ágar Nutriente Difco™ e guardadas a 4ºC.

4.3 LINHAGENS FÚNGICAS

Nove linhagens fúngicas foram testadas. Seis espécies de leveduras: quatro do gênero Candida (*C. krusei, C. parapsilosis, tropicalis, C. glabrata*) e duas do gênero Cryptococcus (*C. gattii and C. neoformans*). Três espécies de dermatófitos também foram avaliadas (*M. gypseum, T. rubrum e T. mentagrophytes)*. Todos os fungos foram mantidos em Ágar Sabouraud Dextrose a 37ºC.

4.4 LINHAGENS DE CÉLULAS TUMORAIS

Duas linhagens celulares foram testadas: MCF-7 (ATCC® HTB-22) e T-47D (ATCC® HTB-133) obtidas do banco de células do Rio de Janeiro (Duque de Caxias, RJ, BR).

4.5 TESTES DE SUSCEPTIBILIDADE DE BACTÉRIAS AO LPSF/NB-14

A metodologia aplicada neste estudo baseou-se microdiluição em placa de 96 poços em caldo Mueller-Hinton (para bactérias) ou Sabouraud (para fungos) para droga isolada e em sinergismo. As suspensões bacterianas foram padronizadas de acordo com a escala 0,5 de MacFarland em PBS a 0,9% que equivale a concentração de aproximadamente $1,5\times10^8$ UFC/mL.

Inicialmente 80 µL do meio MH foi distribuído em todos os poços da placa. Em seguida, adicionou-se 100µL (1 mg/mL) de cada droga/complexo na primeira fileira da microplaca (1º coluna) no sentido vertical. Posteriormente a droga é distribuída com auxílio do multipipetador até a penúltima coluna (11º coluna). A última fileira (12º coluna) é reservada para o controle positivo (solução composta de PBS à 0,9% e Clorafenicol à 500 µg/mL.

Na segunda etapa deste experimento, uma discreta alçada foi retirada da colônia bacteriana e adicionada em tubo contendo 5 mL de PBS 0,9% de modo a alcançar a escala 0,5 de MacFarland. Em seguida 100 µL da suspensão foi adicionado a outro tubo contendo 9 mL de PBS 0,9% para reduzir diluir a solução bacteriana de 1,5x108 para $1,5\times10^6$ UFC/mL. Após a etapa de distribuição do caldo MH e controle positivo, 20µL desta solução bacteriana foi adicionada em todos os poços. A microplaca é então incubada em estufa à 37ºC por 24 horas **(Fig. 15).**

Figura 13 - Esquema de preparação, leitura e análise de dados através do teste de susceptibilidade de bactérias para o DOx em microplaca.

4.6 AVALIAÇÃO DA CONCENTRAÇÃO INIBITÓRIA MÍNIMA (CIM) POR DENSIDADE ÓTICA (DO) EM BACTÉRIAS

Nesta etapa as placas após 24h são submetidas a leitura para obtenção da densidade ótica a 490nm através de espectrofotômetro para microplacas (Polaris, CELER, MG, BR). A CMI é determinada se a diminuição da concentração corresponder igualmente ou maior a 50% da DO em relação ao poço controle. Por fim, a determinação da CMI com efeito bactericida deve ser feita a partir da retirada do poço onde houve inibição para que seja feita em placa de Petri contendo Ágar Nutriente e incubação por 48 h a 37ºC. O experimento só pode ser considerado válido se o desvio-padrão for próximo a zero. A revelação visual com corante supravital pode ser realizada através da inserção de 40 µL de cloreto de trifeniltetrazólio (CTT) onde, células que ainda estão viáveis são coradas em vermelho.

4.7 TESTE DE SUSCEPTIBILIDADE DE FUNGOS PARA O LPSF/NB-14

O método utilizado seguiu as condições descritas no documento em M27-A3 (CLSI, 2008). O meio de cultura utilizado foi o RPMI 1640 (Sigma-Aldrich, EUA) com L-glutamina e sem bicarbonato de sódio, pH 7,0 ± 0,1, com ácido morfolino propano sulfônico (MOPS) à 0,165 mol/L (Sigma-Aldrich, EUA). O meio de cultura foi esterilizado em membranas de 0,22 µm (Millipore, Darmstadt, Alemanha). Os agentes antifúngicos comerciais utilizados foram a anfotericina B (Bristol-Myers Squibb, Princeton, USA) diluída em DMSO e o fluconazol (Pfizer, Nova York, EUA), preparado em água destilada. Concentrações diferentes de ambos antifúngicos foram preparados e usados nos intervalos de 0,03 a 16 µg/mL para anfotericina B e 0,125 a 64 µg/mL para fluconazol. Os DOx foram diluídos em DMSO e as concentrações testadas variaram de 2 a 1.024 µg/mL. As espécies de *Candida, Criptococcus* e dermatófitos utilizadas foram mantidas em meio Sabouraud Dextrose Agar (SDA) e incubadas a 35°C. As suspensões dos isolados foram preparadas em solução salina, e sua densidade foi ajustada de acordo com a escala 0.5 de MacFarland em 90% da transmitância utilizando um espectrofotômetro a 530 nm. O volume do inóculo foi ajustado para 5 mL de solução

salina esterilizada e, posteriormente, diluído em RPMI 1640 para uma concentração de 2-5×10^3 céls.mL^{-1}. Para os testes de sensibilidade, foram utilizadas placas de microtitulação planas de 96 poços. O inóculo foi adicionado aos poços com as drogas a serem testadas, e as placas foram incubadas a 37°C durante 48 horas para determinação da Concentração Inibitória Mínima (CIM). As CIMs para anfotericina B e os DOx foram determinadas para 100% e do fluconazol para ≥50% de inibição em relação aos poços controles **(Fig. 14)**.

Figura 14 - Esquema de preparação, leitura e análise de dados através do teste de susceptibilidade de fungos para o DOx em microplaca.

4.8 PREPARAÇÃO DOS COMPLEXOS DE INCLUSÃO DO DOX COM HP-B-CD

A técnica utilizada neste estudo foi de co-evaporação descrita por Gosh *et al.* (2011) modificada. Quantidades de DOx e HP-β-CD em taxas molares (1:1) foram dissolvidos em acetona: água respectivamente. A solução de droga foi adicionada gota-a-gota em solução de HP-β-CD previamente sob agitação. O conteúdo foi continuamente agitado por 6 horas e rotaevaporado à 45-50°C por aproximadamente 90 minutos. Após a secagem completa do material, o sólido obtido foi liofilizado a 4×10^{-6} Bar for 48 horas estocado em dessecadores para utilização posterior.

4.9 PREPARAÇÃO DE MISTURA FÌSICA

Uma mistura física consistindo de LPSF/NB-14 (5mg) em HP-β-CD (30mg) foi misturada em proporções equimolares e com o auxílio de um almofariz e um pistilo por 10 minutos obteve-se uma mistura homogênea.

4.10 MODELAGEM MOLECULAR DOS COMPLEXOS DE INCLUSÃO DOX:HP-B-CD

Dois aspectos sintéticos de derivados da CD foram levados em consideração para modelagem molecular: 1) regioseletivo: a reação preferivelmente ocorreu no grupo hidroxila primário OH(6), pois estes estão mais acessíveis, seguidos da hidroxila secundária OH(2) com alta acidez (pKa=12.2) (WENZ, 1994); derivados homólogos com razão de substituição (MS) mais baixa e mais elevada (TREIB *et al*., 1999), no qual também são formados na mistura obtida como produto final (WENZ, 1994).

Nossa abordagem foi a de construir praticamente 1000 estruturas (40 configurações com 25 diferentes conformações cada) para o modelo HP-β-CD, a partir da estrutura tridimensional da β-ciclodextrina (β-CD) (SAENGER *et al*., 1998). As 40 configurações foram construídas considerando os dois aspectos sintéticos mencionados anteriormente. Tendo em conta o MS de 0,6, parece razoável considerar que a estrutura de HP-β-CD (7 unidades de glucose) tem, em média, 4 unidades de HP (0,6x7 = 4,2). Assim, foram construídas 20 configurações de HP-β-CD com 4 unidades de HP, 10 configurações com 3 unidades de HP e 10 configurações com unidades de 5 HP-β-CD. Para cada unidade HP adicionada, foi tida em conta a probabilidade de 70% para OH (posição 6), 20% para OH (posição 2) e 10% para OH (posição 3), para selecionar a posição OH para substituição. A busca de confórmeros foi realizada usando *Genetic Algorithm and Energy Score Function* disponível na OpenBabel library (O'BOYLE *et al*., 2011), com parâmetro de convergência padrão. As otimizações geométricas para todos as 1000 estruturas foram computadas usando *MMFF94s force field* (HALGREN, 1999), novamente com a mesma biblioteca e critérios padrões.

Em seguida, uma abordagem de ancoragem (*docking*) molecular para encontrar os complexos de inclusão hospedeiro (*guest*): hóspede (*host)* (HP-β-CD: LPSF/NB-14). Utilizou-se o software Autodock VINA (TROTT E OLSON, 2010), considerando cada estrutura completa de derivado de HP-β-CD como o sítio ativo e ajustando o parâmetro de exaustividade para 8. As energias de interação intermolecular para todos os 1000 complexos foram calculadas. Toda a abordagem utilizada para a modelagem molecular foi realizada de forma automatizada, utilizando uma plataforma desenvolvida pelo nosso grupo de pesquisa, denominada CycloMolder.

4.11CARACTERIZAÇÃO DOS COMPLEXOS DE INCLUSÃO (DOX/ HP-B-CD)

4.11.1 Estudo de Fase de Solubilidade

Os estudos de fase de solubilidade foram conduzidos de acordo com Higuchi & Connors para determinar a razão estequiométrica da droga com HP-β-CD (HIGUCHI E CONNORS, 1965). Seis quantidades de LPSF/NB-14 (1.67 mg) foram misturadas a 2 mL de uma solução aquosa contendo CD variando de 0 até sua solubilidade máxima e, subsequentemente, vigorosamente agitado por 48h a 25ºC. Em seguida, amostras foram centrifugadas a 8972G por 10 minutos e filtradas com membranas PVDF de 0,45µm (Dueren, DE). A solução filtrada foi analisada por espectrofotometria UV-Vis a λ=286 nm. A partir dos valores de inclinação e intersecção (S0) da curva de fase de solubilidade, a constante de estabilidade (Kc) foi determinada (Eq. 1).

$$K_{1:1} = \frac{slope}{[S_0 \times (1 - slope)} \quad (1)$$

A eficiência de complexação (EC) de LPSF/NB-14 foi determinada a partir dos dados obtidos da curva de solubilidade de acordo com a equação a seguir (Eq. 2):

$$CE = \frac{slope}{(1 - slope)} \quad (2)$$

4.11.2 Microscopia eletrônica de varredura

A análise morfológica das amostras (DOX, HP-β-CD e complexo de inclusão) foram realizadas por microscopia eletrônica de varredura. As amostras foram depositadas sobre uma superfície de eletrodo de disco e colocado sobre um suporte de alumínio fixado com cola de carbono. Após este procedimento as amostras foram submetidas a um processo de metalização com ouro utilizando uma evaporadora de revestimento fino EM SCD 500 (Leica Mycrosystems, Wetzlar, DE) e examinado com o uso de um microscópio eletrônico de varredura QUANTA 200 (FEI, OR, USA) a 30 kV.

4.11.3 Análise de Espectro de Infravermelho (FTIR)

Os espectros de infravermelho da droga e do complexo e inclusão (4000 – 400 cm^{-1}) foram obtidos utilizando o método de KBr utilizando um espectrofotômetro com transformada de Fourier Vertek 70 (Bruker, MA, USA). A correção do *baseline* foi realizada utilizando brometo de potássio e então o espectro das misturas secas de droga e complexos de inclusão em brometo de potássio foram gravadas.

4.11.4 Ressonância Magnética Nuclear (^{1}H-NMR)

O espectro de ^{1}H-NMR foi gravado em um espectrofotômetro Varian 400 MHz (Varian, USA) utilizando DMSO-d6 como solvente. Os deslocamentos químicos foram relatados em δ (ppm) em relação ao tetrametilsilano (TMS) como padrão interno.

4.11.5 Difração de Raios-X

Os padrões de difração dos complexos de inclusão foram comparados com o DOxs puro (LPSF/NB-14). Este procedimento foi realizado com um intervalo angular 3-80°, a uma velocidade de 0,03°/segundo e com tempo de análise de 2671 segundos num difratômetro de raio-X D8 Advance (Bruker, MA, USA).

4.11.6 Análise Térmica

A termogravimetria (TGA) e a calorimetria diferencial de varredura (DSC) foram realizadas utilizando um STA 449 F3 Jupiter® (NETZSCH, Asch, CZ). As amostras foram colocadas num cadinho de platina e os termogramas foram registrados com uma taxa de aquecimento de 10°C.min^{-1} num intervalo de 20° to 310°C (LI e XU, 2010).

4.12 ENSAIO DE MTT

A citotoxicidade dos compostos DOx, HP-β-CD e DOx: HP-β-CD foram testadas contra duas linhagens tumorais: MCF-7 (adenocarcinoma de mama) e T47-D (adenocarcinoma ductal mamário). Todas as células foram obtidas do banco de células

obtidos do Rio de Janeiro. As células foram cultivadas em meio RPMI-1640 com 10% de soro bovino fetal, 2 mM de glutamina, 100 mg/mL estreptomicina e 100 U/mL de penicilina a 37ºC com 5% de CO_2. Para os experimentos, as células foram plaqueadas com microplacas de 96 poços (10^4 células/poço). Após 24 horas, os compostos (1 a 100μM) dissolvidos em DMSO a 0.1% (DOx) e H_2O (2-HPβCD e OxD: 2-HPβCD) foram adicionadas em cada poço e incubados por 72h. A doxorubicina foi usada como controle positivo. O crescimento das células tumorais foi quantificado pela habilidade das células vivas de reduzir o corante amarelo, brometo de 3-(4,5-dimetil-2-tiazolil)-2,5-difenil-2H-tetrazolio (MTT) em um produto, o azul de formazan. Após 72h de incubação, 20μL de 0.5 mg/mL de MTT foram adicionados em cada poço, e as células foram incubadas novamente a 37ºC com 5% de CO_2. Três horas depois, a redução do produto de formazan do MTT foi dissolvido em 20% de SDS, e a absorbância foi medida utilizando um leitor de microplaca (EL808, Biotek, USA). O efeito da droga foi quantificado bem como o percentual dos controles da absorbância a partir da redução do produto em 570 nm. Os experimentos foram realizados em triplicata.

4.13 CITOTOXICIDADE EM CÉLULAS MONONUCLEARES DE SANGUE PERIFÉRICO

As células mononucleares de sangue periférico (*PBMCs*) foram obtidas de sangue heparinizado de doadores sadios (n=6), não fumantes dos quais não fizeram uso de drogas por pelo menos 15 dias antes do dia da coleta da amostra. As *PBMC*s foram isoladas via método padrão por centrifugação baseada em diferença de densidade do gradiente com Ficoll-Hypaque (GE Healthcare, UK). As células foram contadas numa câmara de Neubauer, e a viabilidade foi determinada pelo método de exclusão utilizando o azul de tripano. As células foram apenas usadas em casos onde a viabilidade foi >98%. Todos os doadores assinaram o termo de consentimento aprovado pelo comitê de ética e pesquisa da UFPE. As células foram plaqueadas em microplacas de 96 poços (10^6 células/poço). Após 24 horas, os compostos DOx, HP-β-CD e DOx: HP-β-CD em 6 concentrações (1 a 100 μM) foram aplicadas nas placas onde foram incubadas por 48h. Por último, os procedimentos realizados foram os mesmos descritos no tópico acima.

4.13.1 ANÁLISE ESTATÍSTICA

Todos os resultados foram analisados por comparações univariadas usando testes não paramétrico com $p<0.05$ considerado como associação significante. Todos os dados quantitativos foram plotados, bem como, os valores de IC_{50} foram obtidos por regressão não linear desenvolvidos com o software GraphPad Prism 6 (CA, EUA).

5 RESULTADOS E DISCUSSÃO

5.1. RESSONÂNCIA MAGNÉTICA DE HIDROGÊNIO (^{1}H) E CARBONO-13 (^{13}C) DE LPSF/NB-14

RMN-H (LPSF/NB-14): Sólido branco, δ 1.22 ppm (t, 3H, CH_3, j=7,2 Hz), 3.82 ppm (q, 2H, CH_2, j=7,2 Hz), 6.94 ppm (s, 1H, =C-H), 7.49-7.56 (m, 3H, C-H aromático), 7.88 pm (d, 2H, j=8,4 Hz, C-H aromático). **RMN-C13 (LPSF/NB-14):** δ 11.68 ppm (CH_3), 37.73 ppm (CH_2), 112.42 ppm (=C-H), 129.18 – 131.04 (C-H Aromático), 139.10 (C=C), 161.54 (C=S), 183.32 ppm (C=O).

5.2. TESTES DE SUSCEPTIBILIDADE DE BACTÉRIAS COM O LPSF/NB-14

Os testes de susceptibilidade foram realizados para determinar a concentração mínima inibitória do DOx através do método de microdiluição em placa. Inicialmente avaliamos o potencial antibacteriano do DOx em forma livre. As linhagens testadas em linhagens gram-positivas (*Staphyloccoccus aureus* MRSA) e gram-negativas (*Salmonella typhimurium, Shigella flexneri, Enterobacter cloacae*). A validação do CMI é confirmada se a densidade ótima for menor que 50% a densidade ótica do controle positivo com antibiótico de amplo espectro (Clorafenicol 10 μg/mL). Os CMIs de LPSF/NB-14 estão presentes na Tabela 3.

Tabela 3 - Susceptibilidade *in vitro* de linhagens bacterianas de LPSF/NB-14 determinados pelo método de microdiluição em placa

Espécies (no. de isolados)	LPSF/NB-14 (µg/mL)	Clorafenicol
Shigella flexneri (1)	512	8
Staphyloccoccus aureus MRSA (2)	512	8
Salmonella typhimurium (1)	512	8
Enterobacter cloacae	256	8

Em geral, as CMIs apresentados nas linhagens bacterianas testadas foram altas com valores entre 256 µg/mL a 512 µg/mL para o DOx. Levando em consideração os resultados apresentados, o composto apresenta uma atividade bacteriostática porém não apresenta um atividade bactericida. Alguns pesquisadores sugerem que solubilização de alguns antibióticos muito hidrofóbicos poderiam contribuir para a potencialização de uma atividade antibacteriana podendo ter um efeito quatro vezes maior em relação aos compostos puros (ALEEM *et al.*, 2008; SUN *et al.*, 2011).

5.3. TESTES DE SUSCEPTIBILIDADE DE FUNGOS COM DOX

Os testes de susceptibilidade para fungos foram realizados para determinar a concentração mínima inibitória do DOx através do método de microdiluição em placa. Inicialmente, nós testamos a atividade biológica com o DOx em sua forma livre. Dois tipos de leveduras foram avaliados, dos quais quatro espécies foram do gênero *Candida* (*C. krusei, C. parapsilosis, C. tropicalis and C. glabrata*) e dois do gênero Cryptococcus *C. neoformans* and *C. gatti*). Adicionalmente, foram utilizadas três espécies de dermatófitos: um do gênero *Microsporum* (*M. gypseum*) e dois do gênero *Trycophytum* (*T. rubrum, T. mentagrophytes*). A validação do CMI foi confirmada se a densidade ótima for menor que 50% a densidade ótica do controle de crescimento positivo (CP). Além disso, no controle de crescimento negativo (CN) não houve inserção de DOx ou fungo. Os CMIs de LPSF/NB-14 estão presentes na Tabela 4.

Tabela 4 – Susceptibilidade *in vitro* de isolados fúngicos de LPSF/NB-14 determinados pelo método de microdiluição em placa.

Espécies (no. de isolados)	LPSF/NB-14 (μg/mL)	Fluconazol (μg/mL)
C. krusei (1)	512	2
C. parapsilosis (1)	512	2
C. tropicalis (1)	512	2
C. glabrata (1)	512	2
Cryptococcus gattii (2)	128	2
Cryptococcus neoformans (2)	256	2
Microsporum gypseum (1)	128	2
Trichophyton rubrum (1)	16	2
Trichophyton mentagrophytes (2)	16	2

A CMI do DOx para todas as espécies de *Candida* apresentou uma atividade fungistática (512 μg/mL). Em relação as espécies do gênero *Cryptococcus*, observou-se que os valores variaram entre 256 μg/mL e 128 μg/mL para as espécies C. *neoformans* e *C. gatti,* respectivamente. No entanto, os valores de CMI entre dermatófitos apresentaram valores menores em relação a outras espécies. Enquanto a *M. gypseum* apresentou uma 128 μg/mL, as espécies *Trichophyton* (*T. rubrum e T. mentagrophytes*) apresentaram valores menores (16 μg/mL). Tais resultados foram semelhantemente observados em outro derivado testado por Kawai *et al*., o tioxaprofeno. Este derivado apresentou um efeito negativo sobre negativo sobre mitocôndria de dermatofitos das espécies *T. rubrum e T. mentagrophytes* (8 μg/mL) (KAWAI *et al.*, 1983).

5.4. MODELAGEM MOLECULAR DO COMPLEXO DE INCLUSÃO DOX:HP-B-CD

Os resultados da ancoragem molecular demonstraram duas orientações em relação a posição de molécula hóspede (LPSF/NB-14) dentro de molécula hospedeira (HP-β-CD). A primeira, chamada de orientação 1, tem o anel tioxazolidinico dentro da cavidade da HP-β-CD, e o outro, denominado orientação II, tem o anel benzênico dentro da cavidade.

A média de energia de ancoragem para as dez primeiras melhores soluções, considerando a orientação I, é de -5,6 kcal / mol. Por outro lado, a energia média das dez primeiras melhores soluções para orientação II é -5,4 kcal/mol, portanto menos estável. A melhor solução de ancoragem global para a orientação I é mostrada na **Fig. 15a**, com uma energia de atração de -5,9 kcal/mol, enquanto que a melhor solução de ancoragem global para a orientação II pode ser encontrada na **Fig. 15c**, com uma energia de -5,6 kcal/mol.

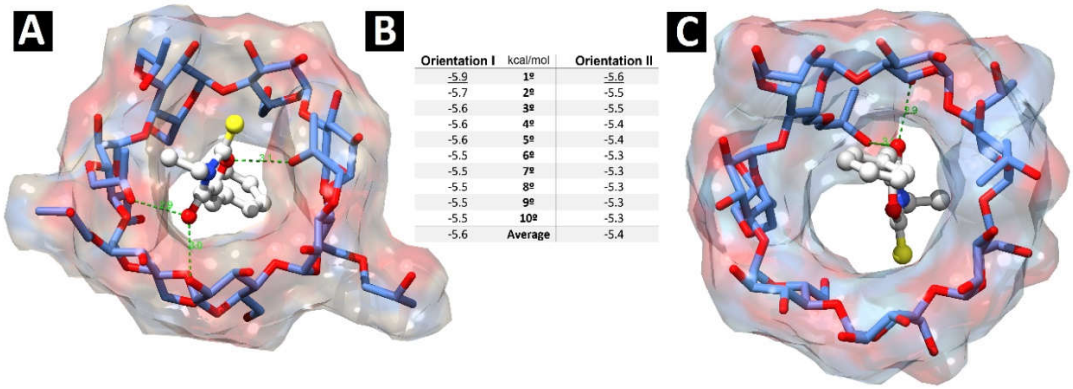

Orientation I	kcal/mol	Orientation II
-5.9	1º	-5.6
-5.7	2º	-5.5
-5.6	3º	-5.5
-5.6	4º	-5.4
-5.6	5º	-5.4
-5.5	6º	-5.3
-5.5	7º	-5.3
-5.5	8º	-5.3
-5.5	9º	-5.3
-5.5	10º	-5.3
-5.6	Average	-5.4

Figura 15 – Resumo dos resultados de ancoragem. A) Melhor solução de ancoragem para a orientação I. B) Tabela de energia de ligação (kcal/mol) das dez melhores soluções para cada orientação. C) Melhor solução para orientação II. Linhas tracejadas representam as ligações de hidrogênio entre HP-β-CD (*host)* e o DOx LPSF/NB-14 (*guest)*.

A melhor solução de acoplamento para a orientação I é estabilizada por vários contatos hidrofóbicos e por três ligações de hidrogénio (2,9 Å, 3,0 Å e 3,1 Å), enquanto a melhor solução para a orientação II é também estabilizada por vários contatos hidrofóbicos, mas apenas por duas ligações de hidrogénio (2,9 Å e 3,1 Å). Os resultados finais de modelação molecular apontam a orientação I como a mais estável, e deve ocorrer na mistura por uma proporção maior, para o complexo de inclusão HP-β-CD: LPSF / NB-14 (*guest: host*).

5.5.CARACTERIZAÇÃO DOS COMPLEXOS DE INCLUSÃO (DOX/ HP-B-CD)

5.5.1 Estudo de Fase de Solubilidade de LPSF/NB-14

O diagrama de fase de solubilidade de LPSF/NB-14 em solução aquosa de HP-β-CD apresentou curvas do tipo AL **(Fig. 16).** Os dados foram ajustados por regressão linear de acordo com a seguinte fórmula $[LPSF/NB\text{-}14]_{água} = 0.1686 \times [HP\text{-}\beta\text{-}CD\ ] + 0.1950$ ($r^2 = 0.99915$). As constantes de solubilidade de LPSF/NB-14 em solução aquosa de HP-β-CD a 25°C foi de K1:1=0.316 onde S_0=0.64mM. O incremento de solubilidade em LPSF/NB-14 com HP-β-CD foi alcançado em 12.62 mM. Este último dado demonstra que houve um aumento na solubilidade vinte vezes maior em relação ao composto puro. O coeficiente de encapsulamento (CE) foi de 0.202 de acordo com a equação 2. De acordo com Loftsson *et al*., se o CE for igual a 0.1, 1 em cada 11 moléculas de CD formam complexo com a droga, no entanto, se o CE > 0.2, uma quantidade menor de moléculas CD interage com a droga. Neste contexto, aproximadamente 1 a cada 5 moléculas de CD formam complexos com a droga, neste caso, o DOx (LOFTSSON *et al.*, 2005).

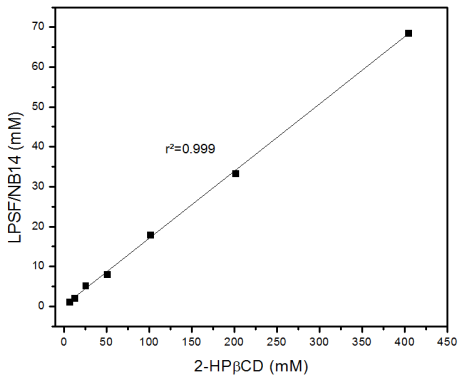

Figura 16 - Diagrama de fase de solubilidade para DOx LPSF/NB-14 a 25ºC na presença de HP-β-CD.

5.5.2. Análise Morfológica

A morfologia de LPSF/NB-14 apresentou uma forma cristalina acicular **(Fig. 17a,a1).** Por outro lado, as imagens relacionadas aos complexos de inclusão **(Fig. 17b, b1)** revelaram uma mudança significante na morfologia demonstrando uma aparência amorfa. Estudos anteriores demonstraram comportamento similar para tais complexos de inclusão devido a formação de agregado de CDs (FAUZIAH *et al.*, 2013; SONGNGAM *et al.*, 2014).

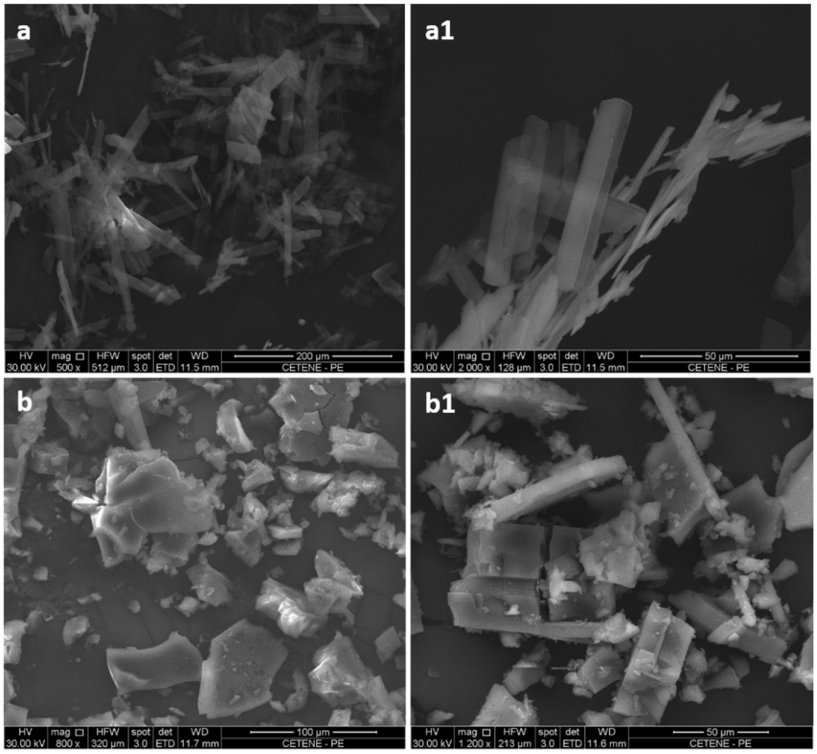

Figura 17 – Micrografias de LPSF/NB-14 (a,a1) e complexo de inclusão LPSF/NB-14:HP-β-CD (b,b1).

5.6. Espectroscopia de infravermelho com transformada de Fourier

O *FTIR* foi utilizado para avaliar a formação dos complexos de inclusão **(Fig. 18).**

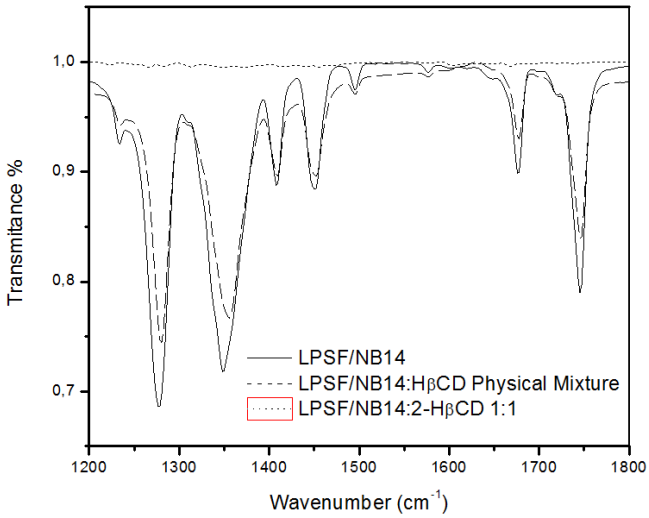

Figura 18. Espectro de FTIR de LPSF/NB-14 e dos complexos de inclusão LPSF/NB-14:HP-β-CD obtidos por mistura física e pelo método de co-evaporação (razão molar 1:1).

Adicionalmente, o espectro de IV foi obtido comparando a eficiência do método de co-evaporação e a mistura física. Os resultados demonstraram a formação dos complexos de inclusão considerando a intensidade das bandas de absorção dos grupos funcionais de DOx. Neste caso uma maior intensidade foi observada através da utilização do método de co-evaporação em relação a mistura física demonstrando que houve uma maior incorporação do composto pelo método de co-evaporação.

O espectro de IV de LPSF/NB-14 apresentou bandas em 1750-1735 cm^{-1} (C=O, alongamento), 1600-1585 cm^{-1} (C–C, alongamento aromático), 1360-1290 cm^{-1} (C-N alongamento, aminas alifáticas). O espectro de IV de LPSF/NB-14 também demonstrou a presença de bandas em (C –H alongamento vibracional), 1745 e 1695 (C=O alongamento), e 1631 cm^{-1} (C=C alongamento). O espectro de IV de HP-β-CD são semelhantes e apresentam bandas de absorção em ~3411 (O–H alongamento vibracional), ~2931 (C−H alongamento vibracional), ~1157, ~1089, e ~1029 cm^{-1} (C−H and C−O alongamento vibracional) (dados não mostrados). Eles apresentam uma grande sobreposição de sinais, com pequenas alterações na intensidade, amplitudes e formas das bandas de absorção, indicando a formação de complexos como novos compostos, com faixas típicas de impressão digital.

5.7. Espectroscopia de Ressonância Magnética Nuclear (RMN-^{1}H)

Os experimentos de RMN-^{1}H foram realizados para confirmar o complexo de inclusão LPSF/NB-14:HP-β-CD, avaliando os deslocamentos químicos (Δδ) de compostos puros (LPSF/NB-14 e HP-β-CD) em uma razão molar 1:1 (Tabela 5).

O LPSF/NB-14 RMN-^{1}H (400 MHz, DMSO-d6) apresentou: δ=1.22 (t, 3H, CH3, J= 7,2 Hz), 3.82 (q, 2H, CH2, J= 7,2 Hz), 6.94 (s, 1H, =C-H), 7.49-7.56 (m, 3H, C-H Ar), 7.88 (d, 2H, J= 8,4 Hz, C-H Ar). As mudanças nos deslocamentos de H_{1-4} foram verificadas com um $\Delta\delta H_4$=0.010 ppm. Outros sítios de ligação de hidrogênio também apresentaram deslocamentos químicos no próton H de 0.020 ppm a 0.030 ppm (Tabela 1).

Tabela 5 – Sinais de ^{1}H-NMR: LPSF/NB-14 e LPSF/NB-14:2–HPβCD (razão molar 1:1).

LPSF/NB-14	$\delta_{LPSF/NB-14\ (ppm)}$	$\delta_{LPSF/NB-14:HP-\beta-CD\ (ppm)}$	$\Delta\delta_{(ppm)}$
H_1 (a)	7.49-7.56	7.51-7.57	0.02-0.01
H_2 (b)	7.88	7.90	0.02
H_3 (c)	6.94	6.96	0.02
H_4 (d)	3.82	3.83	0.01
H_5 (e)	1.22	1.25	0.03

5.8. Difração de Raios-X

A difração de raios X (DRX) é uma técnica eficaz para determinar a natureza do sólido cristalino e considerada essencial para a caracterização de complexos de inclusão. Os padrões XRD de DOx apresentaram dois picos bem definidos para LPSF/NB-14 **(Fig. 19)** que representa uma ordem estrutural típica de um sólido cristalino.

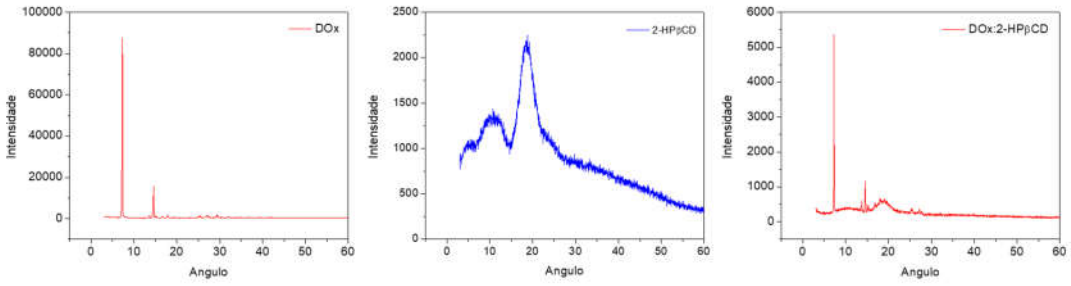

Figura 19 – Difratograma de LPSF/NB-14 (a), LPSF/NB-14: HP-β-CD (b) HP-β-CD (c) (razão molar 1:1).

Em geral, CDs natural e sintético não apresentam picos bem definidos e são caracterizados como materiais amorfos (Choe *et al*., 2003). A HP-β-CD apresentou características amorfas e distintiva de LPSF/NB-14. Uma diminuição na intensidade de pico do complexo de inclusão foi observada quando comparada com ao DOx puro, indicando uma perda de cristalinidade e blindagem devido a incorporação do composto dentro da estrutura da CD.

5.9. Análise Térmica

Avaliou-se o comportamento térmico de LPSF/NB-14, HP-β-CD e complexo de inclusão (razão molar 1: 1). O LPSF/NB-14 apresentou pico exotérmico a 136,57ºC com um calor de reação de 4,19 mW/mg. Este fenômeno surge durante o aquecimento antes da temperatura de decomposição. Por outro lado, a HP-β-CD apresentou pico exotérmico a 103,52 ºC com calor de 1,07 mW/mg. Observando-se o comportamento térmico do complexo de inclusão LPSF / NB-14:HP-β-CD, observou-se a presença de uma mudança exotérmica de 143,77 ºC com uma reação de 0,83 mW/mg. A diferença entre as temperaturas de reação observadas entre as moléculas puras e o complexo de inclusão contribuiu para uma alteração no comportamento térmico do composto LPSF/NB-14 dentro da HP-β-CD **(Fig.20)**.

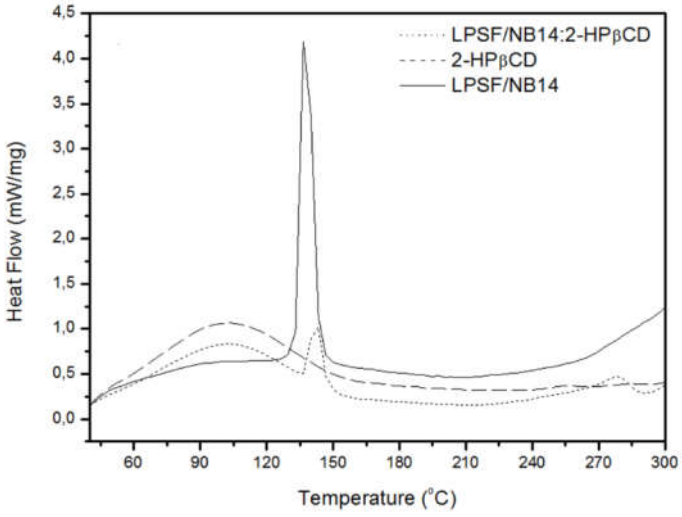

Figura 20. Curvas de CDV de LPSF/NB-14 e do complexo de inclusão LPSF/NB-14:HP-β-CD (razão molar 1:1).

Através da análise de curvas termogravimétricas, é possível observar uma perda de massa significativa de 27,5% de LPSF / NB-14 entre 250ºC e 300ºC. HP-β-CD mostrou uma perda de massa discreta (2,5%) de cerca de 125ºC e 300ºC. Em relação ao complexo de inclusão LPSF/NB-14:HP-β-CD, houve um comportamento de decaimento semelhante ao das duas moléculas isoladas. A perda de massa do complexo de inclusão foi inferior (17,5% vs. 27,5%) em comparação com a molécula de LPSF/NB-14. Inversamente, o complexo de inclusão mostrou uma resposta maior em relação à HP-β-CD (17,5% vs. 2,5%). Estes resultados sugerem que o CD contribuiu positivamente para um deslocamento da temperatura, que está associado à perda da massa em temperaturas mais altas **(Fig. 21).**

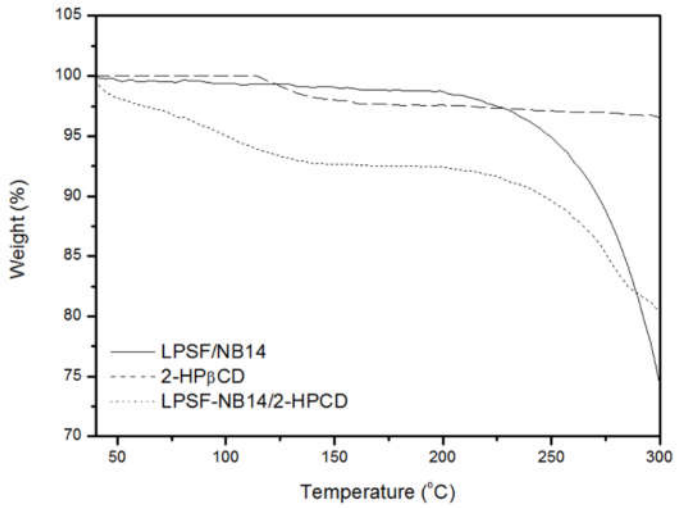

Figura 21. Curvas de TG de LPSF/NB-14, HP-β-CD e do complexo de inclusão LPSF/NB-14:HP-β-CD (razão molar 1:1).

Os resultados TG e DSC do complexo de inclusão LPSF/NB-14: HP-β-CD em comparação com LPSF/NB-14 e HP-β-CD sugerem o sucesso do método de complexação. Além disso, a determinação do ponto de fusão é baseada em interações intermoleculares, que estabilizam a estrutura cristalina do composto. Os resultados sugerem que CD criou uma estabilidade termodinâmica diferente para LPSF/NB-14, o que resultou em um comportamento térmico diferente.

Nossos resultados confirmaram a formação do complexo de inclusão e sugeriram que a molécula LPSF/NB-14 foi inserida na cavidade HP-β-CD substituindo as moléculas de água dentro dela. Além disso, a modelagem molecular corroborou com os resultados experimentais, uma vez que se observou que a estabilidade do complexo de inclusão estava principalmente relacionada com grandes ligações H entre o hóspede (LPSF/NB-14) e o hospedeiro (HP-β-CD).

5.10. Estudo de viabilidade celular por MTT em PBMCs

O percentual de células viáveis foi obtido através da utilização de seis concentrações molares diferentes (1μM a 100 μM) do DOx, 2-HP-β-CD e do complexo de inclusão utilizando o ensaio por MTT em meio RPMI 1640 **(Fig. 22)**.

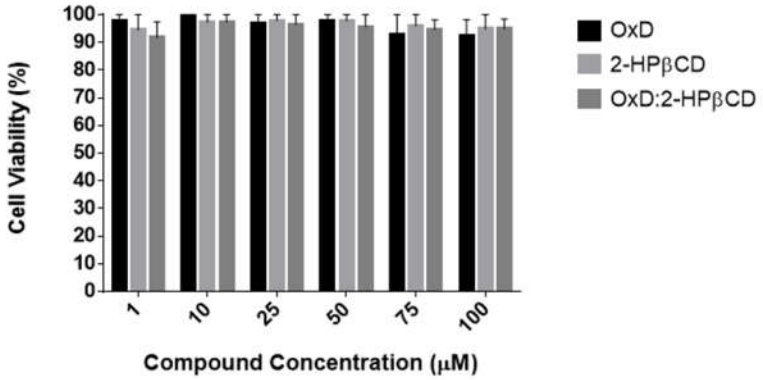

Figura 22 - Citotoxicidade de DOx, HP-β-CD e complexos de inclusão frente a células mononucleares de sangue periférico (PBMCs).

A viabilidade celular das PBMCs em condições com o DOx foi de 95% (± 2.3%) para 1μM a 50μM. A HP-β-CD e o complexo de inclusão demonstraram um percentual semelhante (94% ± 3%) para todas as concentrações estudadas. Estudos anteriores demonstraram que a ciclodextrinas possui uma citotoxicidade específica e que depende da célula envolvida (efeito dose-dependente) (SOFIAN *et al., 2014;* ZHANG *et al*., 2009). Em geral, a diminuição drástica da viabilidade em concentrações >25 μM são indesejadas para eventuais testes *in* vivo sendo necessário estabelecer uma dose ótima levando em consideração a quantidade utilizada. O incremento da solubilidade do DOx foi melhorado ao mesmo tempo que apresentou baixa toxicidade em células normais mesmo sob a forma de complexo de inclusão com a HP-β-CD.

A partir de um percentual de viabilidade, realizamos uma avaliação da atividade antitumoral em linhagens de células tumorais nas mesmas concentrações utilizadas nas PBMCs **(Fig. 23)**.

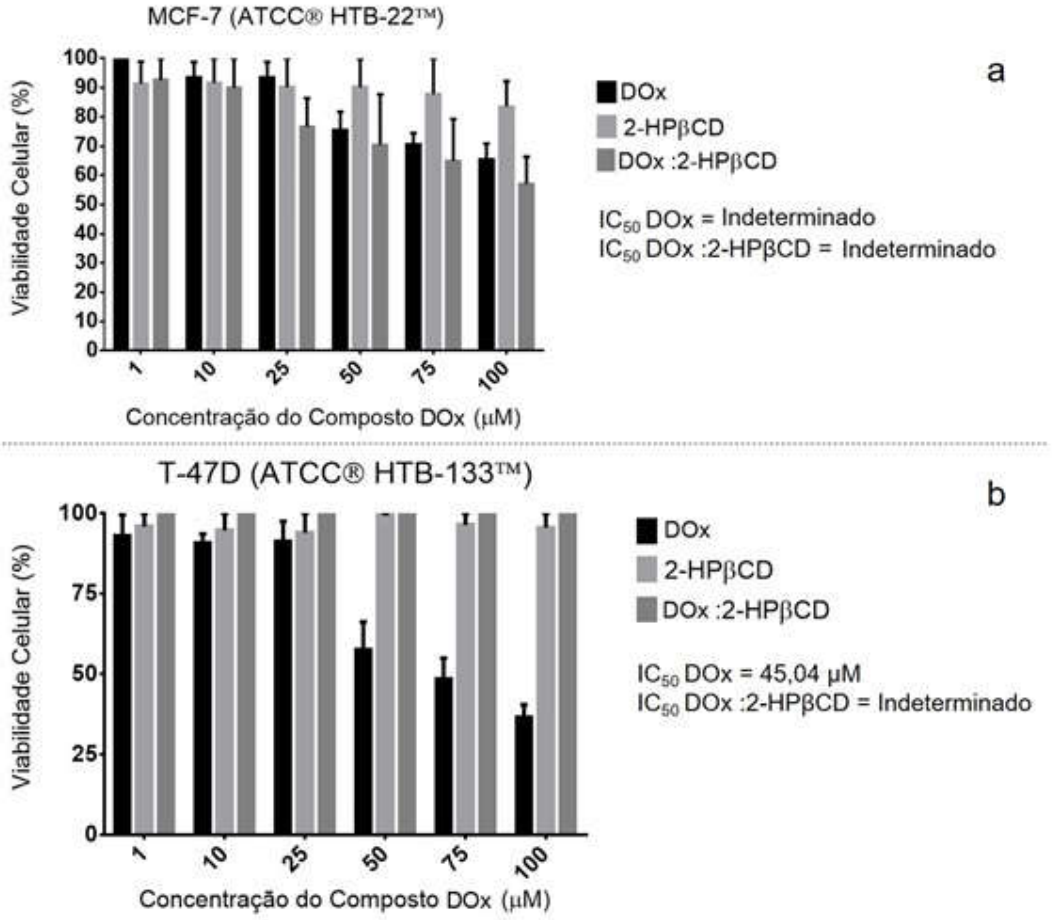

Figura 23 – Citotoxicidade de DOx, HP-β-CD e complexos de inclusão frente a linhagens de células tumorais da mama (MCF-7 e T-47D).

Podemos perceber que o DOx apresentou uma diminuição gradativa na viabilidade celular na linhagem tumoral de MCF-7 a partir de 10μM (93,59%) até 100μM (65,48%) comparado ao complexo de inclusão que obteve valores de 89,92% (10μM) e 57,06% (100μM). Adicionalmente, realizamos um teste t múltiplo para comparar as concentrações aplicadas em relação as mudanças na viabilidade e encontrar valores estatísticos significantes a partir das concentrações utilizadas. A análise demonstrou que a concentração de 25μM comparada entre o DOx e o complexo de inclusão foram próximas da significância estatística (p= 0,0568).

Em relação aos testes aplicados a linhagem tumoral de T-47D, observou-se que a atividade antitumoral foi maior em relação ao DOx em sua forma pura do que em relação ao seu complexo de inclusão. Em relação a análise estatística, exceto a concentração de 1μM e 25μM, o DOx apresentou uma significância estatística relevante (p<0,0001) em relação ao DOx:2-HPβCD. Devido a apresentação destes dados, sugere-se que a região

de interação tenha sido afetada devido a incorporação da molécula dentro da ciclodextrinas.

Um estudo conduzido por Agrawal *et al*., sugeriu que a citotoxicidade em células tumorais ocorra através da interação com os receptores ativados por proliferador de peroxissoma (do inglês, *PPARγ*) (AGRAWAL *et al.*, 2005). Tal observação já foi descrita por Pal *et al*., onde derivados oxazolidínicos apresentaram citotoxicidade contra células de câncer de mama (PAL *et al.*, 2014). Recentemente um estudo realizado por Campos *et al*., demonstrou que os DOX de família semelhante ao apresentado neste estudo, demonstraram uma atividade antitumoral relevante em células hematopoéticas, predominantemente leucêmicas com modulação dos genes envolvidos na apoptose (*PPARγ*), estresse do reticulo endoplasmático, necroptose e inflamação. Adicionalmente, os resultados obtidos a partir da molécula não encapsulada sugeriram que esta molécula possua uma importante função na inibição e indução da apoptose, no entanto, estudo comprobatórios devem ser realizados através de ensaios de biologia molecular com sondas marcadas (*PCR* em tempo real) (CAMPOS *et al.,* 2017) ou citometria de fluxo com marcadores fluorescentes como anexina e iodeto de propidío (*PI*) para esclarecer melhor os mecanismos molecular envolvidos entre este composto e as células-alvo (CROWLEY *et al.*, 2016).

6 CONCLUSÕES

A atividade biológica demonstrada pelo DOX apresentou uma atividade bacteriostática e fungistática na maioria dos microrganismos testados.

O DOX apresentou atividade fungicida em duas espécies de dermatófitos (*T. rubrum e T.* mentagrophytes) em concentrações de 16 μg/mL.

Os estudos *in silico* contribuíram para um maior entendimento sobre o comportamento da molécula em ciclodextrinas demonstrando viabilidade de desenvolver complexos de inclusão.

A metodologia de incremento de solubilidade baseada em ciclodextrinas no DOx foi bem sucedida e confirmada por métodos de caracterização e apresentando um aumento 20 vezes maior na solubilidade em água do que o composto puro.

A HP-β-CD demonstrou-se como um bom veículo de liberação de droga, aumentando sua solubilização em relação a mistura física e ao composto puro.

Os complexos de inclusão contendo DOx apresentou índices percentuais de viabilidade celular em *PBMCs,* demonstrando um baixo efeito citotóxico em células sanguíneas.

REFERÊNCIAS

AGRAWAL, A. K. *et al*. In vitro metabolism of a new oxazolidinedione hypoglycemic agent utilizing liver microsomes and recombinant human cytochrome P450 enzymes. **J Pharm Biomed Anal,** v. 37, n. 2, p. 351-8, fev, 2005.

ALEEM, O. *et al*. Effect of beta-cyclodextrin and hydroxypropyl beta-cyclodextrin complexation on physicochemical properties and antimicrobial activity of cefdinir. **J Pharm Biomed Anal,** v. 47, n. 3, p. 535-40, jul, 15 2008.

ALVES, R. J. *et al*. **N-substituted chiral aromatic oxazolidines, synthesis process, pharmaceutical composition and use**. BR n. PI PCT/BR2013/000347, set, 2012.

ANDERSON, D. J.; KAYE, K. S. Staphylococcal surgical site infections. **Infect Dis Clin North Am,** v. 23, n. 1, p. 53-72, mar, 2009.

ARMSTRONG-JAMES, D.; MEINTJES, G.; BROWN, G. D. A neglected epidemic: fungal infections in HIV/AIDS. **Trends Microbiol,** v. 22, n. 3, p. 120-7, mar, 2014.

AVNI, T.; LEIBOVICI, L.; PAUL, M. PCR diagnosis of invasive candidiasis: systematic review and meta-analysis. **J Clin Microbiol,** v. 49, n. 2, p. 665-70, fev, 2011.

AYATOLLAHI, M. S.; KAZEMI, A. In vitro and in vivo antidermatophytic activities of some Iranian medicinal plants. **Med Mycol**, jun, 2015.

BARTHOLOMEW, D. L.; CAPLOVICH, J. J.; WILDER, A. S. **Fungicidal and bactericidal therapeutic solution of sulfur dioxide**. US3105790A, jun, 1963.

BEGANOV,IC, M. et al. A Review of Combination Antimicrobial Therapy for Enterococcus Faecalis Bloodstream Infections and Infective Endocarditis. **Clin Infect Dis**, jan, 2018.

BEHROOZMAND, A.; KEATING, K.; AUKEN, E. A Review of the Principles and Applications of the NMR Technique for Near-Surface Characterization. **Surveys in Geophysics,** v. 36, n. 1, p. 27-85, out, 2015.

BOVERS, M.; HAGEN, F.; BOEKHOUT, T. Diversity of the Cryptococcus neoformans-Cryptococcus gattii species complex. **Rev Iberoam Micol,** v. 25, n. 1, p. S4-12, mar, 2008.

CAMPOS, J. F. *et al*. Synthesis and in vitro anticancer activity of new 2-thioxo-oxazolidin-4-one derivatives. **Pharmacol Rep,** v. 69, n. 4, p. 633-641, mar, 2017.

CARILLO-MUNOZ, A. J.; TUR-TUR, C. Comparative study of antifungal activity of sertaconazole, terbinafine, and bifonazole against clinical isolates of Candida spp., Cryptococcus neoformans and dermatophytes. **Chemotherapy,** v. 43, n. 6, p. 387-92, dez, 1997.

CHOE, H. W. *et al*. Crystallization and preliminary X-ray diffraction studies of alpha-cyclodextrin glucanotransferase isolated from Bacillus macerans. **Acta Crystallogr D Biol Crystallogr,** v. 59, n. Pt 2, p. 348-9, fev, 2003.

CHOI, J. H. *et al*. Prevalence and risk factors of esophageal candidiasis in healthy individuals: a single center experience in Korea. **Yonsei Med J,** v. 54, n. 1, p. 160-5, jan, 2013.

CIRRI, M. *et al*. Determination of stability constant values of flurbiprofen–cyclodextrin complexes using different techniques. **Journal of Pharmaceutical and Biomedical Analysis,** v. 37, n. 5, p. 995-1002, abr, 2005.

CROWLEY, L. C. *et al*. Quantitation of Apoptosis and Necrosis by Annexin V Binding, Propidium Iodide Uptake, and Flow Cytometry. **Cold Spring Harb Protoc,** v. 2016, n. 11, p. pdb.prot087288, nov, 2016.

D.G., C. **Analytical Chemistry: Solutions Manual.** 5. John Willeys & Sons, 1994. 162.

DARWAZAH, A.; BERG, G.; FARIS, B. Candida parapsilosis: an unusual organism causing prosthetic heart valve infective endocarditis. **J Infect,** v. 38, n. 2, p. 130-1, mar, 1999.

DAVIS, M. E.; BREWSTER, M. E. Cyclodextrin-based pharmaceutics: past, present and future. **Nat Rev Drug Discov,** v. 3, n. 12, p. 1023-1035, dez, 2004.

DE KRAKER, M. E. *et al*. The changing epidemiology of bacteraemias in Europe: trends from the European Antimicrobial Resistance Surveillance System. **Clin Microbiol Infect,** v. 19, n. 9, p. 860-8, set, 2013.

DEL VALLE, E. M. M. Cyclodextrins and their uses: a review. **Process Biochemistry,** v. 39, n. 9, p. 1033-1046, maio, 2004.

DEVI, K. *et al*. An Efficient Approach to the Synthesis of Nov,el Oxazolidinones as Potential Antimicrobial Agents. **Journal of Chemistry,** v. 2013, p. 5, jun, 2013.

DOVNIK, A. *et al*. Treatment of vulvovaginal candidiasis: a review of the literature. **Acta Dermatovenerol Alp Pannonica Adriat,** v. 24, n. 1, p. 5-7, 2015.

DUNN, B. K.; KRAMER, B. S. Cancer Prevention: Lessons Learned and Future Directions. **Trends in cancer,** v. 2, n. 12, p. 713-722, 2016.

DYE, C. After 2015: infectious diseases in a new era of health and development. **Philosophical Transactions of the Royal Society B: Biological Sciences,** v. 369, n. 1645, p. 20130426, 2014.

EASTBURN, S. D.; TAO, B. Y. Applications of modified cyclodextrins. **Biotechnol Adv,** v. 12, n. 2, p. 325-39, 1994.

ELSTNER, E. *et al*. Ligands for peroxisome proliferator-activated receptorgamma and retinoic acid receptor inhibit growth and induce apoptosis of human breast cancer cells in vitro and in BNX mice. **Proc Natl Acad Sci U S A,** v. 95, n. 15, p. 8806-11, jul, 1998.

ENG, S.-K. et al. Salmonella: A review on pathogenesis, epidemiology and antibiotic resistance. **Frontiers in Life Science,** v. 8, n. 3, p. 284-293, mar,. 2015.

ESPINEL-INGROFF, A.; KIDD, S. E. Current trends in the prevalence of Cryptococcus gattii in the United States and Canada. **Infect Drug Resist,** v. 8, p. 89-97, 2015.

FAUZIAH, C. I. *et al*. Thermal Analysis and Surface Morphology Study of Cholesterol: B-Cyclodextrin Inclusion Complex. **Advanced Materials Research,** v. 812, p. 221-225, 2013.

FIRACATIVE, C.; TRILLES, L.; MEYER, W. MALDI-TOF MS enables the rapid identification of the major molecular types within the Cryptococcus neoformans/C. gattii species complex. **PLoS One,** v. 7, n. 5, p. e37566, 2012.

GARCIA-CUESTA, C.; SARRION-PEREZ, M. G.; BAGAN, J. V. Current treatment of oral candidiasis: A literature review. **J Clin Exp Dent,** v. 6, n. 5, p. e576-82, dez, 2014.

GAVALDA, J. *et al*. Invasive fungal infections in solid organ transplant recipients. **Clin Microbiol Infect,** v. 20 Suppl 7, p. 27-48, set, 2014.

GONG, J.; ALKAN, S.; ANAND, S. A Case of Cutaneous Plasmablastic Lymphoma in HIV/AIDS with Disseminated Cryptococcus. **Case Rep Oncol Med,** v. 2013, p. 862585, 2013.

GOULD, I. M. The epidemiology of antibiotic resistance. **Int J Antimicrob Agents,** v. 32 Suppl 1, p. S2-9, nov, 2008.

GROMMES, C.; LANDRETH, G. E.; HENEKA, M. T. Antineoplastic effects of peroxisome proliferator-activated receptor gamma agonists. **Lancet Oncol,** v. 5, n. 7, p. 419-29, jul, 2004.

GROSE, J. H.; CASJENS, S. R. Understanding the enormous diversity of bacteriophages: the tailed phages that infect the bacterial family Enterobacteriaceae. **Virology,** v. 0, p. 421-443, 2014.

HALGREN, T. A. MMFF VI. MMFF94s option for energy minimization studies. **Journal of Computational Chemistry,** v. 20, n. 7, p. 720-729, 1999.

HAWKEY, P. M.; JONES, A. M. The changing epidemiology of resistance. **J Antimicrob Chemother,** v. 64 Suppl 1, p. i3-10, set, 2009.

HEISE, H. M. *et al*. Infrared spectroscopy and Raman spectroscopy of cyclodextrin derivatives and their ferrocene inclusion complexes. **Vibrational Spectroscopy,** v. 53, n. 1, p. 19-23, maio, 2010.

HIGUCHI, T.; CONNORS, K. A. Phase-solubility techniques. **Advances in Analytical Chemistry and Instrumentation,** v. 4, p. 117-212, 1965.

ILLNAIT-ZARAGOZI, M. T. *et al*. Cryptococcus and Cryptococcosis in Cuba. A minireview. **Mycoses,** v. 57, n. 12, p. 707-717, 2014.

IRIMIE, M. *et al*. Prevalence and Antifungal Susceptibility Patterns of Dermatophytes Isolated from Patients with Neoplastic Diseases: A Case Control Study. **Acta Dermatovenerol Croat,** v. 23, n. 2, p. 108-13, jul, 2015.

JAFARI, A. *et al*. Genotypic and phenotypic comparison of enteroaggregative Escherichia coli isolates from HIV-positive and non-HIV diarrheal samples. **Curr HIV Res,** v. 11, n. 8, p. 635-41, dez, 2013.

JOUDIEH, S. *et al*. Cyclodextrin polymers as efficient solubilizers of albendazole: complexation and physico-chemical characterization. **J Nanosci Nanotechnol,** v. 9, n. 1, p. 132-40, jan, 2009.

LA HOZ, R. M.; PAPPAS, P. G. Cryptococcal infections: changing epidemiology and implications for therapy. **Drugs,** v. 73, n. 6, p. 495-504, maio, 2013.

LANTERNIER, F. et al. Primar,y immunodeficiencies underlying fungal infections. **Current opinion in pediatrics,** v. 25, n. 6, p. 736-747, 2013.

LEE, J. D.; CLARKE, J. Cover up or cool it? Sexual intercourse during therapy for bacterial sexually transmitted infections--a discussion of evidence for efficacy of condom use preventing transmission during an acute bacterial STI. **Int J STD AIDS,** v. 15, n. 5, p. 285-8, maio, 2004.

LEMAIRE, S.; TULKENS, P. M.; VAN BAMBEKE, F. Cellular pharmacokinetics of the nov,el biaryloxazolidinone radezolid in phagocytic cells: studies with macrophages and polymorphonuclear neutrophils. **Antimicrob Agents Chemother,** v. 54, n. 6, p. 2540-8, jun, 2010.

LESNAKOVA, A. *et al*. Bacterial meningitis after sinusitis and otitis media: ear, nose, throat infections are still the commonest risk factors for the community acquired meningitis. **Neuro Endocrinol Lett,** v. 28 Suppl 3, p. 14-5, nov, 2007.

LI, N.; XU, L. Thermal analysis of β-cyclodextrin/Berberine chloride inclusion compounds. **Thermochimica Acta,** v. 499, n. 1–2, p. 166-170, fev, 2010.

LOFTSSON, T.; HREINSDÓTTIR, D.; MÁSSON, M. Evaluation of cyclodextrin solubilization of drugs. **International Journal of Pharmaceutics,** v. 302, n. 1–2, p. 18-28, set, 2005.

LOPES, W. A.; FASCIO, M. Esquema para Interpretação de Espectros de Susbtâncias Orgânicas na Região do Infravermelho. **Química Nov,a,** v. 27, n. 4, p. 4, 2004.

MAERTENS, J.; VREBOS, M.; BOOGAERTS, M. Assessing risk factors for systemic fungal infections. **Eur J Cancer Care (Engl),** v. 10, n. 1, p. 56-62, mar, 2001.

MAHABEER, Y. *et al*. Comparison of Etests and Vitek 2 (R) to broth microdilution for the susceptibility testing of Cryptococcus neoformans. **Diagn Microbiol Infect Dis,** v. 80, n. 4, p. 294-8, dez, 2014.

MALEY, C. C. et al. Classifying the evolutionary and ecological features of neoplasms. **Nature reviews. Cancer,** v. 17, n. 10, p. 605-619, set, 2017.

MANGOLIM, C. S. *et al*. Curcumin-beta-cyclodextrin inclusion complex: stability, solubility, characterisation by FT-IR, FT-Raman, X-ray diffraction and photoacoustic spectroscopy, and food application. **Food Chem,** v. 153, p. 361-70, jun, 15 2014.

MAZOLLA, A. A. Ressonância magnética: princípios de formação da imagem e aplicações em imagem funcional. **Revista Brasileira de Física Médica.,** v. 3, n. 1, p. 13, 2009.

MAZU, T. K. et al. The Mechanistic Targets of Antifungal Agents: An Overview. **Mini reviews in medicinal chemistry,** v. 16, n. 7, p. 555-578, 2016.

MCGUIRE, T. M.; SMITH, J.; DEL MAR,, C. The match between common antibiotics packaging and guidelines for their use in Australia. **Aust N Z J Public Health**, jun, 29 2015.

MENDONÇA, E. A. M. *et al*. Enhanced Antiproliferative Activity of the New Anticancer Candidate LPSF/AC04 in Cyclodextrin Inclusion Complexes Encapsulated into Liposomes. **AAPS PharmSciTech**, Boston**,** v. 13, n. 4, p. 1355-1366, set, 2012.

MUELLER, E. *et al*. Terminal differentiation of human breast cancer through PPAR gamma. **Mol Cell,** v. 1, n. 3, p. 465-70, fev, 1998.

MUSKETT, H. *et al*. Risk factors for invasive fungal disease in critically ill adult patients: a systematic review. **Crit Care,** v. 15, n. 6, p. R287, 2011.

NARESH, A. *et al*. Oxazolidinone derivatives: cytoxazone-linezolid hybrids induces apoptosis and senescence in DU145 prostate cancer cells. **Eur J Med Chem,** v. 80, p. 295-307, jun, 2014.

O'BOYLE, N. M. *et al*. Open Babel: An open chemical toolbox. **Journal of Cheminformatics,** v. 3, n. 1, p. 1-14, 2011.

PAL, T.; JOSHI, H.; RAMAA, C. S. Design and development of oxazol-5-ones as potential partial PPAR-gamma agonist against cancer cell lines. **Anticancer Agents Med Chem,** v. 14, n. 6, p. 872-83, 2014.

PAPPAS, P. G. et al. Clinical Practice Guideline for the Management of Candidiasis: 2016 Update by the Infectious Diseases Society of America. **Clinical Infectious Diseases: An Official Publication of the Infectious Diseases Society of America,** v. 62, n. 4, p. e1-e50, nov, 2016.

PENCHOVSKY, R.; TRAYKOVSKA, M. Designing drugs that overcome antibacterial resistance: where do we stand and what should we do? **Expert Opin Drug Discov,** v. 10, n. 6, p. 631-50, jun, 2015.

PIGHETTI, G. M. *et al*. Therapeutic treatment of DMBA-induced mammar,y tumors with PPAR ligands. **Anticancer Res,** v. 21, n. 2A, p. 825-9, abr, 2001.

PITTA, I. R. **Derivados 2-Tioxo-Oxazolidínicos-N-Substituídos potencialmente úteis na terapia anticâncer**. Digital. INDUSTRIAL, I. N. D. P. Brazil. BR1020150160607 2015.

PROSSER, G. A.; DE CARVALHO, L. P. S. Kinetic mechanism and inhibition of Mycobacterium tuberculosis d-alanine:d-alanine ligase by the antibiotic d-cycloserine. **FEV,S Journal,** v. 280, n. 4, p. 1150-1166, 2013.

RIBEIRO, M. A. *et al*. Prevalence and exoenzyme secretion by Candida albicans isolates from oral and vaginal mucosas of HIV-infected women. **Mycopathologia,** v. 157, n. 3, p. 255-61, abr, 2004.

RITZ, N.; CURTIS, N. Nov,el concepts in the epidemiology, diagnosis and prevention of childhood tuberculosis. **Swiss Med Wkly,** v. 144, p. w14000, 2014.

RODRIGUES, J. A. *et al*. Evaluation of biochemical and serological methods to identify and clustering yeast cells of oral Candida species by CHROMagar test, SDS-PAGE and ELISA. **Braz J Biol,** v. 64, n. 2, p. 317-26, maio, 2004.

ROMANO, C. *et al*. Primar,y cutaneous cryptococcosis due to Cryptococcus neoformans in a woman with non-Hodgkin's lymphoma. **Acta Derm Venereol,** v. 81, n. 3, p. 220-1, jul, 2001.

RONCO, C. Lipopolysaccharide (LPS) from the cellular wall of Gram-negative bacteria, also known as endotoxin, is a key molecule in the pathogenesis of set,sis and set,tic shock. Preface. **Blood Purif,** v. 37 Suppl 1, p. 1, 2014.

SADKOWSKA-TODYS, M.; CZARKOWSKI, M. P. Salmonellosis in Poland in 2012. **Przegl Epidemiol,** v. 68, n. 2, p. 243-8, 353-5, 2014.

SAENGER, W. *et al*. Structures of the Common Cyclodextrins and Their Larger Analogues-Beyond the Doughnut. **Chem Rev,** v. 98, n. 5, p. 1787-1802, jul, 1998.

SCHROEDER, G. N.; HILBI, H. Molecular Pathogenesis of Shigella spp.: Controlling Host Cell Signaling, Invasion, and Death by Type III Secretion. **Clinical Microbiology Reviews,** v. 21, n. 1, p. 134-156, jan, 2008.

SHAGHAFI, M. B.; GROTE, R. E.; JARVO, E. R. Oxazolidine synthesis by complementary stereospecific and stereoconvergent methods. **Org Lett,** v. 13, n. 19, p. 5188-91, out, 2011.

SHI, S. H. *et al*. Spectrum and risk factors for invasive candidiasis and non-Candida fungal infections after liver transplantation. **Chin Med J (Engl),** v. 121, n. 7, p. 625-30, abr, 2008.

SHINABARGER, D. Mechanism of action of the oxazolidinone antibacterial agents. **Expert Opin Investig Drugs,** v. 8, n. 8, p. 1195-202, ago, 1999.

SILVERSTEIN, R. M.; BRASSLER, G. C.; MORRILL, T. C. **Identificação espectrométrica de compostos orgânicos.** . 6. Rio de Jan,eiro: Guanabara, 2000. 460.

SIVAKUMAR,, V. G. *et al*. Use of CHROMagar in the differentiation of common species of Candida. **Mycopathologia,** v. 167, n. 1, p. 47-9, jan, 2009.

SOBCZAK, M. *et al*. Polymeric systelms of antimicrobial peptides--strategies and potential applications. **Molecules,** v. 18, n. 11, p. 14122-37, nov, 2013.

SOFIAN, Z. M. *et al*. Evaluation of the Cytotoxicity of Levodopa and its Complex with Hydroxypropyl-ß-Cyclodextrin (HP-ß-CD) to an Astrocyte Cell Line. **The Malaysian Journal of Medical Sciences : MJMS,** v. 21, n. Spec Issue, p. 6-11, nov, 2014.

SONGNGAM, S. *et al*. A 5,7-Dimethoxyflavone/Hydroxypropyl-β-Cyclodextrin Inclusion Complex with Anti-Butyrylcholinesterase Activity. **AAPS PharmSciTech**, Boston**,** v. 15, n. 5, p. 1189-1196, maio, 2014.

SORABJEE, J. S.; GARJE, R. R. Response to . . . successful use of oral linezolide. **J Infect,** v. 48, n. 4, p. 365-6, maio, 2004.

SUH, N. *et al*. A new ligand for the peroxisome proliferator-activated receptor-gamma (PPAR-gamma), GW7845, inhibits rat mammar,y carcinogenesis. **Cancer Res,** v. 59, n. 22, p. 5671-3, Nov, 1999.

SUN, H. *et al*. Antibacterial Activity of β-Cyclodextrin and 2-Hydroxypropyl-β-Cyclodextrin Trimethoprim Complexes **American Journal of Microbiology,** v. 2, n. 1, p. 8, 2011.

SZEJTLI, J. Downstream processing using cyclodextrins. **Trends in Biotechnology,** v. 7, n. 7, p. 170-174, jul, 1989.

TADESSE, M. *et al*. Synoxazolidinone C; a bicyclic member of the synoxazolidinone family with antibacterial and anticancer activities. **Tetrahedron Letters,** v. 52, n. 15, p. 1804-1806, abr, 2011. ISSN 0040-4039.

THEOCHARIS, S. *et al*. Peroxisome proliferator-activated receptor-gamma ligands as cell-cycle modulators. **Cancer Treat Rev,** v. 30, n. 6, p. 545-54, out, 2004.

TOMA, S. H.; TOMA, H. E. Self assembled rotaxane and pseudo-rotaxanes based on b-cyclodextrin inclusion compounds with trans-1,4-bis[(4-pyridyl)ethenyl]benzene-pentacyanoferrate(II) complexes. **Journal of the Brazilian Chemical Society,** v. 18, p. 279-283, 2007.

TORRES-RODRIGUEZ, J. M. *et al*. MICs and minimum fungicidal concentrations of posaconazole, voriconazole and fluconazole for Cryptococcus neoformans and Cryptococcus gattii. **J Antimicrob Chemother,** v. 62, n. 1, p. 205-6, jul, 2008.

TREIB, J. *et al*. An international view of hydroxyethyl starches. **Intensive Care Med,** v. 25, n. 3, p. 258-68, mar, 1999.

TROTT, O.; OLSON, A. J. AutoDock Vina: improving the speed and accuracy of docking with a new scoring function, efficient optimization, and multithreading. **J Comput Chem,** v. 31, n. 2, p. 455-61, jan, 2010.

VILLEMAGNE, B. *et al*. Tuberculosis: The drug development pipeline at a glance. **European Journal of Medicinal Chemistry,** v. 51, n. 0, p. 1-16, 2012.

WASHINGTON, J. A. Principles of Diagnosis. In: BARON, S. (Ed.). **Medical Microbiology**. 4th. Galveston (TX), 1996.

WEITZMAN, I.; SUMMERBELL, R. C. The dermatophytes. **Clin Microbiol Rev,** v. 8, n. 2, p. 240-59, abr, 1995.

WENZ, G. Cyclodextrins as Building Blocks for Supramolecular Structures and Functional Units. **Angewandte Chemie International Edition in English,** v. 33, n. 8, p. 803-822, 1994.

WHO. Antimicrobial resistance. Internet, Abr,il 2015. Disponível em: < http://www.who.int/mediacentre/factsheets/fs194/en/ >. Acesso em: 09 jan, 2015.

YAPAR, N. Epidemiology and risk factors for invasive candidiasis. **Ther Clin Risk Manag,** v. 10, p. 95-105, 2014.

ZHANG, W. F. *et al*. Biocompatibility study of theophylline/chitosan/beta-cyclodextrin microspheres as pulmonary delivery carriers. **J Mater Sci Mater Med,** v. 20, n. 6, p. 1321-30, jul, 2009.

APENDICE A: ARTIGO SUBMETIDO Á PHARMACOLOGICAL REPORTS, ELSEVIER

SOLUBILITY ENHANCEMENT OF OXAZOLIDINE DERIVATIVE BASED ON CYCLODEXTRIN INCLUSION COMPLEX: A MOLECULAR MODELING APPROACH AND PHYSICOCHEMICAL CHARACTERIZATION

Rafael R. Silva[a], Felipe S. Rocha[a], Jamerson F. Oliveira[b], Cézar A.C. Amorim[b], Marina F. Cordeiro[c], Fernanda G. Beserra[c], Moacyr, J.B.M. Rêgo, Maria C.A. Lima[b], Marcelo M. Rabello[d], Marcelo Z. Hernandes [a,d], Moacyr J.B.M. Rêgo[a,c], Maira G.R. Pitta[a,c], Marina G.R. Pitta[e], Maria D.L. Oliveira[a,f], Ivan R. Pitta [a,e], César A.S. Andrade[a,f,*]

[a]Programa de Pós-Graduação em Inovação Terapêutica, Centro de Ciências Biológicas, Universidade Federal de Pernambuco, 50670-901 Recife, PE, Brasil

[b]Laboratório de Química e Inovação Terapêutica, Departamento de Antibióticos, Universidade Federal de Pernambuco, 50670-901 Recife, PE, Brasil

[c]Laboratório de Imunomodulação e Novas Abordagens Terapêuticas, Universidade Federal de Pernambuco, 50670-901 Recife, PE, Brasil

[d]Laboratório de Química Teórica Medicinal, Universidade Federal de Pernambuco, 50670-901 Recife, PE, Brasil

[e]Laboratório de Planejamento e Síntese de Fármacos (LPSF), Universidade Federal de Pernambuco, 50670-901 Recife, PE, Brasil

[f]Laboratório de Biodispositivos Nanoestruturados, Universidade Federal de Pernambuco, 50670-901 Recife, PE, Brasil

***Corresponding Author:** Cesar A.S. Andrade

Laboratório de Biodispositivos Nanoestruturados, Departamento de Bioquímica, UFPE, 50670-901, Recife, PE, Brazil. Phone: +55 81 2126.8450; Fax: +55 81 2126.8547

E-mail: csrandrade@gmail.com

ABSTRACT

Oxazolidine derivatives (OxD) have been described as third-line antibiotics and some reports demonstrated their potential as antitumor agent. However, OxD have low water solubility that limit their use. In this context, the development of inclusion complexes based on cyclodextrin (CD) results in increment of the solubility of these hydrophobic compounds improving the bioavailability. In this study, we developed inclusion complexes based on 2-hydroxy-beta-cyclodextrin (2-HPβCD) and a new synthetic hydrophobic OxD compound (5-benzyl-3-ethyl-2-thioxazolidin 4-one). Initially, we conducted an *in silico* study to evaluate the interaction capacity between a novel OxD and 2-HPβCD. Subsequently, analytical characterization techniques were performed through scanning electron microscopy (SEM), Fourier transformed infrared (FTIR), nuclear magnetic resonance spectroscopy (^{1}H-NMR), X-ray diffraction and thermal analyses. The maximum increment of solubility was obtained at 70 mM OxD using 400 mM 2-HPβCD, resulting in a twenty-fold increase of the solubility comparing OxD in water (0.64 mM). SEM analyses revealed a significant change in the morphology of the molecules after the inclusion process. FTIR spectra indicated the formation of inclusion complexes, considering the decrease in the intensity of the absorption bands of the functional groups of OxD. The chemical shift changes observed in ^{1}H-NMR data indicated 1:1 stoichiometry for the association between OxD and 2-HPβCD. Thermal analyses indicated that the presence of OxD in the inner cavity of 2-HPβCD (inclusion complex) provided different thermal behavior. The degradation time was increased as compared to pure compounds. In conclusion, *in silico* studies provided a foremost insight about the interactions between OxD and 2-HPβCD. The physicochemical characterization confirmed the drug solubility enhancement.

KEYWORDS: *Oxazolidine; Cyclodextrin; Inclusion Complex; Molecular Modelling.*

ABSTRACT

Oxazolidine derivatives (OxD) have been described as third-line antibiotics and antitumoral agents. However, OxD have low water solubility that limit their use. In this context, the inclusion complexes based on cyclodextrin (CD) could improve the solubility and bioavailability of these compounds. In this study, we developed a novel synthetic OxD and inclusion complexes based on 2-hydroxy-beta-cyclodextrin (2-HPβCD). Initially, we conducted an *in silico* study to evaluate the interaction capacity between OxD and 2-HPβCD. Characterization studies were performed through scanning electron microscopy (SEM), Fourier transformed infrared (FTIR), nuclear magnetic resonance spectroscopy (^{1}H-NMR), X-ray diffraction (XRD) and thermal analyses (DSC/TGA). We performed a kinetic profile study of the OxD and cytotoxicity assay using peripheral blood mononuclear cells (PBMCs). The maximum increment of solubility was obtained at 70 mM OxD using 400 mM 2-HPβCD. SEM analyses revealed morphological changes after inclusion process. FTIR spectra indicated the formation of inclusion complexes, considering the intensity decrease of absorption bands from OxD functional groups. ^{1}H-NMR presented chemical shifts that indicated 1:1 stoichiometry from OxD:2-HPβCD. The inclusion complex also indicated different thermal behaviors compared to pure OxD. The pharmacokinetic profile showed a short release time. Pure OxD and its inclusion complex did not exhibit cytotoxicity in PBMCs. In conclusion, *in silico* studies provided a foremost insight about the interactions between OxD and 2-HPβCD.

Keywords: *Oxazolidine; Cyclodextrin; Inclusion Complex; Molecular Modelling.*

1. Introduction

Oxazolidine derivatives (OxDs) are synthetic five ring-membered compounds, which contains at least one oxygen and nitrogen in their molecular structure. In addition, OxD have been used as antitumor agents due to their pharmaceutical properties (ALVES, FERNANDES*, et al.*, 2014a; b). Recently, a previous study demonstrated that a new OxD (5-benzyl-3-ethyl-2-thioxazolidin 4-one) presented cytotoxic activity in leukemic lineage cells (HL-60 ATTC®CCL-240) through apoptosis induction mechanisms (CAMPOS, J. F. *et al.*, 2017). OxDs have a large oral application, however hydrophobic characteristics limit their use *in vivo* (PANDIT *et al.*, 2012). To overcome this limitation, cyclodextrins (CD) have been used as an alternative to increase the solubility through inclusion complexes (SAVJANI, KETAN T. *et al.*, 2012).

CD are cyclic oligosaccharides composed by a hydrophilic outer layer and an internal cavity with the capacity to incorporate hydrophobic drugs. These molecules offers other advantages such as pharmacokinetic profile, chemical stability and low toxicity (TIWARI *et al.*, 2010). 2-hydroxylpropyl-β-cyclodextrin (2-HPβCD) is an alternative to α-, β- and γ-CD, with improved water solubility and low toxicological effects (GOULD e SCOTT, 2005). Furthermore, 2-HPβCD has been pharmaceutically used for parenteral, oral, ophthalmic and nasal applications (CHALLA *et al.*, 2005; RASHEED *et al.*, 2008). In general, analytical techniques to evaluate inclusion complexes involves the use Fourier transformed infrared spectroscopy (FTIR), nuclear magnetic resonance (NMR), scanning electron microscopy (SEM) and thermal analyses (BREWSTER e LOFTSSON, 2007).

In silico studies involve the use of theoretical and computational methods that contribute to mimic the behavior of molecules. There are some previous reports in the literature using molecular modeling of drugs in 2-HPβCD inclusion complexes (CAVALCANTI *et al.*, 2011; MENDONCA *et al.*, 2012; MILETIC *et al.*, 2013; SILVA *et al.*, 2016). One advantage of the molecular modeling is to predict the behavior of the guest molecule with a single carrier or host molecule avoiding expensive assays (ALVIRA *et al.*, 1997; PIEL *et al.*, 2001).

In this study, we performed physicochemical characterization and molecular modeling to elucidate the specific aspects of intermolecular interaction and calculate the interaction energy between a new OxD and 2-HPβCD. To the best of our knowledge there is no previous work reporting the molecular modeling of 5-benzyl-3-ethyl-2-thioxazolidin 4-one and 2-HPβCD.

2. Materials and methods

2.1.Materials

OxD (5-benzyl-3-ethyl-2-thioxazolidin 4-one) (Fig. 1) was kindly provided by Laboratory of Planning and Syntheses of Drugs at Federal University of Pernambuco (Brazil) (PITTA, 2015). 2-HPβCD, acetone, MTT were purchased from Sigma-Aldrich (St. Louis, USA). Deionized (DI) water was obtained from a Milli-Q water purification system (Billerica, MA, USA).

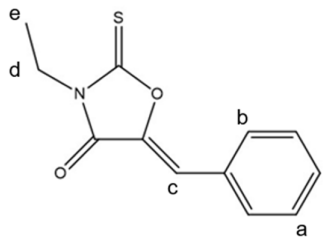

Figure 1. Chemical structure of the new OxD (5-benzyl-3-ethyl-2-thioxazolidin 4-one).

*2.2.*OxD Synthesis

In the first step, Cope esters were obtained from the Knoevenagel condensation reaction. After that, equimolar amounts of 2-cyano-ethyl acetate and substituted benzaldehydes were mixture in the presence of triethylamine (catalyst) and toluene (solvent) at 110ºC. After 24 hours, the obtained product was recrystallized. The product was washed successively with ethanol and separated to the next step [22]. Subsequently, Cope esters reacted with equimolar amounts of 3-ethyl-2-tioxazolidin-4-one via Michael addition reaction in the presence of morpholine (catalyst) and ethanol (solvent) under reflux for 24 hours. The final product was subjected to further purification with absolute ethanol. This procedure was performed to obtain an OxD 5-benzylidene-3-ethyl-2-thioxooxazolidin-4-one (LPSF/NB14) (MOURAO *et al.*, 2005).

2.3.Molecular modelling of the OxD: 2-HPβCD inclusion complex

Two synthetic aspects of 2-HPβCD were taken into consideration for molecular modelling, as follow: a) Regioselective: the reaction preferably occurs at the primary hydroxyl group OH (6), since these are most accessible, followed by the secondary hydroxyl OH (2) with the highest acidity (pKa=12.2) (WENZ, 1994); b) Homologous

derivatives with lower and higher molar substitution ratio (MS) (TREIB *et al.*, 1999), which are also formed in the mixture obtained as the final product (WENZ, 1994).

Our approach was to virtually construct 1000 structures (40 configurations with 25 different conformations each) for the 2-HPβCD model, starting from the tridimensional structure of the βCD (SAENGER *et al.*, 1998). The 40 configurations were built considering both synthetic aspects mentioned before. Taking into account the MS of 0.6, it seems reasonable to consider that the 2-HPβCD structure (7 glucose units) has, on average, 4 HP units (0.6×7=4.2). Thus, 20 configurations of 2-HPβCD were built with 4 HP units, 10 configurations with 3 HP units, and 10 configurations with 5 HP units. For each HP unit added, has been taken into account the probability of 70% for OH (position 6), 20% for OH (position 2), and 10% for OH (position 3), in order to select the OH position for substitution. The conformer search was performed using Genetic Algorithm and Energy Score Function available at the OpenBabel library (O'BOYLE *et al.*, 2011), with default convergence parameters. The geometry optimizations for all the 1000 structures were computed using MMFF94s force field (HALGREN, 1999), again with the same library and default criteria.

Following, a molecular docking approach was applied in order to find the host:guest (OxD: 2-HPβCD) inclusion complexes. The Autodock VINA software (TROTT e OLSON, 2010) was used, considering each entire 2-HPβCD derivative structure as the active site, and adjusting the exhaustiveness parameter to 8. The intermolecular interaction energies for all 1000 complexes were calculated. The entire approach used for molecular modeling was carried out in an automated fashion, using a platform developed by our research group, named CycloMolder (unpublished results).

2.4.Phase Solubility Study of OxD:2-HPβCD

The phase solubility study was carried out according to Higuchi and Connors (HIGUCHI e CONNORS, 1965) to determine the stoichiometric ratio of the host:guest compounds. Six fixed amounts of OxD (1.67 mg) were mixed to 2 mL 2-HPβCD aqueous solution ranging from 0 to maximum solubility (1.38×10^6 mM) and, subsequently, vigorously stirred for 48 h at 25 ºC. After, the samples were centrifuged at 8,972 g for 10 min and filtered with 0.45 μm PVDF membranes (Macherey-Nagel, Dueren, DE). The filtered solution was analyzed using a UV-visible spectrophotometer at $\lambda = 286$ nm. From the slope and intercept value (S_0) of the phase solubility curve, a stability constant (Kc) was determined, as follow:

$$K_{1:1} = \frac{slope}{[S_0 \times (1 - slope)]} \quad (1)$$

The complexation efficiency (CE) of OxD was determined from data of the phase solubility curve according to the following equation:

$$CE = \frac{slope}{(1 - slope)} \quad (2)$$

2.5.Preparation of OxD:2-HPβCD inclusion complexes

Co-precipitation method was used to obtain inclusion complexes (Ghosh *et al*. 2011). Initially, OxD and 2-HPβCD at equimolar ratios (1:1) were dissolved in acetone: water (3:1, v/v). OxD solution was dropwise added to the 2-HPβCD solution and maintained under stirring for 6 h. Subsequently, the samples were submitted to rotary evaporation at 45°C for 90 min. After, the material was partially dried and the solid was lyophilized (4×10^{-6} Barr) for 24 h and stored in desiccators until use. The physical mixture was obtained mixing OxD and 2-HPβCD at equimolar ratios (1:1) in a mortar and pestle for 10 min to obtain a homogeneous mixture.

2.6.Characterization

Morphological analysis were performed using a QUANTA 200 (FEI, OR, USA) scanning electron microscope at 30 kV. The samples were placed on aluminum stubs with double-sided carbon tape and thin gold films were evaporated on the sample surface by using high vacuum film deposition system (SCD 500 Mycrosystems Leica, Wetzlar, DE). Infrared spectra of the OxD and inclusion complexes were recorded using a Vertek 70 Fourier Transform Infrared Spectrophotometer (Bruker, MA, USA) in the range 4000-400 cm^{-1}. All samples were evaluated using KBr pellet method. The baseline correction was performed using a pure KBr disk. ^{13}C and ^{1}H-NMR spectra were recorded on a Varian 400 MHz NMR Spectrometer (Varian, USA) using TMS as internal standard and DMSO-d6 as solvent. The chemical shifts were reported in δ (ppm). XRD diffraction data were collected with a D8 Advance X-ray diffractometer (Bruker, MA, USA) using CuKα radiation in the range of 2θ (30-60)º at 0.03º/second. Simultaneous thermogravimetric (TGA) and differential thermal analysis (DTA) measurements were performed using a STA 449 F3 Jupiter® (NETZSCH, Asch, CZ). The samples were placed in a closed platinum crucible and DSC thermograms were recorded at a heating rate of 10°C.min^{-1} in the range of 20° to 310°C (LI e XU, 2010).

2.7. In vitro release study

In vitro release studies of pure and OxD/2-HPβCD inclusion complexes from physical mixture and co-evaporation method were performed in triplicate according to Ch.P (2010 Edition, Part 2, Appendix XC. No.2 method) and USP 30-NF 25 (2007 Edition, Volume 1, <711> Apparatus 2) using a Rcz-602 Dissolution Apparatus (Shanghai Huanghai Medicine Checking Instrument Co., Ltd). Briefly, 2 mg of OxD or OxD:2-HPβCD inclusion complexes were added to 250 mL of DI water (37 ± 0.5 ºC) and stirred at 50 rpm. At predetermined time intervals, 5 mL of the previous solution was withdrawn and centrifuged at 12,000 rpm for 5 min. The drug content was measured at λ = 282 nm using UV spectrometry. The cumulative release rate was calculated at each time interval.

2.8. PBMC cytotoxicity assay

Peripheral blood mononuclear cells were obtained from heparinized blood from healthy donors (n=5) and the cells were isolated via a standard method of density-gradient centrifugation over Ficoll-Hypaque solution (GE Healthcare). Cells were counted in a Neubauer chamber and viability was determined by trypan blue exclusion method. Cells were used only when the viability was >98%. All donors gave informed consent and the Human Research Ethics Committee of UFPE approved the study. The cells were cultured in RPMI-1640 medium supplemented with 10 % fetal calf serum, 2 mM glutamine, 100 mg/mL streptomycin, and 100 U/mL penicillin at 37ºC with 5 % CO_2. PBMCs were plated in 96-well plates (10^4 cells/well) during the cytotoxicity assay. After, OxD compound (1, 10, 25, 50, 75 and 100 μM) was diluted in a dimethylsulfoxide (DMSO) solution and added to each well. The cells were incubated for 72 h. The control groups were treated with the same amount of 0.1 % DMSO.

The growth of PBMCs was quantified by the ability of living cells to reduce the yellow dye 3-(4,5-dimethyl-2- thiazolyl)-2,5-diphenyl-2H-tetrazolium bromide (MTT) to a blue formazan product. After 72 h of incubation, the medium in each well was replaced with fresh medium (200 μL) containing MTT (0.5 mg/mL). After 3h, the formazan product of MTT reduction was dissolved in 20 % sodium dodecyl sulfate, and the absorbance of the solution was measured at λ = 570 nm with a multiplate reader (EL808, Biotek, USA). The cytotoxicity was expressed as the concentration inhibiting 50% of cell proliferation (IC50), which is the percentage reduction in cell viability calculated from

the ratio between the number of cells treated with OxD, inclusion complexes and untreated cells (control).

3. Results and Discussion

3.1.OxD Molecular Elucidation

RMN^{1}H: (400 MHz, DMSO-d_6): δ=1.22 (t, 3H, CH_3, *J*= 7,2 Hz), 3.82 (q, 2H, CH_2, *J*= 7,2 Hz), 6.94 (s, 1H, =C-H), 7.49-7.56 (m, 3H, C-H Ar), 7.88 (d, 2H, *J*= 8,4 Hz, C-H Ar). RMN ^{13}C (100 MHz, DMSO-d_6): δ= 11.68 (CH_3), 37.73 (CH_2), 112.42 (HC=C), 129.18 (CH Ar), 130.59 (CH Ar), 130.97 (Cq) 131.04 (CH Ar), 139.10 (Cq), 161.54 (C=S), 183.32 (C=O) IV (KBr): $\tilde{\nu}$= 1747 (C=O), 1675 (C=C), 1163 (C=S).

3.2. Molecular modelling of the OxD:2-HPβCD inclusion complex

The molecular docking results showed two main orientations regarding the relative position of the guest molecule (OxD) into the host molecule (2-HPβCD). The first one, called orientation I, has the 2-thioxo-oxazolidine-4-one ring at the wider rim of the 2-HPβCD, and the other one, called orientation II, has the benzene ring at the wider rim. The average docking energy for the ten first best solutions, considering orientation I, is -5.6 kcal/mol. On the other hand, the average energy of the ten first best solutions for orientation II is -5.4 kcal/mol, therefore less stable.

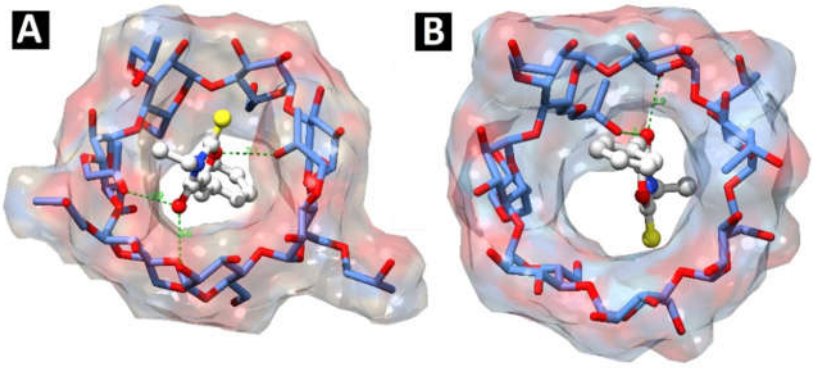

Figure 2. Summary of the molecular docking results. A) Best docking solution for orientation I. B) Binding energy (kcal/mol) table of the ten best docking solutions for each orientation. C) Best docking solution for orientation II. Dashed lines represents intermolecular hydrogen bonds between host (2-HPβCD) and guest (OxD) molecules.

The overall best docking solution for orientation I is shown at Fig. 2a, with a docking energy of -5.9 kcal/mol, while the overall best docking solution for orientation

II can be found at Fig. 2b, with an energy of -5.6 kcal/mol. The best docking solution for orientation I is stabilized by several hydrophobic contacts and by three hydrogen bonds (2.9 Å, 3.0 Å and 3.1 Å), while the best solution for orientation II is also stabilized by several hydrophobic contacts, but only by two hydrogen bonds (2.9 Å and 3.1 Å). The final molecular modeling results point out the orientation I as the most stable, and it should occurs in the mixture by a major ratio, for the OxD:2-HPβCD (host:guest) inclusion complex. Our results indicated the possibility to incorporate OxD into 2-HPβCD and overcome its low aqueous solubility. According to previous studies, 2-HPβCD affects the pharmacokinetic profile associated to a short release time and high amount of mass dissolved in the bulk (DAHIYA e PATHAK, 2006; CAVALCANTI *et al.*, 2011).

3.3. Phase Solubility Study

OxD results in an A_L-curve type phase solubility diagram with 2-HPβCD in water (Fig. 3).

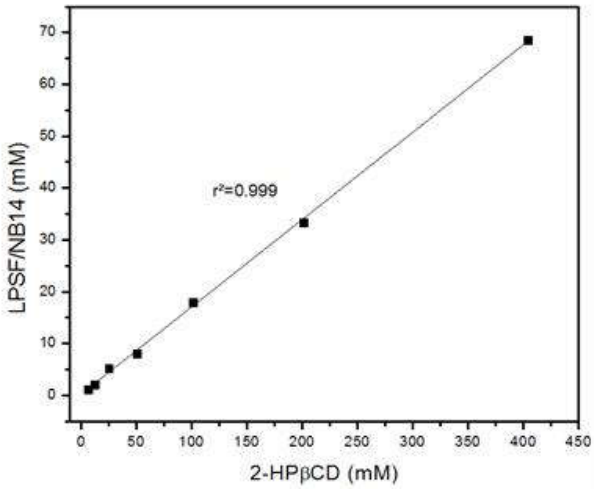

Figure 3. Phase stability diagrams for OxD in the presence of 2-HPβCD at room temperature.

Data were fitted by linear regression leading to the following equation: $[OxD]_{water} = 0.1686 \times [2\text{-HP}\beta\text{CD}] + 0.1950$ ($r^2 = 0.98915$). The solubility constants of OxD with 2-HPβCD in water at 25°C was K1:1=0.316 and S_0=0.64mM. The enhancement of OxD solubility after 2-HPβCD association was obtained initially at 12.62 mM. Of note, it was obtained a twentyfold increase over OxD solubility in water (0.64 mM). The CE was calculated according to Eq. 2 and the result was equivalent to 0.202 for OxD. According

to Loftsson *et al*., if CE is 0.1 then 1 out every 11 CD molecules form a complex with drug. Our results suggest that approximately 1 out 5 CD molecules forms a complex with OxD (LOFTSSON *et al.*, 2005).

3.4. Morphological Analysis

The morphology of OxD and its inclusion complex was evaluated using SEM (Fig. 4).

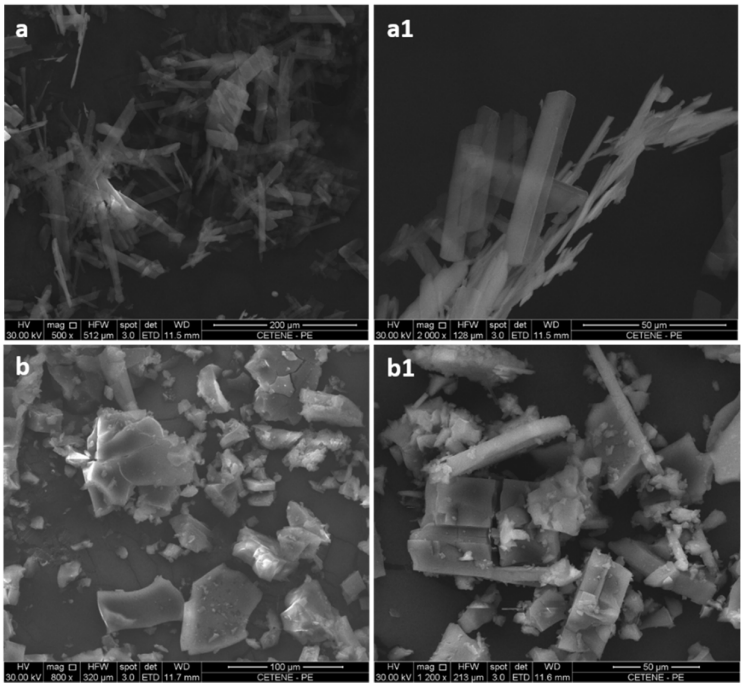

Figure 4. Micrographs of OxD (a) and OxD:2-HPβCD inclusion complex (b).

OxD image demonstrates a long crystal with a smooth surface presenting an acicular shape (Fig. 4a). On the other hand, inclusion complex images revealed significant changes in the morphology showing an amorphous form followed by aggregation (Fig. 4b). The regular shape of the drug is affected since 2-HPBCD is an amorphous material (CIRRI *et al.*, 2005). The morphology of the inclusion complex is similar to other previous studies (FAUZIAH *et al.*, 2013; SONGNGAM *et al.*, 2014). Our data suggest the incorporation of the OxD in the inner cavity of 2-HPβCD.

3.5. FTIR analysis

FTIR spectra from co-evaporation and physical mixture methods were compared to evaluate efficiency between these methodologies (Fig. 5).

Figure 5. FTIR spectra of OxD and OxD:2-HPβCD inclusion complex by physical

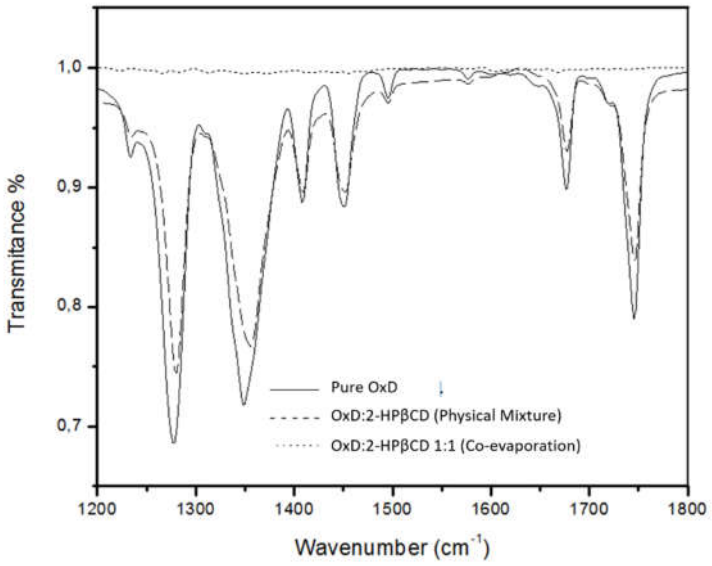

mixture and co-evaporation method at 1:1 molar ratio.

FTIR spectrum of OxD showed the presence of bands at 1750-1735 cm^{-1} (C=O stretch), 1600-1585 cm^{-1} (C–C stretch, aromatic), 1360-1290 cm^{-1} (C–N stretch, aliphatic amines) and 1050-1200 cm^{-1} (C=S stretch, thiocarbonyl). The FTIR spectrum of OxD also shows the presence of bands at ~3016 (C–H stretching vibration), 1745 and 1695 (C=O stretching), and 1631 cm^{-1} (C=C stretching). The FTIR spectrum of 2-HPβCD show prominent absorption bands at ~3411 (O–H stretching vibration), ~2931 (C−H stretching vibration), ~1157, ~1089, and ~1029 cm^{-1} (C−H and C−O stretching vibration). 2-HPβCD presented a large overlap of signals, with small changes in the intensity and broadenings of the absorption bands, indicating the formation of inclusion complexes with typical fingerprint bands. The results showed the formation of the inclusion complexes, considering the decrease in the intensity of the absorption bands of the OxD functional groups. Our results indicate that co-evaporation method was more efficient as compared to the physical mixture method.

3.6. Nuclear magnetic resonance spectroscopy (^{1}H-NMR) measurements

^{1}H-NMR experiments were performed to confirm the formation of OxD:2-HPβCD inclusion complex. The chemical shifts (Δδ) of the pure compounds at 1:1 molar ratio were evaluated (Table 1). The OxD ^{1}H-NMR presented (400 MHz, DMSO-d6):

δ=1.22 (t, 3H, CH_3, J= 7,2 Hz), 3.82 (q, 2H, CH_2, J= 7,2 Hz), 6.94 (s, 1H, =C-H), 7.49-7.56 (m, 3H, C-H Ar), 7.88 (d, 2H, J= 8,4 Hz, C-H Ar). Chemical shift changes of H_4 was verified at 1:1 ($\Delta\delta H_4$=0.010 ppm). Our results indicated the potential of 1:1 stoichiometry for OxD interaction in the inner cavity of 2-HPβCD. However, other conformations are not excluded, given that a higher chemical shift changes in the $H_{1,2,3,5}$ proton ranged from 0.020 ppm to 0.030 ppm (Table 1). The chemical shift changes suggest that hydrogen bonds contribute to the insertion of the compound into the CD cavity (HARA *et al.*, 2006).

3.7. X-ray diffraction measurements

XRD patterns presented two well-defined peaks for OxD (Fig. 6) that represent a typical structural order of a crystalline solid.

Figure 6. X-ray diffraction patterns of the OxD, 2-HPβCD and OxD:2-HPβCD inclusion

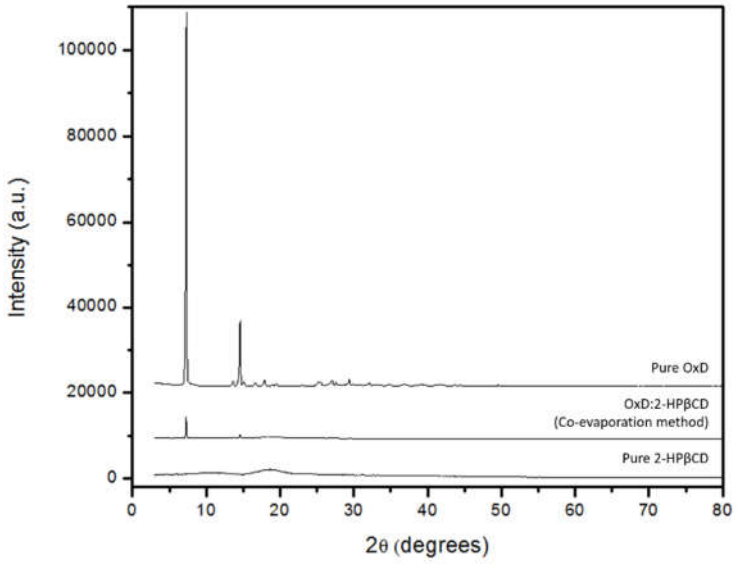

complex.

In general, natural and synthetic CD have no well-defined peaks which are characterized as amorphous materials (CHOE *et al.*, 2003). A decrease in the peak intensity of the inclusion complex is observed indicating a crystallinity loss. In the inclusion complex through our methodology it is possible to observe a small peak of intensity from inclusion complex compared to the pure compound. These data suggest that a greater amount of available cyclodextrin could incorporate into the remainder of the unloaded OxD compounds.

3.8. Thermal Analysis

The thermal behavior of pure compounds and inclusion complex was evaluated. OxD showed an endothermic peak at 136.57 ºC with a reaction heat of 4.19 J/g that occurs before of the decomposition temperature. An exothermic peak at 103.52 ºC with a reaction heat of 1.07 J/g was observed for 2-HPβCD. By observing the thermal behavior of the OxD:2-HPβCD inclusion complex, we noticed the presence of an exothermic shift 143.77 ºC with a reaction heats of 0.83 J/g. A significant shift in the thermal behavior was obtained for the inclusion complex (Fig. 7a).

Figure 7. DSC (a) and TG (b) curves of OxD and OxD:2-HPβCD inclusion complexes at 1:1 molar ratio.

Given the analysis of thermogravimetric curves, it is possible to observe a

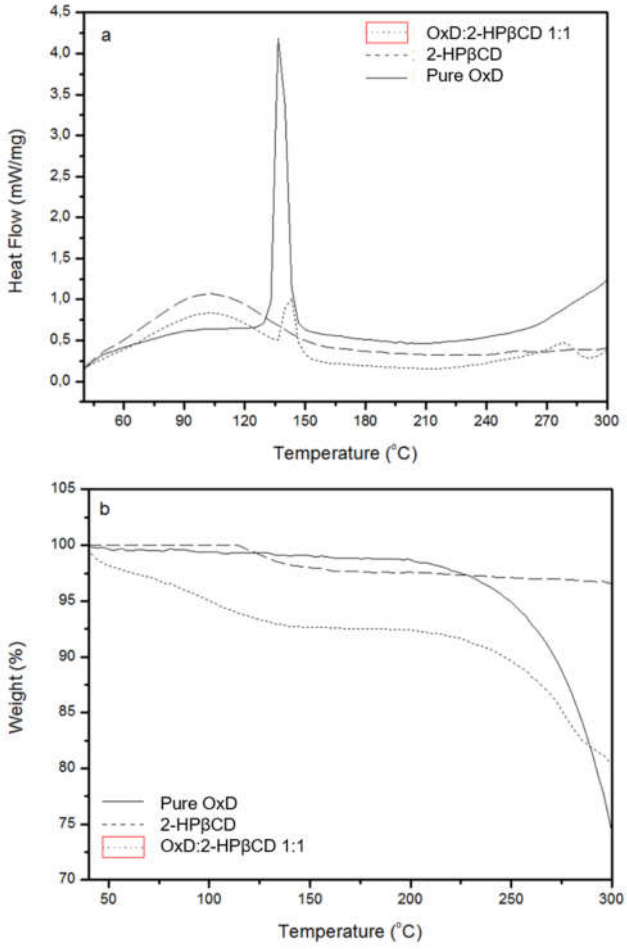

significant mass loss of 27.5% of OxD of about 250-300 ºC. 2-HPβCD showed a discrete mass loss (2.5%) about 125 ºC and 300 ºC. The mass loss of the inclusion complex was lower than pure OxD (17.5% vs. 27.5%, respectively). These results suggest that 2-HPβCD contributed positively to a temperature displacement, which is associated to

weight loss at higher temperatures (Fig. 7b). Then, TG and DSC results demonstrate the effectivity of the complexation method. In addition, melting point determination is based on intermolecular interactions that stabilizes the crystalline structure of the compound. As expected, 2-HPβCD cavity offer thermodynamic stability for OxD resulting in a different thermal behavior.

TG and DSC curves of OxD:2-HPβCD inclusion complex exhibited of pure characteristic of the components. The mass loss is divided into two consecutive processes related to the decomposition of OxD and 2-HPβCD. Of note, two endothermic peaks are associated with each melting point of the molecules. The decomposition process also exhibits two-step pattern, which is associated to the pure OxD and OxD:2-HPβCD inclusion complex decomposition.

3.9. In vitro release study

Fig. 8 shows the dissolution profiles of the OxD and OxD:2-HPβCD inclusion complex. The cumulative release rate of OxD:2-HPβCD obtained by co-evaporation method was significantly higher than the physical mixture of OxD and OxD:2-HPβCD.

The cumulative dissolution percentage for OxD:2-HPβCD CE and OxD:2-HPβCD PM was ~ 90% and 15.5%, respectively, during the first 15min. After, a plateau was observed for OxD:2-HPβCD CE. The dissolution was improved for OxD:2- HPβCD CE as compared to OxD and OxD:2-HPβCD PM. The differences observed in the dissolution profile of OxD and inclusion complex are related to the physical property and microenvironment around of the molecules. The rapid release of OxD was attributed to the fact that β-CD improve the we Fig. 8 shows the dissolution profiles of the OxD and OxD:2-HPβCD inclusion complex. The cumulative release rate of OxD:2-HPβCD obtained by co-evaporation method was significantly higher than the physical mixture of OxD and OxD:2-HPβCD.

The cumulative dissolution percentage for OxD:2-HPβCD CE and OxD:2-HPβCD PM was ~ 90% and 15.5%, respectively, during the first 15min. After, a plateau was observed for OxD:2-HPβCD CE. The dissolution was improved for OxD:2- HPβCD CE as compared to OxD and OxD:2-HPβCD PM. The differences observed in the dissolution profile of OxD and inclusion complex are related to the physical property and microenvironment around of the molecules. The rapid release of OxD was attributed to the fact that β-CD improve the wettability of inclusion complex in dissolution (SAVJANI, K. T. *et al.*, 2012; LIU *et al.*, 2013).

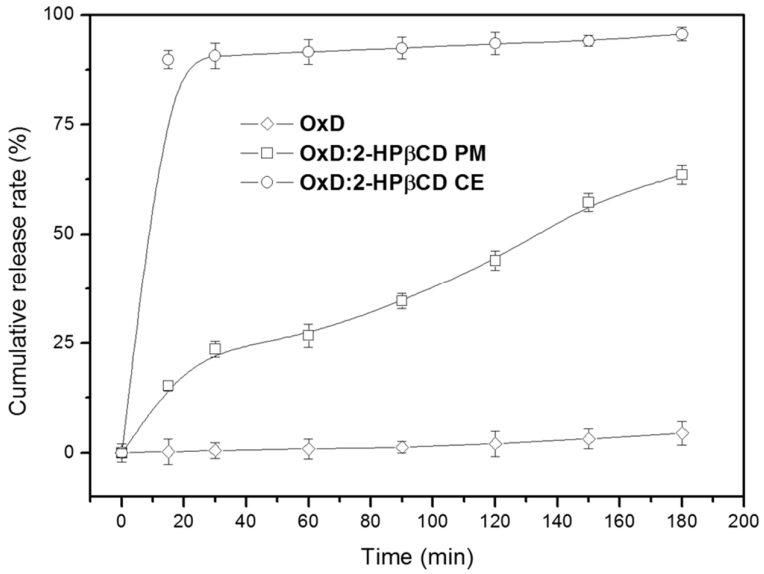

Figure 8. In vitro release kinetics of OxD and OxD:2-HPβCD inclusion complex from physical mixture (PM) and co-evaporation method (CE).

3.10. MTT Cytotoxicity Assay

The percentage of viable cells was obtained for six molar concentrations (1μM, 10 μM, 25 μM, 50 μM, 75 μM and 100 μM) of OxD, 2-HPβCD and inclusion complexes by using MTT assay (RPMI 1640 medium) (Fig. 9).

Figure 9. Cytotoxicity of OxD and inclusion complexes toward PBMCs.

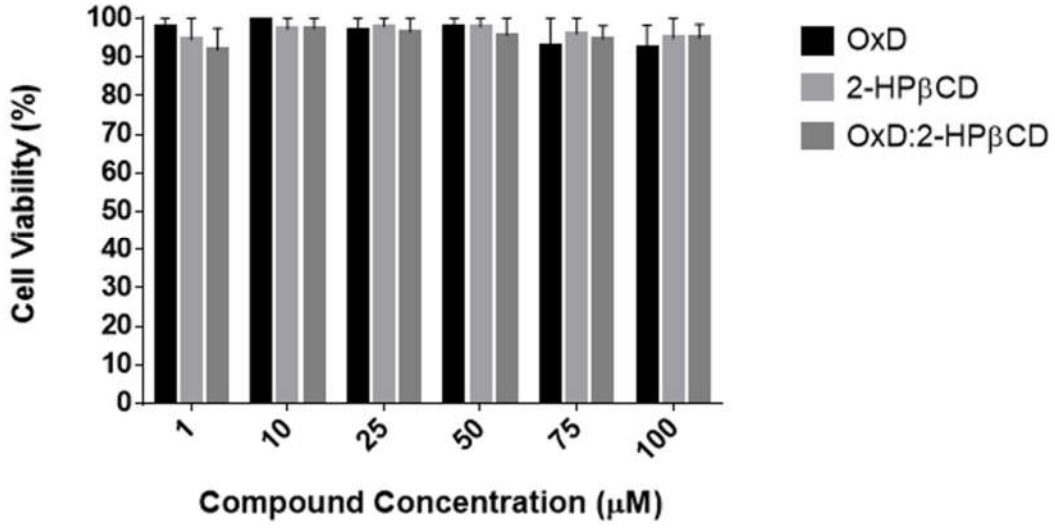

OxD cell viability was 95% (± 2.3%) for 1μM to 50μM. Pure 2-HPβCD and inclusion complexes showed cell viability about 94% (± 3%) for all studied concentrations. Previous studies demonstrated that cyclodextrin has a specific cytotoxicity and depends on the cells involved (dose-dependent) (ZHANG *et al.*, 2009; SOFIAN *et al.*, 2014). In general, concentrations > 25 μM are undesired to eventual *in vivo* tests and therefore it is necessary to establish an optimal dose taking into account the amount used. The increment of the solubility of the OxD has been improved by using 2-HPβCD. In addition, 2-HPβCD and inclusion complexes showed less toxicity in normal cells.

4. CONCLUSION

The molecular modelling studies showed stable intermolecular interactions between OxD and 2-HPβCD. The intermolecular energies and ^{1}H-NMR results of inclusion complex also suggest a hydrogen bonding between guest and host molecules. The stability of inclusion complexes depends of Van der Waals interactions, hydrophobic and electrostatic interactions. Our results demonstrated a solubility enhancement of OxD:2-HPβCD inclusion complex 20 fold more than pure OxD. The inclusion complexes did not have significant cytotoxicity in PBMCs viability. To the best of our knowledge is the first time that 2-HPβCD is applied as inclusion complex involving OxD. The proposed system could be applied as a new oral delivery system for antitumor applications.

ACKNOWLEDGMENT

The authors are grateful for the support provided by the Brazilian National Council for Scientific and Technological Development (CNPq), Instituto Nacional de Ciência e Tecnologia para Inovação Farmacêutica (INCT_if), Fundação de Amparo à Ciência e Tecnologia do Estado de Pernambuco (FACEPE) and Centro de Tecnologias Estratégicas do Nordeste (CETENE). da Silva would like to thank FACEPE for a scholarship.

REFERENCES

AGRAWAL, A. K. et al. In vitro metabolism of a new oxazolidinedione hypoglycemic agent utilizing liver microsomes and recombinant human cytochrome P450 enzymes. **J**

Pharm Biomed Anal, v. 37, n. 2, p. 351-8, Feb 23 2005. ISSN 0731-7085 (Print) 0731-7085 (Linking). Disponível em: < http://www.ncbi.nlm.nih.gov/pubmed/15708677 >.

ALEEM, O. et al. Effect of beta-cyclodextrin and hydroxypropyl beta-cyclodextrin complexation on physicochemical properties and antimicrobial activity of cefdinir. **J Pharm Biomed Anal,** v. 47, n. 3, p. 535-40, Jul 15 2008. ISSN 0731-7085 (Print) 0731-7085 (Linking). Disponível em: < http://www.ncbi.nlm.nih.gov/pubmed/18367363 >.

ALVES, R. J. et al. **Oxazolidinas aromáticas quirais n-substituídas, processo de síntese, composição farmacêutica e uso**: Google Patents 2014.

ALVES, R. J. et al. **N-substituted chiral aromatic oxazolidines, synthesis process, pharmaceutical composition and use**: Google Patents 2014a.

ALVIRA, E.; MAYORAL, J. A.; GARCÍA, J. I. Molecular modelling study of β-cyclodextrin inclusion complexes. **Chemical Physics Letters,** v. 271, n. 1–3, p. 178-184, 6/6/ 1997. ISSN 0009-2614. Disponível em: < http://www.sciencedirect.com/science/article/pii/S000926149700451X >.

ANDERSON, D. J.; KAYE, K. S. Staphylococcal surgical site infections. **Infect Dis Clin North Am,** v. 23, n. 1, p. 53-72, Mar 2009. ISSN 1557-9824 (Electronic) 0891-5520 (Linking). Disponível em: < http://www.ncbi.nlm.nih.gov/pubmed/19135916 >.

ARMSTRONG-JAMES, D.; MEINTJES, G.; BROWN, G. D. A neglected epidemic: fungal infections in HIV/AIDS. **Trends Microbiol,** v. 22, n. 3, p. 120-7, Mar 2014. ISSN 1878-4380 (Electronic) 0966-842X (Linking). Disponível em: < http://www.ncbi.nlm.nih.gov/pubmed/24530175 >.

AVNI, T.; LEIBOVICI, L.; PAUL, M. PCR diagnosis of invasive candidiasis: systematic review and meta-analysis. **J Clin Microbiol,** v. 49, n. 2, p. 665-70, Feb 2011. ISSN 1098-660X (Electronic) 0095-1137 (Linking). Disponível em: < http://www.ncbi.nlm.nih.gov/pubmed/21106797 >.

AYATOLLAHI, M. S.; KAZEMI, A. In vitro and in vivo antidermatophytic activities of some Iranian medicinal plants. **Med Mycol**, Jun 19 2015. ISSN 1369-3786.

BARTHOLOMEW, D. L.; CAPLOVICH, J. J.; WILDER, A. S. **Fungicidal and bactericidal therapeutic solution of sulfur dioxide**: Google Patents 1954.

BEGANOVIC, M. et al. A Review of Combination Antimicrobial Therapy for Enterococcus Faecalis Bloodstream Infections and Infective Endocarditis. **Clin Infect Dis**, Jan 30 2018. ISSN 1058-4838.

BEHROOZMAND, A.; KEATING, K.; AUKEN, E. A Review of the Principles and Applications of the NMR Technique for Near-Surface Characterization. **Surveys in Geophysics,** v. 36, n. 1, p. 27-85, 2015/01/01 2015. ISSN 0169-3298. Disponível em: < http://dx.doi.org/10.1007/s10712-014-9304-0 >.

BOVERS, M.; HAGEN, F.; BOEKHOUT, T. Diversity of the Cryptococcus neoformans-Cryptococcus gattii species complex. **Rev Iberoam Micol,** v. 25, n. 1, p. S4-12, Mar 2008. ISSN 1130-1406 (Print) 1130-1406 (Linking). Disponível em: < http://www.ncbi.nlm.nih.gov/pubmed/18338917 >.

BREWSTER, M. E.; LOFTSSON, T. Cyclodextrins as pharmaceutical solubilizers. **Advanced Drug Delivery Reviews,** v. 59, n. 7, p. 645-666, 7/30/ 2007. ISSN 0169-409X. Disponível em: < http://www.sciencedirect.com/science/article/pii/S0169409X07000841 >.

CAMPOS, J. F. et al. Synthesis and in vitro anticancer activity of new 2-thioxo-oxazolidin-4-one derivatives. **Pharmacol Rep,** v. 69, n. 4, p. 633-641, Mar 18 2017. ISSN 1734-1140 (Print) 1734-1140 (Linking). Disponível em: < http://www.ncbi.nlm.nih.gov/pubmed/28511054 >.

CAMPOS, J. F. et al. Synthesis and in vitro anticancer activity of new 2-thioxo-oxazolidin-4-one derivatives. **Pharmacological Reports,** v. 69, n. 4, p. 633-641, 8// 2017. ISSN 1734-1140. Disponível em: < http://www.sciencedirect.com/science/article/pii/S1734114016301542 >.

CARILLO-MUNOZ, A. J.; TUR-TUR, C. Comparative study of antifungal activity of sertaconazole, terbinafine, and bifonazole against clinical isolates of Candida spp., Cryptococcus neoformans and dermatophytes. **Chemotherapy,** v. 43, n. 6, p. 387-92, Nov-Dec 1997. ISSN 0009-3157 (Print) 0009-3157 (Linking). Disponível em: < http://www.ncbi.nlm.nih.gov/pubmed/9395851 >.

CAVALCANTI, I. M. et al. The encapsulation of beta-lapachone in 2-hydroxypropyl-beta-cyclodextrin inclusion complex into liposomes: a physicochemical evaluation and molecular modeling approach. **Eur J Pharm Sci,** v. 44, n. 3, p. 332-40, Oct 9 2011. ISSN 0928-0987.

CHALLA, R. et al. Cyclodextrins in drug delivery: An updated review. **AAPS PharmSciTech**, New York**,** v. 6, n. 2, p. E329-E357, 10/14 06/11/received 01/26/accepted 2005. ISSN 1530-9932. Disponível em: < http://www.ncbi.nlm.nih.gov/pmc/articles/PMC2750546/ >.

CHOE, H. W. et al. Crystallization and preliminary X-ray diffraction studies of alpha-cyclodextrin glucanotransferase isolated from Bacillus macerans. **Acta Crystallogr D Biol Crystallogr,** v. 59, n. Pt 2, p. 348-9, Feb 2003. ISSN 0907-4449 (Print) 0907-4449 (Linking). Disponível em: < http://www.ncbi.nlm.nih.gov/pubmed/12554949 >.

CHOI, J. H. et al. Prevalence and risk factors of esophageal candidiasis in healthy individuals: a single center experience in Korea. **Yonsei Med J,** v. 54, n. 1, p. 160-5, Jan 1 2013. ISSN 1976-2437 (Electronic) 0513-5796 (Linking). Disponível em: < http://www.ncbi.nlm.nih.gov/pubmed/23225813 >.

CIRRI, M. et al. Determination of stability constant values of flurbiprofen–cyclodextrin complexes using different techniques. **Journal of Pharmaceutical and Biomedical Analysis,** v. 37, n. 5, p. 995-1002, 4/29/ 2005. ISSN 0731-7085. Disponível em: < http://www.sciencedirect.com/science/article/pii/S073170850400473X >.

CROWLEY, L. C. et al. Quantitation of Apoptosis and Necrosis by Annexin V Binding, Propidium Iodide Uptake, and Flow Cytometry. **Cold Spring Harb Protoc,** v. 2016, n. 11, p. pdb.prot087288, Nov 01 2016. ISSN 1559-6095.

D.G., C. **Analytical Chemistry: Solutions Manual.** 5. John Willeys & Sons, 1994. 162.

DAHIYA, S.; PATHAK, K. Physicochemical characterization and dissolution enhancement of aceclofenac-hydroxypropyl beta-cyclodextrin binary systems. **PDA J Pharm Sci Technol,** v. 60, n. 6, p. 378-88, Nov-Dec 2006. ISSN 1079-7440 (Print)

1079-7440.

DARWAZAH, A.; BERG, G.; FARIS, B. Candida parapsilosis: an unusual organism causing prosthetic heart valve infective endocarditis. **J Infect,** v. 38, n. 2, p. 130-1, Mar 1999. ISSN 0163-4453 (Print) 0163-4453 (Linking). Disponível em: < http://www.ncbi.nlm.nih.gov/pubmed/10342657 >.

DAVIS, M. E.; BREWSTER, M. E. Cyclodextrin-based pharmaceutics: past, present and future. **Nat Rev Drug Discov,** v. 3, n. 12, p. 1023-1035, 12//print 2004. ISSN 1474-1776. Disponível em: < http://dx.doi.org/10.1038/nrd1576 >.

DE KRAKER, M. E. et al. The changing epidemiology of bacteraemias in Europe: trends from the European Antimicrobial Resistance Surveillance System. **Clin Microbiol Infect,** v. 19, n. 9, p. 860-8, Sep 2013. ISSN 1469-0691 (Electronic) 1198-743X (Linking). Disponível em: < http://www.ncbi.nlm.nih.gov/pubmed/23039210 >.

DEL VALLE, E. M. M. Cyclodextrins and their uses: a review. **Process Biochemistry,** v. 39, n. 9, p. 1033-1046, 5/31/ 2004. ISSN 1359-5113. Disponível em: < http://www.sciencedirect.com/science/article/pii/S0032959203002589 >.

DEVI, K. et al. An Efficient Approach to the Synthesis of Novel Oxazolidinones as Potential Antimicrobial Agents. **Journal of Chemistry,** v. 2013, p. 5, 2013. Disponível em: < http://dx.doi.org/10.1155/2013/252187 >.

DOVNIK, A. et al. Treatment of vulvovaginal candidiasis: a review of the literature. **Acta Dermatovenerol Alp Pannonica Adriat,** v. 24, n. 1, p. 5-7, 2015. ISSN 1581-2979 (Electronic) 1318-4458 (Linking). Disponível em: < http://www.ncbi.nlm.nih.gov/pubmed/25770305 >.

DUNN, B. K.; KRAMER, B. S. Cancer Prevention: Lessons Learned and Future Directions. **Trends in cancer,** v. 2, n. 12, p. 713-722, 2016. ISSN 2405-8033 2405-8025. Disponível em: < http://www.ncbi.nlm.nih.gov/pmc/articles/PMC5271581/ >.

DYE, C. After 2015: infectious diseases in a new era of health and development. **Philosophical Transactions of the Royal Society B: Biological Sciences,** v. 369, n. 1645, p. 20130426, 2014. ISSN 0962-8436 1471-2970. Disponível em: < http://www.ncbi.nlm.nih.gov/pmc/articles/PMC4024220/ >.

EASTBURN, S. D.; TAO, B. Y. Applications of modified cyclodextrins. **Biotechnol Adv,** v. 12, n. 2, p. 325-39, 1994. ISSN 0734-9750 (Print) 0734-9750 (Linking). Disponível em: < http://www.ncbi.nlm.nih.gov/pubmed/14545896 >.

ELSTNER, E. et al. Ligands for peroxisome proliferator-activated receptorgamma and retinoic acid receptor inhibit growth and induce apoptosis of human breast cancer cells in vitro and in BNX mice. **Proc Natl Acad Sci U S A,** v. 95, n. 15, p. 8806-11, Jul 21 1998. ISSN 0027-8424 (Print) 0027-8424.

ENG, S.-K. et al. Salmonella: A review on pathogenesis, epidemiology and antibiotic resistance. **Frontiers in Life Science,** v. 8, n. 3, p. 284-293, 2015/07/03 2015. ISSN 2155-3769. Disponível em: < https://doi.org/10.1080/21553769.2015.1051243 >.

ESPINEL-INGROFF, A.; KIDD, S. E. Current trends in the prevalence of Cryptococcus gattii in the United States and Canada. **Infect Drug Resist,** v. 8, p. 89-97, 2015. ISSN 1178-6973 (Electronic) 1178-6973 (Linking). Disponível em: < http://www.ncbi.nlm.nih.gov/pubmed/25999744 >.

FAUZIAH, C. I. et al. Thermal Analysis and Surface Morphology Study of Cholesterol: B-Cyclodextrin Inclusion Complex. **Advanced Materials Research,** v. 812, p. 221-225, 2013.

FIRACATIVE, C.; TRILLES, L.; MEYER, W. MALDI-TOF MS enables the rapid identification of the major molecular types within the Cryptococcus neoformans/C. gattii species complex. **PLoS One,** v. 7, n. 5, p. e37566, 2012. ISSN 1932-6203 (Electronic)

1932-6203 (Linking). Disponível em: < http://www.ncbi.nlm.nih.gov/pubmed/22666368 >.

GARCIA-CUESTA, C.; SARRION-PEREZ, M. G.; BAGAN, J. V. Current treatment of oral candidiasis: A literature review. **J Clin Exp Dent,** v. 6, n. 5, p. e576-82, Dec 2014. ISSN 1989-5488 (Electronic) 1989-5488 (Linking). Disponível em: < http://www.ncbi.nlm.nih.gov/pubmed/25674329 >.

GAVALDA, J. et al. Invasive fungal infections in solid organ transplant recipients. **Clin Microbiol Infect,** v. 20 Suppl 7, p. 27-48, Sep 2014. ISSN 1469-0691 (Electronic) 1198-743X (Linking). Disponível em: < http://www.ncbi.nlm.nih.gov/pubmed/24810152 >.

GONG, J.; ALKAN, S.; ANAND, S. A Case of Cutaneous Plasmablastic Lymphoma in HIV/AIDS with Disseminated Cryptococcus. **Case Rep Oncol Med,** v. 2013, p. 862585, 2013. ISSN 2090-6706 (Print). Disponível em: < http://www.ncbi.nlm.nih.gov/pubmed/24371535 >.

GOULD, I. M. The epidemiology of antibiotic resistance. **Int J Antimicrob Agents,** v. 32 Suppl 1, p. S2-9, Nov 2008. ISSN 0924-8579 (Print) 0924-8579 (Linking). Disponível em: < http://www.ncbi.nlm.nih.gov/pubmed/18757182 >.

GOULD, S.; SCOTT, R. C. 2-Hydroxypropyl-β-cyclodextrin (HP-β-CD): A toxicology review. **Food and Chemical Toxicology,** v. 43, n. 10, p. 1451-1459, 10// 2005. ISSN 0278-6915. Disponível em: < http://www.sciencedirect.com/science/article/pii/S0278691505001006 >.

GROMMES, C.; LANDRETH, G. E.; HENEKA, M. T. Antineoplastic effects of peroxisome proliferator-activated receptor gamma agonists. **Lancet Oncol,** v. 5, n. 7, p. 419-29, Jul 2004. ISSN 1470-2045 (Print) 1470-2045 (Linking). Disponível em: < http://www.ncbi.nlm.nih.gov/pubmed/15231248 >.

GROSE, J. H.; CASJENS, S. R. Understanding the enormous diversity of bacteriophages: the tailed phages that infect the bacterial family Enterobacteriaceae. **Virology,** v. 0, p. 421-443, 2014. ISSN 0042-6822 1096-0341. Disponível em: < http://www.ncbi.nlm.nih.gov/pmc/articles/PMC4301999/ >.

HALGREN, T. A. MMFF VI. MMFF94s option for energy minimization studies. **Journal of Computational Chemistry,** v. 20, n. 7, p. 720-729, 1999. ISSN 1096-987X. Disponível em: < http://dx.doi.org/10.1002/(SICI)1096-987X(199905)20:7<720::AID-JCC7>3.0.CO;2-X >.

HARA, T. et al. Prominent Solubilizing Effect of 2-Hydroxypropyl-β-cyclodextrin on a New Thiazolidine Derivative (FPFS-410) with Antidiabetic and Lipid-lowering

Activities through Inclusion Complex Formation. **Journal of inclusion phenomena and macrocyclic chemistry,** v. 56, n. 1, p. 135-139, 2006. ISSN 1573-1111. Disponível em: < http://dx.doi.org/10.1007/s10847-006-9074-5 >.

HAWKEY, P. M.; JONES, A. M. The changing epidemiology of resistance. **J Antimicrob Chemother,** v. 64 Suppl 1, p. i3-10, Sep 2009. ISSN 1460-2091 (Electronic) 0305-7453 (Linking). Disponível em: < http://www.ncbi.nlm.nih.gov/pubmed/19675017 >.

HEISE, H. M. et al. Infrared spectroscopy and Raman spectroscopy of cyclodextrin derivatives and their ferrocene inclusion complexes. **Vibrational Spectroscopy,** v. 53, n. 1, p. 19-23, 5/26/ 2010. ISSN 0924-2031. Disponível em: < http://www.sciencedirect.com/science/article/pii/S0924203110000147 >.

HIGUCHI, T.; CONNORS, K. A. Phase-solubility techniques. **Advances in Analytical Chemistry and Instrumentation,** v. 4, p. 117-212, 1965.

ILLNAIT-ZARAGOZI, M. T. et al. Cryptococcus and Cryptococcosis in Cuba. A minireview. **Mycoses,** v. 57, n. 12, p. 707-717, 2014. ISSN 1439-0507. Disponível em: < http://dx.doi.org/10.1111/myc.12275 >.

IRIMIE, M. et al. Prevalence and Antifungal Susceptibility Patterns of Dermatophytes Isolated from Patients with Neoplastic Diseases: A Case Control Study. **Acta Dermatovenerol Croat,** v. 23, n. 2, p. 108-13, Jul 2015. ISSN 1330-027x.

JAFARI, A. et al. Genotypic and phenotypic comparison of enteroaggregative Escherichia coli isolates from HIV-positive and non-HIV diarrheal samples. **Curr HIV Res,** v. 11, n. 8, p. 635-41, Dec 2013. ISSN 1873-4251 (Electronic) 1570-162X (Linking). Disponível em: < http://www.ncbi.nlm.nih.gov/pubmed/24517190 >.

JOUDIEH, S. et al. Cyclodextrin polymers as efficient solubilizers of albendazole: complexation and physico-chemical characterization. **J Nanosci Nanotechnol,** v. 9, n. 1, p. 132-40, Jan 2009. ISSN 1533-4880 (Print) 1533-4880 (Linking). Disponível em: < http://www.ncbi.nlm.nih.gov/pubmed/19441287 >.

KAWAI, K. et al. A new anti-mycotic drug tioxaprofen and its uncoupling effect on isolated mitochondria. **Experientia,** v. 39, n. 8, p. 889-90, Aug 15 1983. ISSN 0014-4754 (Print) 0014-4754.

LA HOZ, R. M.; PAPPAS, P. G. Cryptococcal infections: changing epidemiology and implications for therapy. **Drugs,** v. 73, n. 6, p. 495-504, May 2013. ISSN 0012-6667 (Print) 0012-6667 (Linking). Disponível em: < http://www.ncbi.nlm.nih.gov/pubmed/23575940 >.

LANTERNIER, F. et al. Primary immunodeficiencies underlying fungal infections. **Current opinion in pediatrics,** v. 25, n. 6, p. 736-747, 2013. ISSN 1040-8703 1531-698X. Disponível em: < http://www.ncbi.nlm.nih.gov/pmc/articles/PMC4098727/ >.

LEE, J. D.; CLARKE, J. Cover up or cool it? Sexual intercourse during therapy for bacterial sexually transmitted infections--a discussion of evidence for efficacy of condom use preventing transmission during an acute bacterial STI. **Int J STD AIDS,** v. 15, n. 5, p. 285-8, May 2004. ISSN 0956-4624 (Print) 0956-4624 (Linking). Disponível em: < http://www.ncbi.nlm.nih.gov/pubmed/15117492 >.

LEMAIRE, S.; TULKENS, P. M.; VAN BAMBEKE, F. Cellular pharmacokinetics of the novel biaryloxazolidinone radezolid in phagocytic cells: studies with macrophages and polymorphonuclear neutrophils. **Antimicrob Agents Chemother,** v. 54, n. 6, p. 2540-8, Jun 2010. ISSN 0066-4804.

LESNAKOVA, A. et al. Bacterial meningitis after sinusitis and otitis media: ear, nose, throat infections are still the commonest risk factors for the community acquired

meningitis. **Neuro Endocrinol Lett,** v. 28 Suppl 3, p. 14-5, Nov 2007. ISSN 0172-780X (Print) 0172-780X (Linking). Disponível em: < http://www.ncbi.nlm.nih.gov/pubmed/18030266 >.

LI, N.; XU, L. Thermal analysis of β-cyclodextrin/Berberine chloride inclusion compounds. **Thermochimica Acta,** v. 499, n. 1–2, p. 166-170, 2/20/ 2010. ISSN 0040-6031. Disponível em: < http://www.sciencedirect.com/science/article/pii/S0040603109003815 >.

LIU, H. et al. Physicochemical characterization and pharmacokinetics evaluation of beta-caryophyllene/beta-cyclodextrin inclusion complex. **Int J Pharm,** v. 450, n. 1-2, p. 304-10, Jun 25 2013. ISSN 1873-3476 (Electronic) 0378-5173 (Linking). Disponível em: < http://www.ncbi.nlm.nih.gov/pubmed/23598076 >.

LOFTSSON, T.; HREINSDÓTTIR, D.; MÁSSON, M. Evaluation of cyclodextrin solubilization of drugs. **International Journal of Pharmaceutics,** v. 302, n. 1–2, p. 18-28, 9/30/ 2005. ISSN 0378-5173. Disponível em: < http://www.sciencedirect.com/science/article/pii/S0378517305004400 >.

LOPES, W. A.; FASCIO, M. Esquema para Interpretação de Espectros de Susbtâncias Orgânicas na Região do Infravermelho. **Química Nova,** v. 27, n. 4, p. 4, 2004.

MAERTENS, J.; VREBOS, M.; BOOGAERTS, M. Assessing risk factors for systemic fungal infections. **Eur J Cancer Care (Engl),** v. 10, n. 1, p. 56-62, Mar 2001. ISSN 0961-5423 (Print) 0961-5423 (Linking). Disponível em: < http://www.ncbi.nlm.nih.gov/pubmed/11827268 >.

MAHABEER, Y. et al. Comparison of Etests and Vitek 2 (R) to broth microdilution for the susceptibility testing of Cryptococcus neoformans. **Diagn Microbiol Infect Dis,** v. 80, n. 4, p. 294-8, Dec 2014. ISSN 1879-0070 (Electronic) 0732-8893 (Linking). Disponível em: < http://www.ncbi.nlm.nih.gov/pubmed/25277745 >.

MALEY, C. C. et al. Classifying the evolutionary and ecological features of neoplasms. **Nature reviews. Cancer,** v. 17, n. 10, p. 605-619, 09/15 2017. ISSN 1474-175X 1474-1768. Disponível em: < http://www.ncbi.nlm.nih.gov/pmc/articles/PMC5811185/ >.

MANGOLIM, C. S. et al. Curcumin-beta-cyclodextrin inclusion complex: stability, solubility, characterisation by FT-IR, FT-Raman, X-ray diffraction and photoacoustic spectroscopy, and food application. **Food Chem,** v. 153, p. 361-70, Jun 15 2014. ISSN 0308-8146 (Print) 0308-8146.

MAZOLLA, A. A. Ressonância magnética: princípios de formação da imagem e aplicações em imagem funcional. **Revista Brasileira de Física Médica.,** v. 3, n. 1, p. 13, 2009.

MAZU, T. K. et al. The Mechanistic Targets of Antifungal Agents: An Overview. **Mini reviews in medicinal chemistry,** v. 16, n. 7, p. 555-578, 2016. ISSN 1389-5575 1875-5607. Disponível em: < http://www.ncbi.nlm.nih.gov/pmc/articles/PMC5215921/ >.

MCGUIRE, T. M.; SMITH, J.; DEL MAR, C. The match between common antibiotics packaging and guidelines for their use in Australia. **Aust N Z J Public Health**, Jun 29 2015. ISSN 1753-6405 (Electronic) 1326-0200 (Linking). Disponível em: < http://www.ncbi.nlm.nih.gov/pubmed/26122469 >.

MENDONCA, E. A. et al. Enhanced antiproliferative activity of the new anticancer candidate LPSF/AC04 in cyclodextrin inclusion complexes encapsulated into liposomes. **AAPS PharmSciTech,** v. 13, n. 4, p. 1355-66, Dec 2012. ISSN 1530-9932.

MENDONÇA, E. A. M. et al. Enhanced Antiproliferative Activity of the New Anticancer Candidate LPSF/AC04 in Cyclodextrin Inclusion Complexes Encapsulated into Liposomes. **AAPS PharmSciTech**, Boston**,** v. 13, n. 4, p. 1355-1366,

10/0204/12/received 09/10/accepted 2012. ISSN 1530-9932. Disponível em: < http://www.ncbi.nlm.nih.gov/pmc/articles/PMC3513461/ >.

MILETIC, T. et al. Spray-dried voriconazole-cyclodextrin complexes: solubility, dissolution rate and chemical stability. **Carbohydr Polym,** v. 98, n. 1, p. 122-31, Oct 15 2013. ISSN 1879-1344 (Electronic) 0144-8617 (Linking). Disponível em: < http://www.ncbi.nlm.nih.gov/pubmed/23987325 >.

MOURAO, R. H. et al. Synthesis and biological activity of novel acridinylidene and benzylidene thiazolidinediones. **Eur J Med Chem,** v. 40, n. 11, p. 1129-33, Nov 2005. ISSN 0223-5234 (Print) 0223-5234.

MUELLER, E. et al. Terminal differentiation of human breast cancer through PPAR gamma. **Mol Cell,** v. 1, n. 3, p. 465-70, Feb 1998. ISSN 1097-2765 (Print) 1097-2765.

MUSKETT, H. et al. Risk factors for invasive fungal disease in critically ill adult patients: a systematic review. **Crit Care,** v. 15, n. 6, p. R287, 2011. ISSN 1466-609X (Electronic) 1364-8535 (Linking). Disponível em: < http://www.ncbi.nlm.nih.gov/pubmed/22126425 >.

N, S. et al. Mode of encapsulation of Linezolid by β-Cyclodextrin and its role in bovine serum albumin binding. **Carbohydrate Polymers,** v. 115, p. 589-597, 2015/01/22/ 2015. ISSN 0144-8617. Disponível em: < http://www.sciencedirect.com/science/article/pii/S0144861714009138 >.

NARESH, A. et al. Oxazolidinone derivatives: cytoxazone-linezolid hybrids induces apoptosis and senescence in DU145 prostate cancer cells. **Eur J Med Chem,** v. 80, p. 295-307, Jun 10 2014. ISSN 1768-3254 (Electronic) 0223-5234 (Linking). Disponível em: < http://www.ncbi.nlm.nih.gov/pubmed/24793880 >.

O'BOYLE, N. M. et al. Open Babel: An open chemical toolbox. **J Cheminform,** v. 3, n. 1, p. 1-14, 2011. ISSN 1758-2946. Disponível em: < http://dx.doi.org/10.1186/1758-2946-3-33 >.

PAL, T.; JOSHI, H.; RAMAA, C. S. Design and development of oxazol-5-ones as potential partial PPAR-gamma agonist against cancer cell lines. **Anticancer Agents Med Chem,** v. 14, n. 6, p. 872-83, 2014. ISSN 1871-5206.

PANDIT, N.; SINGLA, R. K.; SHRIVASTAVA, B. Current updates on oxazolidinone and its significance. **Int J Med Chem,** v. 2012, p. 159285, 2012. ISSN 2090-2069 (Print) 2090-2077 (Linking). Disponível em: < http://www.ncbi.nlm.nih.gov/pubmed/25954524 >.

PAPPAS, P. G. et al. Clinical Practice Guideline for the Management of Candidiasis: 2016 Update by the Infectious Diseases Society of America. **Clinical Infectious Diseases: An Official Publication of the Infectious Diseases Society of America,** v. 62, n. 4, p. e1-e50, 12/1610/28/received 11/02/accepted 2016. ISSN 1058-4838 1537-6591. Disponível em: < http://www.ncbi.nlm.nih.gov/pmc/articles/PMC4725385/ >.

PENCHOVSKY, R.; TRAYKOVSKA, M. Designing drugs that overcome antibacterial resistance: where do we stand and what should we do? **Expert Opin Drug Discov,** v. 10, n. 6, p. 631-50, Jun 2015. ISSN 1746-045X (Electronic) 1746-0441 (Linking). Disponível em: < http://www.ncbi.nlm.nih.gov/pubmed/25981754 >.

PIEL, G. et al. Molecular modeling study of beta- and gamma-cyclodextrin complexes with miconazole. **Eur J Pharm Sci,** v. 13, n. 3, p. 271-9, Jun 2001. ISSN 0928-0987 (Print) 0928-0987.

PIGHETTI, G. M. et al. Therapeutic treatment of DMBA-induced mammary tumors with PPAR ligands. **Anticancer Res,** v. 21, n. 2A, p. 825-9, Mar-Apr 2001. ISSN 0250-7005

(Print) 0250-7005 (Linking). Disponível em: < http://www.ncbi.nlm.nih.gov/pubmed/11396171 >.

PITTA, I. R. **Derivados 2-Tioxo-Oxazolidínicos-N-Substituídos potencialmente úteis na terapia anticâncer**. Digital. INDUSTRIAL, I. N. D. P. Brazil. BR1020150160607 2015.

PROSSER, G. A.; DE CARVALHO, L. P. S. Kinetic mechanism and inhibition of Mycobacterium tuberculosis d-alanine:d-alanine ligase by the antibiotic d-cycloserine. **FEBS Journal,** v. 280, n. 4, p. 1150-1166, 2013. ISSN 1742-4658. Disponível em: < http://dx.doi.org/10.1111/febs.12108 >.

RASHEED, A.; ASHOK KUMAR, C. K.; SRAVANTHI, V. V. N. S. S. **Sci. Pharm.,** v. 76, n. 4, p. 567–598 2008. ISSN 0036-8709.

RIBEIRO, M. A. et al. Prevalence and exoenzyme secretion by Candida albicans isolates from oral and vaginal mucosas of HIV-infected women. **Mycopathologia,** v. 157, n. 3, p. 255-61, Apr 2004. ISSN 0301-486X (Print) 0301-486X (Linking). Disponível em: < http://www.ncbi.nlm.nih.gov/pubmed/15180151 >.

RITZ, N.; CURTIS, N. Novel concepts in the epidemiology, diagnosis and prevention of childhood tuberculosis. **Swiss Med Wkly,** v. 144, p. w14000, 2014. ISSN 1424-3997 (Electronic) 0036-7672 (Linking). Disponível em: < http://www.ncbi.nlm.nih.gov/pubmed/25207918 >.

RODRIGUES, J. A. et al. Evaluation of biochemical and serological methods to identify and clustering yeast cells of oral Candida species by CHROMagar test, SDS-PAGE and ELISA. **Braz J Biol,** v. 64, n. 2, p. 317-26, May 2004. ISSN 1519-6984 (Print) 1519-6984 (Linking). Disponível em: < http://www.ncbi.nlm.nih.gov/pubmed/15462306 >.

ROMANO, C. et al. Primary cutaneous cryptococcosis due to Cryptococcus neoformans in a woman with non-Hodgkin's lymphoma. **Acta Derm Venereol,** v. 81, n. 3, p. 220-1, Jun-Jul 2001. ISSN 0001-5555 (Print) 0001-5555 (Linking). Disponível em: < http://www.ncbi.nlm.nih.gov/pubmed/11558889 >.

RONCO, C. Lipopolysaccharide (LPS) from the cellular wall of Gram-negative bacteria, also known as endotoxin, is a key molecule in the pathogenesis of sepsis and septic shock. Preface. **Blood Purif,** v. 37 Suppl 1, p. 1, 2014. ISSN 1421-9735 (Electronic) 0253-5068 (Linking). Disponível em: < http://www.ncbi.nlm.nih.gov/pubmed/24457486 >.

SADKOWSKA-TODYS, M.; CZARKOWSKI, M. P. Salmonellosis in Poland in 2012. **Przegl Epidemiol,** v. 68, n. 2, p. 243-8, 353-5, 2014. ISSN 0033-2100 (Print) 0033-2100 (Linking). Disponível em: < http://www.ncbi.nlm.nih.gov/pubmed/25135508 >.

SAENGER, W. et al. Structures of the Common Cyclodextrins and Their Larger Analogues-Beyond the Doughnut. **Chem Rev,** v. 98, n. 5, p. 1787-1802, Jul 30 1998. ISSN 0009-2665.

SAVJANI, K. T.; GAJJAR, A. K.; SAVJANI, J. K. Drug solubility: importance and enhancement techniques. **ISRN Pharm,** v. 2012, p. 195727, 2012. ISSN 2090-6153 (Electronic) 2090-6145 (Linking). Disponível em: < http://www.ncbi.nlm.nih.gov/pubmed/22830056 >.

SAVJANI, K. T.; GAJJAR, A. K.; SAVJANI, J. K. Drug Solubility: Importance and Enhancement Techniques. **ISRN Pharmaceutics,** v. 2012, p. 195727, 07/0503/31/received 05/08/accepted 2012. ISSN 2090-6145 2090-6153. Disponível em: < http://www.ncbi.nlm.nih.gov/pmc/articles/PMC3399483/ >.

SCHROEDER, G. N.; HILBI, H. Molecular Pathogenesis of Shigella spp.: Controlling Host Cell Signaling, Invasion, and Death by Type III Secretion. **Clinical Microbiology**

Reviews, v. 21, n. 1, p. 134-156, January 1, 2008 2008. Disponível em: < http://cmr.asm.org/content/21/1/134.abstract >.

SHAGHAFI, M. B.; GROTE, R. E.; JARVO, E. R. Oxazolidine synthesis by complementary stereospecific and stereoconvergent methods. **Org Lett,** v. 13, n. 19, p. 5188-91, Oct 7 2011. ISSN 1523-7052 (Electronic) 1523-7052 (Linking). Disponível em: < http://www.ncbi.nlm.nih.gov/pubmed/21866944 >.

SHI, S. H. et al. Spectrum and risk factors for invasive candidiasis and non-Candida fungal infections after liver transplantation. **Chin Med J (Engl),** v. 121, n. 7, p. 625-30, Apr 5 2008. ISSN 0366-6999 (Print) 0366-6999 (Linking). Disponível em: < http://www.ncbi.nlm.nih.gov/pubmed/18466683 >.

SHINABARGER, D. Mechanism of action of the oxazolidinone antibacterial agents. **Expert Opin Investig Drugs,** v. 8, n. 8, p. 1195-202, Aug 1999. ISSN 1744-7658 (Electronic) 1354-3784 (Linking). Disponível em: < http://www.ncbi.nlm.nih.gov/pubmed/15992144 >.

SILVA, C. V. et al. Molecular modeling and cytotoxicity of diffractaic acid: HP-beta-CD inclusion complex encapsulated in microspheres. **Int J Biol Macromol,** v. 92, p. 494-503, Jul 20 2016. ISSN 1879-0003 (Electronic) 0141-8130 (Linking). Disponível em: < http://www.ncbi.nlm.nih.gov/pubmed/27451026 >.

SILVERSTEIN, R. M.; BRASSLER, G. C.; MORRILL, T. C. **Identificação espectrométrica de compostos orgânicos.** . 6. Rio de Janeiro: Guanabara, 2000. 460.

SIVAKUMAR, V. G. et al. Use of CHROMagar in the differentiation of common species of Candida. **Mycopathologia,** v. 167, n. 1, p. 47-9, Jan 2009. ISSN 0301-486X (Print) 0301-486X (Linking). Disponível em: < http://www.ncbi.nlm.nih.gov/pubmed/18716895 >.

SOFIAN, Z. M. et al. Evaluation of the Cytotoxicity of Levodopa and its Complex with Hydroxypropyl-ß-Cyclodextrin (HP-ß-CD) to an Astrocyte Cell Line. **The Malaysian Journal of Medical Sciences : MJMS,** v. 21, n. Spec Issue, p. 6-11, 09/28/received 11/08/accepted 2014. ISSN 1394-195X 2180-4303. Disponível em: < http://www.ncbi.nlm.nih.gov/pmc/articles/PMC4405804/ >.

SONGNGAM, S. et al. A 5,7-Dimethoxyflavone/Hydroxypropyl-β-Cyclodextrin Inclusion Complex with Anti-Butyrylcholinesterase Activity. **AAPS PharmSciTech**, Boston**,** v. 15, n. 5, p. 1189-1196, 05/3101/30/received 05/20/accepted 2014. ISSN 1530-9932. Disponível em: < http://www.ncbi.nlm.nih.gov/pmc/articles/PMC4179656/ >.

SORABJEE, J. S.; GARJE, R. R. Response to . . . successful use of oral linezolide. **J Infect,** v. 48, n. 4, p. 365-6, May 2004. ISSN 0163-4453 (Print) 0163-4453 (Linking). Disponível em: < http://www.ncbi.nlm.nih.gov/pubmed/15066341 >.

SUH, N. et al. A new ligand for the peroxisome proliferator-activated receptor-gamma (PPAR-gamma), GW7845, inhibits rat mammary carcinogenesis. **Cancer Res,** v. 59, n. 22, p. 5671-3, Nov 15 1999. ISSN 0008-5472 (Print) 0008-5472.

SUN, H. et al. Antibacterial Activity of β-Cyclodextrin and 2-Hydroxypropyl-β-Cyclodextrin Trimethoprim Complexes **American Journal of Microbiology,** v. 2, n. 1, p. 8, 2011. ISSN 1948-982x.

SZEJTLI, J. Downstream processing using cyclodextrins. **Trends in Biotechnology,** v. 7, n. 7, p. 170-174, 1989/07/01 1989. ISSN 0167-7799. Disponível em: < http://www.sciencedirect.com/science/article/pii/0167779989900942 >.

TADESSE, M. et al. Synoxazolidinone C; a bicyclic member of the synoxazolidinone family with antibacterial and anticancer activities. **Tetrahedron Letters,** v. 52, n. 15, p.

1804-1806, 2011/04/13/ 2011. ISSN 0040-4039. Disponível em: < http://www.sciencedirect.com/science/article/pii/S0040403911002395 >.

THEOCHARIS, S. et al. Peroxisome proliferator-activated receptor-gamma ligands as cell-cycle modulators. **Cancer Treat Rev,** v. 30, n. 6, p. 545-54, Oct 2004. ISSN 0305-7372 (Print) 0305-7372.

TIWARI, G.; TIWARI, R.; RAI, A. K. Cyclodextrins in delivery systems: Applications. **J Pharm Bioallied Sci,** v. 2, n. 2, p. 72-9, Apr 2010. ISSN 0975-7406 (Electronic) 0975-7406 (Linking). Disponível em: < http://www.ncbi.nlm.nih.gov/pubmed/21814436 >.

TOMA, S. H.; TOMA, H. E. Self assembled rotaxane and pseudo-rotaxanes based on b-cyclodextrin inclusion compounds with trans-1,4-bis[(4-pyridyl)ethenyl]benzene-pentacyanoferrate(II) complexes. **Journal of the Brazilian Chemical Society,** v. 18, p. 279-283, 2007. ISSN 0103-5053. Disponível em: < http://www.scielo.br/scielo.php?script=sci_arttext&pid=S0103-50532007000200006&nrm=iso >.

TORRES-RODRIGUEZ, J. M. et al. MICs and minimum fungicidal concentrations of posaconazole, voriconazole and fluconazole for Cryptococcus neoformans and Cryptococcus gattii. **J Antimicrob Chemother,** v. 62, n. 1, p. 205-6, Jul 2008. ISSN 1460-2091 (Electronic) 0305-7453 (Linking). Disponível em: < http://www.ncbi.nlm.nih.gov/pubmed/18375969 >.

TREIB, J. et al. An international view of hydroxyethyl starches. **Intensive Care Med,** v. 25, n. 3, p. 258-68, Mar 1999. ISSN 0342-4642 (Print) 0342-4642 (Linking). Disponível em: < http://www.ncbi.nlm.nih.gov/pubmed/10229159 >.

TROTT, O.; OLSON, A. J. AutoDock Vina: improving the speed and accuracy of docking with a new scoring function, efficient optimization, and multithreading. **J**

Comput Chem, v. 31, n. 2, p. 455-61, Jan 30 2010. ISSN 1096-987X (Electronic) 0192-8651 (Linking). Disponível em: < http://www.ncbi.nlm.nih.gov/pubmed/19499576 >.

VILLEMAGNE, B. et al. Tuberculosis: The drug development pipeline at a glance. **European Journal of Medicinal Chemistry,** v. 51, n. 0, p. 1-16, 5// 2012. ISSN 0223-5234. Disponível em: < http://www.sciencedirect.com/science/article/pii/S0223523412001249 >.

WASHINGTON, J. A. Principles of Diagnosis. In: BARON, S. (Ed.). **Medical Microbiology**. 4th. Galveston (TX), 1996. ISBN 0963117211.

WEITZMAN, I.; SUMMERBELL, R. C. The dermatophytes. **Clin Microbiol Rev,** v. 8, n. 2, p. 240-59, Apr 1995. ISSN 0893-8512 (Print) 0893-8512.

WENZ, G. Cyclodextrins as Building Blocks for Supramolecular Structures and Functional Units. **Angewandte Chemie International Edition in English,** v. 33, n. 8, p. 803-822, 1994. ISSN 1521-3773. Disponível em: < http://dx.doi.org/10.1002/anie.199408031 >.

WHO. Antimicrobial resistance. Internet, April 2015 2015. Disponível em: < http://www.who.int/mediacentre/factsheets/fs194/en/ >. Acesso em: 09/01/2015.

YAPAR, N. Epidemiology and risk factors for invasive candidiasis. **Ther Clin Risk Manag,** v. 10, p. 95-105, 2014. ISSN 1176-6336 (Print) 1176-6336 (Linking). Disponível em: < http://www.ncbi.nlm.nih.gov/pubmed/24611015 >.

ZHANG, W. F. et al. Biocompatibility study of theophylline/chitosan/beta-cyclodextrin microspheres as pulmonary delivery carriers. **J Mater Sci Mater Med,** v. 20, n. 6, p. 1321-30, Jun 2009. ISSN 0957-4530.

APENDICE B: DEPÓSITO DE PATENTE

INSTITUTO NACIONAL DA PROPRIEDADE INDUSTRIAL

16/12/2016 870160076203 11:54

00.000.2.2.16.0651587.4

Pedido nacional de Invenção, Modelo de Utilidade, Certificado de Adição de Invenção e entrada na fase nacional do PCT

Número do Processo: BR 10 2016 029610 2

Dados do Depositante (71)

Depositante 1 de 1

Nome ou Razão Social: Universidade Federal de Pernambuco
Tipo de Pessoa: Pessoa Jurídica
CPF/CNPJ: 24134488000108
Nacionalidade: Brasileira
Endereço: Av. Prof. Moraes Rego, 1235 - Cidade Universitária
Cidade: Recife
Estado: PE
CEP: 50670-901
País: Brasil
Telefone: (81)2126 8959
Fax: (81)2126 8959
Email: patentes_dine.propesq@ufpe.br

PETICIONAMENTO ELETRÔNICO Esta solicitação foi enviada pelo sistema Peticionamento Eletrônico em 16/12/2016 às 11:54, Petição 870160076203

Dados do Pedido

Natureza Patente: 10 - Patente de Invenção (PI)

Título da Invenção ou Modelo de Utilidade (54): FORMULAÇÕES FARMACÊUTICAS CONTENDO COMPOSTOS TIOXOOXAZOLIDINONAS 3,5 SUBSTITUÍDOS PARA INCREMENTO DE SOLUBILIDADE E USO ANTITUMORAL

Resumo: Os compostos tioxooxazolidinonas 3,5 substituídos, derivados oxazolidínicos (DOx), têm sido descritos como antibióticos de terceira geração e alguns relatos demonstraram seu potencial como agente antitumoral. Entretanto, a sua baixa solubilidade em água, limita sua utilização. Neste contexto, o desenvolvimento de complexos de inclusão baseados em ciclodextrina podem promover um incremento de solubilidade em compostos hidrofóbicos, oferecendo uma maior eficácia e maior biodisponibilidade. Nesta patente desenvolvemos complexos de inclusão baseados em 2-hidroxipropil-ß-ciclodextrina (2-HPßCD) em DOx hidrofóbicos: 3-etil-5-(4-metóxibenzilideno)-2-tioxooxazolidin-4-ona (LPSF/NB-10) e 5-benzilideno-3-etil-2-tioxooxazolidin-4-ona (LPSF/NB-14). As análises físico-químicos foram realizados através de estudos de fase de solubilidade, espectroscopia de espectroscopia em infravermelho (FTIR), difração de raios-x (DRX) e microscopia eletrônica de varredura (MEV). O estudo de viabilidade celular por MTT também foi conduzido para avaliação e comparação da atividade tumoral em linhagens MCF-7 (câncer de mama) e células controle (fibroblastos HIFF). Os resultados demonstraram que a solubilidade dos compostos foi incrementada em 20 vezes mais se comparados aos compostos puros em água. A análise por MEV também revelou uma mudança significante na morfologia das moléculas após o processo de inclusão. Adicionalmente, os estudos de viabilidade celular por MTT demonstraram uma melhoria na atividade antitumoral do DOx em 2-HPßCD nas linhagens MCF-7 quando comparadas estatisticamente em relação a células controle. Portanto, a presente patente apresentou novos produtos onde foi possível incrementar a solubilidade dos DOx e destinado ao uso antitumoral.

Figura a publicar: 01

FORMULAÇÕES FARMACÊUTICAS CONTENDO COMPOSTOS TIOXOOXAZOLIDINONAS 3,5 SUBSTITUÍDOS PARA INCREMENTO DE SOLUBILIDADE E USO ANTITUMORAL

01. A presente patente de invenção caracteriza-se pela obtenção formulações farmacêuticas contendo compostos tiooxazolidinonas 3,5 substituídos e/ou seus derivados sais, ésteres, amidas ou pró-fármacos farmacologicamente aceitáveis que venham a ser utilizados na saúde humana e/ou animal com fins de tratamento, profilaxia, paliativa.

02. Uma característica da presente invenção é o uso dos compostos tiooxazolidinonas 3,5 substituídos associados a ciclodextrina e/ou seus derivados como agentes antitumorais misturados a excipientes farmaceuticamente aceitáveis, em solução ou no estado sólido.

03. Os compostos da presente invenção são úteis em formulações farmacêuticas com carregadores convencionais ou veículos, para a administração a humanos e/ou animais em dosagens nas formas de tabletes, cápsulas, pílulas, pós, grânulos, supositórios, soluções ou suspensões parenterais estéreis, soluções ou suspensões não parenterais estéreis, soluções ou suspensões orais, suspensões óleo em água ou água em óleo, emulsões e as quantidades necessárias de compostos tiooxazolidinonas 3,5 substituídos e seus derivados.

04 . O núcleo oxazolidínico, foi descoberto pela empresa DuPont e patenteadas em por Fugitt & Luckenbaugh em 1978. Uma outra característica do núcleo oxazolidínico é a capacidade de inibir seletivamente a síntese de proteínas bacterianas através de ligação com a subunidade ribossomal 50S, impedindo a formação de um complexo de iniciação 70S funcional (Zhou et al., 2002; Stevens et al., 2004).

05. O primeiro derivado da oxazolidina, uma oxazolidinona, a ser comercializada foi a Linezolida. Este composto foi aprovado para tratamento de pacientes com infecções causadas por bactérias Gram-positivas (Barrett, 2000; Shaw & Barbachyn, 2011).

06. As oxazolidinas e seus derivados estão presentes em diversas moléculas de interesse farmacêutico. Além da atividade antibacteriana, há relatos na literatura de seus

derivados com atividade antifúngica (Devi *et al.*, 2013), hipoglicêmica (Bodnar *et al.*, 2011), anticonvulsivante (Kombian & Phillips, 2012) e antitumoral (Singh, 2011).

07. Em relação a atividade antitumoral, a presença da oxazolidina têm estado presente em diversos derivados: derivados do Perileno (patente GB8313571, 1983), derivados da sufonil ureia (EP0291269, 1988), ésteres e sais da rizoxina (CN86102020, 1986), taxoides (IL117636, 1996), derivados heteroarila fenil susbtituídos (IL117636, 1996), oxazolidinas aromáticas quiráis N-susbtituídas (WO2014036623, 2012) e 2-tioxo-oxazolidínicos-N-substituídos (BR1020150160607, 2015).

08. Na patente, WO2014036623, as oxazolidinadionas 3,4-dissubistituídas apresentaram atividade citotóxica em linhagem celular HL-60 ATTC®CCL-240 (leucemia promielocítica). Segundo os autores, a origem da diferença de atividade entre os compostos testados não seria devida simplesmente a propriedades físicas como lipofilicidade ou polaridade, mas às características estruturais únicas de cada composto. Os autores afirmaram ainda que a morte das células ocorreu por apoptose, correlacionando-a à tação do DNA.

09. Os mesmos mecanismos foram observados na patente BR1020150160607, 2015 desenvolvidas por nosso grupo de pesquisa. Os compostos apresentaram atividade citotóxica significante nas linhagens celular: leucemia promielocítica (HL-60, ATTC®CCL-240) leucemia linfoblástica aguda (CCRF-CEM, ATCC®CCL-119), leucemia de células T (JURKAT, ATCC®TIB152). O efeito citotóxico foi superior a 90% numa concentração menor de 30μM para todas a linhagens testadas.

10. Embora estes compostos apresentam atividade antitumoral comprovada e significante, eles apresentam uma utilização limitada devido a sua alta lipofilicidade. Essa limitação pode ser solucionada através do desenvolvimento de complexos de inclusão que resultem num incremento de solubilidade destes compostos.

11. Uma das estratégias bem estabelecidas nas ciências farmacêuticas são a utilização das ciclodextrinas. Estas moléculas são oligossacarídeos que apresentam em sua cavidade interna, a capacidade de incorporar drogas hidrofóbicas.

12. As ciclodextrinas também oferecem outras vantagens como uma melhor farmacocinética, estabilidade química e baixa citotoxicidade (Tiwari et al., 2010).

13. Dentre elas a 2-hidroxipropril-β-ciclodextrina (HP-β-CD) é uma das ciclodextrinas mais utilizadas. Esta moléculca além de aumentar consideravelmente a solubilidade de compostos hidrofóbicos, é toxicologicamente benigno. Além do mais a HP-β-CD pode ser administrada em formulações farmacêuticas por via parenteral, oral, oftálmica e nasal (Challa et al., 2005; Rasheed et al., 2008).

14. Em seu primeiro aspecto, nesta patente, utilizamos dois compostos (Fig.3.1 e Fig.3.2) obtidos através síntese estabelecida no pedido de patente BR1020150160607 (2015) de nosso grupo de pesquisa e preparamos os complexos de inclusão baseados em ciclodextrina (Fig.3.3) visando o incremento de solubilidade e/ou seus sais, derivados misturados a excipientes farmaceuticamente aceitáveis em soluções ou no estado sólido.

15. Outro aspecto desta patente foi a sua avaliação de atividade em células tumorais de adenocarcinoma de mama humano (MCF-7, ATCC®HTB-22) através do teste de MTT (3-(4,5-dimetiltiazol-2yl)-2,5-difenil brometo de tetrazolina).

16. Portanto, a presente invenção tem como principal objetivo contribuir com o incremento de solubilidade dos derivados 5-benzilideno-3-etil-2-tioxooxazolidin-4-onas através de complexos de inclusão baseados em ciclodextrina, que podem ser utilizados no tratamento, profilaxia, paliativa.

17. A presente invenção descreve formulações farmacêuticas compreendendo compostos tioxooxazolidinonas 3,5 substituídos visando o incremento de solubilidade destes compostos. As formulações farmacêuticas e/ou seus sais, derivados misturados a excipientes farmaceuticamente aceitáveis em soluções ou no estado sólido são aplicáveis em linhagens tumorais.

18. Entre as vantagens, estão a fácil preparação dos complexos LPSF/NB:2-HP-β-CD 2), aumento da solubilidade 20 vezes maior do que em água em relação aos compostos puros.

19. A seguir, a invenção será descrita em maiores detalhes com o auxílio de exemplos de forma de apresentação apresentados em Figuras e Tabelas.

20. Se mostra:

21. 22. Na figura 1, demonstra-se a estrutura dos derivados oxazolidínicos utilizados nas composições farmacêuticas baseadas em 2-HP-β: 1) 3-etil-5-(4-metóxibenzilideno)-2-tioxooxazolidin-4-ona (LPSF/LPSF/NB-10), 2) 5-benzilideno-3-etil-2-tioxooxazolidin-4-ona (LPSF/NB-14)

23. Na figura 2, está presente o diagrama de fase de solubilidade para LPSF/NB-10 (a) e LPSF/NB-14 (b) em função de concentrações de HP-β-CD em água a 25ºC.

24. Na figura 3, está o espectro de infravermelho do LPSF/NB-10:HP-β-CD (linha vermelha, 4a), LPSF/NB-14:HP-β-CD (linha azul, 4b) através de mistura mecânica e a metodologia aplicada para os complexos de inclusão.

25. Na figura 4, estão presentes os difratogramas de raios-X de LPSF/NB-10 (5a, linha preta), LPSF/NB-14 (5b, linha vermelha), HP-β-CD puro (linhas azuis) e de seus complexos de inclusão com HP-β-CD (a1, linha preta e b1, linha vermelha).

26. Na figura 5 observa-se as imagens de MEV do LPSF/NB-10 (a,a1) e LPSF/NB-14 (6b,b1) , HP-β-CD (6c,c1) e complexos de inclusão LPSF/NB-10/ HP-β-CD (6d, d1) e NB-14/ HP-β-CD (6e,e1).

27. Na tabela 1 demonstra-se os valores médios e desvios-padrão em percentual da viabilidade celular de células tumorais (MCF-7) na presença dos derivados oxazolidinicos e seus complexos de inclusão com HP-β-CD.

TABELAS

Tabela 1.

Concentração	LPSF/ NB-10	LPSF/NB-10:HP-β-CD	Valor de p	LPSF/ NB-14	LPSF/NB-14:HP-β-CD	Valor de p
1μM	97,80 (0,01)	70,22 (0,01)		100,00 (0)	77,93 (0,01)	
10μM	87,56 (0,02)	72,24 (0,01)		87,74 (0,02)	71,79 (0)	
25μM	78,71 (0,02)	67,57 (0,00)	0,357	72,70 (0,03)	65,45 (0,01)	0,008
50μM	67,68 (0,02)	61,46 (0,01)		69,68 (0)	50,98 (0,01)	
75μM	55,13 (0,02)	74,00 (0,01)		70,52 (0,01)	49,37 (0)	
100μM	64,56 (0,02)	66,70 (0,02)		71,37 (0,01)	46,42 (0,01)	

28. Na tabela 2 demonstra-se valores médios e desvios-padrão em percentual da viabilidade celular de células controle (fibroblastos, HIFF) na presença dos derivados oxazolidinicos e seus complexos de inclusão com HP-β-CD.

Tabela 2

Concentração	LPSF/NB-10	LPSF/NB-10:HP-β-CD	Valor de p	LPSF/NB-14	LPSF/NB-14:HP-β-CD	Valor de p
1μM	100 (0)	76,87 (0,03)		98,58 (0,11)	96,02 (0,09)	
10μM	100 (0)	83,62 (0,03)		100,00 (0)	86,25 (0,07	
25μM	100 (0)	82,60 (0,01)		100,00 (0)	82,12 (0,01)	
50μM	97,69 (0,08)	93,78 (0,02)	0,281	100,00 (0)	81,49 (0,07)	0,8450
75μM	89,04 (0,05)	81,24 (0,05)		100,00 (0)	80,90 (0,02)	
100μM	66,41 (0,05)	86,01 (0,05)		88,27 (0,01)	79,88 (0,01)	

29. Na figura 2, foi realizado o estudo de fase de solubilidade obtido a partir de LPSF/NB-10:HP-β-CD (a) e LPSF/NB-14:HP-β-CD (b). Os comportamentos dos valores demonstraram curvas do tipo AL que corresponde a uma razão estequiométrica (K1:1) entre a molécula e a HP-β-CD. As constantes de solubilidade (K1:1) de LPSF/NB-10 e LPSF/NB-14 em solução de HP-β-CD a 25°C foi de 0.320 e 0.316 respectivamente. O incremento da solubilidade destes compostos foi de 12.50 mM e 12.62 mM respectivamente. Isso corresponde a um aumento 20 vezes maior que a solubilidade de LPSF/NB-10 e LPSF/NB-14 em água (0.60 mM e 0.64 mM respectivamente).

30. Na figura 3, está o espectro da HP-β-CD as absorções em 3,411 cm^{-1}, 2,931 cm^{-1}, 1,157 cm^{-1}, 1,089 cm^{-1}, e 1,029 cm^{-1} foram atribuídas às vibrações ν(O –H alongamento vibracional), ν(C –H alongamento vibracional), ν(C –H e C –O alongamento vibracional). No espectro de infravermelho (IV) do LPSF/NB-10 (a) as absorções em 1750-1735 cm^{-1} foram atribuídas às vibrações ν(C=O alongamento), as absorções 1600–1585 cm^{-1} às vibrações ν(C-C alongamento, aromático), as absorções 1360–1290 cm^{-1} às vibrações ν(C-N alongamento, aminas alifáticas), e por fim as

absorções em 1050-1200 cm^{-1} às vibrações ν(C=S alongamento). As absorções semelhantes no espectro de infravermelho do LPSF/NB-14 (b) foram observadas. Absorções em 3,016 cm^{-1} atribuídas às vibrações ν(C–H alongamento vibracional), absorções em 1,745 e 1,695 cm^{-1} às vibrações ν(C=O alongamento), e absorções em 1,631 cm^{-1} às vibrações ν(C=C alongamento). Os resultados mostraram que formação de complexos de inclusão foram bem-sucedidos, considerando a diminuição da intensidade das bandas (linha vermelha em a e b) de absorção dos grupos funcionais dos compostos tiooxazolidina 3,5 substituídos.

31. Na figura 4, a difração de raio-X do LPSF/NB-10 apresentou estes padrões em 12,5 e 25θ (linha preta em a). No entanto, LPSF/NB-14 apresentou também picos de intensidade em 7,5 e 15θ (linha vermelha em b). Isso reflete que uma característica típica de sólidos cristalinos. Em contraste, HP-β-CD naturais e sintéticas não possuem essa característica (linha azul em a1 e b1) são amorfos. Nos compostos de inclusão, os difratogramas sugerem a formação de sistemas mais organizados com uma diminuição nos picos de intensidade se comparadas as moléculas LPSF/NB-10 (a1) e LPSF/NB-14 (b1).

32. Na Figura 5, a imagens de MEV do LPSF/NB-10 (a,a1) e LPSF/NB-14 (b,b1) claramente apresentaram formas cristalinas aciculares, enquanto HP-β-CD (c, c1) apresentou formas esféricas. As imagens relacionadas aos complexos de inclusão para LPSF/NB-10:HP-β-CD (d, d1) e NB-14/ HP-β-CD (e,e1) revelaram uma mudança significativa na morfologia.

33. Na tabela 1, considerando a viabilidade celular da linhagem tumoral MCF-7, percebe-se que houve uma diminuição significativa para os compostos LPSF/NB-14 em relação ao LPSF/NB-10. Os complexos de inclusão demonstram atividade antitumoral até mesmo na mais baixa concentração. A análise estatística demonstrou que a diferença foi mais significante entre LPSF/NB-14 e seu complexo de inclusão em relação ao LPSF/NB-10 e seu complexo de inclusão.

34. Na Tabela 2 é possível perceber através da análise estatística, que as diferenças entre os valores não foram significativas entre si. Os fibroblastos são utilizados como modelo de células padrão (normais) para comparar os efeitos citotóxicos em linhagens tumorais sólidas.

ANEXOS

ANEXO A - ARTIGO PUBLICADO DURANTE O DOUTORADO

[Frontiers in Bioscience, Scholar, 8, 129-142, January 1, 2016]

Chemical immobilization of antimicrobial peptides on biomaterial surfaces

Rafael R. Silva[1], Karen Y.P.S. Avelino[2], Kalline L. Ribeiro[1], Octavio L. Franco[3], Maria D.L. Oliveira[2], Cesar A.S. Andrade[1,2]

[1]Programa de Pos-Graduacao em Inovacao Terapeutica, Universidade Federal de Pernambuco, 50670-901 Recife, PE, Brasil, [2]Departamento de Bioquímica, Universidade Federal de Pernambuco, 50670-901, Recife, PE, Brasil, [3]Centro de Analise Proteomicas e Bioquimicas de Brasilia, Universidade Catolica de Brasilia, 71966-700, Brasilia, DF, Brasil

TABLE OF CONTENTS

1. ABSTRACT

Hospital infections associated with surgical procedures and implants still present a severe problem in modern societies. Therefore, new strategies to combat bacterial infections mainly caused by microorganisms resistant to conventional antibiotics are necessary. In this context, antimicrobial peptides have gained prominence due to their biocompatibility, low toxicity and effectiveness. The immobilization of antimicrobial peptides (AMPs) onto biomaterial surfaces is an excellent alternative for the development of new biodevices with microbicidal properties. Herein, we describe reports related to physical-chemical characterization, *in vitro*/*in vivo* studies and the clinical applicability of such active surfaces. In this review, we focused on the mechanisms of action, different peptide immobilization strategies on solid surfaces and the microbicidal effectiveness of AMPs.

2. INTRODUCTION

Bacterial resistance is still one of the major problems facing public health in modern societies (1). This can occur due to the indiscriminate use of antibiotics, which induces the formation of new species that are resistant to conventional antibiotics (2). A major problem facing modern societies is the health risks stemming from the transmission of new infections that are difficult to treat. In addition, the transmission routes (e.g. airborne or direct contact) can lead to epidemic episodes (3). Thus, many studies have aimed to minimize microbial contamination by developing new drugs. Although there are thousands of new compounds synthesized per year, the difficult process of validation and clinical phase studies decrease the possibility of new drug manufacturing. In this context, the discovery of antimicrobial peptides (AMPs) has shown promise as a way to eradicate some resistant bacterial strains (4).

AMPs are small amino acid sequences obtained by their extraction from many types of organisms (plants, insects and animals) and play an important role in inhibiting the growth of multiple microorganisms (5, 6). Currently, the database that contains detailed information on these peptides (antimicrobial peptides database, APD) contains 2495 types with different functions: antibacterial, antifungal, antiparasitic, anti-cancer, antioxidant, etc. (7). Chemically modified AMPs are obtained from the modifications of natural ones derived from magainin and histidine (8, 9) or through new synthetic forms (e.g. E14LKK, RK1, RK2), aiming to improve microbicidal effectiveness (10, 11).

Some hospital infections come from the adherence of microbes, especially bacterial species on the surfaces of medical devices and implants (e.g. dental or orthopedic) or during surgical procedures due to the lack of adequate hygienization (12, 13). The massive bacterial colonization on solid surfaces could contribute to biofilm formation (14). This process involves the transport of bacterial cells and further attachment commonly mediated by van der Waals and electrostatic charges. The adhesion of proteins and extracellular polymeric substances (EPS) can reinforce bacterial adhesion (15). Once implanted, these microorganisms can maturate and differentiate, forming microcolonies and propagating

infections with detached cells (16). As a result, infections associated with bacteria are difficult to treat, and the removal or replacement of infected medical implants or devices reflects considerable costs for the healthcare system, which leads to patient suffering, prolonged hospitalization and eventually death (17).

In this scenario, the development of new biomaterials to prevent adhesion and microbial infection in hospital equipment and implants are of increased interest. The use of AMPs in adsorption processes, functionalization and immobilization of organic coatings onto substrate surfaces (titanium or silicone) has demonstrated good activity with clinical potential, summarized in Table 1.

Therefore, this review addresses three important aspects for the use of AMPs in antimicrobial coatings: basic concepts and mechanisms of action of peptides against microorganisms (with the emphasis on bacteria), chemical immobilization strategies for the inclusion of peptides associated to solid substrates and the effectiveness of these models in antimicrobial testing.

2.1. Antimicrobial peptides

AMPs are important components of the innate immune systems of living organisms and contribute effectively against exogenous pathogens (18). After a microbial infection, most of these peptides act to neutralize a wide range of microorganisms. In addition, AMPs are efficient at low concentrations, are less likely to promote bacterial resistance and have antitumor properties. Therefore, AMPs are promising candidates for their use as novel therapeutic drugs (4). They comprise a chemically and structurally heterogeneous family yet share molecular masses lower than 5 kDa, aside from having cationic and amphipathic properties (19, 20).

Due to the enormous variety of amino acid sequences and structural features, the exact action mechanism of AMPs is still a controversial issue. However, there is a consensus about the mechanism of positively charged peptides. The cationic charges on the peptide surface favor the electrostatic interaction of negatively charged microbial membranes through bivalent cation exchange (20). In addition, AMPs assume an amphipathic structure after interacting with the bacterial membrane, resulting in a lethal permeabilization (20, 21).

The antimicrobial activity of AMPs is based on four model mechanisms named barrel, carpet, toroidal and detergent. In the barrel model, the hydrophobic part of AMPs interacts with the lipid hydrocarbon chains of membranes, and their hydrophilic part exposes the lumen as a result of transmembrane aqueous channel formation. The carpet model occurs due to the saturation of the bacterial membrane by AMP molecules, resulting in its permeabilization (21, 22). In the toroidal model, the peptides are interspersed with phospholipids, and the polar groups of both molecules interact with each other, resulting in pore formation in the lipid membrane, where peptides are assumed to adopt a transmembrane orientation (23). Finally, the detergent-like model can occur as a consequence of the carpet model. Once attached to membrane surface by electrostatic interactions, AMPs interleave the lipid bilayer until reaching a saturation point with subsequent micelle formation and bacterial membrane destruction (24).

The systemic use of AMPs is restricted, mainly due to their toxicity when used at high concentrations, as well as by its relatively short half-life and susceptibility to proteases (10). The interaction of peptides with bacteria is initially driven by weak attraction forces (van der Waals and electrostatic interactions), which are further enhanced by specific interactions involving peptides and biofilm formation (25). Therefore, the most feasible way to use peptides is through their immobilization onto solid surfaces with the aim of developing new antimicrobial structures. In general, the use of intermediary linkers between solid surfaces and AMPs is required to obtain better microbicidal activity (25).

Bacterial infections associated with implanted devices still present a significant threat to patients and are a serious challenge for physicians. High rates of infection are observed for orthopedic implants, dental devices, vascular grafts, urinary and venous catheters, which results in low performance of these devices in terms of safety and longevity (26, 27). Central venous catheters, commonly used in clinical cases (e.g. chemotherapy, prolonged parenteral nutrition and hemodialysis), contain silicone or polyurethane in their constitution. In addition, catheters are useful for peptide immobilization and, therefore, acquire the potential to be used against biofilms involved in hospital infections post-surgery (28). Furthermore, limitations of biomolecular immobilization could spur the development of new antimicrobial surfaces capable of preventing initial bacterial colonizations or at least reduce active bacterial titles. Thus, modified surfaces could directly affect patient health and reduce costs in public health, making the use of AMPs an excellent alternative to remedy these issues.

3. PHYSICAL METHODS FOR IMMOBILIZATION OF AMPS

Recently, several studies have demonstrated AMP coupling with different substrates and their effectiveness against biofilm formation (29-33). AMPs have unique bioactive properties capable of overcoming limitations of other antibacterial coatings, such as the risk of developing bacterial resistance, short-term antimicrobial protection, limited antimicrobial spectrum and high cytotoxicity (34-37). Therefore, AMP immobilization onto diverse medical devices, including implants, urinary

Chemical immobilization of AMPs on biomaterial surfaces

Table 1. AMP covalent immobilization on solid surfaces and their antimicrobial activity against bacteria, fungi and yeasts

Substratum	AMP	Chemistry Immobilization Strategy	Evaluated microorganisms	References
Polyamide resin (pepsynK)	Novel synthetic peptides and Magainin 2	Grafting of C-terminus to the polymer support during solid-phase peptide synthesis	*E. coli, K. pneumoniae, S. aureus, B. subtilis, C. albicans*	10
PEG[1]-Polystyrene (PEG-PS) resin beads	6K8L	Peptide synthesized by solid-phase peptide synthesis on a PEG-PS resin using Fmoc[2] chemistry	*B. subtilis, E. coli. Kluyveromyces marxianus, L.monocytogenes, P. fluorescens, S. typhimurium, Serratia liquefaciens, S. aureus*	53
PEGylated resin beads (TentaGel S NH2, HypoGel 400 NH2 and HypoGel 200 NH2)	KLAL and Magainin-derived peptide (MK5E)	C-terminal immobilization by standard solid-phase peptide synthesis and Fmoc chemistry; N-terminal and side-chain immobilization by thioalkylation and oxime formation	*E. coli, B. subtilis*	8
PEGylated resin beads (TentaGel S NH2 resin beads)	Melittin, Buforin 2 and Tritrpticin	Thetered modified beads by oxime-forming ligation strategy	*E. coli, B. subtilis*	90
PEG-Polystyrene (PEG-PS) resin beads	amphipathic β-sheet peptides	Covalent binding by Fmoc chemistry on PEG-PS beads	*S. aureus, Micrococcus luteus, P. aeruginosa, E. coli.*	51
Glass coverslips	Melimine	Grafting via ABA[3] and FNA[4] linkers	*P. aeruginosa, S. aureus*	72
Indium-tin-oxide glass	Polymixin B	Silane containing epoxy rings to couple peptides by catalyst	*E. coli. NCTC 8007*	94
Polydimethylsiloxane (PDMS)	CW11	Cross-Linking of peptides to allylglycidil ether modified PDMS surface (PDMS-AGE[5]-PEG) via Sulfhydryl Chemistry	*E. coli, S. aureus, P. aeruginosa*	100
Silicone Urinary Catheter and Polydimethylsiloxane (PDMS)	RK1 and RK2	Cross-linking of peptides to allylglycidil ether modified PDMS surface (PDMS-AGE-PEG) via Sulfhydryl Chemistry	*E. coli, S. aureus, C. albicans*	11
Pretreated Ti with amino silane and epoxy silane	LL-37	Site-specific conjugation through amine reactive NHS-group and the Thiol-reactive maleimide-moiety	*E. coli*	105
Pretreated Tisilanization with CPTES or APTES	hLF[6]-11	Peptide physical adsorption and covalent binding with CPTES[7] or APTES[8]	*S. sanguinis, L. salivarius*	31
-	Nisin, Trp-11, 4K-C16	Covalent immobilization via reaction between amine groups on the peptides and surface epoxy groups on the plasma polymer interlayer	*E. coli, B. subtilis*	85
-	Nisin, Magainin I.	Covalent immobilization through grafting of chitosan, cross-linking agents and peptides	*L. ivanovii*	111

[1]PEG: Polyethylene glycol, [2]Fmoc: 9-fluorenylmethyloxycarbonyl, [3]ABA: 4-azidobenzoic acid, [4]FNA: 4-fluoro-3-nitrophenyl azide, [5]AGE: allylglycidyl ether, [6]hLf: human lactoferrin, [7]CPTES: chloropropyltriethoxysilane, [8]APTES: 3-aminopropyltriethoxysilane

and intravenous catheters, has an undeniable potential for clinical use (38-41). However, new immobilization strategies are required to ensure the applicability of AMPs on solid surfaces, improving the effectiveness and functionality of modified biodevices (35, 42).

AMPs can be immobilized onto solid surfaces through physical methods such as adsorption, self-assembled monolayers (SAM) or through chemical methods via selective or non-selective covalent bonding (35, 42, 43). Physical methods are based on hydrogen bonds, permanent or induced dipole interactions (van der Waals' force or London dispersion force), and hydrophobic or ionic interactions between AMPs and surfaces (44-47). Some substrates have been used for AMP anchoring such as gold (32), titanium (31, 34, 40, 48), titanium dioxide (49), silicon (50), silicone (11, 41), polymeric brushes and resins (8, 51-54). Of note, immobilization onto substrate surfaces can be performed without any shape restriction, such as

planar, spherical or curved geometries (55). However, specific surface properties (nature, composition, charge, hydrophilic or hydrophobic character, topography and roughness) and AMP characteristics (type, charge, molecular size and conformational stability) interfere in the immobilization process (46). In addition, experimental conditions such as time, peptide concentration, pH and temperature should be also considered (46, 53).

The self-assembly technique is one of the main strategies used for physical AMP immobilization (56, 57). This approach is based on the alternating deposition of anionic and cationic layers on a solid substrate (58-60), enabling the obtainment of functionalized films through the insertion of AMPs between polyelectrolytes layers (55) and the control of film thickness and adsorbed biomolecule amounts (56). Moreover, self-assembly is an effective procedure since it does not cause chemical changes in the functional peptide and maintains its conformational stability by retaining water molecules between the matrices (57, 61). One of the main features that make SAM films promising for biotechnological applications is the possibility of temporal control over incorporated AMP release in hydrolytically degradable polymers through surface erosion (57, 62-64).

Several studies have demonstrated good prospects for AMP application in polymeric films. However, some disadvantages could be associated with the self-assembly technique, limiting its application for obtaining implants coated by biomaterials and medical devices (55). An important disadvantage comprises AMP incorporation into the lower layers of the film, which restricts their direct contact with the surrounding bulk (31). AMP bioactivity is dependent on the diffusion process at the interface, being influenced by the tortuosity of the diffusion (64) via film thickness (65) and intermolecular interactions between the polymer and peptide (66). A relatively fast peptide release from the polymeric films results in a decreased amount of anchored AMPs, interfering in the minimum AMP concentration required to inhibit the growth of microorganisms and increase the number of biomolecules in the bulk (55). In addition, a fast release can provide conditions for the development of bacterial resistance, local toxicity and hemolytic activity (45,55). Therefore, the limitations of the self-assembly technique should be considered prior to its use as a strategy for obtaining more effective antimicrobial coatings.

The achievement of antimicrobial coatings with adequate properties results from the improvement of immobilization techniques (16, 39). The development of appropriate methodologies for coating surfaces ensures biological peptide properties including mechanism of action, wide spectrum bioactivity, stability in adverse conditions and low propensity for the development of bacterial resistance (3, 40-42). However, this requires some factors that influence the performance of these biomolecules, such as peptide orientation, surface concentration of bounded AMPs, and spacer length and flexibility, which determine the lateral mobility of AMPs (5, 7). Under these conditions, the use of chemical methods for the immobilization of AMPs onto solid surfaces has increased (27).

4. CHEMICAL APPROACHES FOR COVALENT IMMOBILIZATION OF AMPS ONTO SURFACES

The chemical immobilization of AMPs is an alternative strategy for coating surfaces and improving peptide stability. Consequently, the duration of the antimicrobial efficacy is increased and is further associated with a reduction in the toxicological risks for patients by reducing the leaching of peptides (8, 37, 65, 66). Besides these advantages, adequate AMP orientation on the substrate can provide greater bioactivity (20, 67). For these reasons, covalent bonds have been extensively studied as a tool to overcome the limitations of the physical anchoring methods (20, 54, 68). However, it is important to emphasize that chemical immobilization can alter the conformational structure of the molecule, restrict its mobility and interfere in the mechanism of action (46). Therefore, molecular coupling mechanisms should be thoroughly evaluated for the maintenance of bioactive AMP properties (52).

Chemical immobilization involves the formation of at least one covalent bond between the surface and the responsible biomolecule to provide stability to antimicrobial film (20). Stability is obtained through the strength of covalent bonds, which prevents spontaneous peptide uncoupling (8,10,69). Covalent bonds are classified as selective or non-selective (70). A selective bond between AMPs and substrates can be obtained through the insertion of a specific functional group in the molecular structure of the peptide via chemical synthesis (35). In addition, is possible control the route of reaction and orientation of the biomolecule (8, 48, 71). On the other hand, non-selective immobilization occurs naturally without requiring additional chemical modifications in the peptides. In this case, covalent binding uses the intrinsic functional groups (e.g. carboxylic acid, amino, sulfhydryl and hydroxyl groups) of the peptide sequence to react chemically with activated surfaces. Non-selective immobilization can result in more than one type of covalent bonding with different orientations of the biomolecule (42, 72). However, for non-reactive surfaces, the functional groups should be inserted through spacers to obtain a covalent bond between AMPs and surfaces (73). Substrate modification can be performed using SAM composed by chemically-reactive organic molecules as a simple and effective strategy (35, 74-76). The spacer length can be varied from one to several carbon atoms with a direct influence on AMP bioactivity (35).

Chemical immobilization of AMPs on biomaterial surfaces

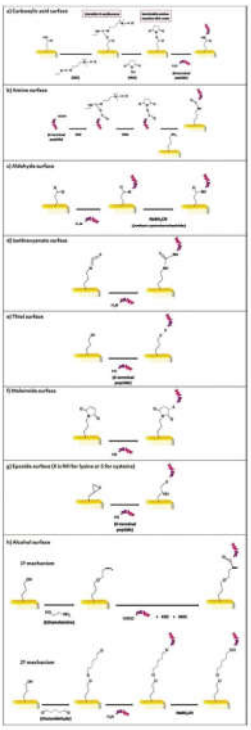

Figure 1. Examples of chemical strategies for controlled covalent attachment of AMPs on surfaces functionalized with different reactive groups. a) Surfaces functionalized with carboxylic acid groups can be used to covalently bind AMPs via coupling agents 1-ethyl-3-(3-dimethylaminopropyl) carbodiimide hydrochloride (EDC) and N-hydroxysuccinimide (NHS) that activate the chemical groups on the surface. b) AMPs can be attached to amino-functionalized surfaces through activation of their carboxylic groups with EDC and NHS before incubating on the surface. c) Aldehyde groups present on functionalized surfaces can chemically react with amine groups of AMPs and establish stable covalent bonds through reducing agents, such as sodium cyanoborohydride ($NaBH_3CN$). AMPs can be immobilized on solid supports functionalized with d) isothiocyanate, e) thiol, f) maleimide and g) epoxide groups. Except for anchoring of AMPs on isothiocyanate modified-surfaces, the use of thiol-bearing peptides is verified for covalent immobilization of AMPs on surfaces functionalized with thiol, maleimide and epoxide groups. In all cases, the chemical coupling occurs in a single step and without the need for additional reagents. h) Surfaces functionalized with alcohol can anchor AMPs via two reaction mechanisms. In the first mechanism, hydroxyl groups of spacers are derivatized with an amino alcohol, such as ethanolamine, and the carboxylic acid groups of AMPs are activated with EDC and NHS for the attachment of the peptides on the surface. In the second mechanism, hydroxyl groups of spacers are derivatized with an aldehyde (e.g. glutaraldehyde), subsequently, the immobilization of AMPs proceeds similarly to the anchoring of peptides on aldehyde-modified surfaces.

Another strategy to covalently immobilize AMPs involves the use of functionalized polymer resins such as polyethylene glycol (PEG) or other 'brushes' that bear reactive groups suitable for coupling peptides (8, 10, 51, 53). PEG is one of the main spacers used in the activation of surfaces by presenting the anti-adhesive property that prevents or minimizes bacterial colonization (77-79). In addition, PEG is an amphiphilic and flexible polymer that allows for a greater lateral mobility of the AMPs and retention of water molecules in its interior. PEG is capable of maintaining the bactericidal activity of peptides after immobilization onto solid supports (25). However, a disadvantage of the use of polymers as spacers consists in the possibility of polymer chain degradation and premature AMP release (53).

A wide variety of chemical coupling methods for the immobilization of AMPs onto surfaces are shown in Figure 1. Carboxylic acid-functionalized surfaces can react with primary amines, leading to the formation of peptide bonds (amide bonds) (73). However, the reactive chemical groups on the surface should be initially activated with 1-ethyl-3-(3-dimethylaminopropyl)carbodiimide hydrochloride (EDC) and N-hydroxysuccinimide (NHS) (Figure 1a) (35, 73). On the other hand, the AMP immobilization onto amino-functionalized surfaces is similarly obtained, as explained previously, for carboxylic acid-functionalized surfaces. In this case, the accessible carboxylic groups of the peptide should be activated with the EDC:NHS coupling method before being added to the functionalized surface (Figure 1b) (35). The carboxyl-amine conjugation reactions based on the use of EDC and NHS occur in two sequential steps. EDC first reacts with a carboxyl group, forming an amine-reactive O-acylisourea intermediate. This unstable intermediate is susceptible to hydrolysis and stabilized through the addition of NHS by converting it to a semistable amine-reactive NHS ester (Figure 1a). After the addition of NHS, it is possible to obtain a stable amide bond with a 10-20 fold increase in coupling efficiency. Carbodiimide cross linker chemistry is widely used for the immobilization of peptides on modified surfaces with carboxyl (Figure 1a) or amino groups (Figure 1b) (80-82). Another strategy for biomolecule immobilization is based on aldehyde groups displayed on functionalized surfaces. This approach can be used to covalently bind AMPs from primary amines, resulting in the formation of imine bonds. However, since the imine bonds are unstable, they should be converted to amine bonds through reducing agents, as sodium cyanoborohydride ($NaBH_3CN$), for the stabilization of anchored peptides (Figure 1c) (71, 83).

The surface coupling strategy also uses isothiocyanate for the attachment of peptides via primary amine groups (Figure 1d) (35). Disulfide bonds can also be used to immobilize many peptides and proteins. Surfaces modified with thiol groups can covalently immobilize AMPs through disulfide bonds established

between the surface and cysteine residues of the peptide (Figure 1e) (70,84). AMPs can be attached to maleimide-functionalized surfaces through covalent bonds established between the thiol group of the peptide and the α,β-unsaturated carboxyl of the maleimide (Figure 1f) (25,52). AMPs containing thiol or primary amino group derivatives (e.g. amino acids cysteine and lysine, respectively) can be easily immobilized onto epoxide-functionalized surfaces through a nucleophilic ring opening in a spontaneous reaction (Figure 1g) (83,85).

There are currently two reaction mechanisms for AMP immobilization onto alcohol-functionalized surfaces (Figure 1h). In the first mechanism, the spacers containing hydroxyl groups are derivatized with an amino alcohol such as ethanolamine. Subsequently, the peptides whose carboxylic acid groups were previously activated with the EDC: NHS solution are added to the modified surface, resulting in a covalent bond (35). In the second mechanism, the spacers presenting the alcohol function are derivatized with an aldehyde (e.g. glutaraldehyde). Therefore, the immobilization of AMPs on aldehyde-modified surfaces occurs similarly, as has been shown previously (35). As explained before, diverse methodologies for AMP immobilization onto solid surfaces are available. However, the advantages and disadvantages of each technique should be evaluated for obtaining effective antibacterial films(46). Therefore, the molecular coupling process should be rigorously controlled for the maintenance of the bioactive properties of the peptides and the functionality of the final product (42,43).

5. EFFECTIVENESS OF AMPS IMMOBILIZED ONTO A BIOMATERIAL SURFACE

Antimicrobial peptides have a well-defined mechanism of action described by interaction models that evaluate the association between the sequence of peptides and the bacterial cell wall (86-88). The search for improving the efficiency of AMP-bacteria interaction also leads to the development of artificial peptides and the discovery of novel, natural peptides extracted from various living organisms. In recent years, there has been increased interest in developing new antimicrobial biomaterials in pre/post-surgery processes to avoid nosocomial infections (25). The applications of immobilized AMPs are an excellent alternative for use against nosocomial infections caused by common pathogens and antibiotic-resistant microorganisms (8, 42). AMPs have been tested on diverse solid surfaces such as resins, glass, silicone, titanium and stainless steel for clinical use (43,89).

Resins are solid polymers obtained from plants or chemical synthesis. Some resins are chemically modified and useful as a substrate for AMP immobilization due to their high molecular weight and amide/amine moieties in its molecular chain (10,90) (Table 1). However, physicochemical characteristics of resins do not contribute to clinical applications. Of note, these materials are important to obtain a better understanding of the mechanisms of action of surface-active peptides (8,53).

Haynie *et al.* studied the bactericidal effects of magainin 2 and various synthetic peptides mainly containing lysine, leucine and glycine in their compositions, utilizing an ethylenediamine-modified polyamide resin (Pepsin K). Altogether, 70% of the tested peptides, which included magainin2, showed bactericidal activity against fungi and Gram-positive and Gram—negative strains. Among them, E14LKK showed the highest antibacterial activity, except for *P. aeruginosa* and *A. niger*. Other studies also used E14LKK immobilized onto polyethylene film containing PEG as the intermediate binder. The peptide remained active and reduced *E. coli* strains up to 3 log (54).

The covalent immobilization of AMPs at different binding sites and with different length spacers also influences biocidal and hemolytic activities. Two α-helical cationic AMPs, MK5E and KLAL, were immobilized on polystyrene resin beads (Table 1). MK5E is an AMP derived from magainin2 having only microbicidal activity while KLAL has both biocidal and hemolytic activities. Bagheri *et al.* used resin beads with different sizes (TentaGel S NH2, HypoGel 200, and 400 NH_2) with covalently-linked peptides via N and C terminal chains. They demonstrated that the antibacterial activity of cationic AMPs was influenced by spacer length. AMP biocidal activity is directly dependent on the spacer length, providing more flexibility and capacity to interact with microorganism surfaces (8).

Bioactive glasses also provide an advantage in forming an interface between implant and organism without inducing immune responses. This type of glass has potential applications in dentistry (91), ophthalmology (92) and orthopedics (93). However, there are still few studies on the immobilization of AMPs onto glass (72,94). These materials have been used for the immobilization of melamine, a cationic peptide modified by covalent bonding. In addition, ligands such as 4-azidobenzoic acid or 4-fluoro-3-nitrophenyl azide are used to modify glass substrate surfaces (72) (Table 1). Glass coated by indium-tin-oxide was also functionalized with silane coatings containing epoxy rings (3-glycidyloxypropyl-trimethoxysilane (94).

Silicone is a synthetic polymer obtained from fluid resin or elastomer forms. Silicone is one of the most cited materials for peptide immobilization and is extensively used in the medical and pharmaceutical fields due to its biocompatibility and wide range of physical forms. In addition, this polymer is applied

in manufacturing prostheses and medical devices (e.g., catheters and stents) (95,96). New approaches have been developed to prevent biofilm formation on pre/post-surgical procedures aiming to decrease mortality rates and costs to public health (97-99).

Some peptides have been immobilized on venous catheters composed of silicone for the development of bactericidal surfaces against bacterial strains (38). The understanding of the interactions between AMPs and bacteria has led to the development of novel synthetic peptides (e.g. CW11, RK1 and RK2) (11,100). CW11, a synthetic peptide, was chemically immobilized on a polydimethylsiloxane (PDMS) surface maintaining an *in vitro* bactericidal effect (Table 1). CW11 is mainly composed of tryptophan and arginine, which contribute to a better adhesion process on bacterial surfaces even under saline conditions. CW11 has low cytotoxicity and excellent antibiotic activity against *E. coli*, *P. aeruginosa* and *S. aureus* as compared to conventional antibiotics. Thus, the CW11 peptide is an alternative for modifying medical devices based on silicone as a substrate (100).

In addition, other peptides such as RK1 and RK2 (both derived from the human beta-defensin-28 variant) showed a broad antimicrobial spectrum, tolerance to saline conditions and use for the modification of silicone surfaces (101) (Table 1). These peptides are rich in arginine, lysine and tryptophan residues, showing antimicrobial activity against *E. coli, S. aureus* and *C. albicans* in phosphate buffered solutions and urine samples. Cultures of smooth muscle cells showed no signs of toxicity, demonstrating biocompatibility for use in urinary catheters. Therefore, the development of new peptides is an alternative for covering catheters and preventing urinary tract infections (11). In addition, new, natural and/or synthetic peptides have been used to modify metal surfaces such as titanium, and have been applied in clinical and preclinical research studies (9, 31, 40, 102).

Titanium (Ti) is another material used for implants in dental and orthopedic applications (12, 13). Likewise, the properties of biocompatibility, corrosion resistance and ability to bind to bone has induced new research studies (103). The use of AMPs and Ti is associated with the lack of toxicity and low immune response. The bactericidal effectiveness of LL-37 on Ti surfaces was evaluated (104, 105) (Table 1). LL-37 is a peptide derived from cathelicidin and extracted from epithelial cells and neutrophil granules. Zanetti *et al.* (104) performed the immobilization of LL37 by covalent bonding strategies using PEG as a spacer between solid surfaces and the peptide. In addition, LL-37 with cysteine (Cys-LL37) was used to assess binding to the spacer. The presence of cysteine ensured stable bonding with PEG and better mobility of LL-37, facilitating the interaction with the evaluated bacterial cell membrane. AMPs conjugated to spacers (copolymer "brushes") with a low density provide a high number of peptide/polymer chains, which results in higher antimicrobial activity (48).

Besides LL-37, another example of AMPs extracted from humans are human lactoferrins (hLF). In addition, hLFs are involved in the activation and differentiation processes and immune responses against microorganisms (106-108). The peptide hLF1-11 is effective against strains of *Streptococcus sanguinis* and *Lactobacillus salivarius*, preventing the formation of biofilms at early stages. Recently, the antimicrobial effect of the hLF1-11 attached to Ti surfaces was demonstrated to be effective for dental applications (31).

On the other hand, stainless steel (SS) is a metal present in several areas where hygiene is essential, including the home, the food industry and the medical field. The presence of SS in hospital environments highlights its importance for developing antimicrobial surfaces in order to avoid pre/postoperative infections (109, 110). In this context, the functionalization of organic polymers deposited by plasma (glow discharge plasma) is essential to immobilize covalent peptides. The process occurred by binding the peptide amine groups and epoxy groups from polymerized interlayers deposited via plasma on SS surfaces. These systems reduced the growth of *E. coli* and *B. subtilis* ranging from 3 to 6 $\log^{10}$ in accordance with the tested peptide (85). In addition, chitosan polymer layers (1,4 linked N-acetyl glucosamine and glucosamine) were used on SS surfaces to immobilize the AMPs nisin and Magainin I. This strategy was possible due to the insertion of terephthalaldehyde cross linker (111). New studies, even at early stages, are essential to contribute to the development and improvement of biomaterials for clinical use and biodevice implantation.

6. CONCLUSION

Since bacterial resistance is still one of the major problems facing modern societies, new strategic therapies to combat microorganisms resistant to conventional antibiotics are required. In this context, antimicrobial peptides are promising due to their biocompatibility, low toxicity and high effectiveness. Synthetic forms of peptides also have increased their microbicidal activity. Currently, chemical methods for immobilization of AMPs on surfaces are considered valuable tools for the construction of modified biodevices. Chemical immobilization provides improvements in peptide stability and ensures an adequate orientation of the biomolecule. Covalent bonding overcomes limitations of the physical anchoring methods, creating films with greater antimicrobial efficacy. Chemical approaches to covalent immobilization of AMPs on solid surfaces, such as orthopedic implants and surgical instruments, represent an advance in the prevention of nosocomial infections. Although many studies are still

in the initial phase, they represent the first step towards the development and improvement of new antimicrobial biomaterials with the capability of reducing infections in hospital environment and improving human health.

7. ACKNOWLEDGEMENTS

The authors are grateful for the support provided by the Brazilian National Council for Scientific and Technological Development (CNPq), Pernambuco State Foundation for Research Support (FACEPE), Nanobiotechnology/CAPES. Silva and Ribeiro would like to thank FACEPE for scholarships.

8. REFERENCES

1. SB Levy, B Marshall: Antibacterial resistance worldwide: causes, challenges and responses. *Nat Med* 10, 122-129 (2004) DOI: 10.1038/nm1145
2. MF Mohamed, MN Seleem: Efficacy of short novel antimicrobial and anti-inflammatory peptides in a mouse model of methicillin-resistant Staphylococcus aureus (MRSA) skin infection. *Drug Des Dev Ther* 8, 1979-1983 (2014) DOI: 10.2147/DDDT.S72129
3. K Molbak: Spread of resistant bacteria and resistance genes from animals to humans--the public health consequences. *J Vet Med B Infect Dis Vet Public Health* 51, 364-369 (2004) DOI: 10.1111/j.1439-0450.2004.00788.x
4. KV Reddy, RD Yedery, C Aranha: Antimicrobial peptides: premises and promises. *Int J Antimicrob Agents* 24, 536-547 (2004) DOI: 10.1016/j.ijantimicag.2004.09.005
5. M Zasloff: Antimicrobial peptides of multicellular organisms. *Nature* 415, 389-395 (2002) DOI: 10.1038/415389a
6. T Ganz: Defensins: antimicrobial peptides of innate immunity. *Nat Rev Immunol* 3, 710-720 (2003) DOI: 10.1038/nri1180
7. Z Wang, G Wang: APD: the Antimicrobial Peptide Database. *Nucleic Acids Res* 32, 590-592 (2004) DOI: 10.1093/nar/gkh025
8. M Bagheri, M Beyermann, M Dathe: Immobilization reduces the activity of surface-bound cationic antimicrobial peptides with no influence upon the activity spectrum. *Antimicrob Agents Chemother* 53, 1132-1141 (2009) DOI: 10.1128/AAC.01254-08
9. S Makihira, H Nikawa, T Shuto, M Nishimura, Y Mine, K Tsuji, K Okamoto, Y Sakai, M Sakai, N Imari, S Iwata, M Takeda, F Suehiro: Evaluation of trabecular bone formation in a canine model surrounding a dental implant fixture immobilized with an antimicrobial peptide derived from histatin. *J Mater Sci Mater Med* 22, 2765-2772 (2011) DOI: 10.1007/s10856-011-4440-2
10. SL Haynie, GA Crum, BA Doele: Antimicrobial activities of amphiphilic peptides covalently bonded to a water-insoluble resin. *Antimicrob Agents Chemother* 39, 301-307 (1995) DOI: 10.1128/AAC.39.2.301
11. X Li, P Li, R Saravanan, A Basu, B Mishra, SH Lim, X Su, PA Tambyah, SS Leong: Antimicrobial functionalization of silicone surfaces with engineered short peptides having broad spectrum antimicrobial and salt-resistant properties. *Acta Biomater* 10, 258-266 (2014) DOI: 10.1016/j.actbio.2013.09.009
12. S Bencharit, WC Byrd, S Altarawneh, B Hosseini, A Leong, G Reside, T Morelli, S Offenbacher: Development and applications of porous tantalum trabecular metal-enhanced titanium dental implants. *Clin Implant Dent Relat Res* 16, 817-826 (2014) DOI: 10.1111/cid.12059
13. E Vanderleyden, S Van Bael, YC Chai, JP Kruth, J Schrooten, P Dubruel: Gelatin functionalised porous titanium alloy implants for orthopaedic applications. *Mater Sci Eng C Mater Biol Appl* 42, 396-404 (2014) DOI: 10.1016/j.msec.2014.05.048
14. JW Costerton, PS Stewart, EP Greenberg: Bacterial biofilms: a common cause of persistent infections. *Science* 284, 1318-1322 (1999) DOI: 10.1126/science.284.5418.1318
15. CC de Carvalho: Biofilms: recent developments on an old battle. *Recent Pat Biotechnol* 1, 49-57 (2007) DOI: 10.2174/187220807779813965
16. WMD Jr: Bacterial adhesion: seen any good biofilms lately? *Clin Microbiol Rev* 15, 155-166 (2002) DOI: 10.1128/CMR.15.2.155-166.2002

17. L Zhao, PK Chu, Y Zhang, Z Wu: Antibacterial coatings on titanium implants. *J Biomed Mater Res B Appl Biomater* 91, 470-480 (2009) DOI: 10.1002/jbm.b.31463
18. A Schmidtchen, M Pasupuleti, M Malmsten: Effect of hydrophobic modifications in antimicrobial peptides. *Adv Colloid Interface Sci* 205, 265-274 (2014) DOI: 10.1016/j.cis.2013.06.009
19. D Andreu, L Rivas: Animal antimicrobial peptides: an overview. *Biopolymers* 47, 415-433 (1998) DOI: 10.1002/(SICI)1097-0282(1998)47:6<415:AID-BIP2>3.0.CO;2-D
20. YJ Gordon, EG Romanowski, AM McDermott: A review of antimicrobial peptides and their therapeutic potential as anti-infective drugs. *Curr Eye Res* 30, 505-515 (2005) DOI: 10.1080/02713680590968637
21. W van 't Hof, EC Veerman, EJ Helmerhorst, AV Amerongen: Antimicrobial peptides: properties and applicability. *Biol Chem* 382, 597-619 (2001)
22. LAC Carvalho, MT Machini: Hemocidinas derivadas da hemoglobina: estruturas, propriedades e perspectivas. *Quim Nova* 36, 1021-1029 (2013) DOI: 10.1590/S0100-40422013000700017
23. KA Brogden: Antimicrobial peptides: pore formers or metabolic inhibitors in bacteria? *Nat Rev Microbiol* 3, 238-250 (2005) DOI: 10.1038/nrmicro1098
24. RR Silva, KY Avelino, KL Ribeiro, OL Franco, MD Oliveira, CAS Andrade: Optical and dielectric sensors based on antimicrobial peptides for microorganism diagnosis. *Front Microbiol* 5, 443 (2014) DOI: 10.3389/fmicb.2014.00443
25. F Costa, IF Carvalho, RC Montelaro, P Gomes, MC Martins: Covalent immobilization of antimicrobial peptides (AMPs) onto biomaterial surfaces. *Acta Biomater* 7, 1431-1440 (2011) DOI: 10.1016/j.actbio.2010.11.005
26. G Gao, D Lange, K Hilpert, J Kindrachuk, Y Zou, JT Cheng, M Kazemzadeh-Narbat, K Yu, R Wang, SK Straus, DE Brooks, BH Chew, RE Hancock, JN Kizhakkedathu: The biocompatibility and biofilm resistance of implant coatings based on hydrophilic polymer brushes conjugated with antimicrobial peptides. *Biomaterials* 32, 3899-3909 (2011) DOI: 10.1016/j.biomaterials.2011.02.013
27. RO Darouiche: Treatment of infections associated with surgical implants. *N Engl J Med* 350, 1422-1429 (2004) DOI: 10.1056/NEJMra035415
28. J Vila, A Soriano, J Mensa: (Molecular basis of microbial adherence to prosthetic materials. Role of biofilms in prosthesis-associated infection). *Enferm Infecc Microbiol Clin* 26, 48-54 (2008) DOI: 10.1157/13114395
29. RT Cleophas, J Sjollema, HJ Busscher, JA Kruijtzer, RM Liskamp: Characterization and activity of an immobilized antimicrobial peptide containing bactericidal PEG-hydrogel. *Biomacromolecules* 15, 3390-3395 (2014) DOI: 10.1021/bm500899r
30. LH Eckhard, A Sol, E Abtew, Y Shai, AJ Domb, G Bachrach, N Beyth: Biohybrid polymer-antimicrobial peptide medium against Enterococcus faecalis. *PLoS One* 9, e109413 (2014) DOI: 10.1371/journal.pone.0109413
31. M Godoy-Gallardo, C Mas-Moruno, MC Fernandez-Calderon, C Perez-Giraldo, JM Manero, F Albericio, FJ Gil, D Rodriguez: Covalent immobilization of hLf1-11 peptide on a titanium surface reduces bacterial adhesion and biofilm formation. *Acta Biomater* 10, 3522-3534 (2014) DOI: 10.1016/j.actbio.2014.03.026
32. A Lombana, Z Raja, S Casale, C M Pradier, T Foulon, A Ladram, V Humblot: Temporin-SHa peptides grafted on gold surfaces display antibacterial activity. *J Pept Sci* 20, 563-569 (2014) DOI: 10.1002/psc.2654
33. M Dawgul, M Maciejewska, M Jaskiewicz, A Karafova, W Kamysz: Antimicrobial peptides as potential tool to fight bacterial biofilm. *Acta Pol Pharm* 71, 39-47 (2014)
34. M Kazemzadeh-Narbat, J Kindrachuk, K Duan, H Jenssen, RE Hancock, R Wang: Antimicrobial peptides on calcium phosphate-coated titanium for the prevention of implant-associated infections. *Biomaterials* 31, 9519-9526 (2010) DOI: 10.1016/j.biomaterials.2010.08.035

35. SA Onaizi, SS Leong: Tethering antimicrobial peptides: current status and potential challenges. *Biotechnol Adv* 29, 67-74 (2011) DOI: 10.1016/j.biotechadv.2010.08.012

36. G Wang, ML Hanke, B Mishra, T Lushnikova, CE Heim, V Chittezham Thomas, KW Bayles, T Kielian: Transformation of human cathelicidin LL-37 into selective, stable, and potent antimicrobial compounds. *ACS Chem Biol* 9, 1997-2002 (2014) DOI: 10.1021/cb500475y

37. L Ferreira, A Zumbuehl: Non-leaching surfaces capable of killing microorganisms on contact. *J Mater Chem* 19, 7796-7806 (2009) DOI: 10.1039/b905668h

38. MB Fontana, MC Bastos, A Brandelli: Peptide-like substances as antimicrobial barriers to Corynebacterium sp. adhesion to silicone catheters. *Lett Appl Microbiol* 45, 324-329 (2007) DOI: 10.1111/j.1472-765X.2007.02193.x

39. PH Kwakman, AA te Velde, CM Vandenbroucke-Grauls, SJ van Deventer, SA Zaat: Treatment and prevention of Staphylococcus epidermidis experimental biomaterial-associated infection by bactericidal peptide 2. *Antimicrob Agents Chemother* 50, 3977-3983 (2006) DOI: 10.1128/AAC.00575-06

40. XW Tan, TW Goh, P Saraswathi, CL Nyein, M Setiawan, A Riau, R Lakshminarayanan, S Liu, D Tan, RW Beuerman, JS Mehta: Effectiveness of antimicrobial peptide immobilization for preventing perioperative cornea implant-associated bacterial infection. *Antimicrob Agents Chemother* 58, 5229-5238 (2014) DOI: 10.1128/AAC.02859-14

41. B Mishra, A Basu, RRY Chua, R Saravanan, PA Tambyah, B Ho, MW Chang, SS J Leong: Site specific immobilization of a potent antimicrobial peptide onto silicone catheters: evaluation against urinary tract infection pathogens. *J Mater Chem B* 2, 1706-1716 (2014) DOI: 10.1039/c3tb21300e

42. K Rapsch, FF Bier, M Tadros, M von Nickisch-Rosenegk: Identification of antimicrobial peptides and immobilization strategy suitable for a covalent surface coating with biocompatible properties. *Bioconjug Chem* 25, 308-319 (2014) DOI: 10.1021/bc4004469

43. D Alves, MO Pereira: Mini-review: Antimicrobial peptides and enzymes as promising candidates to functionalize biomaterial surfaces. *Biofouling* 30, 483-499 (2014) DOI: 10.1080/08927014.2014.889120

44. D Leckband, J Israelachvili: Intermolecular forces in biology. *Q Rev Biophys* 34, 105-267 (2001) DOI: 10.1017/S0033583501003687

45. AD Buckingham: Permanent and induced molecular moments and long-range intermolecular forces. In: Advances in Chemical Physics. Ed: JO Hirschfelder, New Jersey (2007)

46. L Karam, C Jama, P Dhulster, N Chihib: Study of surface interactions between peptides, materials and bacteria for setting up antimicrobial surfaces and active food packaging. *J Mater Environ Sci* 4, 798-821 (2013)

47. JC Stendahl, MS Rao, MO Guler, SI Stupp: Intermolecular forces in the self-assembly of peptide amphiphile nanofibers. *Adv Funct Mater* 16, 499-508 (2006) DOI: 10.1002/adfm.200500161

48. G Gao, K Yu, J Kindrachuk, DE Brooks, RE Hancock, JN Kizhakkedathu: Antibacterial surfaces based on polymer brushes: investigation on the influence of brush properties on antimicrobial peptide immobilization and antimicrobial activity. *Biomacromolecules* 12, 3715-3727 (2011) DOI: 10.1021/bm2009697

49. AR Statz, JP Park, NP Chongsiriwatana, AE Barron, PB Messersmith: Surface-immobilised antimicrobial peptoids. *Biofouling* 24, 439-448 (2008) DOI: 10.1080/08927010802331829

50. A Basu, B Mishra, SSJ Leong: Immobilization of polybia-MPI by allyl glycidyl ether based brush chemistry to generate a novel antimicrobial surface. *J Mater Chem B* 1, 4746-4755 (2013) DOI: 10.1039/c3tb20805b

51. WM Cho, BP Joshi, H Cho, KH Lee: Design and synthesis of novel antibacterial peptide-resin conjugates. *Bioorg Med Chem Lett* 17, 5772-5776 (2007) DOI: 10.1016/j.bmcl.2007.08.056

52. K Glinel, AM Jonas, T Jouenne, J Leprince, L

Galas, WT Huck: Antibacterial and antifouling polymer brushes incorporating antimicrobial peptide. *Bioconjug Chem* 20, 71-77 (2009) DOI: 10.1021/bc800280u

53. P Appendini, JH Hotchkiss: Surface modification of poly(styrene) by the attachment of an antimicrobial peptide. *J Appl Polym Sci* 81, 609-616 (2001) DOI: 10.1002/app.1476
54. MD Steven, JH Hotchkiss: Covalent immobilization of an antimicrobial peptide on poly(ethylene) film. *J Appl Polym Sci* 110, 2665-2670 (2008) DOI: 10.1002/app.27638
55. O Etienne, C Picart, C Taddei, Y Haikel, JL Dimarcq, P Schaaf, JC Voegel, JA Ogier, C Egles: Multilayer polyelectrolyte films functionalized by insertion of defensin: a new approach to protection of implants from bacterial colonization. *Antimicrob Agents Chemother* 48, 3662-3669 (2004) DOI: 10.1128/AAC.48.10.3662-3669.2004
56. DAlves, MO Pereira: Mini-review: Antimicrobial peptides and enzymes as promising candidates to functionalize biomaterial surfaces. *Biofouling* 30, 483-499 (2014) DOI: 10.1080/08927014.2014.889120
57. A Shukla, KE Fleming, HF Chuang, TM Chau, CR Loose, GN Stephanopoulos, PT Hammond: Controlling the release of peptide antimicrobial agents from surfaces. *Biomaterials* 31, 2348-2357 (2010) DOI: 10.1016/j.biomaterials.2009.11.082
58. K Ariga, JP Hill, Q Ji: Layer-by-layer assembly as a versatile bottom-up nanofabrication technique for exploratory research and realistic application. *Phys Chem Chem Phys* 9, 2319-2340 (2007) DOI: 10.1039/b700410a
59. G Decher, JD Hong, J Schmitt: Buildup of ultrathin multilayer films by a self-assembly process: III. Consecutively alternating adsorption of anionic and cationic polyelectrolytes on charged surfaces. *Thin Solid Films* 210-211, Part 2, 831-835 (1992) DOI: 10.1016/0040-6090(92)90417-A
60. G Decher, M Eckle, J Schmitt, B Struth: Layer-by-layer assembled multicomposite films. *Curr Opin Colloid Interface Sci* 3, 32-39 (1998) DOI: 10.1016/S1359-0294(98)80039-3
61. W Soliman, S Bhattacharjee, K Kaur: Adsorption of an antimicrobial peptide on self-assembled monolayers by molecular dynamics simulation. *J Phys Chem B* 114, 11292-11302 (2010) DOI: 10.1021/jp104024d
62. DM Lynn: Peeling back the layers: controlled erosion and triggered disassembly of multilayered polyelectrolyte thin films. *Adv Mater* 19, 4118-4130 (2007) DOI: 10.1002/adma.200701748
63. E Vázquez, DM Dewitt, PT Hammond, DM Lynn: Construction of hydrolytically-degradable thin films via layer-by-layer deposition of degradable polyelectrolytes. *J Am Chem Soc* 124, 13992-13993 (2002) DOI: 10.1021/ja026405w
64. KC Wood, HF Chuang, RD Batten, DM Lynn, PT Hammond: Controlling interlayer diffusion to achieve sustained, multiagent delivery from layer-by-layer thin films. *Proc Natl Acad Sci USA* 103, 10207-10212 (2006) DOI: 10.1073/pnas.0602884103
65. JM Goddard, JH Hotchkiss: Polymer surface modification for the attachment of bioactive compounds. *Prog Polym Sci* 32, 698-725 (2007) DOI: 10.1016/j.progpolymsci.2007.04.002
66. K Vasilev, J Cook, HJ Griesser: Antibacterial surfaces for biomedical devices. *Expert Rev Med Devices* 6, 553-567 (2009) DOI: 10.1586/erd.09.36
67. N Aumsuwan, RC Danyus, S Heinhorst, MW Urban: Attachment of ampicillin to expanded poly(tetrafluoroethylene): surface reactions leading to inhibition of microbial growth. *Biomacromolecules* 9, 1712-1718 (2008) DOI: 10.1021/bm800176t
68. X Qi, G Poernomo, K Wang, Y Chen, MB Chan-Park, R Xu, MW Chang: Covalent immobilization of nisin on multi-walled carbon nanotubes: superior antimicrobial and anti-biofilm properties. *Nanoscale* 3, 1874-1880 (2011) DOI: 10.1039/c1nr10024f
69. P Appendini, JH Hotchkiss: Review of antimicrobial food packagingInnov. *Food Sci Emerg Technol* 3, 113-126 (2002) DOI: 10.1016/S1466-8564(02)00012-7
70. F Rusmini, Z Zhong, J Feijen: Protein

immobilization strategies for protein biochips. *Biomacromolecules* 8, 1775-1789 (2007) DOI: 10.1021/bm061197b

71. P Jonkheijm, D Weinrich, H Schröder, CM Niemeyer, H Waldmann: Chemical strategies for generating protein biochips. *Angew Chem Int* 47, 9618-9647 (2008) DOI: 10.1002/anie.200801711
72. R Chen, N Cole, MD Willcox, J Park, R Rasul, E Carter, N Kumar: Synthesis, characterization and *in vitro* activity of a surface-attached antimicrobial cationic peptide. *Biofouling* 25, 517-524 (2009) DOI: 10.1080/08927010902954207
73. V Humblot, JF Yala, P Thebault, K Boukerma, A Héquet, JM Berjeaud, CM Pradier: The antibacterial activity of Magainin I immobilized onto mixed thiols self-assembled monolayers. *Biomaterials* 30, 3503-3512 (2009) DOI: 10.1016/j.biomaterials.2009.03.025
74. JJ Gooding, F Mearns, W Yang, J Liu: Self-assembled monolayers into the 21st century: recent advances and applications. *Electroanalysis* 15, 81-96 (2003) DOI: 10.1002/elan.200390017
75. TP Sullivan, WTS Huck: Reactions on monolayers: organic synthesis in two dimensions. *Eur J Org Chem* 2003, 17-29 (2003) DOI: 10.1002/1099-0690(200301)2003:1<17 :AID-EJOC17>3.0.CO;2-H
76. A Ulman: Formation and structure of self-assembled monolayers. *Chem Rev* 96, 1533-1554 (1996) DOI: 10.1021/cr9502357
77. F Boulmedais, B Frisch, O Etienne, P Lavalle, C Picart, J Ogier, JC Voegel, P Schaaf, C Egles: Polyelectrolyte multilayer films with pegylated polypeptides as a new type of anti-microbial protection for biomaterials. *Biomaterials* 25, 2003-2011 (2004) DOI: 10.1016/j.biomaterials.2003.08.039
78. LG Harris, S Tosatti, M Wieland, M Textor, RG Richards: Staphylococcus aureus adhesion to titanium oxide surfaces coated with non-functionalized and peptide-functionalized poly(l-lysine)-grafted-poly(ethylene glycol) copolymers. *Biomaterials* 25, 4135-4148 (2004) DOI: 10.1016/j.biomaterials.2003.11.033
79. P Kingshott, J Wei, D Bagge-Ravn, N Gadegaard, L Gram: Covalent attachment of poly(ethylene glycol) to surfaces, critical for reducing bacterial adhesion. *Langmuir* 19, 6912-6921 (2003) DOI: 10.1021/la034032m
80. Y Gao, I Kyratzis: Covalent immobilization of proteins on carbon nanotubes using the cross-linker 1-ethyl-3-(3-dimethylaminopropyl) carbodiimide-a critical assessment. *Bioconjug Chem* 19, 1945-1950 (2008) DOI: 10.1021/bc800051c
81. D Sehgal, IK Vijay: A method for the high efficiency of water-soluble carbodiimide-mediated amidation. *Anal Biochem* 218, 87-91 (1994) DOI: 10.1006/abio.1994.1144
82. JV Staros, RW Wright, DM Swingle: Enhancement by N-hydroxysulfosuccinimide of water-soluble carbodiimide-mediated coupling reactions. *Anal Biochem* 156, 220-222 (1986) DOI: 10.1016/0003-2697(86)90176-4
83. LS Wong, F Khan, J Micklefield: Selective covalent protein immobilization: strategies and applications. *Chem Rev* 109, 4025-4053 (2009) DOI: 10.1021/cr8004668
84. SJ Oh, BJ Hong, KY Choi, JW Park: Surface modification for DNA and protein microarrays. *OMICS* 10, 327-343 (2006) DOI: 10.1089/omi.2006.10.327
85. C Vreuls, G Zocchi, B Thierry, G Garitte, SS Griesser, C Archambeau, C Van de Weerdt, J Martial, H Griesser: Prevention of bacterial biofilms by covalent immobilization of peptides onto plasma polymer functionalized substrates. *J Mater Chem* 20, 8092-8098 (2010) DOI: 10.1039/c0jm01419b
86. M Rahnamaeian: Antimicrobial peptides: modes of mechanism, modulation of defense responses. *Plant Signal Behav* 6, 1325-1332 (2011) DOI: 10.4161/psb.6.9.16319
87. JJ Lopez Cascales, A Garro, RD Porasso, RD Enriz: The dynamic action mechanism of small cationic antimicrobial peptides. *Phys Chem Chem Phys* 16, 21694-21705 (2014) DOI: 10.1039/C4CP02537G
88. KL Lam, H Wang, TA Siaw, MR Chapman, AJ Waring, JT Kindt, KY Lee: Mechanism

of structural transformations induced by antimicrobial peptides in lipid membranes. *Biochim Biophys Acta* 1818, 194-204 (2012) DOI: 10.1016/j.bbamem.2011.11.002

89. RE Hancock, HG Sahl: Antimicrobial and host-defense peptides as new anti-infective therapeutic strategies. *Nat Biotechnol* 24, 1551-1557 (2006) DOI: 10.1038/nbt1267
90. M Bagheri, M Beyermann, M Dathe: Mode of action of cationic antimicrobial peptides defines the tethering position and the efficacy of biocidal surfaces. *Bioconjug Chem* 23, 66-74 (2012) DOI: 10.1021/bc200367f
91. A Kirsten, A Hausmann, M Weber, J Fischer, H Fischer: Bioactive and thermally compatible glass coating on zirconia dental implants. *J Dent Res* 94, 297-303 (2015) DOI: 10.1177/0022034514559250
92. J Ye, J He, C Wang, K Yao, Z Gou: Copper-containing mesoporous bioactive glass coatings on orbital implants for improving drug delivery capacity and antibacterial activity. *Biotechnol Lett* 36, 961-968 (2014) DOI: 10.1007/s10529-014-1465-x
93. N Drnovsek, S Novak, U Dragin, M Ceh, M Gorensek, M Gradisar: Bioactive glass enhances bone ingrowth into the porous titanium coating on orthopaedic implants. *Int Orthop* 36, 1739-1745 (2012) DOI: 10.1007/s00264-012-1520-y
94. M Mohorcic, I Jerman, M Zorko, L Butinar, B Orel, R Jerala, J Friedrich: Surface with antimicrobial activity obtained through silane coating with covalently bound polymyxin B. *J Mater Sci Mater Med* 21, 2775-2782 (2010) DOI: 10.1007/s10856-010-4136-z
95. B Ashar, RSW Jr, LR Turcotte: Development of a silica-free silicone system for medical applications. *J Biomed Mater Res* 15, 663-672 (1981) DOI: 10.1002/jbm.820150505
96. E Briganti, P Losi, A Raffi, M Scoccianti, A Munao, G Soldani: Silicone based polyurethane materials: a promising biocompatible elastomeric formulation for cardiovascular applications. *J Mater Sci Mater Med* 17, 259-266 (2006) DOI: 10.1007/s10856-006-7312-4
97. MC Musolf: Altering the physical properties of silicone elastomers for medical device applications. *Med Device Technol* 1, 26-29 (1990)
98. L Azevedo Calderon, AA Silva, P Ciancaglini, RG Stabeli: Antimicrobial peptides from Phyllomedusa frogs: from biomolecular diversity to potential nanotechnologic medical applications. *Amino Acids* 40, 29-49 (2011) DOI: 10.1007/s00726-010-0622-3
99. A Giacometti, O Cirioni, MS Del Prete, F Barchiesi, AM Paggi, E Petrelli, G Scalise: Comparative activities of polycationic peptides and clinically used antimicrobial agents against multidrug-resistant nosocomial isolates of Acinetobacter baumannii. *J Antimicrob Chemother* 46, 807-810 (2000) DOI: 10.1093/jac/46.5.807
100. K Lim, RR Chua, R Saravanan, A Basu, B Mishra, PA Tambyah, B Ho, SS Leong: Immobilization studies of an engineered arginine-tryptophan-rich peptide on a silicone surface with antimicrobial and antibiofilm activity. *ACS Appl Mater Interfaces* 5, 6412-6422 (2013) DOI: 10.1021/am401629p
101. R Saravanan, X Li, K Lim, H Mohanram, L Peng, B Mishra, A Basu, JM Lee, S Bhattacharjya, SS Leong: Design of short membrane selective antimicrobial peptides containing tryptophan and arginine residues for improved activity, salt-resistance, and biocompatibility. *Biotechnol Bioeng* 111, 37-49 (2014) DOI: 10.1002/bit.25003
102. M Yoshinari, T Kato, K Matsuzaka, T Hayakawa, K Shiba: Prevention of biofilm formation on titanium surfaces modified with conjugated molecules comprised of antimicrobial and titanium-binding peptides. *Biofouling* 26, 103-110 (2010) DOI: 10.1080/08927010903216572
103. E Vasilescu, P Drob, D Raducanu, VD Cojocaru, I Cinca, D Iordachescu, R Ion, M Popa, C Vasilescu: *In vitro* biocompatibility and corrosion resistance of a new implant titanium base alloy. *J Mater Sci Mater Med* 21, 1959-1968 (2010) DOI: 10.1007/s10856-010-4057-x
104. M Zanetti, R Gennaro, D Romeo: Cathelicidins: a novel protein family with a common proregion

ANEXO B - ARTIGO PUBLICADO DURANTE O DOUTORADO

frontiers in MICROBIOLOGY

REVIEW ARTICLE
published: 20 August 2014
doi: 10.3389/fmicb.2014.00443

Optical and dielectric sensors based on antimicrobial peptides for microorganism diagnosis

Rafael R. Silva[1], Karen Y. P. S. Avelino[2], Kalline L. Ribeiro[1], Octavio L. Franco[3], Maria D. L. Oliveira[2] and Cesar A. S. Andrade[1,2]*

[1] *Programa de Pós-Graduação em Inovação Terapêutica, Universidade Federal de Pernambuco, Recife, Brasil*
[2] *Departamento de Bioquímica, Universidade Federal de Pernambuco, Recife, Brasil*
[3] *Centro de Análises Proteômicas e Bioquímicas, Universidade Católica de Brasília, Brasília-DF, Brasil*

Edited by:
Luis Cláudio Nascimento Da Silva, University of Copenhagen, Denmark

Reviewed by:
Margaret E. Bauer, Indiana University School of Medicine, USA
Noton Kumar Dutta, Johns Hopkins University, USA
Stefano Sforza, University of Parma, Italy
Etinosa Igbinosa, University of Benin, Nigeria

Correspondence:
Cesar A. S. Andrade, Departamento de Bioquímica, Universidade Federal de Pernambuco, Avenida Professor Moraes Rêgo S/N, 50670-901 Recife, PE, Brasil
e-mail: csrandrade@gmail.com

Antimicrobial peptides (AMPs) are natural compounds isolated from a wide variety of organisms that include microorganisms, insects, amphibians, plants, and humans. These biomolecules are considered as part of the innate immune system and are known as natural antibiotics, presenting a broad spectrum of activities against bacteria, fungi, and/or viruses. Technological innovations have enabled AMPs to be utilized for the development of novel biodetection devices. Advances in nanotechnology, such as the synthesis of nanocomposites, nanoparticles, and nanotubes have permitted the development of nanostructured platforms with biocompatibility and greater surface areas for the immobilization of biocomponents, arising as additional tools for obtaining more efficient biosensors. Diverse AMPs have been used as biological recognition elements for obtaining biosensors with more specificity and lower detection limits, whose analytical response can be evaluated through electrochemical impedance and fluorescence spectroscopies. AMP-based biosensors have shown potential for applications such as supplementary tools for conventional diagnosis methods of microorganisms. In this review, conventional methods for microorganism diagnosis as well new strategies using AMPs for the development of impedimetric and fluorescent biosensors are highlighted. AMP-based biosensors show promise as methods for diagnosing infections and bacterial contaminations as well as applications in quality control for clinical analyses and microbiological laboratories.

Keywords: antimicrobial peptides, biosensors, bacterial infections, impedance spectroscopy, fluorescence spectroscopy

ANTIMICROBIAL PEPTIDES

Currently, the search for novel compounds with antibiotic ability to overcome bacterial resistance has increased. Antimicrobial peptides (AMPs) appear to be an excellent alternative, since more effective therapeutic approaches are required for many types of pathogens (Brogden et al., 2005; Hancock and Sahl, 2006; Schmidtchen et al., 2014). AMPs are components of the innate immune system, acting in defense against multiple pathogens (Schmidtchen et al., 2014). In general, AMPs may also show other different activities such as antiviral or antitumor properties, making them excellent candidates as new therapeutic drugs (Reddy et al., 2004).

Antimicrobial peptides are biomolecules present in diverse organisms, such as insects, plants, and animals (Mendez et al., 1990; Schnapp and Harris, 1998). In general, AMPs are mainly cationic small molecules composed of 10–50 amino acids residues in length, with molecular masses ranging from 1 to 5 kDa. In addition, AMPs comprise a chemically and structurally heterogeneous family (Andreu and Rivas, 1998; Costa et al., 2011).

In general, AMPs only assume an amphipathic structure after interacting with the bacterial membrane, since it is not a favorable structure in an aqueous environment, allowing lethal permeabilization of the bacterial membrane (van't Hof et al., 2001; Costa et al., 2011). The classical modes of action described previously in the literature are not necessarily exclusive of one other (van't Hof et al., 2001; Brogden et al., 2005; Toke, 2005; Bechinger and Lohner, 2006). In the case of the barrel-stave model, a lipid bilayer disruption by AMPs occurs, until the peptides reach a threshold concentration and insert themselves across the bilayer to obtain peptide-lined pores. Subsequently, a membrane solubilization into micellar structures occurs, resulting in the carpet model or in forming peptide-and-lipid lined pores (toroidal pore model; Rapaport and Shai, 1991).

The mechanisms of action of AMPs (**Figure 1**) were reviewed and described by Nguyen et al. (2011). In this new proposal, pore formation in the disordered toroidal pore model is more stochastic, involving low peptide quantity. The presence of peptides can directly affect the bilayer thickness and, therefore, the membrane is remodeled to form rich domains of anionic lipids on the peptide surface. In addition, AMPs can form non-bilayer intermediates in the membrane coupled to small anions. On the other hand, in the molecular electroporation model, a peptide accumulation occurs on the outer lipid membrane leaflet, making the membrane permeable to various molecules including the AMPs (Nguyen et al., 2011).

Nanotechnology has been widely introduced for multidisciplinary applications, especially associated with the use of AMPs

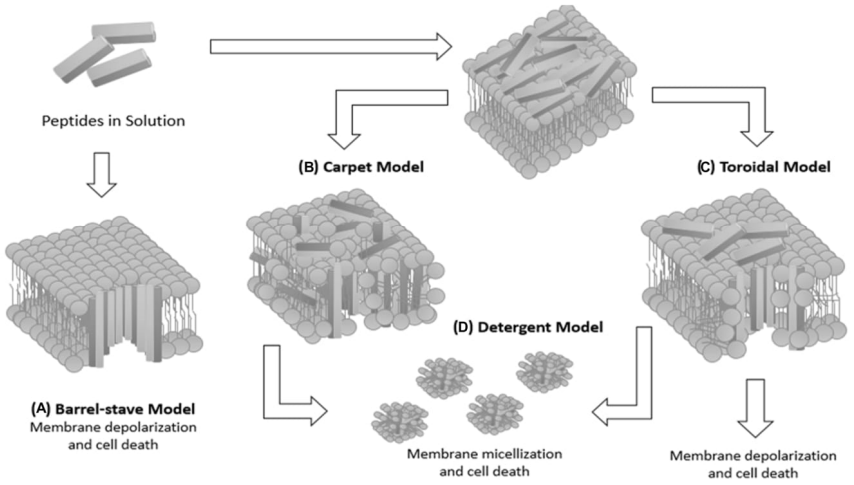

FIGURE 1 | Schematic diagram summarizing the possible mechanisms of peptide–membrane interaction. (A) Barrel-stave model: the peptide assumes an amphipathic helical conformation and organizes itself to form a structure with a central lumen, like a barrel. The hydrophobic part of the AMP interacts with the lipid acyl chains of the membrane and their hydrophilic part is exposed so as to form the lumen of the transmembrane aqueous channel. **(B)** Carpet model: cationic peptides are attracted by anionic phospholipids covering the surface of the bacterial membrane until reaching a saturation point, resulting in solubilization of the bacterial membrane. **(C)** Toroidal model: the peptide helices are inserted parallel to the membrane and cause folding of the lipid monolayers in order to form a pore formed by peptides interspersed with phospholipids. In this model, an association between polar peptide groups with the lipid polar head groups is established. **(D)** Detergent model: membrane solubilization occurs, leading to formation of micellar structures, resulting in the destabilization of the lipid membrane and cell death.

in biology and biomedicine (Barkalina et al., 2014). Among the diverse uses of AMPs have been highlighted quality controls of foods, raising animals, controlled release systems and biosensors (Li et al., 2012; Sobczak et al., 2013). In this context, the peptide nisin has been applied as a milk-derived preservative for quality control in foods (Bi et al., 2011). In animal husbandry, peptides can be used in ruminants as an alternative to common antibiotics, avoiding bacterial resistance or assisting in the immunization of animals for the prevention of diseases (Cheema et al., 2011).

Infectious diseases have been part of humanity for centuries, some of them killing millions of people worldwide. Different types of pathogens (bacteria, viruses, fungi, and parasites) can cause infections from either exogenous (acquired from the environment, animals, or people) or endogenous (from the normal flora) origins (Mazzoni et al., 1987; Murthy et al., 2013). Furthermore, in agribusiness, the use of purified peptides, as well as the development of transgenic plants, aims to minimize plant diseases, avoiding the use of fungicides (Keymanesh et al., 2009). In clinical applications, some AMPs are in the early stages of clinical research to prevent inflammation and sepsis (Schuerholz et al., 2012).

Identification and quantification of pathogenic agents are two important parameters for the diagnosis of bacterial infections and the implementation of effective drug therapy (Lazcka et al., 2007). The most common methods are direct examination by counting bacterial colonies in culture plates and serodiagnosis tests (van Pelt et al., 1999). Direct examination by optical microscopy can identify the morphology using a simple and specific Gram staining. Culture media allow the growth as well as the isolation and identification of specific types of bacteria (Szakal and Pal, 2003; Bragulat et al., 2004). However, these methods are time-consuming and require specialized technicians. Of note, it may require weeks to obtain a correct diagnosis of some pathogens from samples of mucosa, skin, or blood (Benes et al., 1996). Unfortunately, a few days may be sufficient to significantly worsen the clinical status of the patient before receiving appropriate treatment.

Traditional methods of diagnosis also consist of molecular tests or nucleic acid amplification test (NAAT). Techniques based on NAAT include polymerase chain reaction (PCR), ligase chain reaction, transcription mediated amplification, strand displacement amplification, and loop-mediated isothermal amplification (Andersen et al., 2000; Yang et al., 2002; Palka-Santini et al., 2009). Techniques based on nucleic acids enable specific molecular detection through hybridization between a DNA molecule and its complementary strand (Junhui et al., 1997; Wang et al., 1997; Wang, 1998). Although effective, these techniques may present

some limitations, such as the need for sample enrichment and purification prior to analysis, prolonged experimentation time, false-positive results due to cross-reactions, and high cost (Caygill et al., 2010; Singh et al., 2014).

In order to reduce or overcome these restrictions, new detection methods are required, and biosensors are considered promising tools for clinical diagnosis (Abdel-Hamid et al., 1999; Deisingh and Thompson, 2004). In this context, AMPs can be an excellent alternative for the development of biosensors, since their potential use for specific detection of pathogenic bacteria has been demonstrated (Kulagina et al., 2005).

STRATEGIES FOR THE DEVELOPMENT OF AMP-BASED BIOSENSORS

Advances in nanotechnology have contributed to the improvement of biotechnological research associated with the rapid progression of biodetection devices (Jianrong et al., 2004; Fournier-Wirth and Coste, 2010; Yeom et al., 2011). Nanostructures have been extensively used in the biosensor development due to their unique physicochemical characteristics such as quantum size effect, elevated ratio between surface area and volume, and analytical signal amplification capacity (Jianrong et al., 2004; Li et al., 2010). The utilization of AMPs as recognition elements in biosensors is a relatively new concept, but their development is of great relevance due to numerous potential areas for application (Etayash et al., 2014).

Biosensors are chemical devices comprising two basic functional units (**Figure 2**). The first one is a biomolecule responsible for recognition of the target substance through specific intermolecular binding or by means of catalytic reactions (D'Orazio, 2003). The second is the transducer that converts the biochemical response into a measurable electric signal, which is mainly proportional to analyte concentration (Higgins and Lowe, 1987; Hulanicki et al., 1991; Thévenot et al., 2001). In addition, diverse transducers can be used for conversion of the biochemical response into a quantifiable analytical signal, being classified according to their physical principles as electrochemical, electrical, optical, piezoelectric, calorimetric, acoustic, and magnetic (Hulanicki et al., 1991; Sethi, 1994; Marco and Barcelo, 1996; Thévenot et al., 2001).

Electrochemical impedance spectroscopy (EIS) comprises the current main strategy used for the development of biodevices based on AMPs, as shown in **Table 1**. EIS is an effective method for the investigation of modified surfaces and monitoring of interfacial processes, allowing the characterization of electrochemical systems (Stoynov and Savova-Stoynova, 1986; Bard and Faulkner, 2000; Lasia, 2002). In the EIS technique, a signal of perturbation of low amplitude, in the form of sinusoidal potential and different frequency values, is applied to the transducer, forming sinusoidal alternating current (Macdonald, 1990, 1992; Katz and Willner, 2003; Chang and Park, 2010). EIS is a valuable tool for interfacial phenomena analyses occurring between electrode and solution. Dielectric analyses allows for the evaluation of electron charge-transfer parameters, double-layer, electrical layer, and modeling the experimental data to equivalent circuits (Stoynov and Savova-Stoynova, 1986; Macdonald, 1990; Bott, 2001; Oliveira et al., 2011). EIS is a technique of great relevance due to numerous technological applications such as the development of biosensors, studies of dielectric materials, corrosion processes, biofuel cells and rechargeable batteries (Macdonald, 1992; Guan et al., 2004). EIS is a new experimental approach for understanding AMP mechanisms of action through lipid membrane properties by monitoring changes such as thickness, ion permeability and homogeneity after peptide exposure (Chang et al., 2008; Oliveira et al., 2011; Nascimento et al., 2012; Sugihara et al., 2012).

Several biological elements can be used for the manufacturing of biosensitive systems, such as cell receptors, enzymes, antibodies, antigens, nucleic acids, aptamers, lectins, and peptides (Byfield and Abuknesha, 1994; Guan et al., 2004; Caygill et al., 2010). In particular, AMPs are outstanding molecules due to their wide biotechnological applications (Dawson and Liu, 2008; Meng et al., 2010; Seo et al., 2012). In addition, AMPs are promising molecules for the development of biosensors due to the possibility of recognizing a wide variety of pathogenic agents, including bacteria,

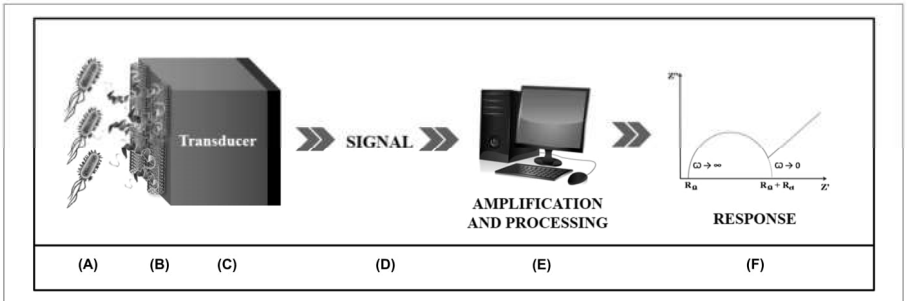

FIGURE 2 | Schematic presentation of an electrochemical biosensor. The detection of the analyte **(A)** is performed through a biological component **(B)** associated to a transducer **(C)**. This is responsible for converting the biochemical response arising from the biospecific interaction into an electrical signal **(D)** which will be amplified and processed by a computer software **(E)** which will describe, through graphs **(F)**, the bioactivity of the system.

Table 1 | Antimicrobial peptides, their immobilization substrates and molecular targets with the respective detection limits obtained through different techniques.

AMPs	Substrate immobilization	Target recognition	Detection limit	Technique	Reference
Magainin I	Gold surface – lipoic acid *N*-hydroxysuccinimide – ferrocene	*Escherichia coli* O157:H7	10^3 CFU · mL^{-1}	Electrochemical impedance	Li et al. (2014)
Magainin I	Glass microbeads – *N*-[γ-maleimidobutyryloxy] succinimide ester (GMBS) – cysteine	Non-pathogenic *Escherichia coli*	10^3 cells · mL^{-1}	Fluorescence microscopy	Yoo et al. (2014)
Magainin I	Gold surface – cysteine	*Salmonella typhimurium*	10^3 CFU · mL^{-1}	Electrical impedance	Mannoor et al. (2010)
Leucocin A	Gold surface – cysteamine	*Listeria monocytogenes*	10^3 CFU · mL^{-1}	Electrical impedance	Etayash et al. (2014)
Bactenecin	Glass slide – 3-mercaptopropyl triethoxysilane (MPTES) – GMBS	*Brucella melitensis* Vaccinia virus Venezuelan equine encephalitis virus *Coxiella burnetti*	5×10^4 cells · mL^{-1} $<5 \times 10^5$ PFU · mL^{-1} $<5 \times 10^5$ PFU · mL^{-1} 5×10^5 cells · mL^{-1}	Fluorescence spectroscopy	Kulagina et al. (2007)
G10KHc	Gold surface – cysteine	*Pseudomonas aeruginosa*	10^5 CFU · mL^{-1}	Electrical impedance	Lillehoj et al. (2014)
C16G2cys	Gold surface – cysteine	*Streptococcus mutans*	10^5 CFU · mL^{-1}	Electrical impedance	Lillehoj et al. (2014)
Cecoprin A	Glass slide – poly(dimethyl) siloxane (PDMS)	Botulinum toxin A	1 ng · mL^{-1}	Fluorescence spectroscopy	Kulagina et al. (2006)
Melittin	Glass slide – PDMS	Botulinum toxin B	10 ng · mL^{-1}	Fluorescence spectroscopy	Kulagina et al. (2006)

**CFU, colony forming units; PFU, plaque forming units.*

fungi, toxins, and viruses with lipoprotein envelope (Zasloff, 2002; De Smet and Contreras, 2005; Kulagina et al., 2007).

The basic principle that enables the use of AMPs in biosensors is its ability to selectively interact with the cell membrane components of pathogens (Kulagina et al., 2005). The (bio) interaction is mainly driven by electrostatic forces, hydrogen bonds, and hydrophobic interactions (Seelig, 2004). Biological recognition thermodynamics depends on lipid membrane composition and peptide properties such as hydrophobicity, amphipathicity, molecular charge, and degree of secondary structure angle (Mozsolits et al., 2001; Papo and Shai, 2003; Fernandes et al., 2012; Oliveira et al., 2013). Therefore, AMP specificity is based on the different molecular affinities, allowing their employment in diagnostic tests (Kulagina et al., 2005; Etayash et al., 2014; Li et al., 2014).

Interdigitated electrodes are an excellent alternative for biosensor development. Mannoor et al. (2010) reported the development of an interdigitated capacitive biosensor for detection of *Escherichia coli* and *Salmonella typhimurium*. In this study, magainin I was immobilized on gold microelectrodes via its *C*-terminal cysteine residue, and the binding capacity to bacterial cells was evaluated by EIS. The changes in the dielectric properties of the modified electrode surface allowed the determination of selectivity for pathogenic Gram-negative bacteria *E. coli* and *Salmonella typhimurium* in relation to non-pathogenic *E. coli* and the Gram-positive species *Listeria monocytogenes* (Mannoor et al., 2010).

Recently, Li et al. (2014) developed an impedimetric biosensor with magainin I conjugated to a structured film of ferrocene for bacterial detection. The biosensor showed a preferential selectivity for *E. coli* O157: H7 followed by non-pathogenic *E. coli* K12, *Bacillus subtilis* and *Staphylococcus epidermidis*. In addition, a detection limit was observed for *E. coli* O157: H7 of 10^3 CFU mL^{-1}.

A microelectromechanical sensor using two synthetic peptides (C16G2cys or G10KHc) was developed for the detection of *Streptococcus mutans* and *Pseudomonas aeruginosa* (Lillehoj et al., 2014). It is important to note that C16G2cys and G10KHc have a cysteine amino acid residue in the *C*-terminus, and the -SH group of the cysteine can be used to promote binding on the gold surface, resulting in the vertical orientation of the recognition molecules.

Among the optical properties explored for the construction of biosensors, one of the most prevalent is fluorescence, evaluated by a significant number of techniques that allow the analysis of the systems conjugated with fluorophores and molecular targets quantification (Gauglitz, 2005; Altschuh et al., 2006; Lazcka et al., 2007; Fan et al., 2008). Fluorescence is a phenomenon of photon emissions, resulting from the passage of a valence electron in

an orbital of ground state to an orbital of higher energy to the absorption of radiation of appropriate wavelength. Upon returning to the state of origin, photons are liberated with bottom energy to absorbed light. Fluorescence spectroscopy allows for the quantification of the analyte with sensibility, low cost, and easy implementation (Eaton, 1990; Lazcka et al., 2007). Thus, the molecular recognition is assessed through variations in fluorescence properties after the interaction of the bioreceptor with the specific target (McFarland and Finney, 2001; Altschuh et al., 2006).

In this context, magainin I was immobilized on glass slides modified with 3-mercaptopropyl triethoxysilane (MPTES) and *N*-(γ-maleimidobutyryloxy) succinimide ester (GMBS) through direct covalent binding or by avidin–biotin coupling, being used as a recognition molecule for *E. coli* O157: H7 and *Salmonella typhimurium* (Kulagina et al., 2005). The immobilization method interferes with biosensor sensitivity, and the direct binding of magainin I reduces non-specific interactions, resulting in detection limits of 1.6×10^5 and 6.5×10^4 cells mL^{-1} for *E. coli* and *Salmonella typhimurium* labeled with Cy5, respectively. Through the indirect method values of 6.8×10^5 and 5.6×10^5 cells mL^{-1} were obtained (Kulagina et al., 2005). Moreover, cecropin A, parasin, magainin I, and polymyxin B and E, immobilized on a glass slide modified with MPTES and GMBS, were also used in screening fluorescent assays for detection of *E. coli* O157:H7 and *Salmonella typhimurium* (Kulagina et al., 2006). The assay in "sandwich" format, with the employment of Cy3-labeled anti-*E. coli* or anti-*Salmonella,* demonstrated different AMP affinities for pathogenic species (Kulagina et al., 2006). In another study, cecropin (A, B, and P), parasin, magainin I, polymyxin (B and E), melittin, and bactenecin were evaluated for the biodetection of viral particles and bacterial cells using Cy3 (Kulagina et al., 2007).

Cecropin P1 (CP1), SMAP-29, and PGQ were used as alternative molecules for detection of *E. coli* O157:H7 in substitution of the *anti-E. coli* O157:H7 antibody (Arcidiacono et al., 2008). Through screening in solution and quantification of fluorescence, it was verified that the detection limits for Cy5 CP1, Cy5 SMAP, and Cy5 PGQ were 10^4, 10^5 e10^6 CFU mL^{-1}, respectively, in comparison to 10^5 CFU mL^{-1} for Cy5 anti-*E. coli* O157 antibody. Because of the high sensitivity of the CP1 and specificity of the anti-*E. coli* O157:H7 antibody, a prototype immuno-magnetic bead biosensor was developed, resulting in a 10-fold improvement in sensitivity (Arcidiacono et al., 2008).

Glass microspheres (GMs) based on microfluidic chip were used for magainin I immobilization as a new method for *E. coli* biodetection (Yoo et al., 2014). GMs provided greater detection efficiency through the increase of superficial area of adsorption relative to the volume, enabling a greater number of bonds between microorganism-AMPs. The biodevice presented a good detection efficiency of 87% in a limit of 10^3 cells mL^{-1} obtained by image analysis under fluorescence microscopy (Yoo et al., 2014).

The most common application of AMP-based biosensors is the identification of diverse bacteria such as *E. coli*, *Salmonella typhimurium*, *L. monocytogenes*, *Streptococcus mutans*, *P. aeruginosa*, and others (Mannoor et al., 2010; Li et al., 2014). In this scenario, AMPs stand out for presenting differential characteristics and large applicability potential, since AMPs are highly stable under unsuitable conditions and can be continuously exposed to natural surroundings (Casteels et al., 1989; Mannoor et al., 2010; Laverty et al., 2011; Hassan et al., 2012; Dawgul et al., 2014). AMPs are capable of interacting with invariant components of the target surfaces (Kulagina et al., 2006), providing each peptide with the possibility of recognizing a variety of pathogens (Zasloff, 2002; De Smet and Contreras, 2005; Kulagina et al., 2007). Despite the importance of bacterial diagnosis, diverse studies have undertaken to develop detection systems for other microorganisms and toxins (Zasloff, 2002; De Smet and Contreras, 2005; Kulagina et al., 2007).

Therefore, AMPs can be used in nanostructured platforms for the detection of pathogenic agents due to their singular properties, ease of acquisition, and relevant biological activity (Kulagina et al., 2005; Yonekita et al., 2013). AMPs are an excellent alternative for obtaining new, sensitive, inexpensive, portable, versatile, and fast methods of diagnostics for analyte identification and quantification (Caygill et al., 2010; Yoo et al., 2014). Thus, nanobiosensors based on AMPs can be used in basic and applied research, clinical analysis, commercial applications, microbiological quality control, and environmental monitoring (Higgins and Lowe, 1987; D'Orazio, 2003; Mehrvar and Abdi, 2004).

CONCLUSION

Antimicrobial peptides are considered promising molecules in the development of biodetection devices. Nanotechnology has enabled the construction of biosensors based on AMPs with more specificity and sensitivity for detection of pathogenic agents. Biosensors based on AMPs are a useful tool since it is possible to investigate a wide variety of molecular targets in real time, providing quantitative or semi-quantitative analytical information that is both specific and selective. In spite of AMP-based biosensors being prototypes and their remaining challenges to commercialization such as reproducibility, validation and proper standardization, they may be considered valuable alternatives for obtaining new diagnostic methods.

ACKNOWLEDGMENTS

The authors are grateful for the support provided by the FACEPE and Rede de Nanobiotecnologia/CAPES. Andrade and Oliveira are also gratefully for CNPq financial support (grant 310305/2012-8 and 310361/2012-5, respectively). Ribeiro and da Silva would like to thank FACEPE for M.Sc. and Ph.D. scholarships, respectively.

REFERENCES

Abdel-Hamid, I., Ivnitski, D., Atanasov, P., and Wilkins, E. (1999). Flow-through immunofiltration assay system for rapid detection of *E. coli* O157:H7. *Biosens. Bioelectron.* 14, 309–316. doi: 10.1016/S0956-5663(99)00004-4

Altschuh, D., Oncul, S., and Demchenko, A. P. (2006). Fluorescence sensing of intermolecular interactions and development of direct molecular biosensors. *J. Mol. Recognit.* 19, 459–477. doi: 10.1002/jmr.807

Andersen, P., Munk, M. E., Pollock, J. M., and Doherty, T. M. (2000). Specific immune-based diagnosis of tuberculosis. *Lancet* 356, 1099–1104. doi: 10.1016/S0140-6736(00)02742-2

Andreu, D., and Rivas, L. (1998). Animal antimicrobial peptides: an overview. *Biopolymers* 47, 415–433. doi: 10.1002/(SICI)1097-0282(1998)47:6<415::AID-BIP2>3.0.CO;2-D

Arcidiacono, S., Pivarnik, P., Mello, C. M., and Senecal, A. (2008). Cy5 labeled antimicrobial peptides for enhanced detection of *Escherichia coli* O157:H7. *Biosens. Bioelectron.* 23, 1721–1727. doi: 10.1016/j.bios.2008.02.005

Bard, J. B. F., and Faulkner, L. R. (2000). *Electrochemical Methods: Fundamentals and Applications.* New York, NY: Wiley.

Barkalina, N., Charalambous, C., Jones, C., and Coward, K. (2014). Nanotechnology in reproductive medicine: emerging applications of nanomaterials. *Nanomedicine* 14, 1549–9634. doi: 10.1016/j.nano.2014.01.001

Bechinger, B., and Lohner, K. (2006). Detergent-like actions of linear amphipathic cationic antimicrobial peptides. *Biochim. Biophys. Acta* 1758, 1529–1539. doi: 10.1016/j.bbamem.2006.07.001

Benes, J., Gabrielova, A., Horova, B., Zitko, K., Rozsypal, H., Dzupova, O., et al. (1996). [Comparison of various methods of hemoculture tests]. *Epidemiol. Mikrobiol. Imunol.* 45, 101–107. doi: 10.4103/0974-2727.129084

Bi, L., Yang, L., Narsimhan, G., Bhunia, A. K., and Yao, Y. (2011). Designing carbohydrate nanoparticles for prolonged efficacy of antimicrobial peptide. *J. Control. Release* 150, 150–156. doi: 10.1016/j.jconrel.2010.11.024

Bott, A. W. (2001). Eletrochemical techniques for the characterization of redox polymers. *Curr. Sep.* 19, 71–75.

Bragulat, M. R., Martinez, E., Castella, G., and Cabanes, F. J. (2004). Selective efficacy of culture media recommended for isolation and enumeration of *Fusarium* spp. *J. Food Prot.* 67, 207–211.

Brogden, K. A., Guthmiller, J. M., Salzet, M., and Zasloff, M. (2005). The nervous system and innate immunity: the neuropeptide connection. *Nat. Immunol.* 6, 558–564. doi: 10.1038/ni1209

Byfield, M. P., and Abuknesha, R. A. (1994). Biochemical aspects of biosensors. *Biosens. Bioelectron.* 9, 373–400. doi: 10.1016/0956-5663(94)80038-3

Casteels, P., Ampe, C., Jacobs, F., Vaeck, M., and Tempst, P. (1989). Apidaecins: antibacterial peptides from honeybees. *EMBO J.* 8, 2387–2391.

Caygill, R. L., Blair, G. E., and Millner, P. A. (2010). A review on viral biosensors to detect human pathogens. *Anal. Chim. Acta* 681, 8–15. doi: 10.1016/j.aca.2010.09.038

Chang, B. Y., and Park, S. M. (2010). Electrochemical impedance spectroscopy. *Annu. Rev. Anal. Chem. (Palo Alto Calif)* 3, 207–229. doi: 10.1146/annurev.anchem.012809.102211

Chang, W. K., Wimley, W. C., Searson, P. C., Hristova, K., and Merzlyakov, M. (2008). Characterization of antimicrobial peptide activity by electrochemical impedance spectroscopy. *Biochim. Biophys. Acta* 1778, 2430–2436. doi: 10.1016/j.bbamem.2008.06.016

Cheema, U. B., Younas, M., Sultan, J. I., Iqbal, A., Tariq, M., and Waheed, A. (2011). Antimicrobial peptides: an alternative of antibiotics in ruminants. *Adv. Agric. Biotechnol.* 2, 15–21.

Costa, F., Carvalho, I. F., Montelaro, R. C., Gomes, P., and Martins, M. C. (2011). Covalent immobilization of antimicrobial peptides (AMPs) onto biomaterial surfaces. *Acta Biomater.* 7, 1431–1440. doi: 10.1016/j.actbio.2010.11.005

Dawgul, M., Maciejewska, M., Jaskiewicz, M., Karafova, A., and Kamysz, W. (2014). Antimicrobial peptides as potential tool to fight bacterial biofilm. *Acta Pol. Pharm.* 71, 39–47.

Dawson, R. M., and Liu, C. Q. (2008). Properties and applications of antimicrobial peptides in biodefense against biological warfare threat agents. *Crit. Rev. Microbiol.* 34, 89–107. doi: 10.1080/10408410802143808

Deisingh, A. K., and Thompson, M. (2004). Biosensors for the detection of bacteria. *Can. J. Microbiol.* 50, 69–77. doi: 10.1139/w03-095

De Smet, K., and Contreras, R. (2005). Human antimicrobial peptides: defensins, cathelicidins and histatins. *Biotechnol. Lett.* 27, 1337–1347. doi: 10.1007/s10529-005-0936-5

D'Orazio, P. (2003). Biosensors in clinical chemistry. *Clin. Chim. Acta* 334, 41–69. doi: 10.1016/S0009-8981(03)00241-9

Eaton, D. F. (1990). Recommended methods for fluorescence decay analysis. *Pure Appl. Chem.* 62, 1631–1648. doi: 10.1351/pac199062081631

Etayash, H., Jiang, K., Thundat, T., and Kaur, K. (2014). Impedimetric detection of pathogenic gram-positive bacteria using an antimicrobial peptide from class IIa bacteriocins. *Anal. Chem.* 86, 1693–1700. doi: 10.1021/ac4034938

Fan, X. D., White, I. M., Shopova, S. I., Zhu, H. Y., Suter, J. D., and Sun, Y. Z. (2008). Sensitive optical biosensors for unlabeled targets: a review. *Anal. Chim. Acta* 620, 8–26. doi: 10.1016/j.aca.2008.05.022

Fernandes, F. C., Rigden, D. J., and Franco, O. L. (2012). Prediction of antimicrobial peptides based on the adaptive neuro-fuzzy inference system application. *Biopolymers* 98, 280–287. doi: 10.1002/bip.22066

Fournier-Wirth, C., and Coste, J. (2010). Nanotechnologies for pathogen detection: future alternatives? *Biologicals* 38, 9–13. doi: 10.1016/j.biologicals.2009.10.010

Gauglitz, G. (2005). Direct optical sensors: principles and selected applications. *Anal. Bioanal. Chem.* 381, 141–155. doi: 10.1007/s00216-004-2895-4

Guan, J. G., Miao, Y. Q., and Zhang, Q. J. (2004). Impedimetric biosensors. *J. Biosci. Bioeng.* 97, 219–226. doi: 10.1016/S1389-1723(04)70195-4

Hancock, R. E. W., and Sahl, H. G. (2006). Antimicrobial and host-defense peptides as new anti-infective therapeutic strategies. *Nat. Biotechnol.* 24, 1551–1557. doi: 10.1038/nbt1267

Hassan, M., Kjos, M., Nes, I. F., Diep, D. B., and Lotfipour, F. (2012). Natural antimicrobial peptides from bacteria: characteristics and potential applications to fight against antibiotic resistance. *J. Appl. Microbiol.* 113, 723–736. doi: 10.1111/j.1365-2672.2012.05338.x

Higgins, I. J., and Lowe, C. R. (1987). Introduction to the principles and applications of biosensors. *Philos. Trans. R. Soc. Lond. B Biol. Sci.* 316, 3–11. doi: 10.1098/rstb.1987.0013

Hulanicki, A., Glab, S., and Ingman, F. (1991). Chemical sensors definitions and classification. *Pure Appl. Chem.* 63, 1247–1250. doi: 10.1351/pac199163091247

Jianrong, C., Yuqing, M., Nongyue, H., Xiaohua, W., and Sijiao, L. (2004). Nanotechnology and biosensors. *Biotechnol. Adv.* 22, 505–518. doi: 10.1016/j.biotechadv.2004.03.004

Junhui, Z., Hong, C., and Ruifu, Y. (1997). DNA based biosensors. *Biotechnol. Adv.* 15, 43–58. doi: 10.1016/S0734-9750(97)00003-7

Katz, E., and Willner, I. (2003). Probing biomolecular interactions at conductive and semiconductive surfaces by impedance spectroscopy: routes to impedimetric immunosensors, DNA-Sensors, and enzyme biosensors. *Electroanalysis* 15, 913–947. doi: 10.1002/elan.200390114

Keymanesh, K., Soltani, S., and Sardari, S. (2009). Application of antimicrobial peptides in agriculture and food industry. *World J. Microb. Biotechnol.* 25, 933–944. doi: 10.1007/s11274-009-9984-7

Kulagina, N. V., Lassman, M. E., Ligler, F. S., and Taitt, C. R. (2005). Antimicrobial peptides for detection of bacteria in biosensor assays. *Anal. Chem.* 77, 6504–6508. doi: 10.1021/ac050639r

Kulagina, N. V., Shaffer, K. M., Anderson, G. P., Ligler, F. S., and Taitt, C. R. (2006). Antimicrobial peptide-based array for *Escherichia coli* and *Salmonella* screening. *Anal. Chim. Acta* 575, 9–15. doi: 10.1016/j.aca.2006.05.082

Kulagina, N. V., Shaffer, K. M., Ligler, F. S., and Taitt, C. R. (2007). Antimicrobial peptides as new recognition molecules for screening challenging species. *Sens. Actuators B Chem.* 121, 150–157. doi: 10.1016/j.snb.2006.09.044

Lasia, A. (2002). "Electrochemical impedance spectroscopy and its applications," in *Modern Aspects of Electrochemistry*, 1st Edn, eds B. E. Conway, J. O. M. Bockris, and R. White (New York: Springer), 143–248.

Laverty, G., Gorman, S. P., and Gilmore, B. F. (2011). The potential of antimicrobial peptides as biocides. *Int. J. Mol. Sci.* 12, 6566–6596. doi: 10.3390/ijms12106566

Lazcka, O., Del Campo, F. J., and Munoz, F. X. (2007). Pathogen detection: a perspective of traditional methods and biosensors. *Biosens. Bioelectron.* 22, 1205–1217. doi: 10.1016/j.bios.2006.06.036

Lillehoj, P. B., Kaplan, C. W., He, J., Shi, W. Y., and Ho, C. M. (2014). Rapid, electrical impedance detection of bacterial pathogens using immobilized antimicrobial peptides. *J. Lab. Autom.* 19, 42–49. doi: 10.1177/2211068213495207

Li, Y., Afrasiabi, R., Fathi, F., Wang, N., Xiang, C., Love, R., et al. (2014). Impedance based detection of pathogenic *E. coli* O157:H7 using a ferrocene-antimicrobial peptide modified biosensor. *Biosens. Bioelectron.* 58, 193–199. doi: 10.1016/j.bios.2014.02.045

Li, Y., Schluesener, H. J., and Xu, S. (2010). Gold nanoparticle-based biosensors. *Gold Bull.* 43, 29–41. doi: 10.1007/BF03214964

Li, Y., Xiang, Q., Zhang, Q., Huang, Y., and Su, Z. (2012). Overview on the recent study of antimicrobial peptides: origins, functions, relative mechanisms and application. *Peptides* 37, 207–215. doi: 10.1016/j.peptides.2012.07.001

Macdonald, D. D. (1990). Review of mechanistic analysis by electrochemical impedance spectroscopy. *Electrochim. Acta* 35, 1509–1525. doi: 10.1016/0013-4686(90)80005-9

Macdonald, J. R. (1992). Impedance spectroscopy. *Ann. Biomed. Eng.* 20, 289–305. doi: 10.1007/BF02368532

Mannoor, M. S., Zhang, S., Link, A. J., and McAlpine, M. C. (2010). Electrical detection of pathogenic bacteria via immobilized antimicrobial peptides. *Proc. Natl. Acad. Sci. U.S.A.* 107, 19207–19212. doi: 10.1073/pnas.1008768107

Marco, M. P., and Barcelo, D. (1996). Environmental applications of analytical biosensors. *Meas. Sci. Technol.* 7, 1547–1562. doi: 10.1088/0957-0233/7/11/002

Mazzoni, A., Fiacchini, M., Cevenini, R., Gatti, M., and Nanetti, A. (1987). Incidence of endogenous and exogenous opportunistic fungal infections in relation to different prophylactic measures: clinical and microbiological study of 431 immunocompromised patients. *Chemioterapia* 6, 374–376.

McFarland, S. A., and Finney, N. S. (2001). Fluorescent chemosensors based on conformational restriction of a biaryl fluorophore. *J. Am. Chem. Soc.* 123, 1260–1261. doi: 10.1021/ja005701a

Mehrvar, M., and Abdi, M. (2004). Recent developments, characteristics, and potential applications of electrochemical biosensors. *Anal. Sci.* 20, 1113–1126. doi: 10.2116/analsci.20.1113

Mendez, E., Moreno, A., Colilla, F., Pelaez, F., Limas, G. G., Mendez, R., et al. (1990). Primary structure and inhibition of protein synthesis in eukaryotic cell-free system of a novel thionin, gamma-hordothionin, from barley endosperm. *Eur. J. Biochem.* 194, 533–539. doi: 10.1111/j.1432-1033.1990.tb15649.x

Meng, S., Xu, H., and Wang, F. (2010). Research advances of antimicrobial peptides and applications in food industry and agriculture. *Curr. Prot. Pept. Sci.* 11, 264–273. doi: 10.2174/138920310791233369

Mozsolits, H., Wirth, H. J., Werkmeister, J., and Aguilar, M. I. (2001). Analysis of antimicrobial peptide interactions with hybrid bilayer membrane systems using surface plasmonresonance. *Biochim. Biophys. Acta* 1512, 64–76. doi: 10.1016/S0005-2736(01)00303-0

Murthy, S., Keystone, J., and Kissoon, N. (2013). Infections of the developing world. *Crit. Care Clin.* 29, 485–507. doi: 10.1016/j.ccc.2013.03.005

Nascimento, J. M., Franco, O. L., Oliveira, M. D. L., and Andrade, C. A. S. (2012). Evaluation of magainin I interactions with lipid membranes: an optical and electrochemical study. *Chem. Phys. Lipids* 165, 537–544. doi: 10.1016/j.chemphyslip.2012.05.002

Nguyen, L. T., Haney, E. F., and Vogel, H. J. (2011). The expanding scope of antimicrobial peptide structures and their modes of action. *Trends Biotechnol.* 29, 464–472. doi: 10.1016/j.tibtech.2011.05.001

Oliveira, M. D. L., Abdalla, D. S. P., Guilherme, D. F., Faulin, T. E. S., and Andrade, C. A. S. (2011). Impedimetric immunosensor for electronegative low density lipoprotein (LDL-) based on monoclonal antibody adsorbed on (polyvinyl formal)-gold nanoparticles matrix. *Sens. Actuators B Chem.* 155, 775–781. doi: 10.1016/j.snb.2011.01.046

Oliveira, M. D. L., Franco, O. L., Nascimento, J. M., Melo, C. P., and Andrade, C. A. S. (2013). Mechanistic aspects of peptide-membrane interactions determined by optical, dielectric and piezoelectric techniques: an overview. *Curr. Prot. Pept. Sci.* 14, 543–555. doi: 10.2174/13892037113149990070

Palka-Santini, M., Cleven, B. E., Eichinger, L., Krönke, M., and Krut, O. (2009). Large scale multiplex PCR improves pathogen detection by DNA microarrays. *BMC Microbiol.* 9:1. doi: 10.1186/1471-2180-9-1

Papo, N., and Shai, Y. (2003). Exploring peptide membrane interaction using surface plasmon resonance: differentiation between pore formation versus membrane disruption by lytic peptides. *Biochemistry* 42, 458–466. doi: 10.1021/bi0267846

Rapaport, D., and Shai, Y. (1991). Interaction of fluorescently labeled pardaxin and its analogs with lipid bilayers. *J. Biol. Chem.* 266, 23769–23775.

Reddy, K. V. R., Yedery, R. D., and Aranha, C. (2004). Antimicrobial peptides: premises and promises. *Int. J. Antimicrob. Agents* 24, 536–547. doi: 10.1016/j.ijantimicag.2004.09.005

Schmidtchen, A., Pasupuleti, M., and Malmsten, M. (2014). Effect of hydrophobic modifications in antimicrobial peptides. *Adv. Colloid Interface Sci.* 205, 265–274. doi: 10.1016/j.cis.2013.06.009

Schnapp, D., and Harris, A. (1998). Antibacterial peptides in bronchoalveolar lavage fluid. *Am. J. Respir. Cell Mol. Biol.* 19, 352–356. doi: 10.1165/ajrcmb.19.3.3384

Schuerholz, T., Brandenburg, K., and Marx, G. (2012). Antimicrobial peptides and their potential application in inflammation and sepsis. *Crit. Care* 16:207. doi: 10.1186/cc11220

Seelig, J. (2004). Thermodynamics of lipid-peptide interactions. *Biochim. Biophys. Acta* 1666, 40–50. doi: 10.1016/j.bbamem.2004.08.004

Seo, M. D., Won, H. S., Kim, J. H., Mishig-Ochir, T., and Lee, B. J. (2012). Antimicrobial peptides for therapeutic applications: a review. *Molecules* 17, 12276–12286. doi: 10.3390/molecules171012276

Sethi, R. S. (1994). Transducer aspects of biosensors. *Biosens. Bioelectron.* 9, 243–264. doi: 10.1016/0956-5663(94)80127-4

Singh, P. K., Shiha, M. J., and Kumar, A. (2014). Antibacterial responses of retinal Muller gia: production of antimicrobial peptides, oxidative burst and phagocytosis. *J. Neuroinflammation* 11:33. doi: 10.1186/1742-2094-11-33

Sobczak, M., Debek, C., Oledzka, E., and Kozlowski, R. (2013). Polymeric systems of antimicrobial peptides -strategies and potential applications. *Molecules* 18, 14122–14137. doi: 10.3390/molecules181114122

Stoynov, Z. B., and Savova-Stoynova, B. (1986). Structural simulation of electrochemical impedances. *J. Electroanal. Chem.* 209, 11–18. doi: 10.1016/0022-0728(86)80181-4

Sugihara, K., Delaia, M., Szendro, I., Guillaume-Gentil, O., Vörös, J., and Zambelli, T. (2012). Simultaneous OWLS and EIS monitoring of supported lipid bilayers with the pore forming peptide melittin. *Sens. Actuators B Chem.* 161, 600–606. doi: 10.1016/j.snb.2011.11.007

Szakal, D., and Pal, T. (2003). Comparison of media for the selective culture of enteroinvasive *Escherichia coli*. *Eur. J. Clin. Microbiol. Infect. Dis.* 22, 235–241.

Thévenot, D. R., Toth, K., Durst, R. A., and Wilson, G. S. (2001). Electrochemical biosensors: recommended definitions and classification. *Biosens. Bioelectron.* 16, 121–131. doi: 10.1016/S0956-5663(01)00115-4

Toke, O. (2005). Antimicrobial peptides: new candidates in the fight against bacterial infections. *Biopolymers* 80, 717–735. doi: 10.1002/bip.20286

van't Hof, W., Veerman, E. C., Helmerhorst, E. J., and Amerongen, A. V. (2001). Antimicrobial peptides: properties and applicability. *Biol. Chem.* 382, 597–619. doi: 10.1515/BC.2001.072

van Pelt, C., Verduin, C. M., Goessens, W. H., Vos, M. C., Tümmler, B., Segonds, C., et al. (1999). Identification of *Burkholderia* spp. in the clinical microbiology laboratory: comparison of conventional and molecular methods. *J. Clin. Microbiol.* 37, 2158–2164.

Wang, J. (1998). DNA biosensors based on Peptide Nucleic Acid (PNA) recognition layers. A review. *Biosens. Bioelectron.* 13, 757–762. doi: 10.1016/S0956-5663(98)00039-6

Wang, J., Rivas, G., Cai, X., Palecek, E., Nielsen, P., Shiraish, H., et al. (1997). DNA electrochemical biosensors for environmental monitoring. A review. *Anal. Chim. Acta* 347, 1–8. doi: 10.1016/S0003-2670(96)00598-3

Yang, S., Lin, S., Kelen, G. D., Quinn, T. C., Dick, J. D., Gaydos, C. A., et al. (2002). Quantitative multiprobe PCR assay for simultaneous detection and identification to species level of bacterial pathogens. *J. Clin. Microbiol.* 40, 3449–3454. doi: 10.1128/JCM.40.9.3449-3454.2002

Yeom, S. H., Kang, B. H., Kim, K. J., and Kang, S. W. (2011). Nanostructures in biosensor-a review. *Front. Biosci.* 16:997–1023. doi: 10.2741/3731

Yonekita, T., Ohtsuki, R., Hojo, E., Morishita, N., Matsumoto, T., Aizawa, T., et al. (2013). Development of a novel multiplex lateral flow assay using an antimicrobial peptide for the detection of Shiga toxin-producing *Escherichia coli*. *J. Microbiol. Methods* 93, 251–256. doi: 10.1016/j.mimet.2013.03.006

Yoo, J. H., Woo, D. H., Chang, M.-S., and Chun, M.-S. (2014). Microfluidic based biosensing for *Escherichia coli* detection by embedding antimicrobial peptide-labeled beads. *Sens. Actuators B Chem.* 191, 211–218. doi: 10.1016/j.snb.2013.09.105

Zasloff, M. (2002). Antimicrobial peptides of multicellular organisms. *Nature* 415, 389–395. doi: 10.1038/415389a

Conflict of Interest Statement: The authors declare that the research was conducted in the absence of any commercial or financial relationships that could be construed as a potential conflict of interest.

Received: 30 May 2014; accepted: 04 August 2014; published online: 20 August 2014.
Citation: Silva RR, Avelino KYPS, Ribeiro KL, Franco OL, Oliveira MDL and Andrade CAS (2014) Optical and dielectric sensors based on antimicrobial peptides for microorganism diagnosis. Front. Microbiol. 5:443. doi: 10.3389/fmicb.2014.00443
This article was submitted to Antimicrobials, Resistance and Chemotherapy, a section of the journal Frontiers in Microbiology.

ANEXO C - ARTIGO PUBLICADO DURANTE O DOUTORADO

http://dx.doi.org/10.5935/0103-5053.20150249
J. Braz. Chem. Soc., Vol. 27, No. 1, 77-83, 2016.
Printed in Brazil - ©2016 Sociedade Brasileira de Química
0103 - 5053 $6.00+0.00

Article

Dielectric Behavior of Alginate-Based Hydrogel Containing Neomycin-Loaded Lipid Nanovesicles under Influence of Electrical Potentials

Rafael R. Silva,[a] Sandro V. de Lima,[b] Gustavo H. R. C. Silva,[c] Helinando P. de Oliveira,[d] Maria D. L. Oliveira[c] and Cesar A. S. Andrade[a,c]*

[a]*Programa de Pós-Graduação em Inovação Terapêutica,* [b]*Departamento de Física and* [c]*Departamento de Bioquímica, Universidade Federal de Pernambuco, 50670-901 Recife-PE, Brazil*

[d]*Colegiado de Pós-Graduação em Ciência dos Materiais, Universidade Federal do Vale do São Francisco, 48902-300 Juazeiro-BA, Brazil*

Dielectric characterization has been applied as a convenient tool for evaluation of transport and polarization mechanisms in soft materials. In this work, we have explored the study of charge transport mechanisms in alginate hydrogel containing neomycin-loaded liposomes. For comparison, drug release kinetic was evaluated by using UV-Vis spectrophotometry and electrical impedance spectroscopy (EIS) at different external direct current (DC) polarization (100 mV and 1 V). The charge transfer resistance (Rct) was proportional to DC electrical stimulation and inversely to the amount of released neomycin. Optical and electrical measurements confirmed the dependence of neomycin release under influence of electrical potentials. The kinetic profile of these systems was described by zero-order model. In addition, the Korsmeyer-Peppas model also suggested a diffusion mechanism based on super case II transport (non-Fickian). These results encouraged the use of EIS as a "dark" spectroscopy technique, since EIS is effective for studies of release kinetics controlled by DC external electrical excitation.

Keywords: controlled release, hydrogel, alginate, liposomes, impedance spectroscopy

Introduction

Hydrogels are semi-solid materials soluble in polar solvent with potential application in the development of new controlled release systems.[1] Therapeutic use of hydrogels is associated with diverse applications such as ophthalmic ointments,[2] wound healing for venous ulcers[3] and treatment for skin infections.[4] A variety of synthetic and natural molecules, extracted from animals, plants or algae serves as a basis for gel preparation.[5]

Alginate (Alg), an anionic polysaccharide isolated from brown seaweed with linear structure containing homopolymeric blocks of guluronate and mannuronate residues, has been extensively used in the pharmaceutical industry for production of natural ointments. Alg is an electro-responsive polymer due to the presence of ionizable groups (–COOH) and counterions (Na^+ and Ca^+), with an important role during ion exchange process.[6-8]

The advantages of Alg, viz., high solubility in polar solvents, biodegradability and non-toxicity[9] contribute to development of new promising controlled release systems for antibacterial applications.[10] In addition, the association between liposomes (Lipo) and Alg hydrogel improves the controlled release of resulting systems.[11] Lipo are nanometric spherical lipid vesicles with different properties, viz., varying size, number of lipid layers, lipid constitution, biocompatibility and different routes of administration.[12]

Neomycin (Neo) is a well-known antibiotic with effective action against Gram-negative bacteria, such as *Klebsiella pneumoniae*, *Escherichia coli* and *Pseudomonas aeruginosa*.[13,14] The system composed by Neo-loaded Lipo could be considered as an ideal model for development of topical formulations.

In general, drug release kinetic profile is evaluated by different methods such as UV-Vis spectrophotometry,[15] fluorescence spectrometry[16] and high performance liquid chromatography.[17] On the other hand, electrochemical impedance spectroscopy (EIS) is an alternative and effective method applied in the study of drug release and hydrogel swelling behavior. EIS is also applied in the study of dielectric behavior and relaxation processes in

*e-mail: csrandrade@gmail.com

soft materials, such as polymers.[18,19] Furthermore, the analysis of the alternating current (AC) response of the materials using equivalent electric circuit models allows the evaluation of diverse parameters such as charge transfer resistance (Rct), double electric layer, bulk resistance and others.[20]

In this study, we analyzed NeoLipoAlg systems at zero direct current (DC) external excitation and under influence of two external applied potentials (100 mV and 1 V). Neo release kinetic profiles from LipoAlg system under influence of electrical potentials were monitored using the alternative viewpoint of the EIS. For comparison, the amount of the drug released was also evaluated using an optical conventional technique.

Experimental

Materials

Neomycin trisulfate salt hydrate, *L*-α-phosphatidylcholine (PC), cholesterol (CHOL), sodium alginate, chloroform and methanol were purchased from Sigma Aldrich. Deionized (DI) water was obtained from a Sinergy Millipore System.

Preparation of NeoLipoAlg system

Liposomal colloidal solution was synthesized using a mixture of PC:CHOL (7:1 m/m) dissolved in chloroform:methanol (9:1 v/v) solution. Subsequently, the solvent mixture was removed under reduced pressure during 5 min at 37 ± 1 °C at 80 rpm. After that, the resulting dried thin lipid film was hydrated with 5 mL of 10 mmol L^{-1} Neo aqueous solution. Resulting sample was sonicated for 5 min at 15 kHz (UNIQUE DES500) in order to obtain large unilamellar vesicles (LUV). Finally, 1 mL NeoLipo solution was added to 300 mg of Alg to obtain a homogeneous mixture of hydrogel (NeoLipoAlg system).

Particle size and zeta potential measurements

Size distribution and zeta potential of NeoLipo samples were determined by photon correlation spectroscopy (Zetasizer Nano ZS90, Malvern Instruments) with a laser wavelength of 633 nm at a fixed angle of 90° at 25 °C. All measurements were performed in triplicate.

Calculation of drug entrapment efficiency

Drug entrapment efficiency (%EE) of the liposomes was evaluated after ultracentrifugation at 8,792 g for 1 h. Subsequently, the supernatant was diluted with DI water (1:10 v/v). The drug content was evaluated by UV-Vis spectroscopy at $\lambda = 282$ nm and calculated as follows:

$$\%EE = \frac{(\text{NeoLipo}) - (\text{Neounl})}{(\text{NeoLipo})} \times 100 \quad (1)$$

NeoLipo and Neounl represent the amount of the drug encapsulated and non-encapsulated in the liposomes, respectively.

UV-Vis measurements

Neo calibration curve was performed using eight different concentrations (1.0 to 10 mmol L^{-1}) dissolved in DI water. Subsequently, the samples were analyzed by UV-Vis spectrophotometer (FEMTO 800) at fixed wavelength ($\lambda = 282$ nm).

The experiments were performed using two parallel stainless steel electrodes (area of 59 mm × 19 mm) connected to an external high-voltage source measurement unit (Model 237, Keithley). Experiments were performed at zero DC excitation and under influence of two external DC voltage (100 mV and 1 V). Aliquots of 2 mL were collected during 1 h with intervals of 5 min and, after each removal, 2 mL of fresh DI water were replenished carefully to keep the total volume. The amount of drug released was calculated according to the following equation:

$$Neo_{Abs} = NeoLipoAlg_{Abs} - LipoAlg_{Abs} \quad (2)$$

Neo absorbance (Neo_{Abs}) corresponds to the difference between optical absorption of NeoLipoAlg and LipoAlg. The calculation of difference excludes the interference of hydrogel absorption on measurement of UV-Vis absorption.

Drug release kinetic models

Five mathematical models (Table 1) were applied to analyze drug release mechanism, as follows: zero-order, first-order, Higuchi, Korsmeyer-Peppas and Baker-Lonsdale. These models are applied to systems which present a porous polymers composition, loaded hydrophilic drugs and pharmaceutical forms in general including spherical geometry.[21]

The values for the parameters present for each equation were determined by linear or non-linear least squares fitting methods. A regression analysis was performed and the best fittings were calculated based on correlation factors as r^2.

Table 1. Mathematical models used to analyze drug release mechanisms

Model	Equation	Graph presentation
Zero-order	$Q_t = Q_0 + kt$	cumulative amount of drug released *vs.* time
First-order	$\log C = \log C - kt / 2.303$	log cumulative percentage of drug remaining *vs.* time
Higuchi	$Q_t = k\sqrt{t} + C$	cumulative percentage drug release *vs.* square root of time
Korsmeyer-Peppas	$M_t / M_\infty = kt^n$	log cumulative percentage drug release *vs.* log time
Baker-Lonsdale	$3/2[1 - (1 - M_t/M_\infty)^{2/3}] - M_t/M_\infty = kt$	$[3/2[1 - (1 - M_t/M_\infty)^{2/3}] - M_t/M_\infty = kt]$ with respect to the time

Q_t: drug released fraction at time t; Q_0: initial amount of drug in the solution; k: release rate constant; C: initial concentration of drug; n: exponent that determines release mechanism; M_t / M_∞: fraction of drug released at time t.

Morphological analysis under influence of electrical potentials

A homemade apparatus composed of a Petri plate, two parallel stainless steel electrodes (area of 59 mm × 19 mm) and a power supply for electro-stimulation was used to stimulate the drug release. The morphology and behavior of gel at unstimulated condition and under influence of external electric potentials (100 mV and 1 V) were evaluated using an optical microscope (CKX31, Olympus). The images were captured using a high-resolution digital camera (CCD) and analyzed by ImageJ software (NIH Image).

Dielectric impedance measurements

Dielectric measurements were performed using two parallel stainless steel electrodes (area of 59 × 19 mm) into a beaker containing 50 mL DI water placed inside a Faraday cage. Analyses were carried out at neutral and stimulated (100 mV and 1 V) conditions using an external high-voltage source measurement unit (Model 237, Keithley).

The experiments were carried out using a PGSTAT 128N Autolab potentiostat/galvanostat (Metrohm). The impedance spectra were recorded in a frequency range from 0.1 to 10^5 Hz with AC voltage of 10 mV. In addition, the standard deviation is approximately 5% for all measurements. The collected data were recorded during 1 h with interval of 10 min. Results are shown in terms of cumulative percentage release as a function of time, as follows:

$$\text{Cumulative percentage release} = \frac{N_l}{N_d} \times 100\% \qquad (3)$$

where N_l is the cumulative amount of Neo released from LipoAlg and N_d is the total amount of Neo loaded into LipoAlg.

Statistical and data analysis

Statistical and data analysis were carried out using Prism software (version 5, GraphPad). The paired *t*-test (one-tailed) was used considering p values less than 0.05 as statistically significant. The graphical representation was obtained using OriginPro software (version 8, OriginLab).

Results and Discussion

Particle size and zeta potential analysis

Three independent samples of Lipo and NeoLipo systems were analysed. Dynamic light scattering measurements indicated significant differences in the diameters of Lipo (125.80 ± 4.32 nm) and NeoLipo (132.10 ± 5.25 nm) samples. Zeta potential values also showed differences ($p = 0.012$) in the electrical double layer of Lipo (–1.59 ± 0.12 mV) compared to NeoLipo system (–1.06 ± 0.02 mV). The differences observed for zeta values could be attributed to the presence of non-encapsulated drug[22] or electrostatic interactions with liposomes,[23] since Neo has a positive charge.

Drug entrapment efficiency and kinetics profile determination

The maximum absorbance (λ_{max} = 282 nm) was used to evaluate %EE. The value of r^2 in the calibration curve is nearly 1 (r^2 = 0.999). Results demonstrated a drug entrapment efficiency of 92.5%. The polymer dissolution is involved with two transport processes as solvent diffusion and chain disentanglement.[24] The excess of solvent results in increase of dissolution degree associated with subsequent swelling of hydrogel. Moreover, drug release can be improved during electrical stimulation of the hydrogel.[7,25,26]

In the order to elucidate the release mechanism, the data were fitted considering the correlation coefficient (r^2) and the release rate constant (k) for unstimulated and estimulated conditions (Table 2).

As observed in Table 2, r^2 for zero-order for all three conditions (unstimulated, 100 mV and 1 V) ranged from 0.9957, 0.9928 and 0.9937, respectively, demonstrating that drug release followed zero-order kinetics. It is noteworthy to mention that this model is applied to several

Table 2. Simulated results for the release profile according to mathematical models

Model	Potential / V					
	0		0.1		1	
	k	r^2	k	r^2	k	r^2
Zero-order	1.07	0.9957	1.45	0.9928	1.55	0.9937
First-order	3.13×10^{-3}	0.9728	5.87×10^{-3}	0.9196	6.51×10^{-3}	0.9174
Higuchi	8.72	0.8802	11.82	0.8695	12.73	0.8783
Korsmeyer-Peppas	1.06	0.9966	1.00	0.9890	1.16	0.9967
Baker-Lonsdale	1.6×10^{-3}	0.8805	3.8×10^{-3}	0.8449	4.2×10^{-3}	0.8437

k: release rate constant; r^2: correlation coefficient.

pharmaceutical forms involving hydrophilic drugs and a constant release from polymer matrices independent of time.[27,28] However, the electrical stimulation suggested an influence in the polymer, demonstrating a higher amount of drug release in 100 mV and 1 V compared to unstimulated condition.

The correlation coefficient (r^2) for Korsmeyer-Peppas equation also presented good correlation for all three conditions (0.9728, 0.9890, and 0.9967, respectively). Considering our drug delivery system, which has spherical geometry, a limiting n value of 0.45 corresponds to a Fickian diffusion of the drug. The n values from 0.45 to 0.85 indicate a diffusion-dependent drug mechanism and considering the erosion of the polymer matrix. The n values > 0.85 are associated with previous description and may indicate that the drug-release is controlled by multiple process. The n value higher than 1, which may be regarded as super case II transport (non-Fickian model)[29] was observed for all NeoLipoAlg conditions (n = 1.07). This mechanism involves the superposition of swelling, relaxation and dissolution of the polymer. The log% cumulative release under electrical potentials was higher than unstimulated condition (Supplementary Information Figure S1d). The statistical differences were observed for electrically stimulated systems compared to unstimulated condition ($p < 0.0001$).

A recent report demonstrated the relationship between drug release and external applied potentials.[7] On the other hand, no significant differences were observed between the responses of the NeoLipoAlg under electrical potentials ($p = 0.4991$). The similarity in release profiles between stimulated conditions suggests that 100 mV is sufficient to increase the amount of drug released at NeoLipoAlg system. Other models have no better correlation coefficients than the models discussed above.

Morphological analysis under influence of electrical potentials

Optical and electrical experiments were performed to evaluate gel morphology and behavior at unstimulated and under electrical stimulated conditions. The gel motion was proportional to the applied potential (Figures 1 and 2). NeoLipoAlg system (Figure 1) revealed strong motion in comparison with neat Alg (Figure 2). The presence of amine groups in the Neo molecule promote a better ion exchange contributing to the increase of electrical conductivity.[30]

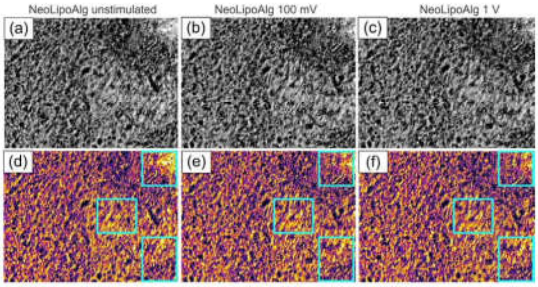

Figure 1. Digital images of NeoLipoAlg system before (a-c) and after editing (d-f) with ImageJ software. The edited images represent the gel at three different conditions, as follows: unstimulated condition (a and d) and under influence of electric potential at 100 mV (b and e) and 1 V (c and f). The lighter areas (yellow) represent surface regions while the darker areas (purple) represent the deepest regions of the gel. The electrical stimulation induced a discrete motion in the gel mesh. It is possible to observe this phenomenon in highlighted areas (blue cyan rectangles).

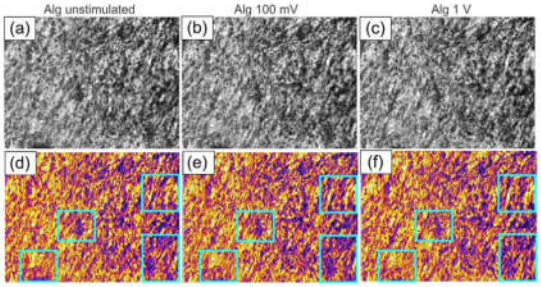

Figure 2. Digital images of pure alginate before (a-c) and after editing (d-f) with ImageJ software. The edited images represent the gel at three different conditions, as follows: unstimulated condition (a and d) and under influence of electric potential at 100 mV (b and e) and 1 V (c and f). The lighter areas (yellow) represent surface regions while the darker areas (purple) represent the deepest regions of the gel. The electrical stimulation induced a discrete motion in the gel mesh. It is possible to observe this phenomenon in highlighted areas (blue cyan rectangles).

Electrochemical impedance spectroscopy analysis

The Nyquist plot (–Z'' *vs.* Z') of the three NeoLipoAlg conditions are shown in Figure 3. In general, the plots present two well-defined regions: a semicircle at high frequencies and non-vertical spike at lower frequencies. The semicircle formation is associated with the bulk effect of electrolytes whereas a non-vertical spike can be attributed to the polarization of the electrode-electrolyte interface. Since Alg and Neo are highly conductive, the semicircle formation was not fully formed. The bulk resistance was obtained from the intersection of the high frequency impedance semicircle with the real axis (Z').[29,30]

We observed that a reduction in the real part of the impedance varies inversely with values of external DC polarization. Real values of impedance (Z') are lower due to the higher rate of Neo release (Z' 1 V < Z' 100 mV < Z' unstimulated condition). It was observed that gradual decrease in the magnitude of impedance with increasing time resulted in a reduction of characteristic semicircle in the Nyquist diagram. The bulk electrical response was dependent on the amount of dispersed analytes.[31]

Equivalent circuit

Detailed information about impedimetric spectra can be obtained using equivalent circuit. Impedimetric results were fitted using a modified Randles circuit (Figure 4), which consists of ohmic resistance of the solution (Rs) assigned to the ion migration in the solution (bulk resistance). Rct is associated with resistance for electric current transportation in the electrode/solution interface. The capacitance of the double layer (Cdl) represents the ability to store charge in the electrode and constant phase element (Cpe) introducing additional mechanisms that

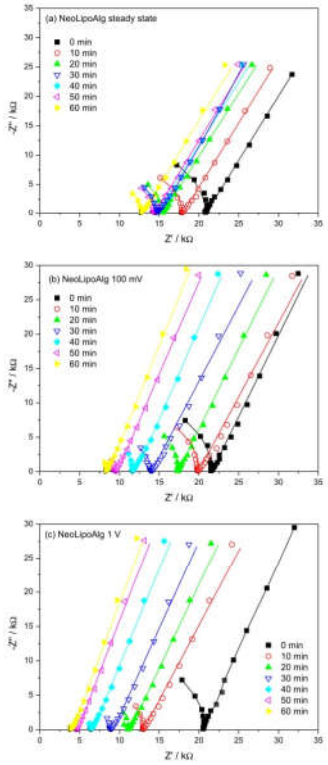

Figure 3. Nyquist diagrams of NeoLipoAlg at different conditions: (a) unstimulated, (b) 100 mV and (c) 1 V. The results were recorded every 10 min during a maximum period of 1h.

contributes with a depressed semicircle response such as diffusion.[32,33]

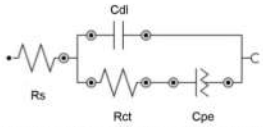

Figure 4. Equivalent circuit adopted to fit the impedance data.

Fitted curves exhibited an excellent agreement with experimental impedance plots. Parameters calculated from the fitting are shown in Table S1. As explained before, a notable Rct decrease was observed for all experiments and the impedimetric response of NeoLipoAlg at 100 mV and 1 V was more pronounced than at unstimulated condition. In addition, the obtained response can be explained by different conditions of the interaction between the polymer and water resulting in degradation, passive diffusion and electric induction of the drug.[8,34]

The impedimetric response of NeoLipoAlg at unstimulated condition in a period of 1 h has no statistical significance if compared to an external excitation of 100 mV ($p = 0.0966$). Significant Rct values ($p = 0.01401$) are observed at high potential values (1 V). The Rct curve showed a similar behavior during the first 20 min for all analyzed systems (Figure 5).

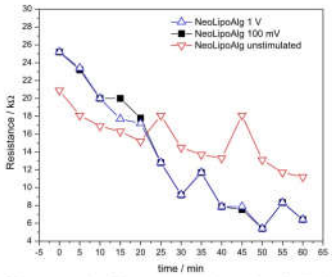

Figure 5. Representation of the resistance values *vs.* time for NeoLipoAlg systems at unstimulated condition, 100 mV and 1 V conditions.

NeoLipoAlg resistances at 100 mV and 1 V were significantly reduced ($p = 0.0032$ for both conditions) compared to the unstimulated condition, which means that the resistivity decreases while the capacitance increases.

Conclusions

The electro-responsive property of the gel contributed to its induced movement and drug controlled release. The drug release kinetic profile was characterized as a superposition of both Fickian diffusion and case-II transport. The degree of drug release was directly dependent on the electro-stimulation. Our results suggest that EIS can be an additional tool to monitor the drug release from polymers in aqueous solution. The solubility, swelling, electro-responsiveness and diffusion of the drug through the hydrogel matrix contributed to a gradual drug release with potential use for *in vivo* applications.

Supplementary Information

Supplementary data are available free of charge at http://jbcs.sbq.org.br as PDF file.

Acknowledgements

The authors are grateful for the support provided by FACEPE, CNPq and Rede de Nanobiotecnologia/CAPES. C. A. S. Andrade and M. D. L. Oliveira are also gratefully for CNPq financial support (grants 310305/2012-8 and 310361/2012-5, respectively). R. R. Silva would like to thank FACEPE for PhD scholarship.

References

1. Jones, D. S.; Lorimer, C. P.; McCoy, C. P.; Gorman, S. P.; *J. Biomed. Mater. Res., Part B* **2008**, *85*, 417.
2. Kushwaha, S. K.; Saxena, P.; Rai, A.; *Int. J. Pharm. Invest.* **2012**, *2*, 54.
3. Dumville, J. C.; O'Meara, S.; Deshpande, S.; Speak, K.; *Cochrane Database Syst. Rev.* **2003**, CD009110.
4. Miguel, S. P.; Ribeiro, M. P.; Brancal, H.; Coutinho, P.; Correia, I. J.; *Carbohydr. Polym.* **2014**, *111*, 366.
5. Kataoka, K.; Suzuki, Y.; Kitada, M.; Ohnishi, K.; Suzuki, K.; Tanihara, M.; *J. Biomed. Mater. Res.* **2001**, *54*, 373.
6. Zvitov, R.; Nussinovitch, A.; *Food Hydrocolloids* **2003**, *17*, 255.
7. Kulkarni, R. V.; Setty, C. M.; Sa, B.; *J. Appl. Polym. Sci.* **2010**, *115*, 1180.
8. Ko, Y. G.; Lee, H. J.; Chun, Y. J.; Choi, U. S.; Yoo, K. P.; *ACS Appl. Mater. Interfaces* **2013**, *5*, 1122.
9. Lee, W. R.; Park, J. H.; Kim, K. H.; Kim, S. J.; Park, D. H.; Chae, M. H.; *Wound Repair Regen.* **2009**, *17*, 505.
10. Rao, K. M.; Rao, K. S. V. K.; Ramanjaneyulu, G.; Rao, K. C.; Subha, M. C. S.; Ha, C.-S.; *J. Biomed. Mater. Res., Part A, in press*, DOI: 10.1002/jbma.34991.
11. Gao, W.; Vecchio, D.; Li, J.; Zhu, J.; Zhang, Q.; Fu, V.; *ACS Nano* **2014**, *8*, 2900.
12. Akbarzadeh, A.; Rezaei-Sadabady, R.; Davaran, S.; Joo, S. W.; Zarghami, N.; Hanifehpour, Y.; *Nanoscale Res. Lett.* **2013**, *8*, 102.

13. Brewer, N. S.; *Mayo Clin. Proc.* **1977**, *52*, 675.
14. Saidkarimov, S.; *Antibiotiki* **1962**, *7*, 339.
15. Rathore, N.; Qi, W.; Ji, W.; *Biotechnol. Prog.* **2008**, *24*, 684.
16. Delie, F.; Gurny, R.; Zimmer, A.; *Biol. Chem.* **2001**, *382*, 487.
17. Mondal, N.; Pal, T. K.; Ghosal, S. K.; *Acta Pol. Pharm.* **2009**, *66*, 11.
18. Lasia, A.; *Electrochemical Impedance Spectroscopy and Its Applications*, vol. 32, 1st ed.; Springer: New York, 2002.
19. Bard, A. J.; Faulkner, L. R.; *Electrochemical Methods: Fundamentals and Applications*, vol. 2, 2nd ed.; Wiley: New York, 1980.
20. Oliveira, M. D.; Franco, O. L.; Nascimento, J. M.; de Melo, C. P.; Andrade, C. A.; *Curr. Protein Pept. Sci.* **2013**, *14*, 543.
21. Dash, S.; Murthy, P. N.; Nath, L.; Chowdhury, P.; *Acta Pol. Pharm.* **2010**, *67*, 217.
22. Hernández-Caselles, T.; Villalaín, J.; Gómez-Fernández, J. C.; *Mol. Cell. Biochem.* **1993**, *120*, 119.
23. Ogiso, T.; Yamaguchi, T.; Iwaki, M.; Tanino, T.; Miyake, Y.; *J. Drug Targeting* **2001**, *9*, 49.
24. Dash, S.; Murthy, P. N.; Nath, L.; Chowdhury, P.; *Acta Pol. Pharm.* **2010**, *67*, 217.
25. Fu, Y.; Kao, W. J.; *Expert Opin. Drug Delivery* **2010**, *7*, 429.
26. Murdan, S.; *J. Controlled Release* **2003**, *92*, 1.
27. Narashimhan, B.; Mallapragada, S. K.; Peppas, N. A.; *Encyclopedia of Controlled Drug Delivery*, vol. 2; Wiley: New York, 1999.
28. Hadjiioannou, T. P.; Christian, G. D.; Koupparis, M. A.; Macheras, P. E.; *Quantitative Calculations in Pharmaceutical Practice and Research*; VCH Publishers: New York, 1993.
29. Kurzawa, M.; Jastrzębska, A.; Szłyk, E.; *Chem. Pap.* **2009**, *63*, 255.
30. Sheybani, R.; Cabrera-Munoz, N. E.; Sanchez, T.; Meng, E.; *Conf. Proc. IEEE Eng. Med. Biol. Soc.* **2012**, 519.
31. Shi, X.; Zheng, Y.; Wang, G.; Lin, Q.; Fan, J.; *RSC Adv.* **2014**, 1.
32. Katz, E.; Willner, I.; *Electroanalysis* **2003**, *15*, 913.
33. Lima, S. V.; Oliveira, H. P.; *Quim. Nova* **2010**, *33*, 1928.
34. Jarek, S.; Thonstad, J.; *J. Appl. Electrochem.* **1987**, *17*, 1203.

Submitted: August 10, 2015
Published online: September 25, 2015

ANEXO D - ARTIGOS PUBLICADOS DURANTE O DOUTORADO

Hindawi Publishing Corporation
Journal of Sensors
Volume 2015, Article ID 913640, 16 pages
http://dx.doi.org/10.1155/2015/913640

Hindawi

Research Article

Trends in Biosensors for HPV: Identification and Diagnosis

Isaac A. M. Frías,[1] Karen Y. P. S. Avelino,[2] Rafael R. Silva,[3] César A. S. Andrade,[2,3] and Maria D. L. Oliveira[2]

[1]*Programa de Pós-Graduação em Ciência de Materiais, Universidade Federal de Pernambuco, 50670-901 Recife, PE, Brazil*
[2]*Departamento de Bioquímica, Universidade Federal de Pernambuco, 50670-901 Recife, PE, Brazil*
[3]*Programa de Pós-Graduação em Inovação Terapêutica, Universidade Federal de Pernambuco, 50670-901 Recife, PE, Brazil*

Correspondence should be addressed to César A. S. Andrade; csrandrade@gmail.com

Received 2 April 2015; Revised 21 June 2015; Accepted 5 August 2015

Academic Editor: Michele Giordano

The conventional methodologies used for the detection of human papillomavirus (HPV) present actually robust and reproducible advantages. However, at the same time, they involve complex protocols that sometimes are difficult to popularize. Over the first half of XX century, the adequate treatment of complex and delicate processes from a simple instrumental base seemed a fundamental and intrinsic contradiction. However, interdisciplinary trends have allowed the manipulation of tissues, proteins, and nucleic acids through innovative increasingly smaller devices. The proper diagnosis of HPV has seen great advances since biosensor researchers are employing its virus strains as models to study the interactions between the biorecognition element and the transducer. Additionally, all recent improvements and trends that material sciences, biotechnology, and data processing scientists excel for biosensors can be applied for the HPV detection platforms. In this review, we highlight the recent trends on materials, nanomaterials, and transducers for the specific detection and differentiation of HPV strains. The most influential methods for the detection and identification of these papillomaviruses include optical, electrochemical, and piezoelectric transducers; we will visit their sensibility and advantages. Additionally, we highlight the factors that contributed to the increasing importance of these biodevices as potential substitutes to conventional diagnostic methods.

1. Introduction

Perplexing as it may seem, the cancer research community has significantly underappreciated the enormous amount of cancer cases caused by viral infections [1], mostly because it is known that just a small proportion of humans infected with any of the oncogenic viruses will develop tumors. In the last century, at least seven human viruses have been pointed as the cause for 10–15% of worldwide human cancers cases [2]. Cancers are serious public health concerns in the developed countries and, for sure, most of aggressive cases could be avoided in first place by preventing the initial infection. Behavioral changes and vaccination, as well as the early screening of precancerous lesions, have shown to be plausible palliatives to prevent the disease.

At first glance, human papillomavirus (HPV) viruses may sound like an evolutionary machinery programmed to cause cancer; however, from the 150 HPV genotypes that have been already identified, only about a dozen are high-risk or oncogenic types [3, 4]. A routine practice in the medical community consists in the association of major risk factors to cancer incidences. Tobacco and alcohol consumption are regularly associated to oropharyngeal cancer as much as sexual behavior risk is assigned to anogenital cancer. However, the astonishing proportion of confirmed presence of viruses on healthy individuals that have never had those risk factors is overwhelming [5]. Although most patients infected by HPV can spontaneously eliminate the virus by their own immune system [6], some individuals can remain asymptomatic by maintaining the virus in latent form and some other immunocompromised patients may present recurrent infections [7]. Several factors such as the lesion type, size, spread, and localization will establish the risk level of the infection and will help to endorse the correct treatment.

Conventional treatments have different effectiveness levels and are selected according to the patient tolerance. Some

of the leading conventional methods include chemotherapy [8, 9], immunotherapy [10], surgery [11], or the collective application of these techniques [12, 13]. Additionally, nanoparticle based delivery of anticancer drugs and therapeutic vaccines have increased the treatment efficacy while simultaneously decreasing the side effects of the traditional therapeutics [14]. The occurrence of visible epidermal manifestations as warts or condylomas is one of the symptoms of HPV infection; however, since only 1% of infected patients present the symptomatology, the diagnosis is difficult [15, 16]. The identification of the disease in these asymptomatic cases requires specialized equipment to carefully search for internal lesions at the mucous membranes. In cases of proven cervical injury, a routine cytological analysis known as Papanicolaou test is performed over a local biopsy for histopathological analysis [17, 18]. Beyond visual and cytological identification, molecular diagnosis is taking over as an essential method for the accurate differentiation between HPV strains, which are categorized with respect to their potential for low, intermediate, or high oncogenic risk.

Since all HPV strains are related, researchers have battled to understand and find the characteristics that differentiate every discovered strain. Often the distinction relies on the peculiar metabolism that a particular strain endures. The most common ways to differentiate the HPV involve the analysis of the protein expression ratio that provides a molecular fingerprint of the oncogenic potential within a histopathological sample [19, 20]. Considering the fact that some HPV strains are more related between them than to the others, DNA analyses are often required for the accurate identification of the strain. DNA analyses are quite heterogeneous and are based on the complementarity principle of the DNA strands. For instance, we can identify the target amplification of a precise fragment of nucleic material by the polymerase chain reaction (PCR) and by signal amplification of an oligonucleotide hybridization assay [21, 22]. Although PCR associated techniques present high rates of sensitivity and specificity, most of these techniques are mainly used by research centers and/or specific health services. Some of the reasons include the time consuming and complex protocols that usually require specialized skills for the correct operation of the instruments and fulfillment of the methods [23].

Fortunately, the research on cancer has reached a maturity level of awareness that allows the population to realize that viruses are in fact the cause of a great proportion of cancers. The alarming discovery that certain high-risk strains of HPV caused assured 100% of invasive cervical cancer has instigate a global awareness about cervical cancer prevention and, most essentially, the development of other cancers prophylactic vaccines [24]. Regular vaccines use viral vectors to promote immune response, and, more recently, DNA vaccines have been developed to control tumor-expressed antigens [25]. The employed plasmid vectors are safe and present low immunogenicity, so they can be constantly administered. Further researches have been demonstrated to increase their efficiency by designing nanometrical delivery systems as nanoparticles, micelles, and fibers [26].

After HPV16 and HPV18, 10 more HPV strains are known to cause cervical carcinomas [61]. Some researchers have reached a milestone, where the precise identification of HPV types has become extremely important. They propose to follow the ecological competitive exclusion principle to create an artificial substitution of high-risk HPV types for those of reduced risk [3]. In addition, the detailed identification of all different strains within a sample is of great importance to epidemiological studies and involves major and interesting new obstacles to overcome, for example, the correct identification of HPV strains that are known to be genetically close related like HPV6 and HPV11.

Because of the large amount of different HPV types, it is reasonable to think that the current competence of vaccine design technology is insufficient to provide enough protection. Despite the fact that the research on individual strains proceeds slowly, the research on biosensors has not delayed its development. Nowadays, biosensor researchers have more tools to design better techniques to apply and help to control viral epidemics. Live vectors characterization, peptide/protein expression and interaction, DNA vaccine design, and whole cell-based treatment approaches [62] are some of the explored topics that are applied on viral sensing and detection. In the case of genosensors, as much as the genomic databases improve, cancers will be easier to detect and diagnose.

2. Biosensors for HPV as Alternative Diagnostic Tools

Over the years, the progress of biotechnological research has contributed to the development of biologic sensor devices [63, 64]. Biosensors are portable analytical devices constituted by at least one biological molecule. The strategies to obtain these biosensors combine the specificity of the biological probe with the analytical capacity of the transduction methods [65, 66]. In addition, materials at the nanometer scale as nanoparticles [67], nanotubes [28], nanofibers [68], and nanocomposites [69] have been used to achieve the nanostructuration of these devices. The diversity of structures provides tailored interfacial modification alternatives with the purpose of amplifying the analytical signal and increasing the sensibility of the biosensor [63]. The challenge to construct these nanometrical systems relies in the need to preserve the biological activity of the probe as well as the transducing activity of the nanostructure [70]. For these reasons, a detailed study of the physical-chemical properties of both constituents should be performed.

The device requires the efficient immobilization of antibodies, peptides, aptamers, or nucleic acids over the surface of a transducer, which are responsible for the analyte recognition and will execute a measurable response signal proportional to the analyte concentration [71–74]. Besides covalent functionalization of nanoparticles (known for allowing a strong and controlled immobilization of the probe over the surface of the sensor), most immobilization strategies involve simple methods. In general, mixtures or emulsions of two or more materials previously known for their individual properties are performed, for example, nanoparticles

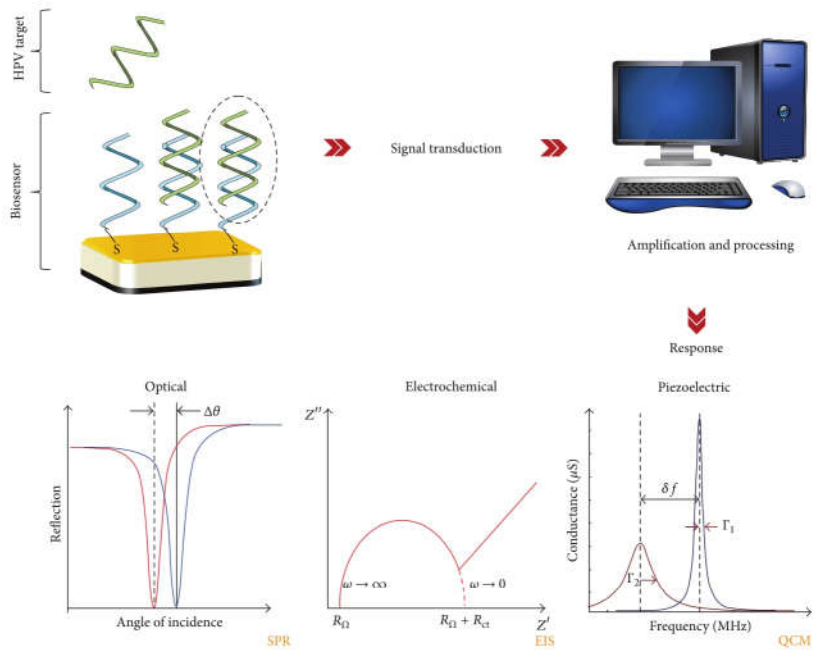

FIGURE 1: Schematic representation of a biosensor developed to detect HPV. The response arising from the biospecific interaction between the oligonucleotide probe and the HPV target DNA will be transduced into a measurable signal, which will be amplified and processed by computer software. The main types of signal transduction methods used in biosensors for HPV are optical, electrochemical, and piezoelectric. In addition, the signal conversion can be accomplished through SPR, EIS, and QCM techniques [31, 70, 103].

of biodegradable polymers as poly(lactic acid), poly(D,L-glycolide), and chitosan, among others, which are conjugated with biorecognition drugs as therapeutic cancer vaccine formulations [75, 76]. As another example of versatility, we find magnetic nanoparticles. These nanomaterials have been conjugated with an enormous amount of fluorescent dyes, polymeric matrixes, and biologic macromolecules, among others, to provide the magnetic property to innumerous *in situ* HPV biosensor applications [77, 78].

The incursion of nanotechnology into biology has been catalyzed by the positive and important role that analytical methodologies and automation have over the equipment efficiency and effectivity, thus allowing the rapid progression of sensor systems [63, 79]. Nowadays, we are presented with innumerous types of transducers that can be used for the construction of biosensors, and according to the physical principle of transduction, we find it easy to classify them into electrochemical, optical, piezoelectric, and magnetic [72, 73, 80, 81]. Along with a representation of a generic biosensor constructed for HPV detection, we show in Figure 1 the main signal transduction methods currently used.

Compared to the conventional identification techniques, the biosensors dedicated to the molecular diagnosis and detection of HPV strains prove themselves less complicated and exempt from prolonged experimentation processes and purification requirements [35, 38, 68]. The interest towards biosensors is growing due to the broad potential that these devices provide in terms of high sensitivity, simplicity, low cost, and small sample volume requirement. The amount of recent publications in biosensors is the proof of the interest that researchers have in the development of effective and stable sensor platforms for application in clinical analysis [82, 83]. In this review, we will provide an overview of the trends and advances in the field of biosensors developed for the diagnosis and detection of HPV. We will compare the detection limits obtained for each transduction technique and the convenience of their use.

2.1. Electrochemical Biosensors. The improvement on electrochemical biosensors walks along with the advances of analytical chemistry, a science dedicated to measure the

structure, composition, distribution, and interaction of matter. The purpose of the electrochemical research is to design sensitive, selective, and specific detection strategies, measuring principles and analytical methodologies. In addition, the automation processes provided better construction strategies for obtaining biosensors with increased analytical performance [63, 64, 84]. Since Clark and Lyons first developed an electrochemical biosensor for glucose in 1962, this transduction method represents the main class of biosensors reported in the literature and they are by far the most commercially successful [74, 80, 85, 86]. In fact, Vernon et al. developed a bioelectronic detection platform for the detection of multiple HPV types. The design of the model system is structured on gold electrodes where self-assembled monolayers of immobilized oligonucleotides that are specific for HPV genotypes are formed [27].

The electrochemical biosensor is a device composed of a biological recognition element that is associated with an electrochemical transducer capable of providing selective quantitative or semiquantitative analytical information [72, 87]. These biosensors require electroanalytical techniques (such as potentiometry, amperometry, voltammetry, conductometry, and impedometry) [73, 88] to measure the transduced output signal and to characterize the electrochemical changes in the system caused by the molecular recognition process.

As we have already stated, electrochemical biosensors are the most utilized devices for screening and diagnosing clinical analysis [65, 74]. In this sense, we show in Table 1 the trends on electrochemical techniques for biodetection of HPV [35, 38, 68]. The electrochemical biosensors are promising diagnostic techniques for HPV, because of their tendency to miniaturization and due to their fast response, simplicity, and low cost instrumentation [88]. Although the regeneration of the sensor platform might minimize the cost of the analysis, only a few publications report reusable electrochemical biosensors [28, 32].

The actual interest on multiplex assays [31], which refers to the fulfilment of a full range of laboratory tests in the form of a centimeter square microarray, is evident. Also the incorporation of technological advances as microfluidic channels is starting to venture willing to improve the already stablished multiplex assays. The most frequent platform to immobilize the oligonucleotides is a gold electrode, achieving the interaction through thiol-gold covalent bonding. The process can be performed in the presence of a secondary reporter probe (which will serve as a label during the measurement process) as tetramethylbenzidine (TMB), horseradish peroxidase, methylene blue, or hematoxylin providing an amplified electrochemical response combined with greater specificity [29, 31, 32, 36].

Besides the already mentioned gold electrodes, in the last five years, label-free electrochemical microarrays have been used extensively for the detection of different HPV16 antibodies [34, 35, 37, 39]. These label-free platforms are developed through the immobilization of the biorecognition probe atop of an interdigitated gold or platinum electrode. The signal transducers are widely diverse, pencil graphite surfaces [30, 33], carbon surfaces modified with linear polysaccharides [35], plain glassy carbon surface [34], or poly(methylmethacrylate) substrate recovered with a thin gold film [38]. Additionally, more sophisticated nanostructured ones as graphene/gold nanoparticles (AuNPs), nanorod/poly(thionine), or polyaniline-multiwall carbon nanotube (MWCNT) film [39, 68] have been used to construct biosensors committed to detect and differentiate HPV strains. These platforms facilitate the study of the output signal by cyclic voltammetry (CV), square wave voltammetry (SWV) [33, 35], differential pulse voltammetry (DPV) [30, 68], and electrochemical impedance spectroscopy (EIS) [68].

After analyzing the most recent developed electrochemical biosensors for the identification of HPV, we noticed that the sensor platform constructed by Wang et al. holds the lowest detection limit reported in the literature for the DNA of HPV16. Interestingly, the transducer of the platform was designed from single walled carbon nanotube arrays coated with gold nanoparticles, atop of which the self-assembly of single-stranded DNA probe was promoted. Electrochemical impedance was used to verify the high sensitivity, great stability, and good regeneration ability of the biosensor with a detection limit up to one attomole of HPV16 DNA [89].

From the presented alternatives, we highlight the use of nanomaterials, particularly carbon nanotubes and gold nanoparticles, as strategic components to improve the analytical performance of electrochemical biosensors [38, 39, 68, 89]. The cited nanomaterials exhibit not only combined dielectric and optical properties but also a high surface-to-volume ratio, biocompatibility, and high conductivity, allowing direct charge transfer between the biomolecule and the electrode surface [90–92]. Thus, it is possible to obtain biosensors with higher sensibility and ultralow detection limit.

In addition, there is a notable interest on the development of ultrasensitive methods for the detection of particular papillomavirus strains, especially the high-risk associated HPV types 16, 18, and 45 [31, 32, 68]. In spite of these electrochemical biosensors being prototypes and requiring additional studies of reproducibility, stability, and validation, they show potential to become valuable alternatives or even the new conventional diagnostic methods [93].

2.2. Optical Biosensors. Visual differentiation techniques are widely spread over important areas of modern life like food safety, security, and environmental monitoring, in medicine and, of course, in HPV detection [66]. Several of the first methods to detect diseases and pathological infections were optical based methods. The Papanicolaou test, a worldwide famous cervical cytology exam performed to detect HPV, was developed to exploit optical techniques as microscopy. In recent decades, other optical alternatives in the form of optical biosensor, also named *optrodes*, have grown robust because of the facility to differentiate the positive and negative samples by color changes produced by differential staining and fluorescence labeling [94, 95]. In Table 2, we present the comparison of some features used on recent publications for

Table 1: Electrochemical techniques applied for HPV detection.

HPV type	Sensor platform	Sensing method	Technique	Detection limit	Detection range	Detection time	Reusability	References
21 different types of HPV	Gold surface/capture oligonucleotides	Two hybridization events must occur for electrochemical detection. The first between the capture probe and the target, and the second between an adjacent region of the target and ferrocene labeled signal probe.	CV	—	—	2 to 8 hours	—	[27]
HPV 16	Single walled carbon nanotube arrays/gold nanoparticles/HPV 16 E7 probe	Hybridization between the capture probe and the HPV target (specific to HPV-16, E7 region).	EIS	1aM (Atto molar)	1 aM to 1 μM	2 hours	6 tests	[28]
HPV 16	Gold surface/L-cysteine/HPV 16 oligonucleotide	The measurement was based on the reduction signals of methylene blue (MB) before and after hybridization between the probe and the synthetic target or extracted DNA from clinical samples.	DPV	18.13 nM	18.75 nM to 1000 nM	10 minutes	—	[29]
HPV 16	Pencil graphite surface/HPV 16 E6 probe	The hybridization between the capture probe and the HPV 16 E6 gene was directly detected through guanine oxidation signals.	DPV	16 pg/μL	5 pg/μL to 40 pg/μL	5 minutes	—	[30]
HPV 16 and HPV 45	Gold surface/thiolated HPV 16 E7p and HPV 45 E6 probes	The hybridization was detected by incorporating a horseradish peroxidase- (HRP-) labelled reporter probe that pairs with the target. The 3,3′,5,5′-tetramethylbenzidine (TMB) was used as a chromogenic substrate for enzyme.	CV	490 pM for HPV 16 E7p 110 pM for HPV 45 E6	0.1 nM to 50 nM	1 hour	—	[31]
HPV 16, HPV 18, and HPV 45	Gold surface/oligoethylene glycol-terminated bipodal thiol/thiolated HPV 16 E7p, HPV 18 E6, and HPV 45 E6 probes	The detection was carried with the target hybridized between a surface immobilized probe and a HRP-labelled secondary reporter probe. The TMB was used as a chromogenic substrate for HRP.	CV	220 pM for HPV 16 E7p 170 pM for HPV 18 E6, and 110 pM for HPV 45 E6	0.1 nM to 50 nM	20 minutes	5 tests	[32]
HPV (L1 gene)	Pencil graphite surface/HPV probe	The hybridization between the probe and HPV target was studied by measurement of MB signal accumulated on the pencil graphite electrode.	SWV	1.2 ng/μL	1.2 ng/μL to 50 ng/μL	3 minutes	—	[33]

Table 1: Continued.

HPV type	Sensor platform	Sensing method	Technique	Detection limit	Detection range	Detection time	Reusability	References
HPV 16	Glassy carbon surface/conjugated copolymer poly(5-hydroxy-1,4-naphthoquinone-co-5-hydroxy-2-carboxyethyl-1,4-naphthoquinone)/antigenic peptide L1	Interaction between antigenic peptide L1 and HPV-16 antibody.	SWV	50 nM	—	1 hour	—	[34]
HPV 16	Carbon surface/chitosan/anthraquinone-labeled pyrrolidinyl peptide nucleic acid (acpcPNA) probe	The hybridization with the HPV 16 DNA was studied by measuring the electrochemical signal of the label anthraquinone attached to the acpcPNA probe.	SWV	4 nM	0.02 mM to 12 nM	15 minutes	—	[35]
HPV (L1 gene)	Gold surface/alkanethiol HPV probe	The study was performed based on the interaction of hematoxylin with an alkanethiol DNA probe and its hybridized form.	CV and DPV	3.8 nM	12.5 nM to 400 nM	2 hours	—	[36]
HPV 16	Glassy carbon surface/graphene/Au nanorod/polythionine/HPV 16 probe	Besides the capture probe, two auxiliary probes were designed for the hybridization with HPV DNA. 1,10-Phenanthroline ruthenium dichloride ($[Ru(phen)_3]^{2+}$) was used as the electrochemical indicator.	EIS and DPV	4.03×10^{-14} mol/L	1×10^{-13} mol/L to 1×10^{-10} mol/L	90 minutes	—	[37]
HPV 16	Polymethylmethacrylate substrate/gold nanolayer/4-aminothiophenol/monoclonal antibody (mAb) 5051	Interaction between mAb 5051 and HPV 16.	CV and EIS	—	—	1 hour	—	[38]
HPV 16	Platinum surface/polyaniline-multiwalled carbon nanotube composite/HPV 16-L1 peptide aptamer	Interaction between the antigen peptide aptamer HPV-16-L1 and HPV-16 antibody.	CV and SWV	490 pM	10 nM to 80 nM	15 minutes	—	[39]

Table 2: Optical techniques applied for HPV detection.

HPV type	Sensor platform	Sensing method	Technique	Detection limit	Detection range	Detection time	Reusability	References
HPVs 16, 18, 31, 33, 35	Aqueous solution.	Fluorescent reporter dye covalently linked to the 5′ end, and a quencher dye linked to the 3′ end.	Fluorescence PCR.	Differential detection of samples mimicking mixed infections up to 1% of the total DNA.	10^1–10^6 DNA copies.	75 minutes after DNA extraction and preparation of PCR solutions.	—	[40]
Ratios between HPVs 6/11, 16/18, and 31/33/35	*In situ* histological sample.	Fluorescently labeled oligonucleotides with biotin-streptavidin modification.	*In situ* PCR/FISH/LSCM.	1-2 DNA copies.	1 to 50 DNA copies per cell.	Overnight hybridization, no DNA extraction needed.	—	[41]
HPVs 16, 18	*In situ* histological sample.	Oligonucleotides labeled with digoxigenin-11 -dUTP by random priming.	FISH, automatic image cytometry.	1 DNA copy.	1-500 DNA copies per cell.	6 hours after cell culture, no DNA extraction needed.	—	[42]
HPVs 16, 18	Avidin coated (LKB, Sweden) sensor chip.	Biotinylated oligonucleotide bound to oncoproteins.	Plasmon resonance.	0.18 μM.	0.1–4 μM.	—	—	[43]
HPVs 16, 18	Nitrocellulose DNA chip.	Biotin labeled oligonucleotides sandwich of streptavidin to fluorescence dye.	PCR/chromatography fluorescence.	Qualitative.	—	30 minutes.	—	[44]
HPVs 6, 11	DNA amplification.	Oligonucleotides labeled with fluorescent probes optimized for FRET.	Real-time PCR FRET-fluorescence.	25–43 DNA copies.	$1\text{-}3 \times 10^7$ DNA copies.	90 minutes.	—	[45]
13 different types of HPV	Nitrocellulose chip.	Fluorescently labeled oligonucleotides immobilized via biotin-avidin.	PCR amplification.	10–10^2 plasmid copies.	0–10^3 DNA copies.	30 minutes for incubation, 30 seconds for reading.	Lateral flow, 60 tests.	[46]
HPVs 16, 18	Photonic crystal on silicon.	Antibody immobilization.	Optical detection of resonant modes.	1.50 nM.	0–1.5 nM.	16 hours.	—	[47]
HPV 16	CM5 sensor chip (GE Healthcare).	Pairwise antibody footprinting.	SPR.	10 μg/mL.	50–200 μg.	30 minutes.	3 tests.	[48]
24 different types of HPV	Gold chip.	DNA-probe hybridization.	PCR/SPR.	Qualitative.	—	4 hours.	—	[49]
HPV 16	QuantumDot (75 nm)/Maghemite (46 nm).	Oligonucleotides labeled with superparamagnetic nanoparticles and QDs.	Fluorescence spectroscopy.	Qualitative.	—	1 hour.	—	[50]
HPV 16	Silica nanoparticles (75 nM).	Folate functionalization.	Fluorescence microscopy.	Qualitative.	—	15 minutes.	—	[51]

Table 2: Continued.

HPV type	Sensor platform	Sensing method	Technique	Detection limit	Detection range	Detection time	Reusability	References
High risk selector software (HPVs 16, 18)	Fluorescent dyed silica nanoparticles (250 nm).	Biotin-streptavidin sandwich functionalization.	Microarray DNA amplification.	150 pM.	5 pM–10 nM.	3 hours for incubation time after 13 hours of amplification and sample preparation.	—	[52]
HPVs 16, 18	Silica nanoparticles (60 nm).	Biotin-avidin sandwich with oligonucleotides fluorescently labeled.	Fluorescence spectroscopy.	13–15 pmol.	0–0.78 nM.	90 minutes.	—	[53]
HPVs 6, 11, 16, 18	Glass.	Immobilized PCR product, oligonucleotide labelled with gold, silver nanoparticles (15 nM).	Optical signal to background ratio.	0.05 pmol/μL.	0.05–0.50 pmol/μL.	—	—	[54]

*Polymerase chain reaction (PCR), *fluorescent in situ* hybridization (FISH), laser scanning confocal microscopy (LSCM), and fluorescent resonance energy transfer (FRET).

the identification and detection of HPV strains by optical transducers. When applied to conventional methods, fluorescent and color labels provide an upgrade in the analysis of tissue samples, allowing fast and automatized diagnosis based on the differential staining of cancerous cells. A technique frequently employed to diagnose HPV is the fluorescent *in situ* hybridization (FISH); this technique provides the possibility to examine the tissue sample at the same time that the fluorescent label probe signals the specific DNA region for which it was designed.

When PCR assays reached HPV diagnosis [96], the use of fluorescent molecules impelled not only the detection but the quantitation of oncogenic HPV strains by real-time PCR (RT-PCR) [40]. Mostly, fluorescent nanoparticles provide a labeled transduction methodology that has proven to be very useful for the identification of HPV viral genome after PCR amplification [44]. To date, RT-PCR is the only technique capable of identifying closely related HPV strains. The group of Poljack has demonstrated a beautiful use of fluorescence resonance energy transfer (FRET) coupled with RT-PCR to achieve the identification of 19 different HPV strains that are important because of their oncogenic risk [45]. They successfully identified several HPV strains mixed in the same sample, with a presence as low as 25–43 DNA strands per strain. Despite the advances on terms of specificity and sensibility, PCR based methodologies are being rapidly challenge by *optrode* methodologies. Some of these alternative biosensors provide a significant reduction in diagnosis time besides an increased portability and facility of use out of controlled laboratory environment. Although *optrodes* do not hold the lowest detection limit, when they are combined with spectroscopic techniques, they represent one of the methodologies with the highest sensibility. For instance, Li and col. [54] developed a glass chip with immobilized HPVs 6, 11, 16, and 18 oligonucleotides. The hybridized target DNA was labeled with gold and silver nanoparticles besides a fluorescent molecule. Their strategy attained a 0.05 pmol/μL detection limit.

The most common analytical techniques used to measure the transduced signal of optical biosensors include absorption, fluorescence, phosphorescence, Raman, refraction, and dispersion spectroscopies; also, there is surface plasmon resonance (SPR) [97]. Biosensors that make use of the surface plasmonic waves of metallic substrates to detect the interaction between the target analyte and the biorecognition element are actually monitoring the change in the refractive index (RI) at the analyte-sensor interface. The RI changes produce a variation in the propagation constant of the surface plasmon wave that will produce the reading [98]. One of the signatures of SPR is its convenience as a label-free sensing principle, avoiding the use of radioactive and fluorescence markers. Since SPR measures the mass of the material binding to the sensor surface [99], the technique is not suitable for studying small analytes <2 kDa; however, SPR has been proposed as an optimal transducer to identify HPV strains among other viruses [100] based on size and mass differences or as an immunologic methodology. In addition, the proper functionalization of the SPR substrate provides high specificity towards selected HPV strains. Once the substrate is properly functionalized, the methodology can perform several diagnoses and regeneration cycles in a row, resulting in a reduction of time when compared to PCR based methodologies. As an immunologic methodology, SPR achieved the detection limit of 10 μg of HPV16 expressed protein per mL.

The use of fluorescent nanoparticles as transducers requires the synergy between the nanostructure and one or several distinct biological materials as enzymes, nucleic acids, or antibodies to the capsid of the target virus. Some of the most important characteristics of nanoparticles are its surface and then the transduction method that the nature of the nanoparticle involves. In the case of fluorescent nanoparticles, quantum dots (QD) are semiconductor nanoparticles with exceptional optical properties such as fluorescent emission controlled by the size of the nanoparticle. Some quantum dots are assembled as core-shell structures where magnetic core plays an important role in recovering the particles from the sample. Nanoparticles are generally exploited by bioconjugation, that is, by the intelligent mixing of the nanostructure with some biological molecules as DNA or RNA oligonucleotides; this conjugation is made to favor the binding of small oligonucleotides that are complementary to HPV DNA. These kinds of bioconjugated systems have demonstrated to differentiate between HPV16 and HPV18 strains mixed in the same sample [101]. Usually utilized as reporters or signal enhancers [52, 54], nanoparticles are designed based on their combination with another technique. In this manner, silica nanoparticles (SiNPs) are commonly mixed with fluorescent molecules to achieve the prescreening of many HPV genotypes [51]. Nanoparticles can also be covalently linked to oligonucleotides as Yu-Hong and col. described [50]. In their method to detect HPV16, they functionalize QD and magnetic nanoparticles to DNA probes. When both probes attach to a HPV16 DNA specific region, then the labeled DNA responds to an applied magnetic field and, at the same time, presents luminescence from the QD. Even though these kinds of qualitative diagnostic methods are developed to serve a single sample, they are advantageous because they are portable and feature simplified handling.

Fluorescence is an important luminescent property of certain molecules. When fluorescent systems are engineered to recognize a certain HPV strain, not only does the fluorescence of the molecule provide *in situ* evidence of the existence of the expected strain but also its quantification can be easily achieved. An exact amount of energy must be supplied to the molecule so that it can get into the excited state, from which the luminescence will occur. Electromagnetic radiation is the most common way to provide this energy, but there are other quite rare and convenient ways to supply this energy as by heat, by frictional force, and by electron impact or crystallization [102]; all these alternatives are still to be exploited for the specific detection of HPV. For the most part, optical transducers and optical biosensors are gaining research interest; actually, Qiagen N.V., a molecular diagnostics company, has developed and commercialized the first molecular diagnostic to screen for high-risk HPV strains designed for low-resource clinical settings [103].

Table 3: Piezoelectric biosensors for HPV detection.

HPV type	Sensor platform	Techniques	Application	Sensibility	Detection limit	References
HPVs 6, 11, 16, 18	HPV probes with a disulfide group	QCM	Qualitative results from QCM versus dot-blot hybridization	25 μM of predigested PCR products	$-\Delta F = 48 \pm 5$ Hz	[55]
HPVs 16, 18	Biotinylated HPV probes via streptavidin anchoring	QCM	Simultaneous identification and genotyping HPVs 16 and 18	50 nM of PCR products	$-\Delta F = \leq 3$ Hz	[56]
HPVs 6. 11	HPV probes	QCM	Detection of single strand-PCR products in temperature changes by metal clamping piezoelectric sensor	25 μM	$-\Delta F = 82 \pm 3.7$ Hz	[57]
HPV 58	Biotinylated LAMP HPV products via avidin anchoring	LAMP-QCM	Real-time amplification and hybridization to HPV 58 probe	1–10^6 plasmid clones	$\Delta F = 28.3$ Hz	[58]
11 different types of HPV	Biotinylated HPV probes via avidin anchoring	QCM	QCM sensor replacement of traditional method, HPV detection in gel electrophoresis for QCM system	10^3 plasmid clones	$\Delta F = 44.7$ Hz	[59]
HPV 16	Alkanethiol self-assembling monolayer	QCM-D	Detection of antigens (cytoplasmic proteins) from cancer cell lines by HPV	Bayesian classifier dependent		[60]

*Loop-mediated isothermal amplification (LAMP).

2.3. Piezoelectric Biosensors. The recent success in the molecular diagnosis of HPV by electrochemical and optical transducers based on the sequence-specific detection of nucleic acids (DNA or RNA) encouraged the development of diagnostic tools based in other novel transducer methods as the piezoelectric biosensors. Biosensors are important alternatives to the conventional molecular biology techniques like the blotting methods, because they hold associated advantages in terms of cost, run time, and real-time monitoring [104]. Piezoelectric biosensors exploit a secondary but not less important aspect of the electrochemical biosensor, the gravimetric analysis of the biosensor surface. In each electrochemical reaction, mass changes occur as material is deposited or lost from the surface of the transducer, and the monitoring of these changes simultaneously with the electrochemical response provides the piezoelectric biosensor with clear advantages over the electrochemical biosensor alone. These gravimetric transducers have shown to be able to achieve good sensitivity and specificity for the target molecule [105, 106].

The quartz crystal microbalance (QCM) sensors consist of cavity resonators constructed over a piezoelectric crystal substrate, which will accumulate electrical charge in response to the applied mechanical stress. The most common method to immobilize the biocompatible layer is achieved by the physical adsorption of the biological probe over the quartz balance; this kind of nonspecific interaction results in the strong collective action of a large number of relative weak bonding interactions. However, the recent trend for the use of QCM biosensors for the detection of HPV viruses prefers a more specific strategy of immobilization involving biotinylated HPV probes. In Table 3, we present the comparison of some features used in recent publications for the identification and detection of HPV strains by piezoelectric transducers.

The specificity of the biotin/streptavidin bonding is used in conventional assays as the enzyme-linked immunosorbent assay (ELISA). The binding mechanism between biotin and streptavidin results in long-term stable anchoring [107]. Dell'Atti et al. developed a biosensor based on such processes of immobilization for the recognition of HPV 16 and 18 types. Their methodology allowed monitoring real-time hybridization by frequency changes, which resulted in HPV type differentiation. They achieve the identification within a 50 nM detection limit of PCR-amplified short DNA strands. Furthermore, the stability of the probe-surface interaction allowed the regeneration of the system up to fifteen times without losing sensitivity [56]. Moreover, this technique presented some advantages over conventional molecular techniques that require many steps to achieve the same result [108, 109].

Fu et al. have constructed one of the first HPV genosensors based on QCM piezoelectric. This group aimed at the detection and identification of HPV types 6, 11, 16, and 18 from pathologic biopsy samples. The strategy involved the adsorption of HPV oligonucleotides functionalized with disulfide groups atop the surface of a QCM disc. The system presented high sensibility (up to 95%), which is comparable to the result obtained by the combination of PCR and dot-blot technique [55, 110]. This label-free technique offers some benefits like rapidness, convenience, low cost, and feasible multiple sensors building on several QCM plates [103].

One important aspect that is relevant for the correct use of DNA based QCM piezoelectrics is temperature. Maintaining a constant temperature during the formation of the biocompatible layer has been shown to influence its eventual thickness. As a result, the frequency pattern of the samples is modified as well [111]. Consequently, the complementary principle of nucleic acids allows real-time monitoring of the hybridization processes that result from the change in

oscillation frequency of the QCM system after the double strand is formed [57, 112, 113]. Chen et al. [57] demonstrated that by maintaining the PCR products (amplicon) at low temperatures (~4°C) they could avoid the self-hybridization of DNA, resulting in a diagnosis with increased sensibility and accuracy.

Because of the deep impact that temperature has over the stability of the resonance frequency, techniques that depend on thermal cycling are severely limited. For this reason, alternatives that provide the amplification of a genomic region at constant temperature have been of great advantage. Loop-mediated isothermal amplification (LAMP) has adhered to QCM piezoelectrics with tremendous success. LAMP provides genomic amplification with high sensitivity, specificity, and rapidity [114]. Recently, Prakrankamanant et al. developed a prototype system to monitor the differences in the resonance frequency by QCM-LAMP to detect the high-risk strain HPV 58. The amplicon obtained by LAMP was biotinylated and then anchored to the avidin-coated surface of the sensor platform. Differently from conventional LAMP, the incorporation of QCM real-time monitoring system allowed a rapid and quantitative detection of HPV [58].

The same research groups aimed to increase the scope of their biosensor by immobilizing biotinylated probes for 11 high-risk types of HPV. This technique showed good accuracy for all probes with sensitivity up to 10^3 copies/μL; their results are showed to be comparable to coupled PCR amplification and electrophoresis based analysis. Although the operational time of QCM-LAMP is similar to the conventional PCR/electrophoresis technique, the QCM prototype stands out since no labeling is required and because the constant system temperature is close to 4°C. For certain, this new tool represents a milestone for piezoelectric biosensors and opens the path to complement the exploration of the interactions occurring on top of the electrochemical biosensor [59].

As an alternative to the previously described DNA biosensors, Mobley et al. used a different approach for the QCM piezoelectric technique; it is by the dissipation frequency monitoring (QCM-D) instead of the resonance frequency. Commonly applied in the fields of biophysics, biomaterials, cell adhesion, and drug discovery, this interfacial acoustic technique is a special type of QCM that serves to analyze the thickness of a film in a liquid environment [60]. In their study, they attained to distinguish between HPV-positive and HPV-negative cells based on antigen protein expression from a prelysed cancer cell line. Furthermore, their theoretical guidelines, based on linear discrimination, were useful for the analysis of the output signals of other immunosensor platforms and for the diagnosis of diseases. However, these models still require standardization to validate their results.

2.4. Magnetic Biosensors. Biosensors based on magnetic materials have presented a distinctive alternative to identify and diagnose diseases. The response signal occurs in a similar fashion than in other transducers; at the surface of the magnetic material, there is a specific biological probe immobilized and ready to interact with its counterpart found on a sample suspected to contain biologic traces of HPV. Not only have these methodologies allowed the physical separation of the substrates by magnetic field, but also there are some magnetic transducers that are able to compete with the specificity and sensibility threshold that optical transducers might detent in terms of quantification of the transduced signal [115–117].

Throughout Section 2, we have given several examples about how magnetic materials are employed in the form of nanoparticles to provide, not only but mostly, their magnetic characteristic in order to physically separate the functionalized magnetic beads from the working solution. However, over the last decade, magnetoresistive materials have been explored in the form of multilayered films (alternating layers of magnetic and nonmagnetic materials) or granulated substrates (magnetic islands inserted into a nonmagnetic material) to determine the advantages of their use as transducer materials in biosensors. In simple words, the magnetoresistance effect occurs when, under the presence of a magnetic field, the magnetic material experiences a change in its global electrical resistance.

These materials are very susceptible to magnetic fields; for this reason, even a 10 nm size magnetic nanoparticle might create a measurable signature of its close proximity to the magnetoresistive substrate [118], and actually this is the sensing principle behind its known great sensibility.

In spite of the novelty of the methodology, there are few reports about its use in the detection of HPV [119]. For instance, Xu et al. developed a multilayered system for the selective detection of HPV 16, 18, 33, and 45 subtypes. The respective DNA probes were immobilized over the surface of the biosensor to propitiate the capture, by hybridization, of the complementary targeted DNA (if present on the sample); the methodology of immobilization follows the trend used in other transducers (Figure 2).

To immobilize the probe on the surface, the interaction between amine and carboxylic acid groups is used, while the target DNA is functionalized at the loose end with biotin. To quantify the amount of hybridized target DNA, the biosensor is then exposed to magnetic nanoparticles that will bind to the biotin, because they were previously functionalized with avidin. Finally, the close presence of the magnetic nanoparticles interferes with the magnetoresistive material, creating a response signal equivalent to the amount of hybridized target DNA. This methodology was able to reach 90% of accuracy and a sensitivity around 10 pM of target DNA; in addition, the development of these biodevices presents low cost, rapid detection, and reliability [120].

3. Conclusion

The proper diagnosis of HPV infection is essential for the prevention of cervical cancer. The implementation of effective therapeutic strategies requires the development of biosensors for the detection and identification of HPV types. To this date, optical, electrochemical, and piezoelectric materials are the main transducers used to develop biosensors. Among

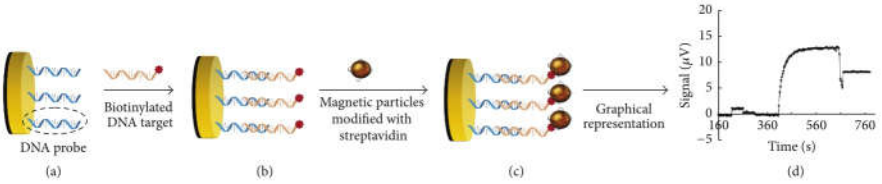

FIGURE 2: Schematic representation of a magnetic genosensor for the detection of HPV. The DNA probe was immobilized on the transducer surface (a). Then, biotinylated DNA target was hybridized (b). Magnetic particles modified with streptavidin were added on the genosensor (c). Measuring the magnetic signal could characterize the bioactivity of biodevice (d). It is important to highlight that the magnetic signal intensity is proportional to the number of biospecific interactions between the streptavidin molecules and the biotin groups.

the most sensitive techniques available to study the biorecognition activity of the sensors, we highlight the fluorescent spectroscopy, EIS, and QCM.

We notice a rapid growth in technological improvements for the development of simple, cost-effective, and accurate rapid diagnostic tests. The sensitivity and detection limit are essential parameters for the evaluation of these biodetection methodologies. However, other characteristics as the specificity, propensity to cross-binding interference, experimental simplicity, and cost should be considered. For instance, it was verified that the use of nanostructures (as carbon nanotubes and gold nanoparticles) enables the construction of electrochemical biosensors with lower detection limits. Notwithstanding, improvements in the design and manufacturing should be considered to achieve the commercial incursion of these devices, since their reuse is limited.

The ability to fast regenerate the substrate after a diagnosed sample is of great importance and affects directly the cost of the methodology. In this sense, QCM and nitrocellulose substrates have managed to get more than 10 diagnoses without losing sensibility; also, microfluidics are helping to create in-flow diagnostics to first allow the sensing to occur, quickly wash the substrate, and then offer a new sample to diagnose.

Thus, future researches should explore new strategies to enhance the immobilization and to increase the stability of bioreceptors. The development of methodologies that facilitate the use of biosensors out of controlled laboratory environment is of great importance for the popularization of these methodologies. Furthermore, evaluating the performance of the biosensors by facing real samples, such as blood and other body fluids, will verify the real potential of these new molecular methods to confirm the clinical diagnosis of HPV.

Conflict of Interests

The authors declare that there is no conflict of interests regarding the publication of this paper.

Acknowledgments

The authors are grateful for the support provided by the Brazilian National Council for Scientific and Technological Development (CNPq Grants 310305/2012-8 and 310361/2012-5), Fundação de Amparo à Ciência e Tecnologia do Estado de Pernambuco (FACEPE), and Rede de Nanobiotecnologia/CAPES. Silva and Morales would like to thank FACEPE and CAPES for their respective scholarships.

References

[1] P. S. Moore and Y. Chang, "Why do viruses cause cancer? Highlights of the first century of human tumour virology," *Nature Reviews Cancer*, vol. 10, no. 12, pp. 878–889, 2010.

[2] D. M. Parkin, "The global health burden of infection-associated cancers in the year 2002," *International Journal of Cancer*, vol. 118, no. 12, pp. 3030–3044, 2006.

[3] J. E. Tota, A. V. Ramanakumar, M. Jiang et al., "Epidemiologic approaches to evaluating the potential for human papillomavirus type replacement postvaccination," *American Journal of Epidemiology*, vol. 178, no. 4, pp. 625–634, 2013.

[4] M. Schmitt, B. Dondog, T. Waterboer, M. Pawlita, M. Tommasino, and T. Gheit, "Abundance of multiple high-risk human papillomavirus (HPV) infections found in cervical cells analyzed by use of an ultrasensitive HPV genotyping assay," *Journal of Clinical Microbiology*, vol. 48, no. 1, pp. 143–149, 2010.

[5] A. R. Kreimer, A. Villa, A. G. Nyitray et al., "The epidemiology of oral hpv infection among a multinational sample of healthy men," *Cancer Epidemiology Biomarkers & Prevention*, vol. 20, no. 1, pp. 172–182, 2011.

[6] I. Frazer, "Correlating immunity with protection for HPV infection," *International Journal of Infectious Diseases*, vol. 11, supplement 2, pp. S10–S16, 2007.

[7] O. Aynaud, D. Piron, R. Barrasso, and J.-D. Poveda, "Comparison of clinical, histological, and virological symptoms of HPV in HIV-1 infected men and immunocompetent subjects," *Sexually Transmitted Infections*, vol. 74, no. 1, pp. 32–34, 1998.

[8] W.-Y. Zhu, A. Blauvelt, B. A. Goldstein, C. Leonardi, and N. S. Penneys, "Detection with the polymerase chain reaction of human papillomavirus DNA in condylomata acuminata treated in vitro with liquid nitrogen, trichloroacetic acid, and podophyllin," *Journal of the American Academy of Dermatology*, vol. 26, no. 5, part 1, pp. 710–714, 1992.

[9] K. Niwa, K. Tagami, Z. Lian, J. Gao, H. Mori, and T. Tamaya, "Topical vidarabine or 5-fluorouracil treatment against persistent HPV in genital (pre)cancerous lesions," *Oncology Reports*, vol. 10, no. 5, pp. 1437–1441, 2003.

[10] C.-M. Chuang, A. Monie, C.-F. Hung, and T.-C. Wu, "Treatment with Imiquimod enhances antitumor immunity induced by therapeutic HPV DNA vaccination," *Journal of Biomedical Science*, vol. 17, no. 1, article 32, 2010.

[11] L. O. Sarian, S. F. M. Derchain, L. A. A. Andrade, J. Tambascia, S. S. Morais, and K. J. Syrjänen, "HPV DNA test and Pap smear in detection of residual and recurrent disease following loop electrosurgical excision procedure of high-grade cervical intraepithelial neoplasia," *Gynecologic Oncology*, vol. 94, no. 1, pp. 181–186, 2004.

[12] C. Facchini, G. A. Eremita, and A. Bernabei, "Combination of beta-interferon and laser-CO2 therapy in female HPV genitalis," *Minerva Ginecologica*, vol. 48, no. 9, pp. 345–349, 1996.

[13] P. Nieminen, M. Aho, M. Lehtinen, E. Vesterinen, A. Vaheri, and J. Paavonen, "Treatment of genital HPV infection with carbon dioxide laser and systemic interferon alpha-2b," *Sexually Transmitted Diseases*, vol. 21, no. 2, pp. 65–69, 1994.

[14] J. Chen, W. Gu, L. Yang et al., "Nanotechnology in the management of cervical cancer," *Reviews in Medical Virology*, vol. 25, pp. 72–83, 2015.

[15] K. Morshed, D. Polz-Gruszka, M. Szymański, and M. Polz-Dacewicz, "Human Papillomavirus (HPV)—structure, epidemiology and pathogenesis," *Otolaryngologia Polska*, vol. 68, no. 5, pp. 213–219, 2014.

[16] M. Stanley, "The epidemiology and burden of HPV disease," *Nursing Times*, vol. 104, no. 36, pp. 38–40, 2008.

[17] D. Ertoy Baydar, I. Kulac, A. Ozagari, and G. Guler Tezel, "Occurrence of dysplasia and human papilloma virus typing in penile condylomas," *Urology*, vol. 81, no. 1, pp. 211.e9–211.e15, 2013.

[18] E. Beerens, L. van Renterghem, M. Praet et al., "Human papillomavirus DNA detection in women with primary abnormal cytology of the cervix: prevalence and distribution of HPV genotypes," *Cytopathology*, vol. 16, no. 4, pp. 199–205, 2005.

[19] I. Salimović-Bešić, A. Tomić-Čiča, A. Smailji, and M. Hukić, "Comparison of the detection of HPV-16, 18, 31, 33, and 45 by type-specific DNA- and E6/E7 mRNA-based assays of HPV DNA positive women with abnormal Pap smears," *Journal of Virological Methods*, vol. 194, no. 1-2, pp. 222–228, 2013.

[20] P. G. Rossi, M. Benevolo, A. Vocaturo et al., "Prognostic value of HPV E6/E7 mRNA assay in women with negative colposcopy or CIN1 histology result: a follow-up study," *PLoS ONE*, vol. 8, no. 2, Article ID e57600, 2013.

[21] A. Vince and S. Ž. Lepej, "Diagnostic methods and techniques in cervical cancer prevention Part II: molecular diagnostics of HPV infection," *Medicinski Glasnik*, vol. 7, no. 1, pp. 18–25, 2010.

[22] W. Weichert, C. Schewe, C. Denkert, L. Morawietz, M. Dietel, and I. Petersen, "Molecular HPV typing as a diagnostic tool to discriminate primary from metastatic squamous cell carcinoma of the lung," *The American Journal of Surgical Pathology*, vol. 33, no. 4, pp. 513–520, 2009.

[23] K. D. Tardif, K. E. Simmon, Ø. Kommedal, M. T. Pyne, and R. Schlaberg, "Sequencing-based genotyping of mixed human papillomavirus infections by use of ripseq software," *Journal of Clinical Microbiology*, vol. 51, no. 4, pp. 1278–1280, 2013.

[24] L. Shi, H. L. Sings, J. T. Bryan et al., "GARDASIL: prophylactic human papillomavirus vaccine development—from bench top to bed-side," *Clinical Pharmacology & Therapeutics*, vol. 81, no. 2, pp. 259–264, 2007.

[25] A. Monie, S.-W. D. Tsen, C.-F. Hung, and T.-C. Wu, "Therapeutic HPV DNA vaccines," *Expert Review of Vaccines*, vol. 8, no. 9, pp. 1221–1235, 2009.

[26] A. Tahamtan, A. Ghaemi, A. Gorji et al., "Antitumor effect of therapeutic HPV DNA vaccines with chitosan-based nanodelivery systems," *Journal of Biomedical Science*, vol. 21, no. 1, article 69, 2014.

[27] S. D. Vernon, D. H. Farkas, E. R. Unger et al., "Bioelectronic DNA detection of human papillomaviruses using eSensor: a model system for detection of multiple pathogens," *BMC Infectious Diseases*, vol. 3, article 12, 2003.

[28] S. Wang, L. Li, H. Jin et al., "Electrochemical detection of hepatitis B and papilloma virus DNAs using SWCNT array coated with gold nanoparticles," *Biosensors and Bioelectronics*, vol. 41, no. 1, pp. 205–210, 2013.

[29] D. S. Campos-Ferreira, G. A. Nascimento, E. V. M. Souza et al., "Electrochemical DNA biosensor for human papillomavirus 16 detection in real samples," *Analytica Chimica Acta*, vol. 804, pp. 258–263, 2013.

[30] D. S. Campos-Ferreira, E. V. M. Souza, G. A. Nascimento et al., "Electrochemical DNA biosensor for the detection of human papillomavirus E6 gene inserted in recombinant plasmid," *Arabian Journal of Chemistry*, 2014.

[31] L. Civit, A. Fragoso, and C. K. O'Sullivan, "Electrochemical biosensor for the multiplexed detection of human papillomavirus genes," *Biosensors and Bioelectronics*, vol. 26, no. 4, pp. 1684–1687, 2010.

[32] L. Civit, A. Fragoso, S. Hölters, M. Dürst, and C. K. O'Sullivan, "Electrochemical genosensor array for the simultaneous detection of multiple high-risk human papillomavirus sequences in clinical samples," *Analytica Chimica Acta*, vol. 715, pp. 93–98, 2012.

[33] R. E. Sabzi, B. Sehatnia, M. H. Pournaghi-Azar, and M. S. Hejazi, "Electrochemical detection of human papilloma virus (HPV) target DNA using MB on pencil graphite electrode," *Journal of the Iranian Chemical Society*, vol. 5, no. 3, pp. 476–483, 2008.

[34] B. Piro, A. Kapella, V. H. Le et al., "Towards the detection of human papillomavirus infection by a reagentless electrochemical peptide biosensor," *Electrochimica Acta*, vol. 56, no. 28, pp. 10688–10693, 2011.

[35] S. Jampasa, W. Wonsawat, N. Rodthongkum et al., "Electrochemical detection of human papillomavirus DNA type 16 using a pyrrolidinyl peptide nucleic acid probe immobilized on screen-printed carbon electrodes," *Biosensors & Bioelectronics*, vol. 54, pp. 428–434, 2014.

[36] N. Nasirizadeh, H. R. Zare, M. H. Pournaghi-Azar, and M. S. Hejazi, "Introduction of hematoxylin as an electroactive label for DNA biosensors and its employment in detection of target DNA sequence and single-base mismatch in human papilloma virus corresponding to oligonucleotide," *Biosensors and Bioelectronics*, vol. 26, no. 5, pp. 2638–2644, 2011.

[37] K.-J. Huang, Y.-J. Liu, J.-Z. Zhang, J.-T. Cao, and Y.-M. Liu, "Aptamer/Au nanoparticles/cobalt sulfide nanosheets biosensor for 17beta-estradiol detection using a guanine-rich complementary DNA sequence for signal amplification," *Biosensors and Bioelectronics*, vol. 67, pp. 184–191, 2015.

[38] L. F. Urrego, D. I. Lopez, K. A. Ramirez, C. Ramirez, and J. F. Osma, "Biomicrosystem design and fabrication for the human papilloma virus 16 detection," *Sensors and Actuators B: Chemical*, vol. 207, pp. 97–104, 2015.

[39] L. D. Tran, D. T. Nguyen, B. H. Nguyen, Q. P. Do, and H. Le Nguyen, "Development of interdigitated arrays coated with

functional polyaniline/MWCNT for electrochemical biodetection: application for human papilloma virus," *Talanta*, vol. 85, no. 3, pp. 1560–1565, 2011.

[40] A. Josefsson, K. Livak, and U. Gyllensten, "Detection and quantitation of human papillomavirus by using the fluorescent 5′ exonuclease assay," *Journal of Clinical Microbiology*, vol. 37, no. 3, pp. 490–496, 1999.

[41] G. Lizard, M.-C. Chignol, C. Souchier, P. Roignot, Y. Chardonnet, and D. Schmitt, "Detection of low copy numbers of HPV DNA by fluorescent in situ hybridization combined with confocal microscopy as an alternative to in situ polymerase chain reaction," *Journal of Virological Methods*, vol. 72, no. 1, pp. 15–25, 1998.

[42] M. Siadat-Pajouh, A. Periasamy, A. H. Ayscue et al., "Detection of human papillomavirus Type 16/18 DNA in cervicovaginal cells by fluorescence based in situ hybridization and automated image cytometry," *Cytometry*, vol. 15, no. 3, pp. 245–257, 1994.

[43] M. Chinami, M. Inoue, K. Masunaga, T. Fukuma, M. Shingu, and T. Toyoda, "Nucleic acid binding by zinc finger-like motif of human papillomavirus type 16 E7 oncoprotein," *Journal of Virological Methods*, vol. 59, no. 1-2, pp. 173–176, 1996.

[44] S. J. Kim, K. B. Nahm, J. B. Lim, S. W. Oh, and E. Y. Choi, "A rapid and sensitive detection of HPV by combined assay of PCR and fluorescence DNA chip," *Biochip Journal*, vol. 8, no. 1, pp. 48–54, 2014.

[45] B. J. Kocjan, K. Seme, and M. Poljak, "Detection and differentiation of human papillomavirus genotypes HPV-6 and HPV-11 by FRET-based real-time PCR," *Journal of Virological Methods*, vol. 153, no. 2, pp. 245–249, 2008.

[46] Y. Xu, Y. Liu, Y. Wu, X. Xia, Y. Liao, and Q. Li, "Fluorescent probe-based lateral flow assay for multiplex nucleic acid detection," *Analytical Chemistry*, vol. 86, no. 12, pp. 5611–5614, 2014.

[47] S. Pal, A. R. Yadav, M. A. Lifson, J. E. Baker, P. M. Fauchet, and B. L. Miller, "Selective virus detection in complex sample matrices with photonic crystal optical cavities," *Biosensors and Bioelectronics*, vol. 44, pp. 229–234, 2013.

[48] V. Towne, Q. Zhao, M. Brown, and A. C. Finnefrock, "Pairwise antibody footprinting using surface plasmon resonance technology to characterize human papillomavirus type 16 virus-like particles with direct anti-HPV antibody immobilization," *Journal of Immunological Methods*, vol. 388, no. 1-2, pp. 1–7, 2013.

[49] S. Wang, H. Yang, H. Zhang et al., "A surface plasmon resonance-based system to genotype human papillomavirus," *Cancer Genetics and Cytogenetics*, vol. 200, no. 2, pp. 100–105, 2010.

[50] W. Yu-Hong, C. Rui, and L. Ding, "A quantum dots and superparamagnetic nanoparticle-based method for the detection of HPV DNA," *Nanoscale Research Letters*, vol. 6, no. 1, article 461, 2011.

[51] S. Palantavida, N. V. Guz, C. D. Woodworth, and I. Sokolov, "Ultrabright fluorescent mesoporous silica nanoparticles for prescreening of cervical cancer," *Nanomedicine: Nanotechnology, Biology, and Medicine*, vol. 9, no. 8, pp. 1255–1262, 2013.

[52] R. Riccò, A. Meneghello, and F. Enrichi, "Signal enhancement in DNA microarray using dye doped silica nanoparticles: application to Human Papilloma Virus (HPV) detection," *Biosensors and Bioelectronics*, vol. 26, no. 5, pp. 2761–2765, 2011.

[53] W. Wang, D.-W. Pang, and H.-W. Tang, "Sensitive multiplexed DNA detection using silica nanoparticles as the target capturing platform," *Talanta*, vol. 128, pp. 263–267, 2014.

[54] X. Z. Li, S. Kim, W. Cho, and S.-Y. Lee, "Optical detection of nanoparticle-enhanced human papillomavirus genotyping microarrays," *Biomedical Optics Express*, vol. 4, no. 2, pp. 187–192, 2013.

[55] W. Fu, Q. Huang, J. Wang, M. Liu, J. Huang, and B. Chen, "Detection of human papilloma virus with piezoelectric quartz crystal genesensors," *Sensors & Transducers Magazine*, vol. 42, no. 4, 6 pages, 2004.

[56] D. Dell'Atti, M. Zavaglia, S. Tombelli et al., "Development of combined DNA-based piezoelectric biosensors for the simultaneous detection and genotyping of high risk Human Papilloma Virus strains," *Clinica Chimica Acta*, vol. 383, no. 1-2, pp. 140–146, 2007.

[57] Q. Chen, Z. Bian, X. Hua et al., "Detection of hybridization of single-strand DNA PCR products in temperature change process by a novel metal-clamping piezoelectric sensor," *Biosensors and Bioelectronics*, vol. 25, no. 9, pp. 2161–2166, 2010.

[58] P. Prakrankamanant, C. Leelayuwat, C. Promptmas et al., "The development of DNA-based quartz crystal microbalance integrated with isothermal DNA amplification system for human papillomavirus type 58 detection," *Biosensors and Bioelectronics*, vol. 40, no. 1, pp. 252–257, 2013.

[59] P. Parsongdee, T. Limpaiboon, C. Leelayuwat, C. Promptmas, and P. Jearanaikoon, "Development of biosensor for high risk HPV detection in cervical cancer," *KKU Research Journal (Graduate Studies)*, vol. 8, no. 1, 2008.

[60] S. Mobley, S. Yalamanchili, H. Zhang et al., "Procedure for developing linear and Bayesian classification models based on immunosensor measurements," *Sensors and Actuators, B: Chemical*, vol. 190, pp. 165–170, 2014.

[61] N. Li, S. Franceschi, R. Howell-Jones, P. J. F. Snijders, and G. M. Clifford, "Human papillomavirus type distribution in 30,848 invasive cervical cancers worldwide: variation by geographical region, histological type and year of publication," *International Journal of Cancer*, vol. 128, no. 4, pp. 927–935, 2011.

[62] J.-H. Su, A. Wu, E. Scotney et al., "Immunotherapy for cervical cancer," *BioDrugs*, vol. 24, no. 2, pp. 109–129, 2010.

[63] C. Jianrong, M. Yuqing, H. Nongyue, W. Xiaohua, and L. Sijiao, "Nanotechnology and biosensors," *Biotechnology Advances*, vol. 22, no. 7, pp. 505–518, 2004.

[64] S.-H. Yeom, B.-H. Kang, K.-J. Kim, and S.-W. Kang, "Nanostructures in biosensor—a review," *Frontiers in Bioscience*, vol. 16, no. 3, pp. 997–1023, 2011.

[65] M. Mehrvar and M. Abdi, "Recent developments, characteristics, and potential applications of electrochemical biosensors," *Analytical Sciences*, vol. 20, no. 8, pp. 1113–1126, 2004.

[66] R. L. Caygill, G. E. Blair, and P. A. Millner, "A review on viral biosensors to detect human pathogens," *Analytica Chimica Acta*, vol. 681, no. 1-2, pp. 8–15, 2010.

[67] S. Guo and S. Dong, "Biomolecule-nanoparticle hybrids for electrochemical biosensors," *TrAC—Trends in Analytical Chemistry*, vol. 28, no. 1, pp. 96–109, 2009.

[68] H. Huang, W. Bai, C. Dong, R. Guo, and Z. Liu, "An ultrasensitive electrochemical DNA biosensor based on graphene/Au nanorod/polythionine for human papillomavirus DNA detection," *Biosensors and Bioelectronics*, vol. 68, pp. 442–446, 2015.

[69] Rajesh, T. Ahuja, and D. Kumar, "Recent progress in the development of nano-structured conducting polymers/nanocomposites for sensor applications," *Sensors and Actuators B: Chemical*, vol. 136, no. 1, pp. 275–286, 2009.

[70] D. C. Ferrier, M. P. Shaver, and P. J. W. Hands, "Micro- and nano-structure based oligonucleotide sensors," *Biosensors and Bioelectronics*, vol. 68, pp. 798–810, 2015.

[71] I. J. Higgins and C. R. Lowe, "Introduction to the principles and applications of biosensors," *Philosophical Transactions of the Royal Society of London. Series B: Biological Sciences*, vol. 316, no. 1176, pp. 3–11, 1987.

[72] A. Hulanicki, S. Glab, and F. Ingman, "Chemical sensors: definitions and classification," *Pure and Applied Chemistry*, vol. 63, no. 9, pp. 1247–1250, 1991.

[73] D. R. Thévenot, K. Toth, R. A. Durst, and G. S. Wilson, "Electrochemical biosensors: recommended definitions and classification," *Biosensors & Bioelectronics*, vol. 16, no. 1-2, pp. 121–131, 2001.

[74] P. D'Orazio, "Biosensors in clinical chemistry," *Clinica Chimica Acta*, vol. 334, no. 1-2, pp. 41–69, 2003.

[75] K. S. Soppimath, T. M. Aminabhavi, A. R. Kulkarni, and W. E. Rudzinski, "Biodegradable polymeric nanoparticles as drug delivery devices," *Journal of Controlled Release*, vol. 70, no. 1-2, pp. 1–20, 2001.

[76] S. Rahimian, M. F. Fransen, J. W. Kleinovink et al., "Polymeric nanoparticles for co-delivery of synthetic long peptide antigen and poly IC as therapeutic cancer vaccine formulation," *Journal of Controlled Release*, vol. 203, pp. 16–22, 2015.

[77] J. Devkota, J. Wingo, T. T. T. Mai et al., "A highly sensitive magnetic biosensor for detection and quantification of anticancer drugs tagged to superparamagnetic nanoparticles," *Journal of Applied Physics*, vol. 115, no. 17, Article ID 17B503, 2014.

[78] X. Zhang, L. Jiang, C. Zhang et al., "A silicon dioxide modified magnetic nanoparticles-labeled lateral flow strips for HBs antigen," *Journal of Biomedical Nanotechnology*, vol. 7, no. 6, pp. 776–781, 2011.

[79] K. K. Jain, "Applications of nanobiotechnology in clinical diagnostics," *Clinical Chemistry*, vol. 53, no. 11, pp. 2002–2009, 2007.

[80] R. S. Sethi, "Transducer aspects of biosensors (reprinted from Gec Journal Research Vol 9, Pg 81, 1991)," *Biosensors & Bioelectronics*, vol. 9, no. 3, pp. 243–264, 1994.

[81] M.-P. Marco and D. Barceló, "Environmental applications of analytical biosensors," *Measurement Science & Technology*, vol. 7, no. 11, pp. 1547–1562, 1996.

[82] P. D'Orazio, "Biosensors in clinical chemistry—2011 update," *Clinica Chimica Acta*, vol. 412, no. 19-20, pp. 1749–1761, 2011.

[83] C. I. L. Justino, T. A. Rocha-Santos, A. C. Duarte, and T. A. Rocha-Santos, "Review of analytical figures of merit of sensors and biosensors in clinical applications," *TrAC Trends in Analytical Chemistry*, vol. 29, no. 10, pp. 1172–1183, 2010.

[84] C. Fournier-Wirth and J. Coste, "Nanotechnologies for pathogen detection: future alternatives?" *Biologicals*, vol. 38, no. 1, pp. 9–13, 2010.

[85] D. Grieshaber, R. MacKenzie, J. Vörös, and E. Reimhult, "Electrochemical biosensors—sensor principles and architectures," *Sensors*, vol. 8, no. 3, pp. 1400–1458, 2008.

[86] L. C. Clark Jr. and C. Lyons, "Electrode systems for continuous monitoring in cardiovascular surgery," *Annals of the New York Academy of Sciences*, vol. 102, pp. 29–45, 1962.

[87] D. R. Thevenot, K. Tóth, R. A. Durst, and G. S. Wilson, "Electrochemical biosensors: recommended definitions and classification," *Pure and Applied Chemistry*, vol. 71, no. 12, pp. 2333–2348, 1999.

[88] N. J. Ronkainen, H. B. Halsall, and W. R. Heineman, "Electrochemical biosensors," *Chemical Society Reviews*, vol. 39, no. 5, pp. 1747–1763, 2010.

[89] S. Wang, L. Li, H. L. Jin et al., "Electrochemical detection of hepatitis B and papilloma virus DNAs using SWCNT array coated with gold nanoparticles," *Biosensors & Bioelectronics*, vol. 41, no. 1, pp. 205–210, 2013.

[90] E. T. Thostenson, Z. Ren, and T.-W. Chou, "Advances in the science and technology of carbon nanotubes and their composites: a review," *Composites Science and Technology*, vol. 61, no. 13, pp. 1899–1912, 2001.

[91] J. J. Gooding, "Nanostructuring electrodes with carbon nanotubes: a review on electrochemistry and applications for sensing," *Electrochimica Acta*, vol. 50, no. 15, pp. 3049–3060, 2005.

[92] J. M. Pingarrón, P. Yáñez-Sedeño, and A. González-Cortés, "Gold nanoparticle-based electrochemical biosensors," *Electrochimica Acta*, vol. 53, no. 19, pp. 5848–5866, 2008.

[93] F. S. R. R. Teles, "Biosensors and rapid diagnostic tests on the frontier between analytical and clinical chemistry for biomolecular diagnosis of dengue disease: a review," *Analytica Chimica Acta*, vol. 687, no. 1, pp. 28–42, 2011.

[94] M. F. Mitchell, S. B. Cantor, N. Ramanujam, G. Tortolero-Luna, and R. Richards-Kortum, "Fluorescence spectroscopy for diagnosis of squamous intraepithelial lesions of the cervix," *Obstetrics & Gynecology*, vol. 93, no. 3, pp. 462–470, 1999.

[95] J. Rao, A. Dragulescu-Andrasi, and H. Yao, "Fluorescence imaging in vivo: recent advances," *Current Opinion in Biotechnology*, vol. 18, no. 1, pp. 17–25, 2007.

[96] F. Chang, S. SyrjÄnen, J. Nuutinen, J. KÄrjÄ, and K. SyrjÄnen, "Detection of human papillomavirus (HPV) DNA in oral squamous cell carcinomas by in situ hybridization and polymerase chain reaction," *Archives of Dermatological Research*, vol. 282, no. 8, pp. 493–497, 1990.

[97] I. Abdulhalim, M. Zourob, and A. Lakhtakia, "Overview of optical biosensing techniques," in *Handbook of Biosensors and Biochips*, John Wiley & Sons, 2008.

[98] T. J. Park, M. S. Hyun, H. J. Lee, S. Y. Lee, and S. Ko, "A self-assembled fusion protein-based surface plasmon resonance biosensor for rapid diagnosis of severe acute respiratory syndrome," *Talanta*, vol. 79, no. 2, pp. 295–301, 2009.

[99] A. Olaru, C. Bala, N. Jaffrezic-Renault, and H. Y. Aboul-Enein, "Surface plasmon resonance (SPR) biosensors in pharmaceutical analysis," *Critical Reviews in Analytical Chemistry*, vol. 45, no. 2, pp. 97–105, 2015.

[100] A. Mitra, B. Deutsch, F. Ignatovich, C. Dykes, and L. Novotny, "Nano-optofluidic detection of single viruses and nanoparticles," *ACS Nano*, vol. 4, no. 3, pp. 1305–1312, 2010.

[101] D.-S. Xiang, G.-P. Zeng, and Z.-K. He, "Magnetic microparticle-based multiplexed DNA detection with biobarcoded quantum dot probes," *Biosensors and Bioelectronics*, vol. 26, no. 11, pp. 4405–4410, 2011.

[102] C. Dodeigne, L. Thunus, and R. Lejeune, "Chemiluminescence as a diagnostic tool. A review," *Talanta*, vol. 51, no. 3, pp. 415–439, 2000.

[103] Y.-L. Qiao, J. W. Sellors, P. S. Eder et al., "A new HPV-DNA test for cervical-cancer screening in developing regions: a cross-sectional study of clinical accuracy in rural China," *The Lancet Oncology*, vol. 9, no. 10, pp. 929–936, 2008.

[104] F. R. R. Teles and L. P. Fonseca, "Trends in DNA biosensors," *Talanta*, vol. 77, no. 2, pp. 606–623, 2008.

[105] A. Tinelli, G. Leo, D. Dell'Edera et al., "Molecular methods for a correct diagnosis of multiple HPV infections and clinical implications for vaccine," *International Journal of Gynecological Cancer*, vol. 21, no. 3, pp. 545–550, 2011.

[106] A. Molijn, B. Kleter, W. Quint, and L.-J. van Doorn, "Molecular diagnosis of human papillomavirus (HPV) infections," *Journal of Clinical Virology*, vol. 32, supplement 1, pp. S43–S51, 2005.

[107] A. Holmberg, A. Blomstergren, O. Nord, M. Lukacs, J. Lundeberg, and M. Uhlén, "The biotin-streptavidin interaction can be reversibly broken using water at elevated temperatures," *Electrophoresis*, vol. 26, no. 3, pp. 501–510, 2005.

[108] K. Sotlar, D. Diemer, A. Dethleffs et al., "Detection and typing of human papillomavirus by E6 nested multiplex PCR," *Journal of Clinical Microbiology*, vol. 42, no. 7, pp. 3176–3184, 2004.

[109] A. Roda, M. Mirasoli, S. Venturoli et al., "Microtiter format for simultaneous multianalyte detection and development of a PCR-chemiluminescent enzyme immunoassay for typing human papillomavirus DNAs," *Clinical Chemistry*, vol. 48, no. 10, pp. 1654–1660, 2002.

[110] Y. Okahata, M. Kawase, K. Niikura, F. Ohtake, H. Furusawa, and Y. Ebara, "Kinetic measurements of DNA hybridization on an oligonucleotide-immobilized 27-MHz quartz crystal microbalance," *Analytical Chemistry*, vol. 70, no. 7, pp. 1288–1296, 1998.

[111] I. Burda, A. Silaghi, A. Tunyagi, S. Simon, and O. Popescu, "Note: sensitivity multiplication module for quartz crystal microbalance applications," *Review of Scientific Instruments*, vol. 85, no. 2, Article ID 026116, 2014.

[112] D. S. Lee and C. S. Chen, "Development of a temperature sensor array chip and a chip-based real-time PCR machine for DNA amplification efficiency-based quantification," *Biosensors and Bioelectronics*, vol. 23, no. 7, pp. 971–979, 2008.

[113] Y. Mao, C. Luo, and Q. Ouyang, "Studies of temperature-dependent electronic transduction on DNA hairpin loop sensor," *Nucleic Acids Research*, vol. 31, no. 18, article e108, 2003.

[114] T. Notomi, H. Okayama, H. Masubuchi et al., "Loop-mediated isothermal amplification of DNA," *Nucleic Acids Research*, vol. 28, no. 12, article e63, 2000.

[115] H.-T. Kuo, J. Z. Yeh, C.-M. Jiang, and M.-C. Wu, "Magnetic particle-linked anti hCG beta antibody for immunoassay of human chorionic gonadotropin (hCG), potential application to early pregnancy diagnosis," *Journal of Immunological Methods*, vol. 381, no. 1-2, pp. 32–40, 2012.

[116] X. Yi, Y. Ding, Y. Zeng et al., "Magnetic resonance imaging contrast agent: cRGD-ferric oxide nanometer particle and its role in the diagnosis of tumor," *Journal of Nanoscience and Nanotechnology*, vol. 11, no. 5, pp. 3800–3807, 2011.

[117] D. L. Graham, H. A. Ferreira, and P. P. Freitas, "Magnetoresistive-based biosensors and biochips," *Trends in Biotechnology*, vol. 22, no. 9, pp. 455–462, 2004.

[118] S. X. Wang and G. Li, "Advances in giant magnetoresistance biosensors with magnetic nanoparticle tags: review and outlook," *IEEE Transactions on Magnetics*, vol. 44, no. 7, pp. 1687–1702, 2008.

[119] K. S. Kim, S. Choi, G. J. Lee et al., "Effects of stray field distribution generated by magnetic beads on giant magnetoresistance sensor for biochip applications," in *26th Southern Biomedical Engineering Conference SBEC 2010, April 30–May 2, 2010, College Park, Maryland, USA*, vol. 32 of *IFMBE Proceedings*, pp. 293–296, Springer, Berlin, Germany, 2010.

[120] L. Xu, H. Yu, M. S. Akhras et al., "Giant magnetoresistive biochip for DNA detection and HPV genotyping," *Biosensors and Bioelectronics*, vol. 24, no. 1, pp. 99–103, 2008.